doi : 10.17596/0003053

R/V *Mirai* Cruise Report

MR12-05

WOCE-revisit in the western Pacific and Southern oceans

5th November 2012 – 15th February 2013

Japan Agency for Marine-Earth Science and Technology

(JAMSTEC)

Cruise Report ERRATA of the Nutrients part

page	Error	Correction
119	potassium nitrate CAS No. 7757-91-1	potassium nitrate CAS No. 7757-79-1

Content

I. Introduction

II. Observation

1. Cruise Information
2. Underway Observation
   2.1 Navigation
   2.2 Swath Bathymetry
   2.3 Surface Meteorology
   2.4 Thermo-salinograph
   2.5 pCO_2
   2.6 PCO_2 and pCH_4 by Cavity Ring-Down Spectroscopy
   2.7 Ceilometer
   2.8 Isotopes in rainfall and water vapor
   2.9 Aerosol optical characteristics measured by Ship-borne Sky radiometer
   2.10 Lidar
   2.11 ADCP
   2.12 Sea surface gravity
   2.13 On-board geomagnetic measurement
   2.14 Bathymetry of the Lyra Basin
   2.15 PAR

3. Station Observation
   3.1 CTDO2 Measurements
   3.2 Bottle Salinity
   3.3 Density
   3.4 Oxygen
   3.5 Nutrients
   3.6 Chlorofluorocarbons and Sulfur hexafluoride
   3.7 Carbon items
   3.8 DMS and isoprene
   3.9 Chlorophyll-a
   3.10 Pigment and bacterial abundance
   3.11 Chlorophyll isotope
   3.12 Carbon isotopes

3.13 Radioactive cesium
3.14 Delta O18
3.15 Ocean orign gases
3.16 PFASs (perfluoro alkyl substances)
3.17 Distribution and ecology of oceanic *Halobates* inhabiting tropical area of Pacific Ocean and their responding system to several environmental factors
3.18 LADCP
3.19 XCTD
3.20 XMP

4. Floats, Drifters and Moorings
4.1 Argo floats
4.2 Southern Ocean flux mooring (Recovery of the Southern Ocean buoy)

III. Notice on Using

I. Introduction

It is well established that oceans play important roles in the global climate system, but quantitative description of the oceans' roles and their variabilities are still yet to be made. Given natural variabilities of the oceans, it is necessary to observe them as frequently as practicable and as accurate as possible. In this research cruise, we observed, with state-of-art precision, the Southwestern Pacific and Southern oceans, which are known to be one of the most sensitive regions in the world oceans to the global climate change, particularly as a likely source of the recently-established Pacific near-bottom warming. These oceans are also known to ventilate the intermediate-depth and deep oceans and exchange anthropogenic carbon. We also recovered a JAMSTEC southern ocean mooring, which continuously measured the air-sea flux in this region for the first time. This expedition was conducted under the Global Ocean Ship-based Hydrographic Investigation Programme (GO-SHIP http://www.go-ship.org).

II. Observation

.

1. Cruise Information

Katsuro Katsumata (JAMSTEC)

Hiroshi Uchida (JAMSTEC)

1.1. Basic Information

Cruise track:	See Fig. 1.1.1
Cruise code:	MR12-05
Expocode	Leg 1: 49NZ20121105 Leg 2: 49NZ20121128 Leg 3: 49NZ20130106
GHPO section designation:	P14S, S4I
Ship name:	R/V Mirai
Ports of call:	Leg 1, Sekinehama, Japan; Hachinohe, Japan – Auckland, New Zealand Leg 2, Auckland, New Zealand – Hobart, Australia Leg 3, Hobart, Australia – Fremantle, Australia
Cruise date:	Leg 1, 5 November 2012 – 26 November 2012 Leg 2, 28 November 2012 – 4 January 2013 Leg 3, 6 January 2013 – 15 February 2013
Chief scientists:	Legs 1 and 2, Katsuro Katsumata (k.katsumata@jamstec.go.jp) Leg 3, Hiroshi Uchida (huchida@jamstec.go.jp) Ocean Climate Change Research Program Research Institute for Global Change (RIGC) Japan Agency for Marine-Earth Science and Technology (JAMSTEC) 2-15 Natsushima, Yokosuka, Kanagawa, Japan 237-0061 Fax: +81-46-867-9835
Number of Stations:	Leg 1, 3 stations Leg 2, 54 stations including 6 XCTD-only stations Leg 3, 77 stations

.

Floats and drifters deployed: 3 floats (Leg 1), 4 floats (Leg 2)

Mooring recovery : 2 including 1 emergency recovery of Southern Ocean Flux Buoy (Bureau of Meteorology, Australia)

Research area: the Southwestern Pacific and Southern ocean

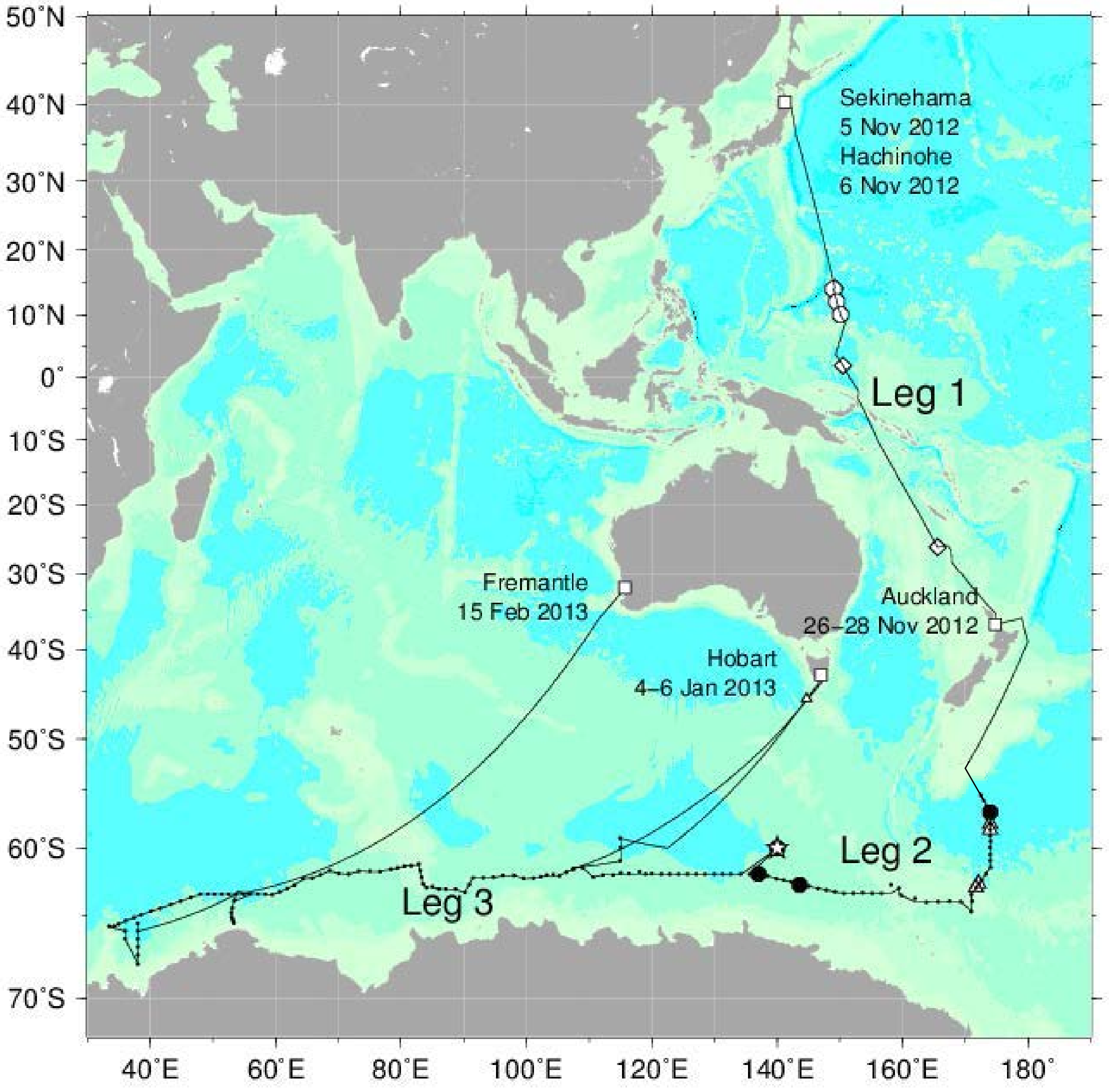

Fig. 1.1.1 MR12-05 cruise. White circles show the deployment position of Argo floats. White diamonds show neuston net sampling (the northernmost station overlaps the northern most Argo deployment). White large triangles show the XMP deployment stations. Star is the flux-buoy recovery position. Black dots shows CTD/bottom sampling stations. Black circles show the Deep Ninja deployment positions (one position overlaps the flux-buoy position). Small white triangle is Australian SOFS buoy recover position.

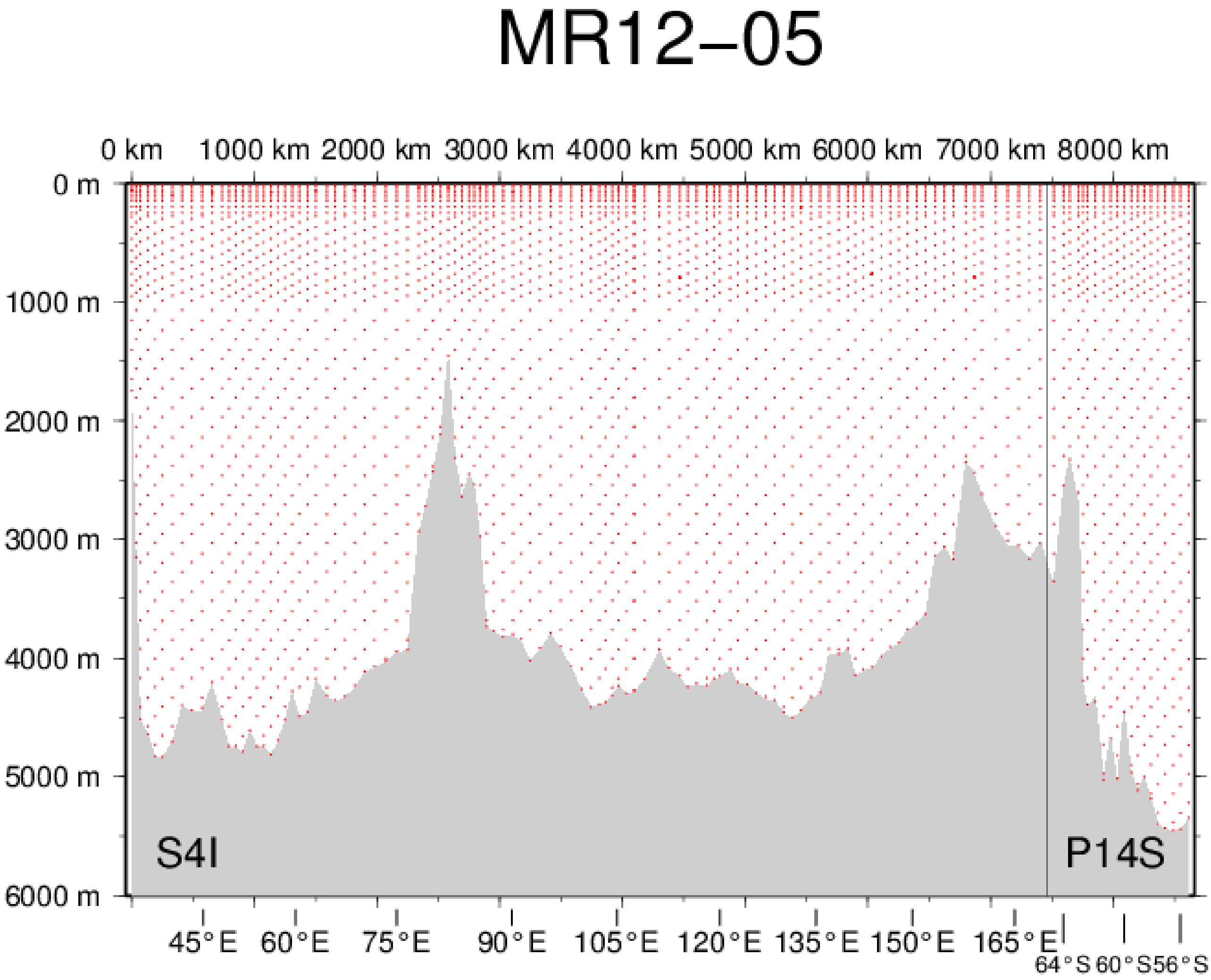

Fig. 1.1.2 Water sampling positions. Meridional segments on S4I are not included.

1.2. Cruise Participants

List of Participants for leg 1

Katsuro Katsumata	Chief scientist	RIGC/JAMSTEC
Yuichiro Kumamoto	C14/radioactive cesium	RIGC/JAMSTEC
Hiroshi Uchida	Thermosalinograph/Chlorophyll	RIGC/JAMSTEC
Tetsuo Harada	*Halobates*	Kochi University
Ryuta Ide	*Halobates*	Kochi University
Takero Sekimoto	*Halobates*	Kochi University

.

Kentaro Emi	*Halobates*	Kochi University
Tomonori Watai	Chief technician/carbon items preparation	MWJ
Tatsuya Tanaka	CTD/Float	MWJ
Makoto Takada	Carbon items preparation	MWJ
Shinsuke Toyoda	CTD	MWJ
Katsunori Sagishima	CFCs preparation	MWJ
Hironori Sato	CFCs preparation	MWJ
Kanako Yoshida	Thermosalinograph	MWJ
Emi Deguchi	Carbon items preparation	MWJ
Soichiro Sueyoshi	Chief technician/meteorology/geophysics/ADCP	GODI
Koichi Inagaki	Meteorology/geophysics/ADCP	GODI

List of Participants for leg 2

Katsuro Katsumata	Chief scientist/XMP/water sampling	RIGC/JAMSTEC
Yuichiro Kumamoto	DO/Δ^{14}C/radioactive cesium	RIGC/JAMSTEC
Hiroshi Uchida	CTD/density/water sampling	RIGC/JAMSTEC
Shinya Kouketsu	LADCP/ADCP/water sampling	RIGC/JAMSTEC
Kazuhiko Hayashi	Water sampling chief/ δ O18	RIGC/JAMSTEC
Ken’ichi Sasaki	CFCs	MIO/JAMSTEC
Shoichiro Baba	Mooring/water sampling	MARITEC/JAMSTEC
Takero Sekimoto	*Halobates*/water sampling	Kochi University
Nobuyoshi Yamashita	PFASs/water sampling	AIST
Eriko Yamazaki	PFASs/water sampling	AIST
Sohiko Kameyama	DMS/isoprene/water sampling	Hokkaido University
Tomohide Noguchi	Chief technician/mooring/water sampling chief	MWJ
Tomonori Watai	pH/total alkalinity	MWJ
Tatsuya Tanaka	Salinity/mooring	MWJ
Shinsuke Toyoda	CTD/mooring/water sampling	MWJ
Atsushi Ono	DIC	MWJ
Emi Deguchi	pH/total alkalinity	MWJ
Shungo Oshitani	CTD/mooring/water sampling	MWJ
Tomoyuki Takamori	CTD/mooring/water sampling	MWJ
Rei Ito	CTD/mooring/water sampling	MWJ
Minoru Kamata	Nutrients	MWJ
Yoshiko Ishikawa	DIC	MWJ
Yasuhiro Arii	Nutrients	MWJ
Hideki Yamamoto	CFCs	MWJ

.

Shoko Tatamisashi	CFCs	MWJ
Misato Kuwahara	DO/thermosalinograph	MWJ
Masahiro Orui	CFCs	MWJ
Keitaro Matsumoto	DO/mooring/water sampling	MWJ
Keisuke Tsubata	Salinity	MWJ
Takuhiro Osumi	DO/water sampling	MWJ
Kohei Miura	Nutrients	MWJ
Yuki Komuro	Water sampling	MWJ
Takehiro Shibuya	Water sampling	MWJ
Saeko Kumagai	Water sampling	MWJ
Mizuho Yasui	Water sampling	MWJ
Hitomi Takahashi	Water sampling	MWJ
Ai Ozaki	Water sampling	MWJ
Kazuho Yoshida	Chief technician/meterology/geophysics/ADCP/XCTD	GODI
Shinya Okumura	Meteorlology/geophysics/ADCP/XCTD	GODI
Masanori Murakami	Meteorology/geophysics/ADCP/XCTD	GODI

List of Participants for leg 3

Hiroshi Uchida	Chief scientist/CTD/density	RIGC/JAMSTEC
Akihiko Murata	Carbon items/water sampling	RIGC/JAMSTEC
Toshimasa Doi	LADCP/water sampling	RIGC/JAMSTEC
Kazuhiko Hayashi	Water sampling chief/ δ O18	RIGC/JAMSTEC
Ken’ichi Sasaki	CFCs	MIO / JAMSTEC
Osamu Yoshida	CH_4 and N_2O/water sampling	Rakuno Gakuen University
Haruka Tamada	CH_4 and N_2O/water sampling	Rakuno Gakuen University
Yuko Kanayama	CH_4 and N_2O/water sampling	Rakuno Gakuen University
Okura Shinozaki	CH_4 and N_2O/water sampling	Rakuno Gakuen University
Sohiko Kameyama	DMS/isoprene/water sampling	Hokkaido University
Hideki Yamamoto	Chief technician/water sampling chief	MWJ
Tomonori Watai	pH/total alkalinity	MWJ
Minoru Kamata	Nutrients	MWJ
Yoshiko Ishikawa	DIC	MWJ
Misato Kuwahara	DO/thermosalinograph/water sampling	MWJ
Masahiro Orui	CFCs	MWJ
Satoshi Ozawa	CTD/water sampling	MWJ
Tamami Ueno	Salinity	MWJ
Hiroshi Matsunaga	CTD/water sampling	MWJ

.

Naoko Miyamoto	CTD/water sampling	MWJ
Hiroki Ushiromura	Salinity	MWJ
Takami Mori	CTD/water sampling	MWJ
Masanori Enoki	Nutrients	MWJ
Atsushi Ono	pH/total alkalinity	MWJ
Elena Hayashi	Nutrients	MWJ
Kanako Yoshida	DO/water sampling	MWJ
Katsunori Sagishima	CFCs	MWJ
Hironori Sato	CFCs	MWJ
Keisuke Tsubata	DIC	MWJ
Takuhiro Osumi	DO/water sampling	MWJ
Aiko Miura	Water sampling	MWJ
Manami Kamei	Water sampling	MWJ
Sachi Miyake	Water sampling	MWJ
Yuta Furukawa	Water sampling	MWJ
Iori Fujiwara	Water sampling	MWJ
Yuki Kawabuchi	Water sampling	MWJ
Soichiro Sueyoshi	Chief technician/meteorology/geophysics/ADCP/XCTD	GODI
Katsuhisa Maeno	Meteorology/geophysics/ADCP/XCTD	GODI
Koichi Inagaki	Meteorology/geophysics/ADCP/XCTD	GODI

.

2. Underway Observation

2.1 Navigation

(1) Personnel

Souichiro Sueyoshi	*(Global Ocean Development Inc., GODI)*	*-leg1, leg3-*
Koichi Inagaki	*(GODI)*	*-leg1, leg3-*
Kazuho Yoshida	*(GODI)*	*-leg2-*
Shinya Okumura	*(GODI)*	*-leg2-*
Masanori Murakami	*(GODI)*	*-leg2-*
Katsuhisa Maeno	*(GODI)*	*-leg3-*
Ryo Kimura	*(MIRAI Crew)*	*-leg1, leg2-*
Ryo Ohyama	*(MIRAI Crew)*	*-leg3-*

(2) System description

Ship's position and velocity were provided by Radio Navigation System on R/V Mirai. This system integrates GPS position, log speed, gyro compass heading and other basic data for navigation, and calculated speed/course over ground on workstation. Radio navigation System also distributed ship's standard time synchronized to GPS time server via Network Time Protocol. These data were logged on the network server as "SOJ" data every 5 seconds.

Sensors for navigation data are listed below;

i) GPS system: MultiFix6 (software version 1.01), Differential GPS system.
Receiver: Trimble SPS751, with two GPS antennas located on navigation deck, starboard side and port side, manually switched as to GPS receiving state and offset to radar-mast position, datum point.
Decoder: Fugro STARFIX 4100LR
ii) Doppler log: Furuno DS-30, which use three acoustic beam for current measurement under the hull.
iii) Gyrocompass: Tokimec TG-6000, sperry type mechanical gyrocompass.
iv) GPS time server: SEIKO TS-2540 Time Server, synchronizing to GPS satellite every 1 second.

(3) Period (Times in UTC)

Leg1: 07:00, 05 Nov. 2012 - 20:30, 25 Nov. 2012
Leg2: 21:10, 27 Nov. 2012 - 23:20, 03 Jan. 2013
Leg3: 22:50, 05 Jan. 2013 - 06:23, 15 Feb. 2013

(4) Remarks (Times in UTC)

i) The following periods, navigation data was invalid due to the system error.

23:25:05, 22 Nov. 2012
23:30:40, 22 Nov. 2012 - 23:36:30, 22 Nov. 2012
23:38:15, 22 Nov. 2012 - 23:38:30, 22 Nov. 2012
23:38:40, 22 Nov. 2012 - 23:38:55, 22 Nov. 2012

23:39:05, 22 Nov. 2012

18:07:50, 04 Dec. 2012

15:26:05, 05 Dec. 2012

21:32:10, 07 Dec. 2012

18:01:50, 09 Dec. 2012

15:33:50, 10 Dec. 2012

15:16:20, 15 Dec. 2012

16:07:00, 16 Dec. 2012

16:07:05, 16 Dec. 2012

20:50:55, 20 Dec. 2012

ii) The following periods, navigation data was invalid due to GPS position fix error.

12:14:15, 22 Dec. 2012

12:15:45, 22 Dec. 2012

11:47:40, 28 Dec. 2012 - 11:52:40, 28 Dec. 2012

12:39:25, 28 Dec. 2012 - 12:41:55, 28 Dec. 2012

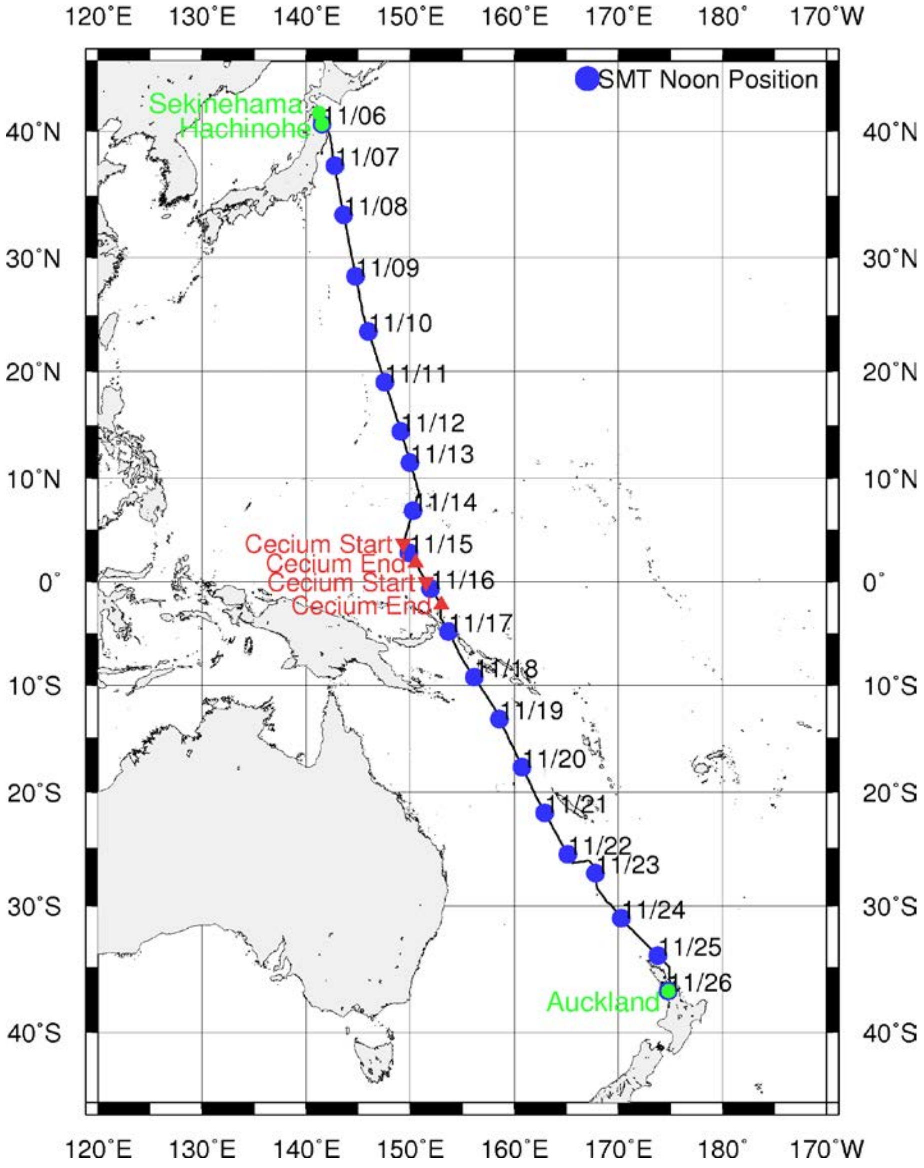

Fig.2.1-1 Cruise Track of MR12-05 Leg1

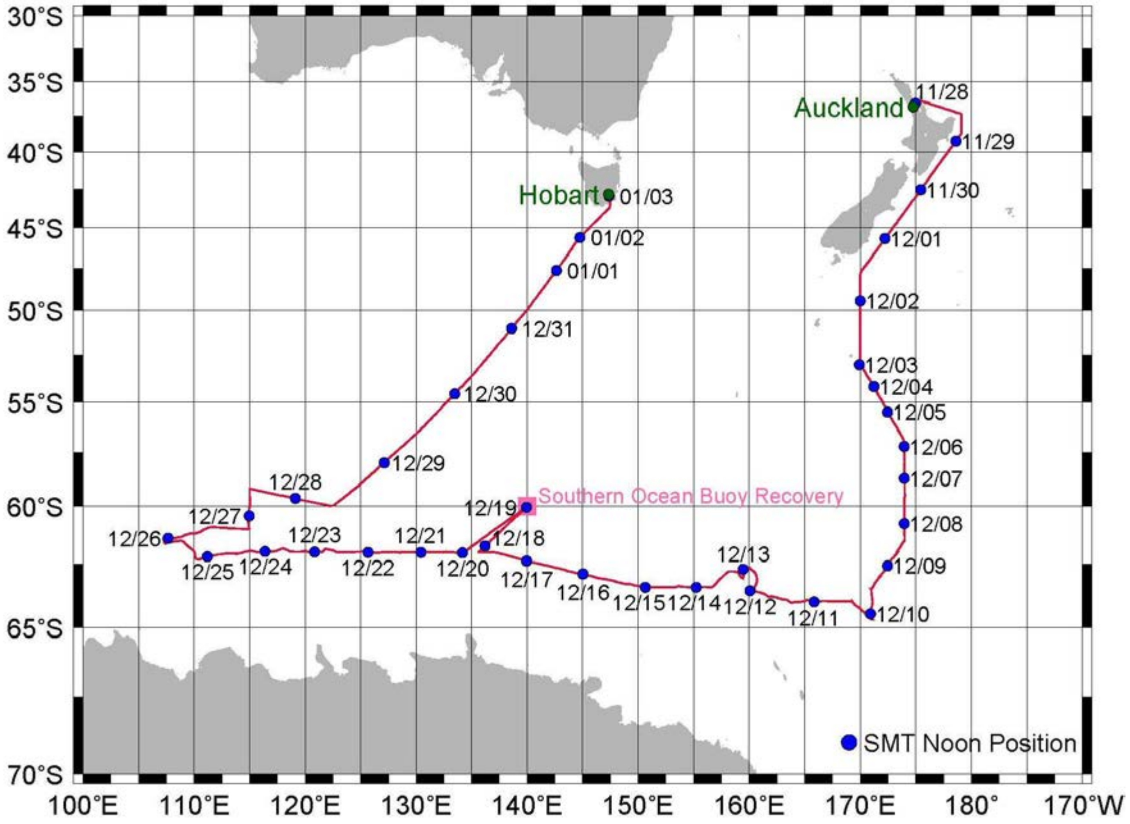

Fig.2.1-2 Cruise Track of MR12-05 Leg2

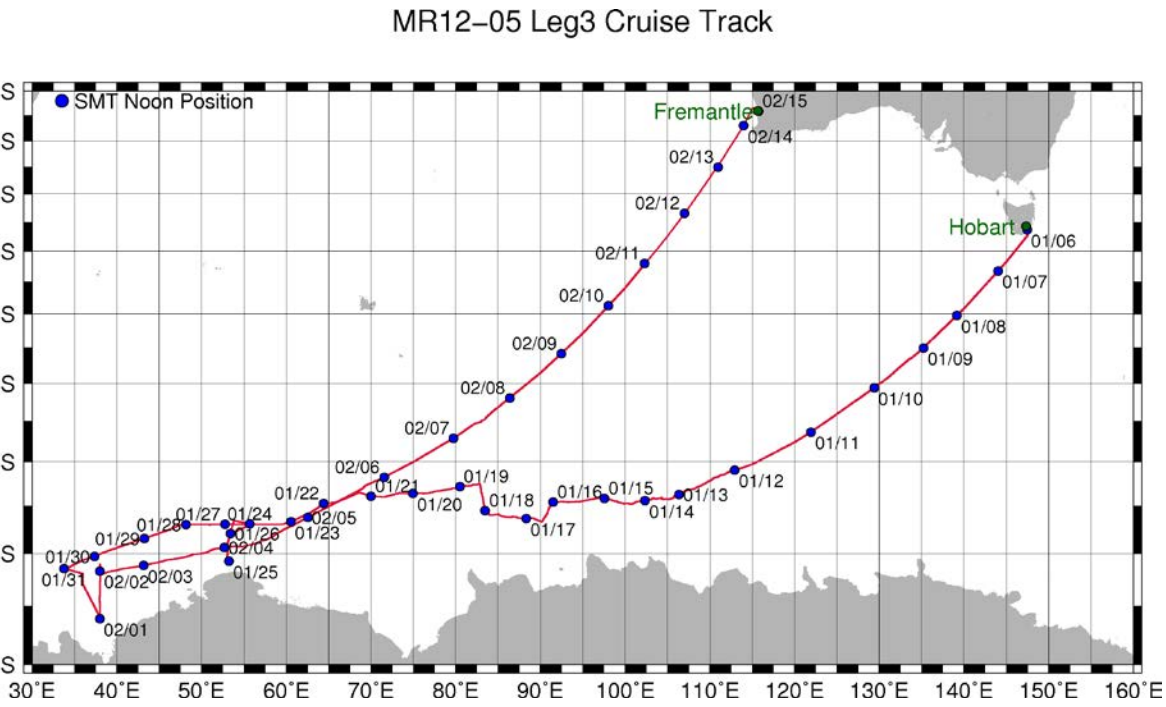

Fig.2.1-3 Cruise Track of MR12-05 Leg3

2.2 Swath Bathymetry

1) Multi beam echo sounding system

(1) Personnel

Takeshi Matsumoto	*(University of the Ryukyus): Principal investigator (not on-board)*	
Masao Nakanishi	*(Chiba University): Principal investigator (not on-board)*	
Souichiro Sueyoshi	*(Global Ocean Development Inc., GODI)*	*-leg1, leg3-*
Koichi Inagaki	*(GODI)*	*-leg1, leg3-*
Kazuho Yoshida	*(GODI)*	*-leg2-*
Shinya Okumura	*(GODI)*	*-leg2-*
Masanori Murakami	*(GODI)*	*-leg2-*
Katsuhisa Maeno	*(GODI)*	*-leg3-*
Ryo Kimura	*(MIRAI Crew)*	*-leg1, leg2-*
Ryo Ohyama	*(MIRAI Crew)*	*-leg3-*

(2) Introduction

R/V MIRAI is equipped with a Multi narrow Beam Echo Sounding system (MBES), SEABEAM 3012 Upgraded Model (L3 Communications ELAC Nautik). The objective of MBES is collecting continuous bathymetric data along ship's track to make a contribution to geological and geophysical investigations and global datasets.

(3) Data Acquisition

The "SEABEAM 3012 Upgrade Model" on R/V MIRAI was used for bathymetry mapping during the MR12-05 cruise from 5th November 2012 to 15th February 2013.

To get accurate sound velocity of water column for ray-path correction of acoustic multibeam, we used Surface Sound Velocimeter (SSV) data to get the sea surface sound velocity (at 6.62m), and the deeper depth sound velocity profiles were calculated by temperature and salinity profiles from CTD and XCTD data by the equation in Del Grosso (1974) during this cruise.

Table 2.2-1 shows system configuration and performance of SEABEAM 3012Upgraded Model.

Table 2.2-1 System configuration and performance

SEABEAM 3012 (12 kHz system)

Frequency:	12 kHz
Transmit beam width:	1.6 degree
Transmit power:	20 kW
Transmit pulse length:	2 to 20 msec.
Receive beam width:	1.8 degree
Depth range:	100 to 11,000 m
Beam spacing:	0.5 degree athwart ship
Swath width:	150 degree (max)
	120 degree to 4,500 m

	100 degree to 6,000 m
	90 degree to 11,000 m
Depth accuracy:	Within < 0.5% of depth or +/-1m, whichever is greater, over the entire swath. (Nadir beam has greater accuracy; typically within < 0.2% of depth or +/-1m, whichever is greater)

(4) Data processing

i. Sound velocity correction

Each bathymetry data was corrected with a sound velocity profile calculated from the nearest CTD or XCTD data in the distance. The equation of Del Grosso (1974) was used for calculating sound velocity. The data correction was carried out using the HIPS software version 7.1 (CARIS, Canada)

ii. Editing and Gridding

Gridding for the bathymetry data were carried out using the HIPS. Firstly, the bathymetry data during ship's turning was basically deleted, and spike noise of each swath data was removed. Then the bathymetry data was gridded by "Interpolate" function of the software with the parameters shown as table 2.2-2

Table 2.2-2 Parameters for interpolate of bathymetry data

BASE surface resolution:	50m
Interpolate matrix size:	5 x 5
Minimum number of neighbors for interpolate:	10

Finally, interpolated data were exported as ASCII data, and converted to 150m grid data using "xyz2grd" utility of GMT (Generic Mapping Tool) software.

(5) Data Archives

Bathymetric data obtained during this cruise will be submitted to the Data Management Group (DMG) of JAMSTEC, and will be archived there.

(6) Remarks (Times in UTC)

1) The following periods, the observation was carried out.

Leg1:	14:24, 06 Nov. 2012 - 13:05, 16 Nov. 2012
	04:28, 17 Nov. 2012 - 07:00, 25 Nov. 2012
Leg2:	08:15, 28 Nov. 2012 - 07:00, 01 Jan. 2013

.

Leg3: 02:25, 7 Jan. 2013 - 12:06, 13 Feb 2013.

2) The following periods, data acquisition was suspended due to the system error and maintenance.

12:22 - 13:12, 11 Dec. 2012
07:12 - 09:02, 12 Dec. 2012
08:06 - 08:31, 23 Jan. 2013

3) The following periods, navigation data was invalid due to GPS position fix error..

23:30:30 - 23:39:05, 22 Nov. 2012 (intermittently)
11:47:37 - 11:52:42, 28 Dec. 2012
12:39:23 - 12:41:55, 28 Dec. 2012

2) Sub-bottom profiler

(1) Personnel

Takeshi Matsumoto	***(University of the Ryukyus): Principal investigator (not on-board)***	
Masao Nakanishi	***(Chiba University): Principal investigator (not on-board)***	
Souichiro Sueyoshi	***(Global Ocean Development Inc., GODI)***	***-leg1-***
Koichi Inagaki	***(GODI)***	***-leg1-***
Ryo Kimura	***(MIRAI Crew)***	***-leg1-***

(2) Introduction

R/V MIRAI is equipped with a Sub-bottom Profiler (SBP), Bathy2010 (SyQwest). The objective of SBP is collecting sub-bottom data along ship's track.

(3) Data Acquisition

Bathy2010 on R/V MIRAI was used for sub-bottom mapping during the following periods.

01:24, 13 Nov. 2012 – 03:52, 13 Nov. 2012
13:48, 14 Nov. 2012 – 13:06, 16 Nov. 2012

Table 2.2.3 shows system configuration and performance of Bathy2010 system.

Table 2.3.3 Bathy2010 System configuration and performance

Frequency:	3.5 kHz
Transmit beam width:	23 degree
Transmit pulse length:	0.5 to 50 msec
Strata resolution:	Up to 8 cm with 300+ Meters of bottom penetration; bottom type dependant
Depth resolution:	0.1 Feet, 0.1 Meters
Depth accuracy:	±10 cm to 100 m, ± .3% to 6,000 m

(4) Data Archives

Sub-bottom data obtained during this cruise will be submitted to the Data Management Group (DMG) in

.

JAMSTEC, and will be archived there.

.

2.3 Surface Meteorology

(1) Personnel

Souichiro Sueyoshi	***(Global Ocean Development Inc., GODI)***	***-leg1, leg3-***
Koichi Inagaki	***(GODI)***	***-leg1, leg3-***
Kazuho Yoshida	***(GODI)***	***-leg2-***
Shinya Okumura	***(GODI)***	***-leg2-***
Masanori Murakami	***(GODI)***	***-leg2-***
Katsuhisa Maeno	***(GODI)***	***-leg3-***
Ryo Kimura	***(MIRAI Crew)***	***-leg1, leg2-***
Ryo Ohyama	***(MIRAI Crew)***	***-leg3-***

(2) Objectives

Surface meteorological parameters are observed as a basic dataset of the meteorology. These parameters provide the temporal variation of the meteorological condition surrounding the ship.

(3) Methods

Surface meteorological parameters were observed during the MR12-05 cruise from 5th November 2012 to 15th February 2013. In this cruise, we used two systems for the observation.

i. *MIRAI Surface Meteorological observation (SMet) system*

Instruments of SMet system are listed in Table 2.3-1 and measured parameters are listed in Table 2.3-2. Data were collected and processed by KOAC-7800 weather data processor made by Koshin-Denki, Japan. The data set consists of 6-second averaged data.

ii. *Shipboard Oceanographic and Atmospheric Radiation (SOAR) measurement system*

SOAR system designed by BNL (Brookhaven National Laboratory, USA) consists of major three parts.

a) Portable Radiation Package (PRP) designed by BNL – short and long wave downward radiation.
b) Zeno Meteorological (Zeno/Met) system designed by BNL – wind, air temperature, relative humidity, pressure, and rainfall measurement.
c) Scientific Computer System (SCS) developed by NOAA (National Oceanic and Atmospheric Administration, USA) – centralized data acquisition and logging of all data sets.

SCS recorded PRP data every 6 seconds, Zeno/Met data every 10 seconds. Instruments and their locations are listed in Table 2.3-3 and measured parameters are listed in Table 2.3-4.;

For the quality control as post processing, we checked the following sensors, before and after the cruise.

i. Young Rain gauge (SMet and SOAR)

Inspect of the linearity of output value from the rain gauge sensor to change Input value by adding fixed quantity of test water.

ii. Barometer (SMet and SOAR)

Comparison with the portable barometer value, PTB220, VAISALA

iii. Thermometer (air temperature and relative humidity) (SMet and SOAR)

.

Comparison with the portable thermometer value, HMP41/45, VAISALA

(4) Preliminary results

Fig. 2.3-1 shows the time series of the following parameters;

Wind (SMet)
Air temperature (SMet)
Relative humidity (SOAR)
Precipitation (SOAR, rain gauge)
Short/long wave radiation (SOAR)
Pressure (SMet)
Sea surface temperature (SMet)
Significant wave height (SMet)

(5) Data archives

These meteorological data will be submitted to the Data Management Group (DMG) of JAMSTEC just after the cruise.

(6) Remarks (Times in UTC)

1) The following periods, observation was carried out.

Leg1: 00:00, 05 Nov. 2012 to 15:00, 16 Nov. 2012
03:00, 17 Nov. 2012 to 07:00, 25 Nov. 2012
Leg2: 06:00, 28 Nov. 2012 to 07:00, 01 Jan. 2013
Leg3: 02:00, 07 Jan. 2013 to 12:00, 13. Feb 2013

2) The following periods, navigation data of SMet data was invalid due to GPS position fix error.

Leg1: 23:30 - 23:39, 22 Nov. 2012 (intermittently)
Leg2: 12:21, 18 Dec. 2012
11:47 to 11:51, 28 Dec. 2012
12:39 to 12:41, 28 Dec. 2012

3) The following periods, FRSR data acquisition was suspended to prevent damage to the shadow-band from freezing.

Leg2: 08:01, 08 Dec. 2012 to 20:45, 28 Dec. 2012
Leg3: 19:20, 12 Jan. 2013 to 10:21, 08 Feb. 2013

4) The following time, SMet rain gauge amount values were increased because of test transmitting for MF/HF radio.

Leg1: 23:01 - 23:16, 11 Nov. 2012
Leg2: 08:54, 06 Dec. 2012
00:35, 18 Dec. 2012
22:41, 25 Dec. 2012
Leg3: 06:15, 24 Jan. 2013
01:25, 13 Feb. 2013

Table 2.3-1 Instruments and installation locations of MIRAI Surface Meteorological observation system

Sensors	Type	Manufacturer	Location (altitude from surface)
Anemometer	KE-500	Koshin Denki, Japan	foremast (24 m)
Tair/RH	HMP45A	Vaisala, Finland	
with 43408 Gill aspirated radiation shield		R.M. Young, USA	compass deck (21 m) starboard side and port side
Thermometer: SST	RFN1-0	Koshin Denki, Japan	4th deck (-1m, inlet -5m)
Barometer	Model-370	Setra System, USA	captain deck (13 m) weather observation room
Rain gauge	50202	R. M. Young, USA	compass deck (19 m)
Optical rain gauge	ORG-815DR	Osi, USA	compass deck (19 m)
Radiometer (short wave)	MS-802	Eko Seiki, Japan	radar mast (28 m)
Radiometer (long wave)	MS-202	Eko Seiki, Japan	radar mast (28 m)
Wave height meter	WM-2	Tsurumi-seiki, Japan	bow (10 m)

Table 2.3-2 Parameters of MIRAI Surface Meteorological observation system

Parameter	Units	Remarks
1 Latitude	degree	
2 Longitude	degree	
3 Ship’s speed	knot	Mirai log, DS-30 Furuno
4 Ship’s heading	degree	Mirai gyro, TG-6000, Tokimec
5 Relative wind speed	m/s	6sec./10min. averaged
6 Relative wind direction	degree	6sec./10min. averaged
7 True wind speed	m/s	6sec./10min. averaged
8 True wind direction	degree	6sec./10min. averaged
9 Barometric pressure	hPa	adjusted to sea surface level 6sec. averaged
10 Air temperature (starboard side)	degC	6sec. averaged
11 Air temperature (port side)	degC	6sec. averaged
12 Dewpoint temperature (starboard side)	degC	6sec. averaged
13 Dewpoint temperature (port side)	degC	6sec. averaged
14 Relative humidity (starboard side)	%	6sec. averaged
15 Relative humidity (port side)	%	6sec. averaged
16 Sea surface temperature	degC	6sec. averaged
17 Rain rate (optical rain gauge)	mm/hr	hourly accumulation
18 Rain rate (capacitive rain gauge)	mm/hr	hourly accumulation
19 Down welling shortwave radiation	W/m2	6sec. averaged
20 Down welling infra-red radiation	W/m2	6sec. averaged
21 Significant wave height (bow)	m	hourly
22 Significant wave height (aft)	m	hourly
23 Significant wave period (bow)	second	hourly
24 Significant wave period (aft)	second	hourly

Table 2.3-3 Instruments and installation locations of SOAR system

Sensors (Zeno/Met)	Type	Manufacturer	Location (altitude from surface)
Anemometer	05106	R.M. Young, USA	foremast (25 m)
Tair/RH	HMP45A	Vaisala, Finland	
with 43408 Gill aspirated radiation shield		R.M. Young, USA	foremast (23 m)
Barometer	61302V	R.M. Young, USA	
with 61002 Gill pressure port		R.M. Young, USA	foremast (23 m)
Rain gauge	50202	R.M. Young, USA	foremast (24 m)
Optical rain gauge	ORG-815DA	Osi, USA	foremast (24 m)

Sensors (PRP)	Type	Manufacturer	Location (altitude from surface)
Radiometer (short wave)	PSP	Epply Labs, USA	foremast (25 m)
Radiometer (long wave)	PIR	Epply Labs, USA	foremast (25 m)
Fast rotating shadowband radiometer		Yankee, USA	foremast (25 m)

Table 2.3-4 Parameters of SOAR system

Parameter	Units	Remarks
1 Latitude	degree	
2 Longitude	degree	
3 SOG	knot	
4 COG	degree	
5 Relative wind speed	m/s	
6 Relative wind direction	degree	
7 Barometric pressure	hPa	
8 Air temperature	degC	
9 Relative humidity	%	
10 Rain rate (optical rain gauge)	mm/hr	
11 Precipitation (capacitive rain gauge)	mm	reset at 50 mm
12 Down welling shortwave radiation	W/m2	
13 Down welling infra-red radiation	W/m2	
14 Defuse irradiance	W/m2	

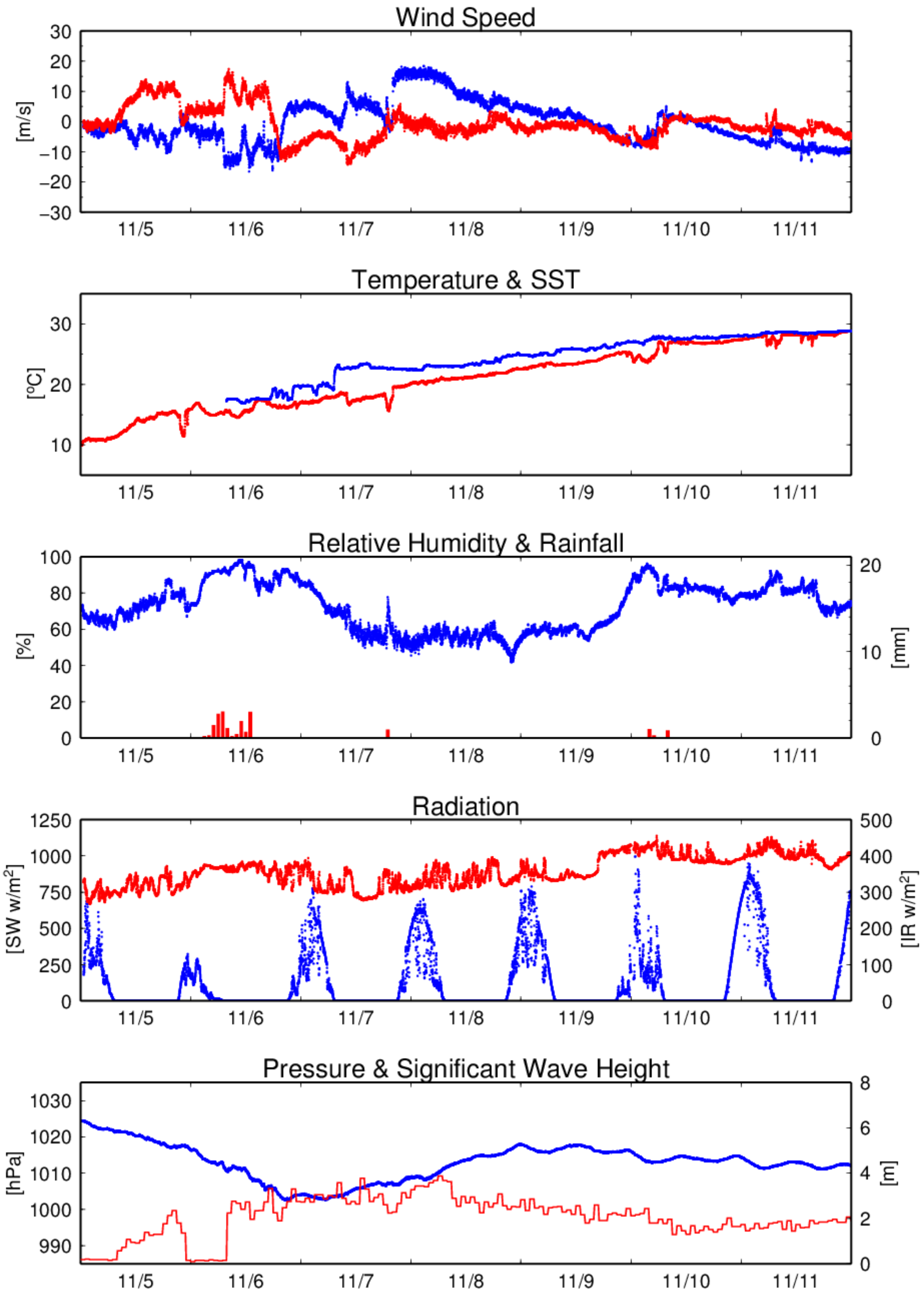

Fig. 2.3-1 Time series of surface meteorological parameters during the MR12-05 leg1 cruise

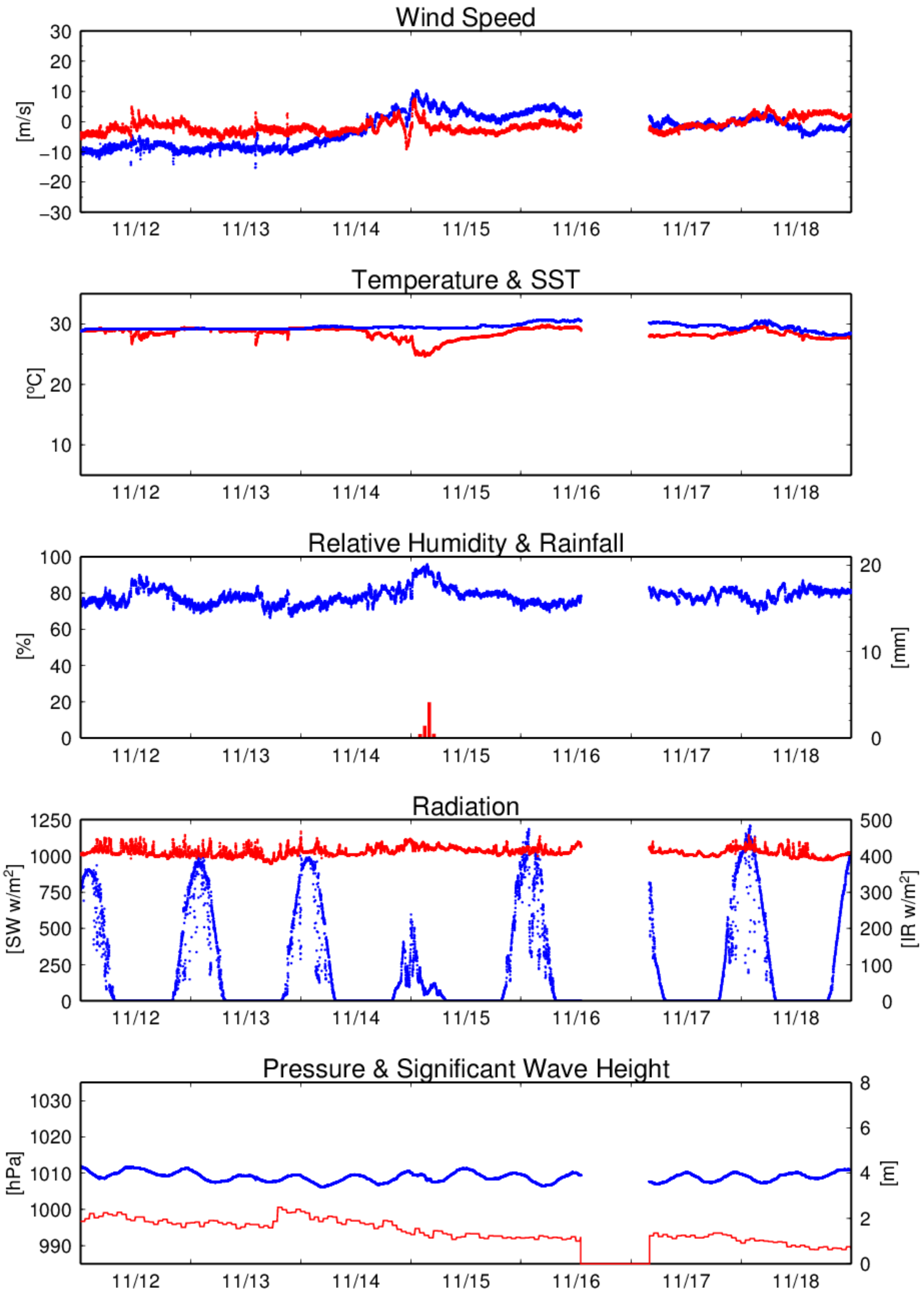

Fig. 2.3-1 (Continued)

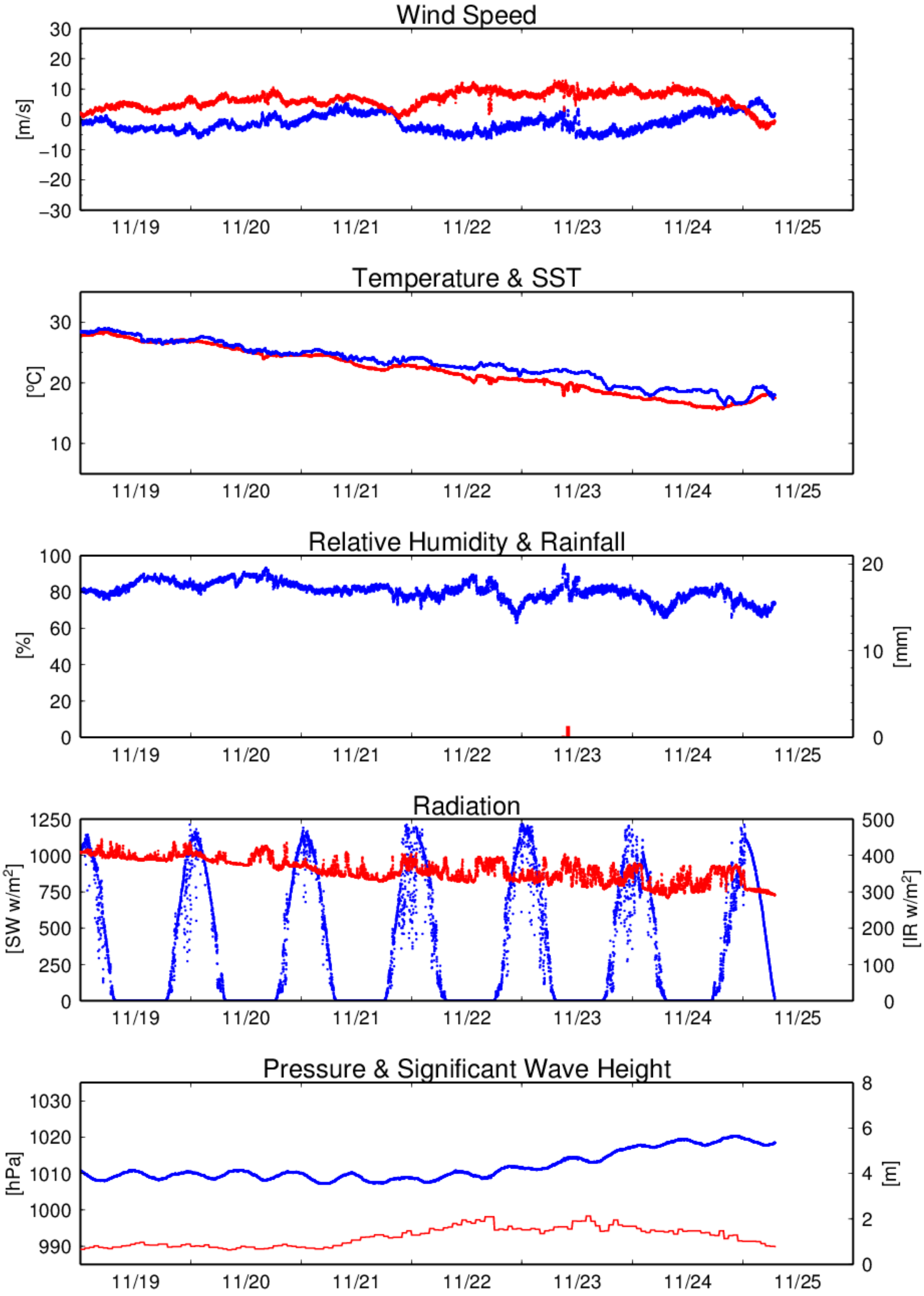

Fig. 2.3-1 (Continued)

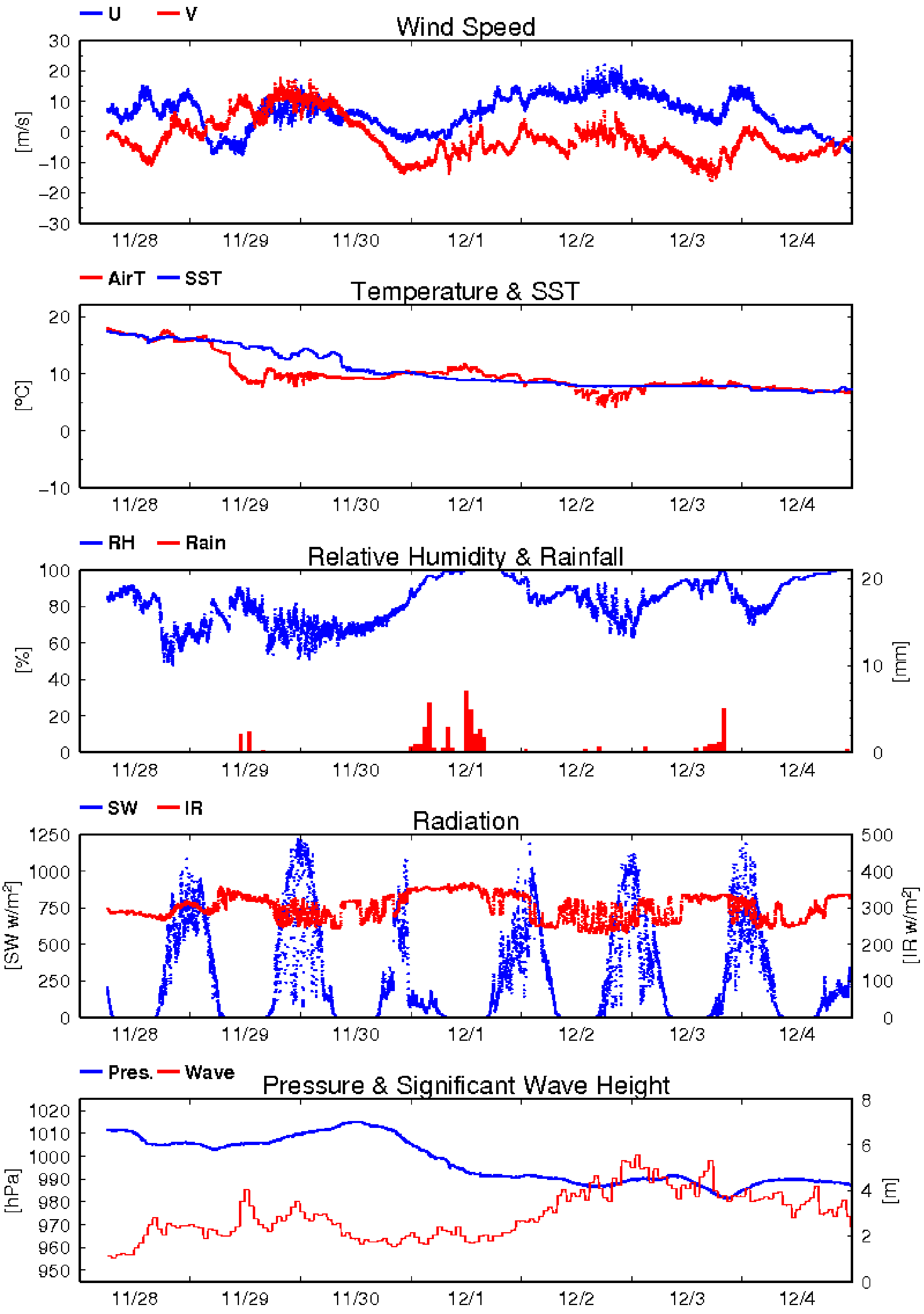

Fig. 2.3-2 Time series of surface meteorological parameters during the MR12-05 leg2 cruise

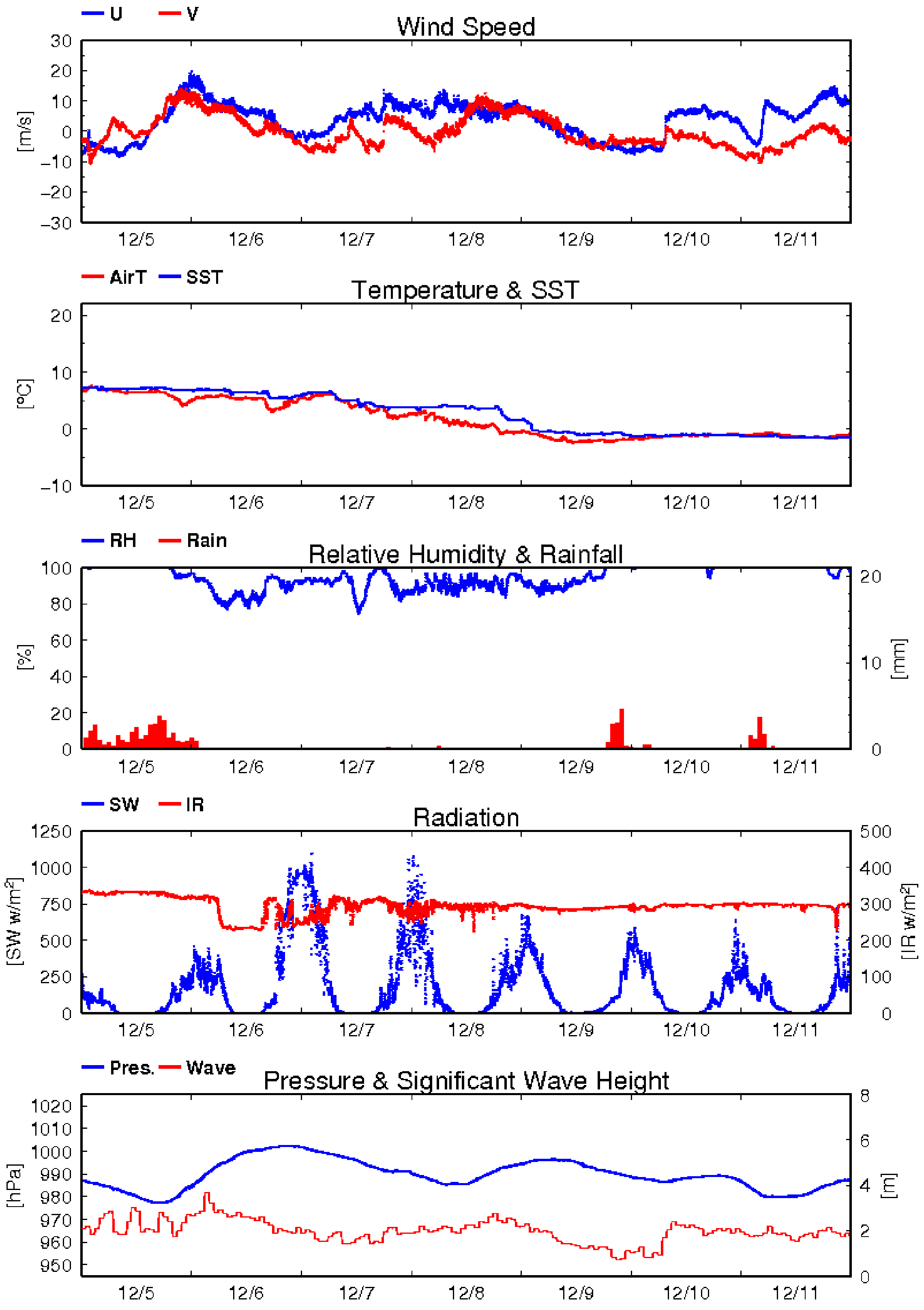

Fig. 2.3-2 (Continued)

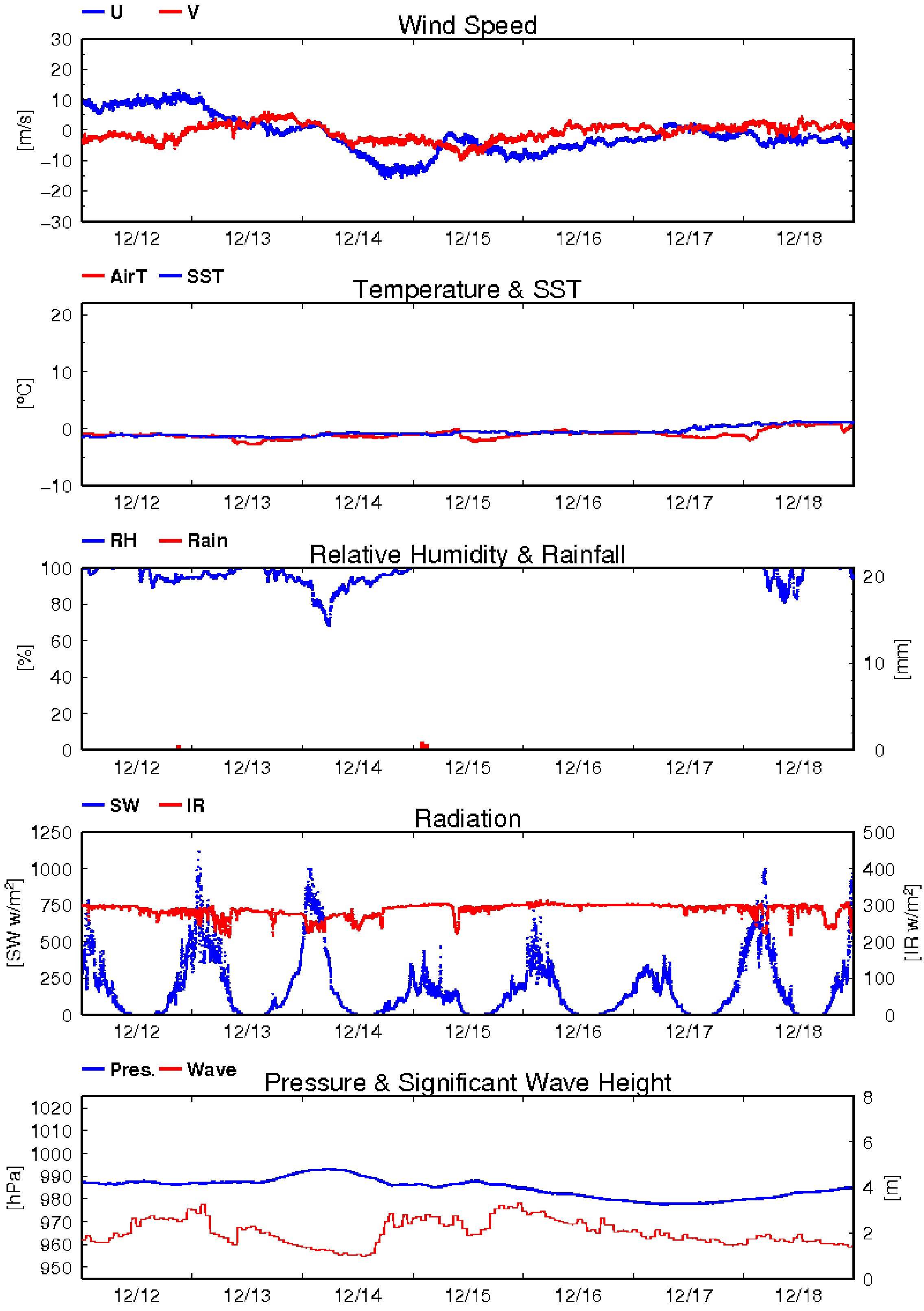

Fig. 2.3-2 (Continued)

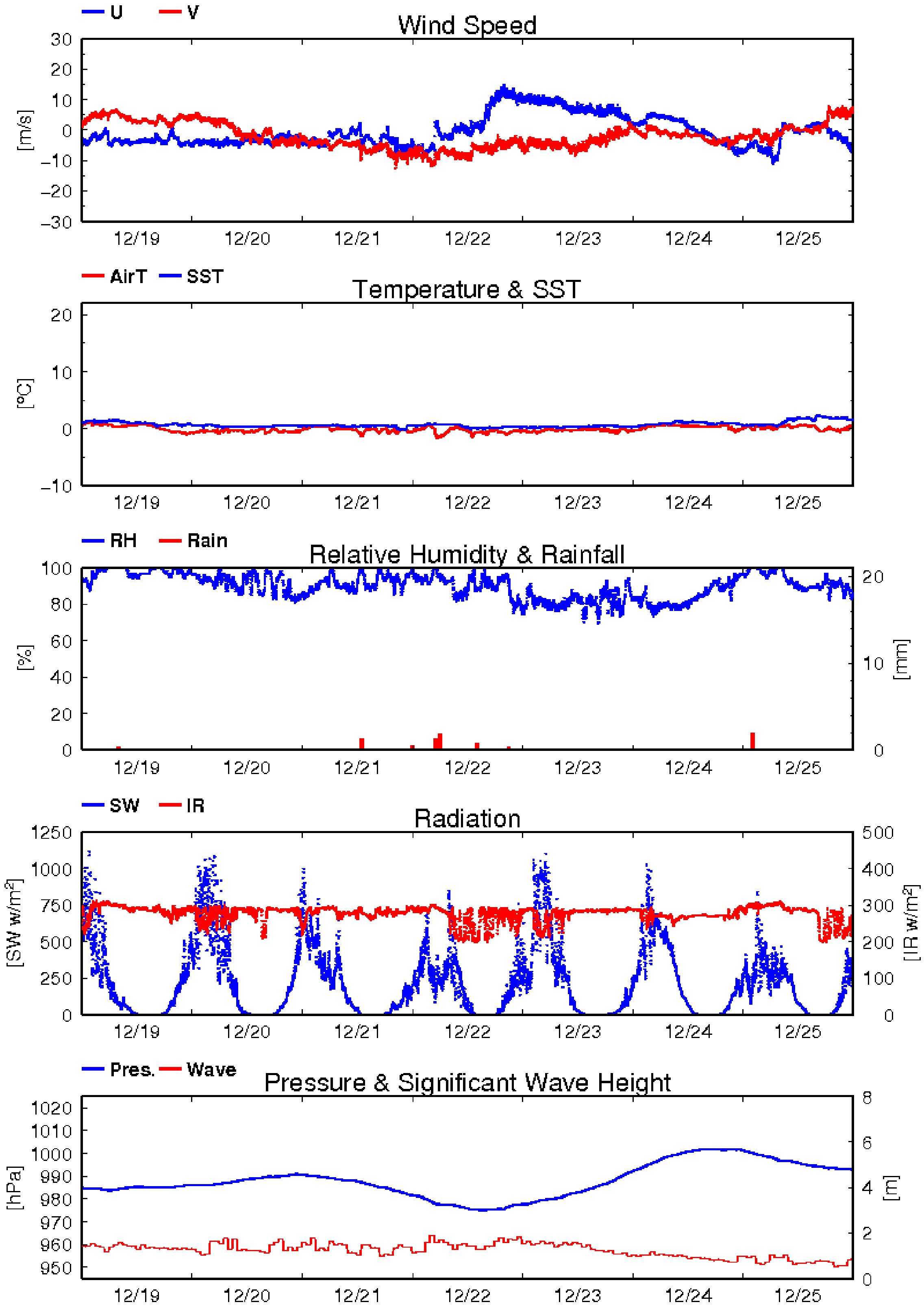

Fig. 2.3-2 (Continued)

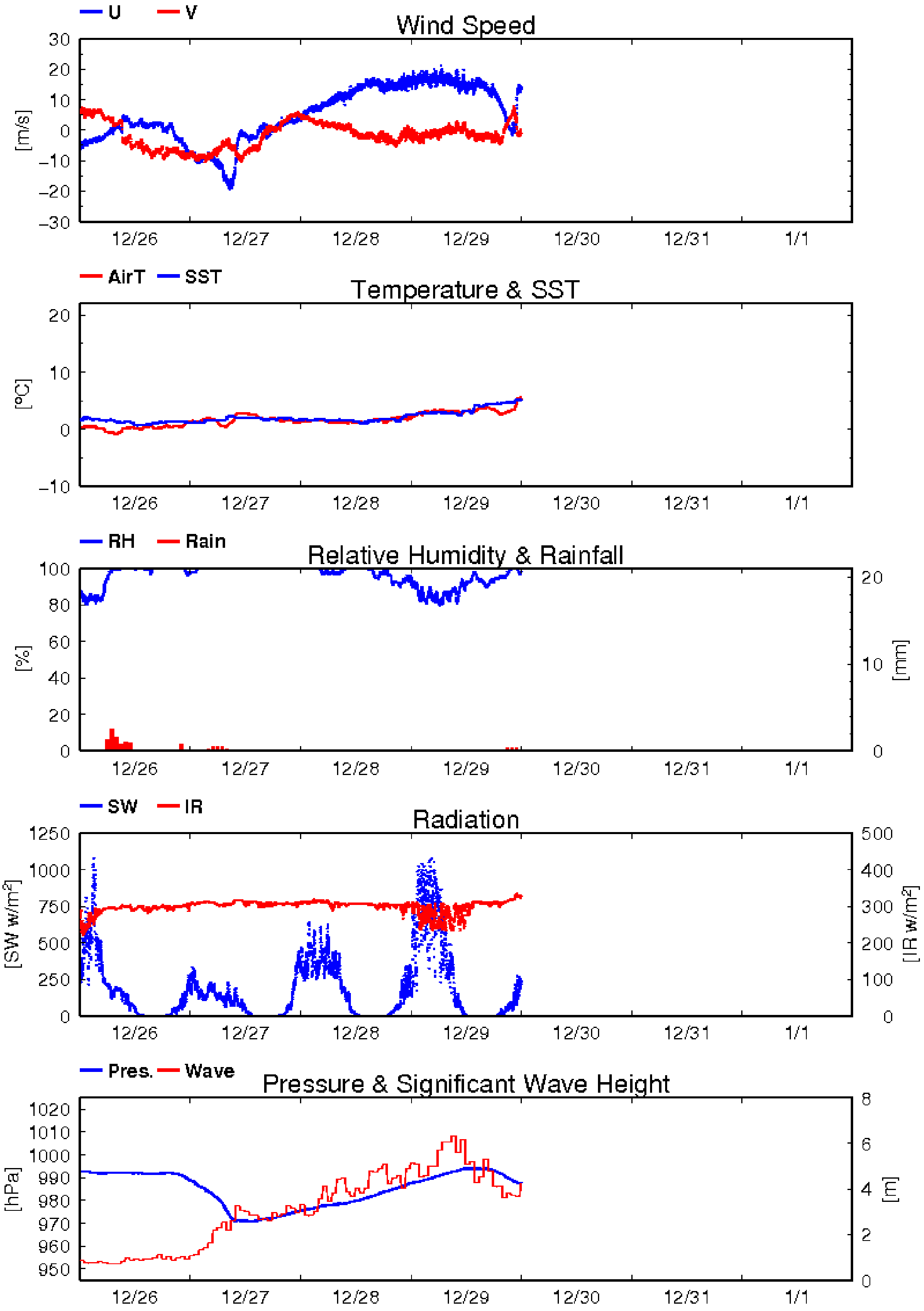

Fig. 2.3-2 (Continued)

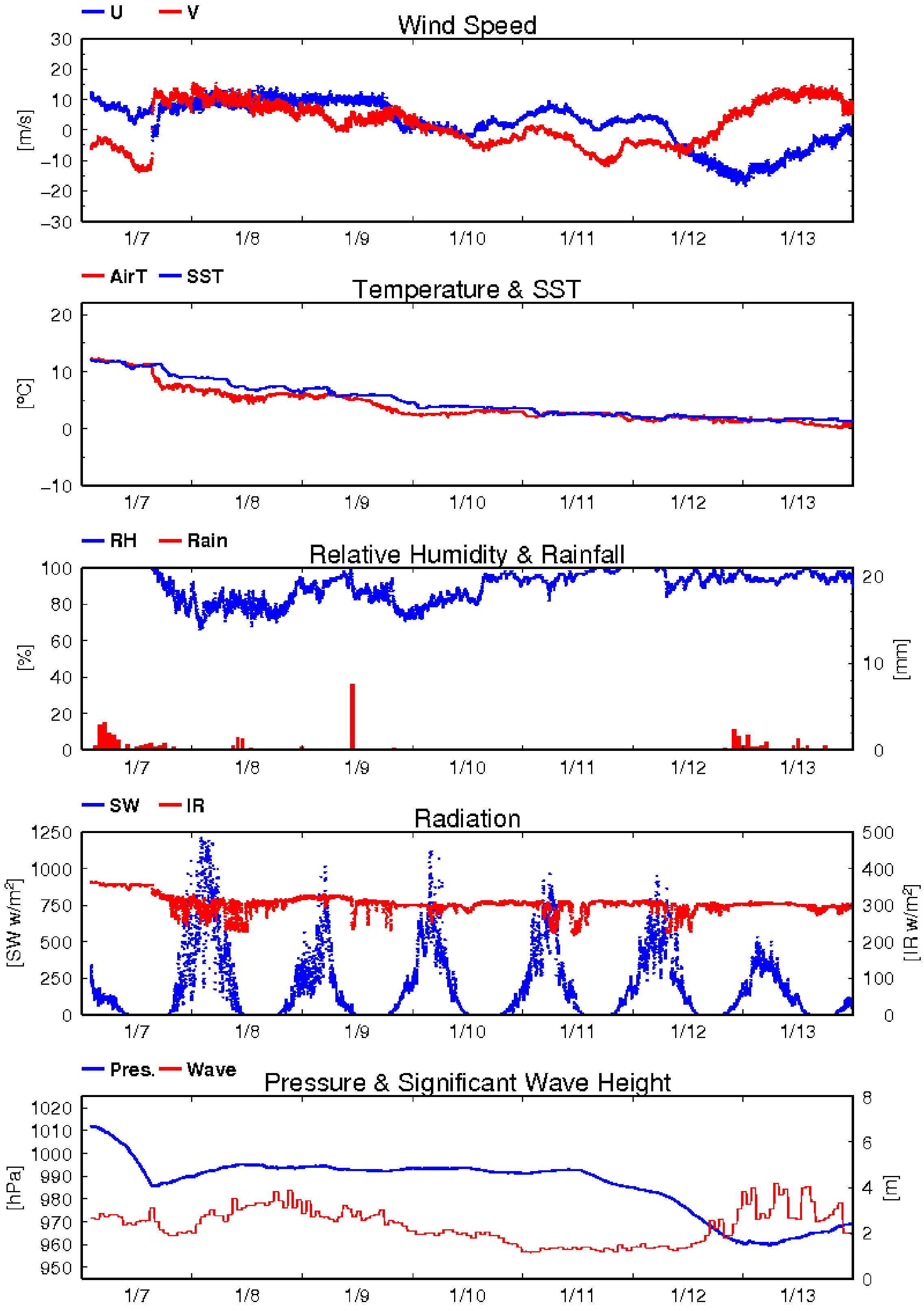

Fig. 2.3-3 Time series of surface meteorological parameters during the MR12-05 leg3 cruise

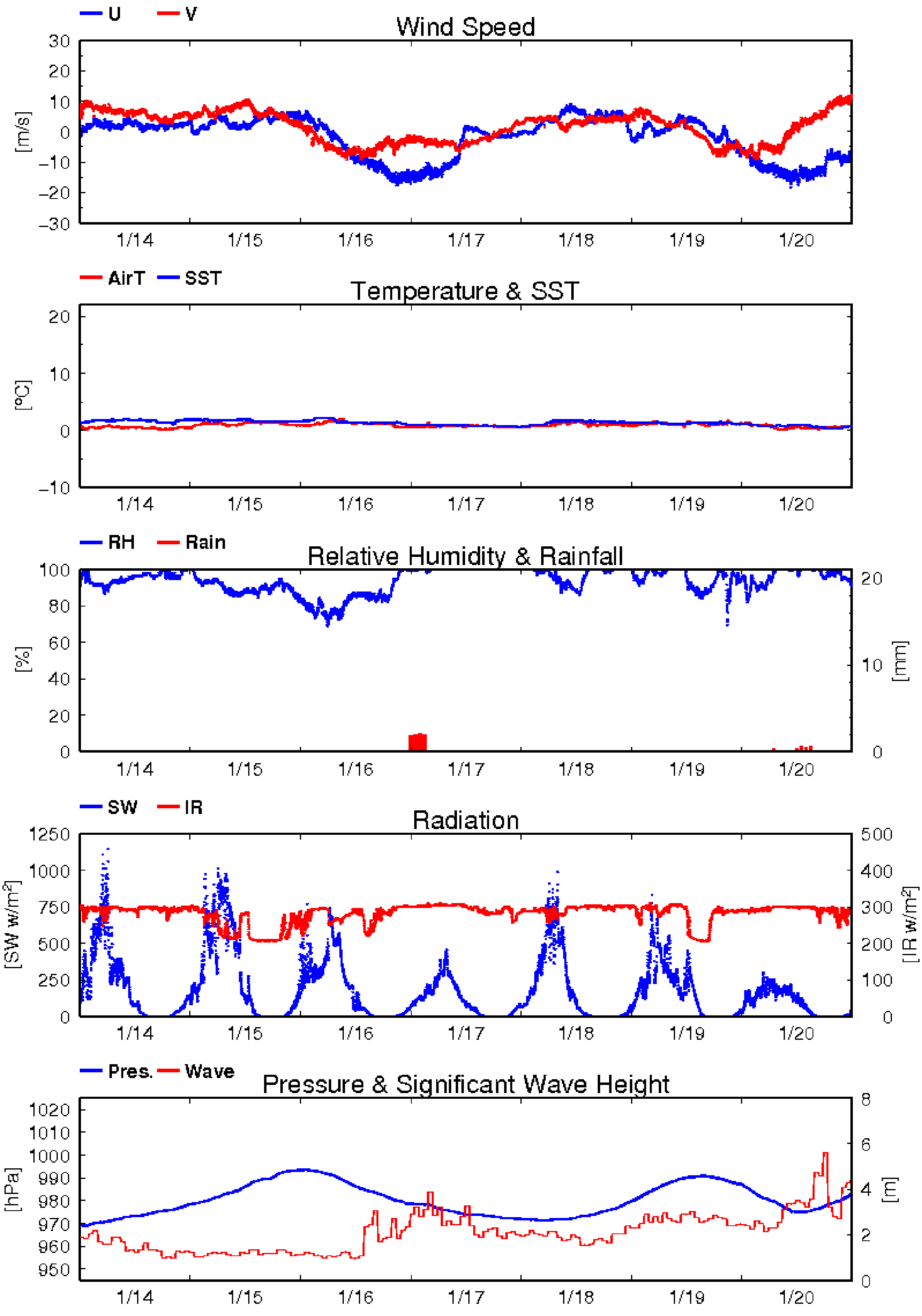

Fig. 2.3-3 (Continued)

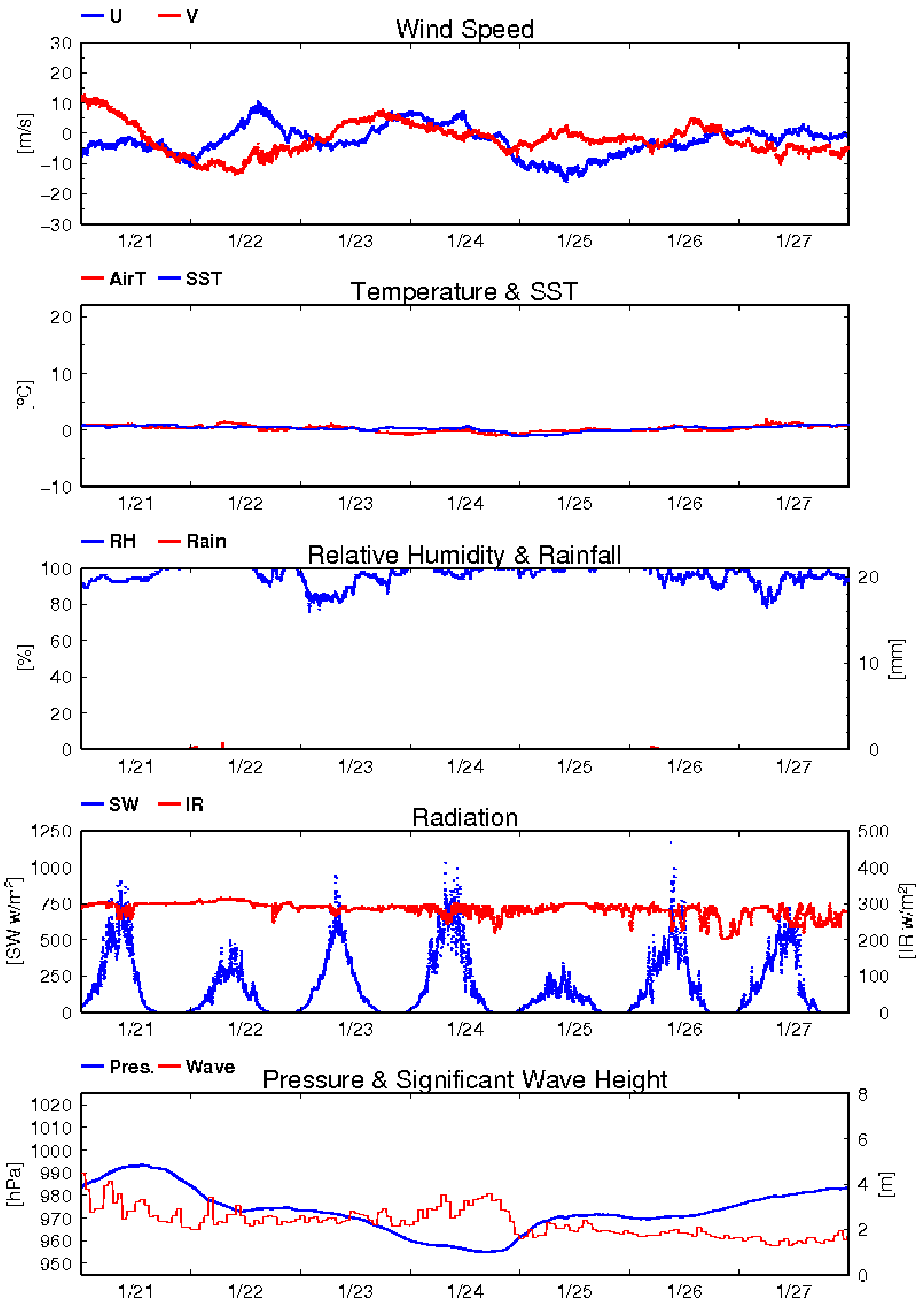

Fig. 2.3-3 (Continued)

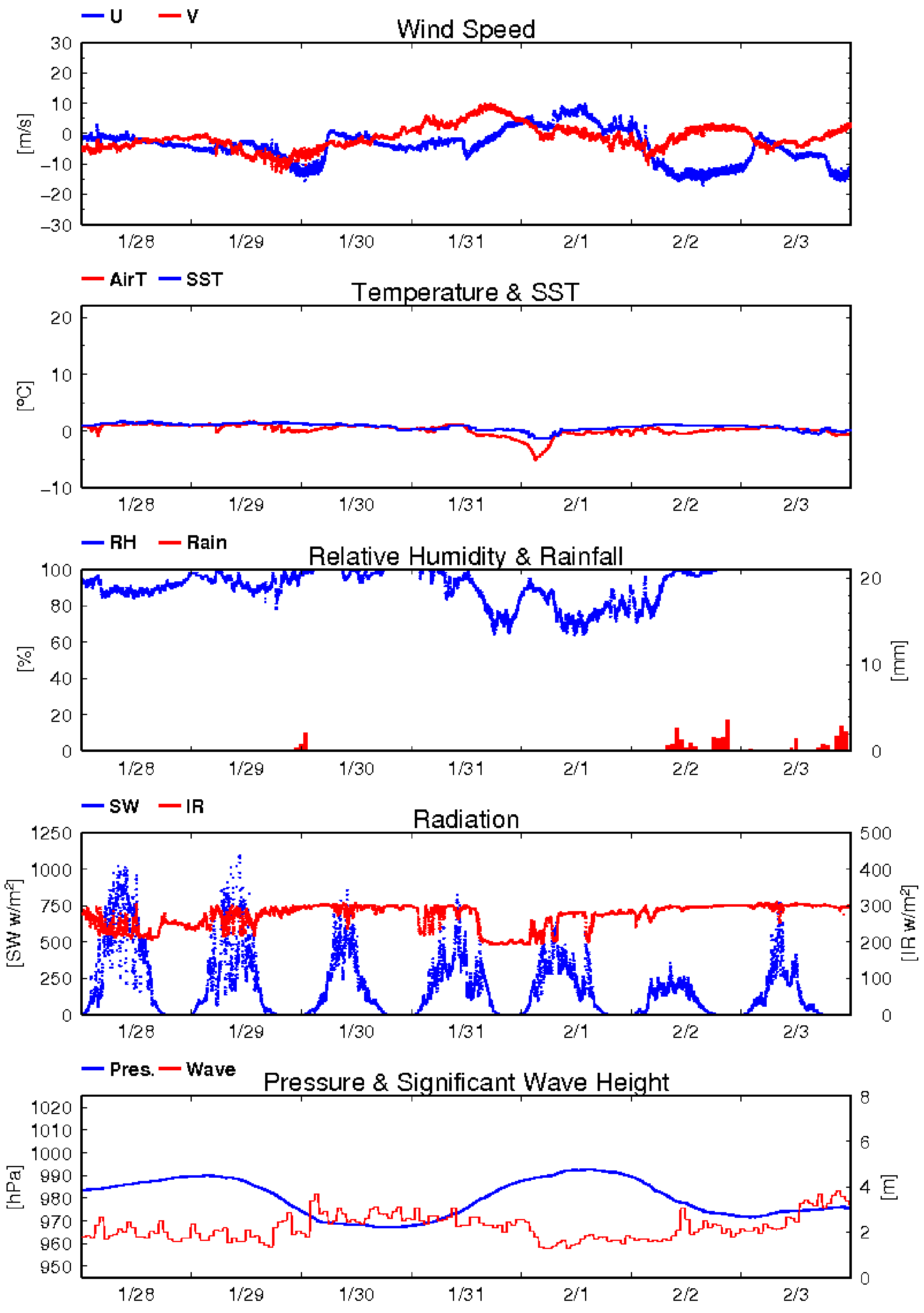

Fig. 2.3-3 (Continued)

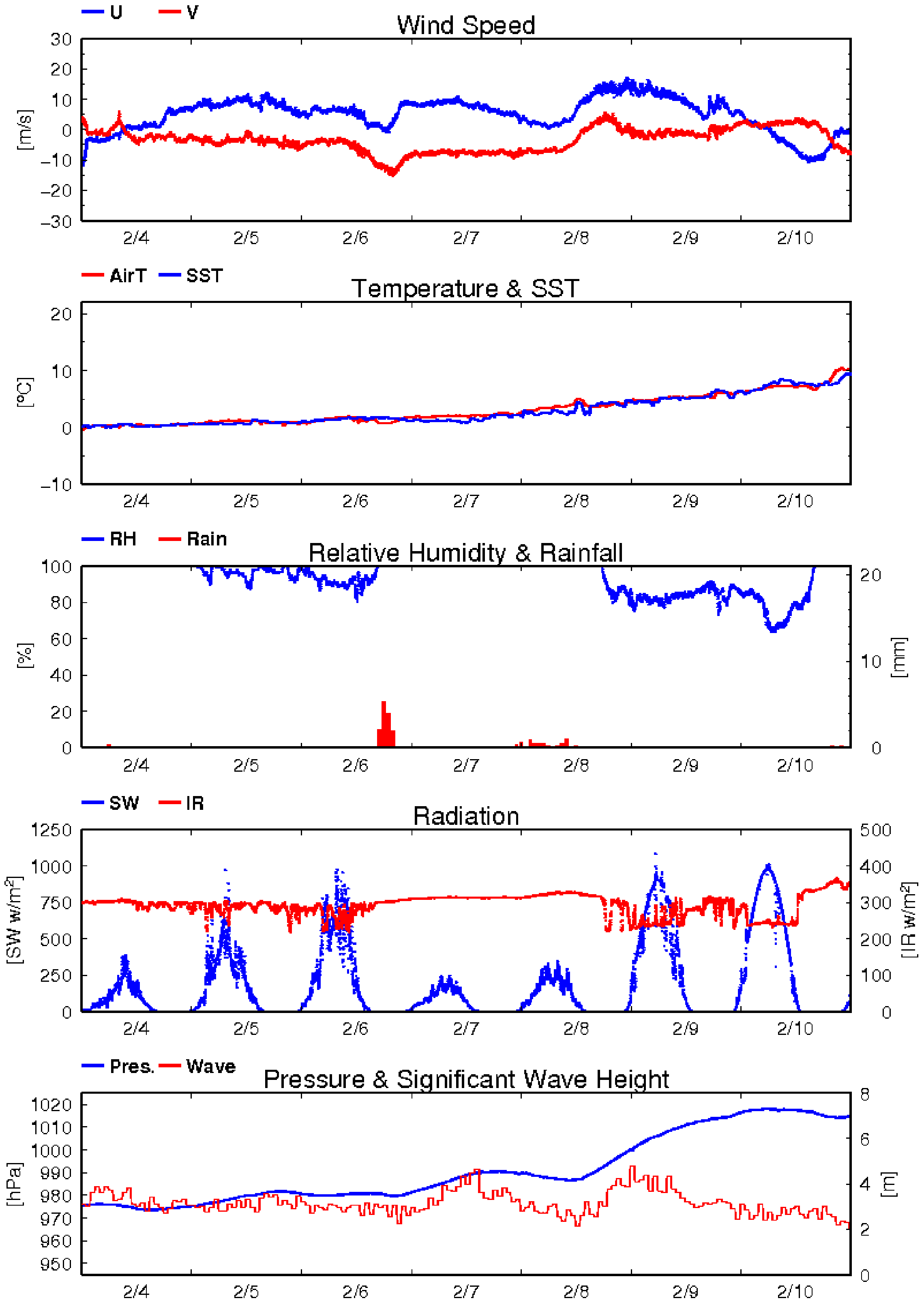

Fig. 2.3-3 (Continued)

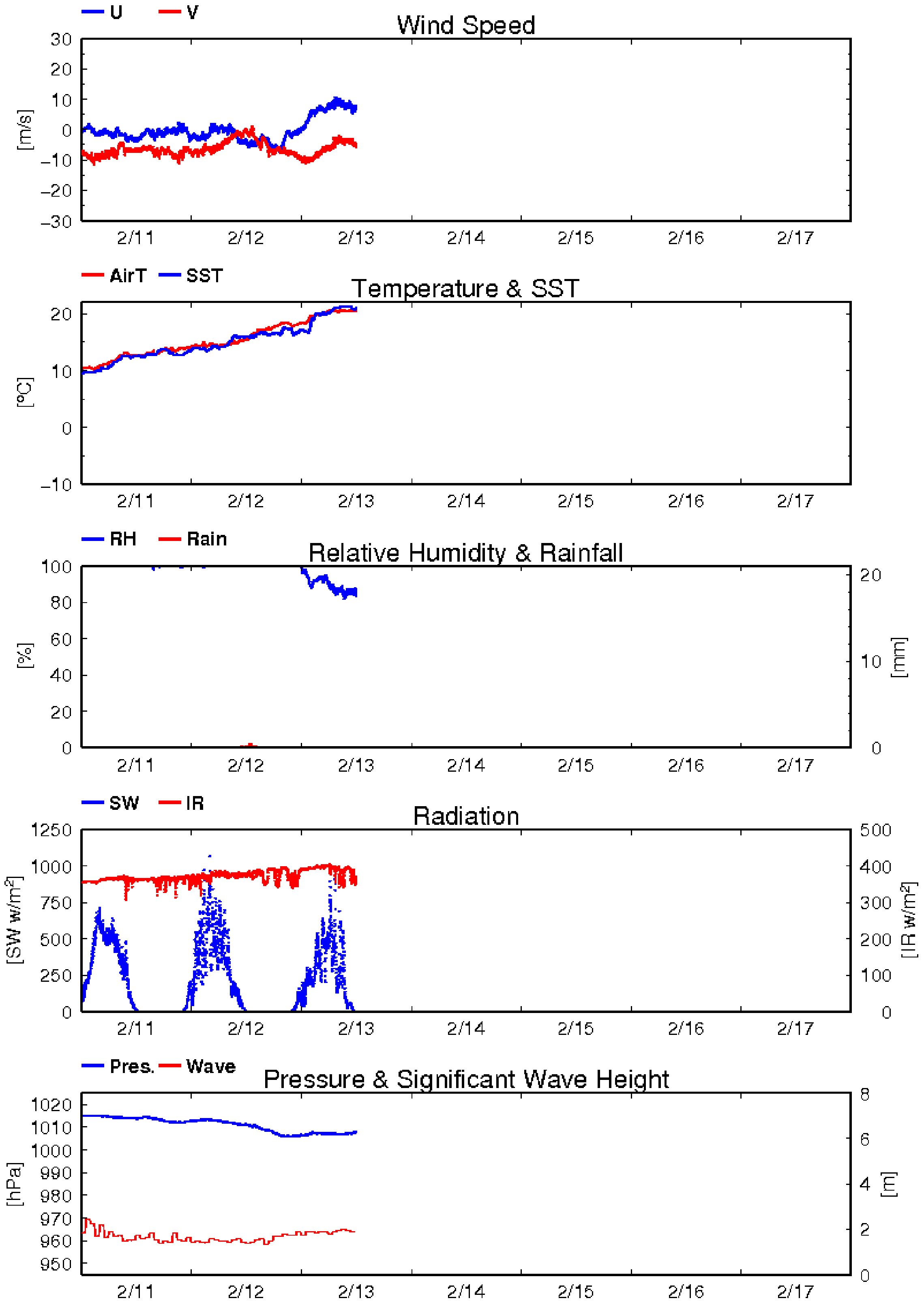

Fig. 2.3-3 (Continued)

.

2.4 Thermo-salinograph (TSG)

(1) Personnel

Hiroshi Uchida (JAMSTEC)
Kanako Yoshida (MWJ) (Legs 1, 3)
Misato Kuwahara (MWJ) (Legs 2, 3)
Keitaro Matsumoto (MWJ) (Leg 2)

(2) Objectives

The objective is to collect sea surface salinity, temperature, dissolved oxygen, and fluorescence data continuously along the cruise track.

(3) Materials and methods

The Continuous Sea Surface Water Monitoring System (Marine Works Japan Co, Ltd.) has six sensors and automatically measures salinity, temperature, dissolved oxygen, and fluorescence in sea surface water every one minute. This system is located in the sea surface monitoring laboratory and connected to shipboard LAN system. Measured data along with time and location of the ship were displayed on a monitor and stored in a desktop computer. The sea surface water was continuously pumped up to the laboratory from about 5 m water depth and flowed into the system through a vinyl-chloride pipe. The flow rate of the surface seawater was controlled to be 5 dm^3/min. Manufacturer's specifications of the each sensor in this system are listed below.

i. Software

Seamoni-kun Ver.1.30

ii. Sensors

Temperature and conductivity sensor

Model:	SBE-45, SEA-BIRD ELECTRONICS, INC.
Serial number:	4563325-0362
Measurement range:	Temperature –5 to 35 ºC
	Conductivity 0 to 7 S m^{-1}
Initial accuracy:	Temperature 0.002 ºC
	Conductivity 0.0003 S m^{-1}
Typical stability (per month):	Temperature 0.0002 ºC
	Conductivity 0.0003 S m^{-1}
Resolution:	Temperatures 0.0001 ºC
	Conductivity 0.00001 S m^{-1}

Bottom of ship thermometer

Model:	SBE 38, SEA-BIRD ELECTRONICS, INC.
Serial number:	3857820-0540

Measurement range: –5 to +35 ºC
Initial accuracy: ±0.001 ºC
Typical stability (per 6 month): 0.001 ºC
Resolution: 0.00025 ºC

Dissolved oxygen sensor
Model: OPTODE 3835, Aanderaa Data Instruments, AS.
Serial number: 985
Measuring range: 0 - 500 μmol L^{-1}
Resolution: < 1 μmol L^{-1}
Accuracy: < 8 μmol L^{-1} or 5% whichever is greater
Settling time (63%): < 25 s

Medel: RINKO-II, JFE Advantech Co. Ltd.
Serial number: 13

Fluorometer
Model: C3, TURNER DESIGNS
Serial number: 2300123

(4) Data Processing and Quality Control

Data from the Continuous Sea Surface Water Monitoring System were processed as follows. Data gaps were linearly interpolated when the gap was ≤ 7 minutes. Spikes in the temperature and salinity data were removed using a median filter with a window of 3 scans (3 minutes) when difference between the original data and the median filtered data was larger than 0.1 ºC for temperature and 0.5 for salinity. Fluorometer data were low-pass filtered using a median filter with a window of 3 scans (3 minutes) to remove spikes. Raw data from the RINKO oxygen sensor and the fluorometer data were low-pass filtered using a Hamming filter with a window of 15 scans (15 minutes).

Salinity (S [PSU]), dissolved oxygen (O [μmol/kg]) and fluorescence (Fl [RFU]) data were corrected using the water sampled data. Details of the measurement methods are described in Sections 3.2, 3.4, and 3.8 for salinity, dissolved oxygen and chlorophyll-a, respectively. Corrected salinity (S_{cor}), dissolved oxygen (O_{cor}), and estimated chlorophyll *a* (Chl-a) were calculated from following equations

$$S_{cor}\ [\mathrm{PSU}] = c_0 + c_1\, S + c_2\, t$$

$$O_{cor}\ [\mu\mathrm{mol/kg}] = c_0 + c_1\, O + c_2\, T + c_3\, t$$

$$\text{Chl-a}\ [\mu\mathrm{g/L}] = c_0 + c_1\, Fl$$

where t is days from a reference time, T is temperature in ºC. The best fit sets of calibration coefficients (c_0~c_3) were determined by a least square technique to minimize the deviation from the water sampled data. The reference times were listed in Table 2.4.1. The calibration coefficients were listed in Table 2.4.2. Comparisons between the Continuous Sea Surface Water Monitoring System data and water sampled data are shown in from Figs. 2.4.1 to 2.4.9. For fluorometer data, water sampled data obtained at night [PAR (Photosynthetically Available Radiation) < 50 μE/(m^2 sec), see Section

2.15] were used for the calibration, since sensitivity of the fluorometer to chlorophyll *a* is different at nighttime and daytime (Fig. 2.4.10). For leg 1, sensitivity of the fluorometer to chlorophyll *a* is also different at around Solomon Sea and other area. Therefore, slope (c_1) of the calibration coefficients was changed for each area (Table 2.4.2). For latitude between 14ºS and 13ºS, chlorophyll *a* was estimated from weighted mean of the two equations as

$$\text{Chl-a} = \text{Chl-a}_1\ f_1 + \text{Chl-a}_2\ f_2$$

$$f_1 = 1 - (\text{latitude}+14)$$

$$f_2 = 1 - f_1$$

where Chl-a1 is chlorophyll *a* calculated by using the set of coefficients A, and Chl-a_2 is chlorophyll *a* calculated by using the set of coefficients B (Table 2.4.2).

Table 2.4.1. Reference time used in the calibration equations for salinity and dissolved oxygen.

Leg	Date	Time (UTC)
1	2012/11/06	08:09
2	2012/11/28	06:00
3	2013/01/07	02:00

Table 2.4.2. Calibration coefficients for the salinity, dissolved oxygen, and chlorophyll *a*.

	Leg	c0	c1	c2	c3
Salinity					
	1	-8.264243e-04	1.000025	-3.094205e-06	
	2	-4.901493e-04	1.000014	-8.007142e-08	
	3	4.116161e-04	0.9999879	1.490024e-07	
Dissolved oxygen					
	1	8.682632e-03	0.9999764	-1.111354e-04	-3.665007e-05
	2	9.983204e-03	0.9999737	-1.391134e-04	-3.103317e-05
	3	-1.566883e-02	1.000044	2.854348e-04	8.284769e-06
Chlorophyll a					
	1	5.352958e-02	0.1296275 (A: for latitude ≤ 14ºS or latitude ≥ 5ºS)		
		5.352958e-02	0.3467123 (B: for latitude > 13ºS and latitude < 5ºS)		
	2	0.1141853	5.968889e-02		
	3	1.445487e-02	5.716477e-02		

.

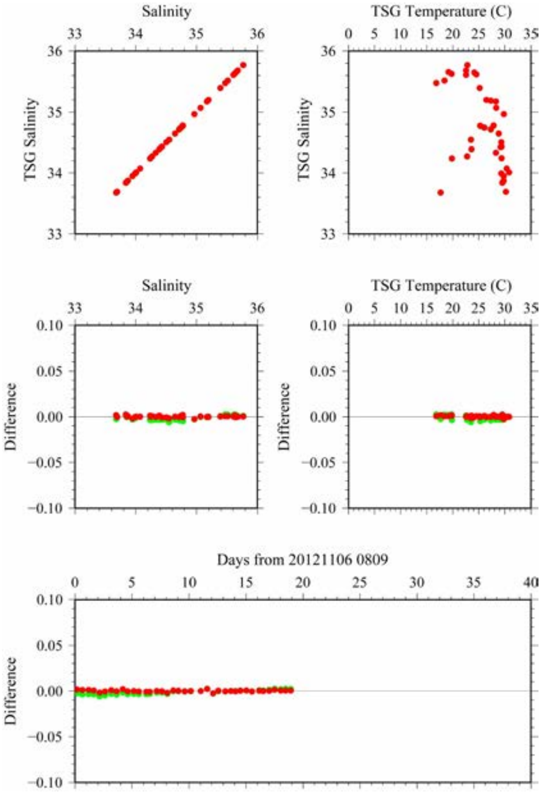

Figure 2.4.1. Comparison between TSG salinity (green: before correction, red: after correction) and sampled salinity for leg 1.

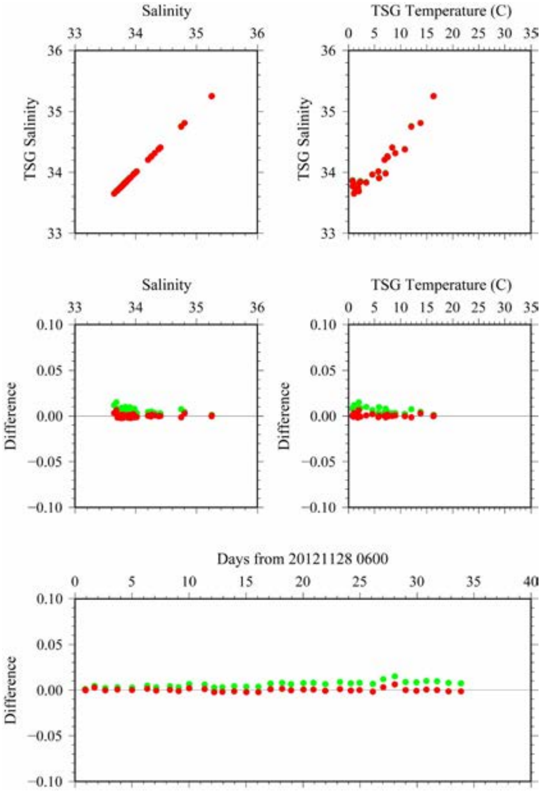

Figure 2.4.2. Same as Fig. 2.4.1, but for leg 2.

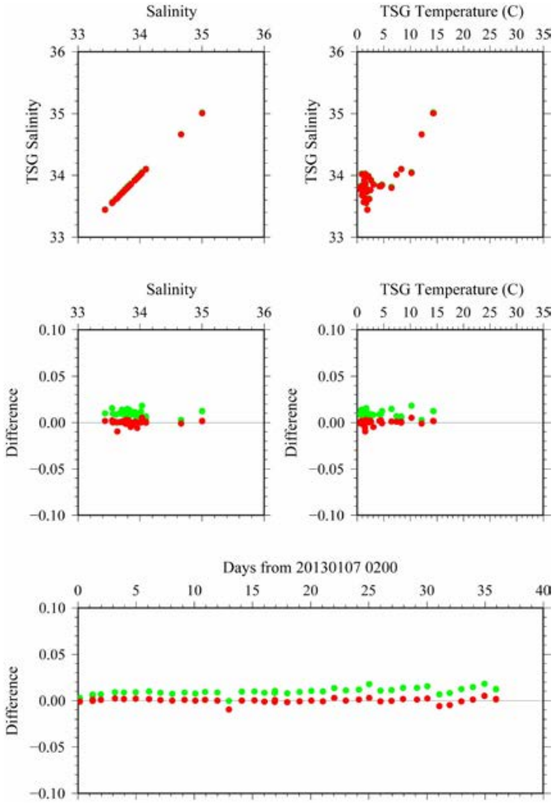

Figure 2.4.3. Same as Fig. 2.4.1, but for leg 3.

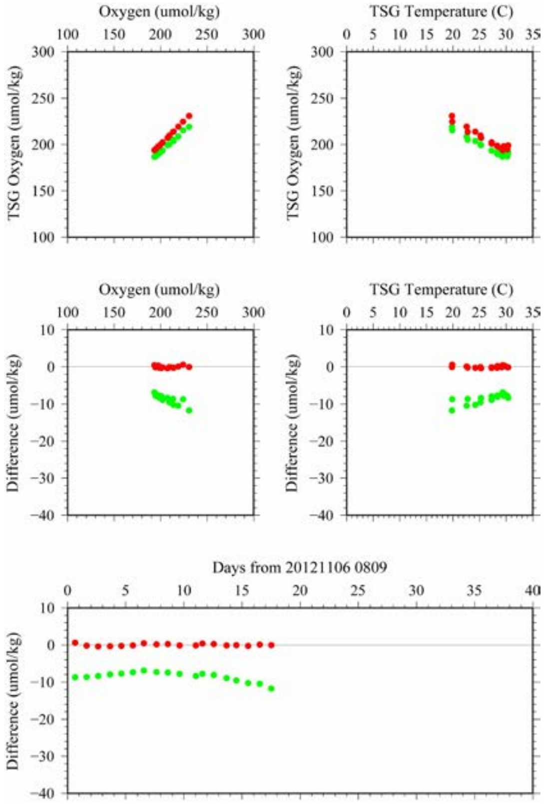

Figure 2.4.4. Comparison between TSG oxygen (green: before correction, red: after correction) and sampled oxygen for leg 1.

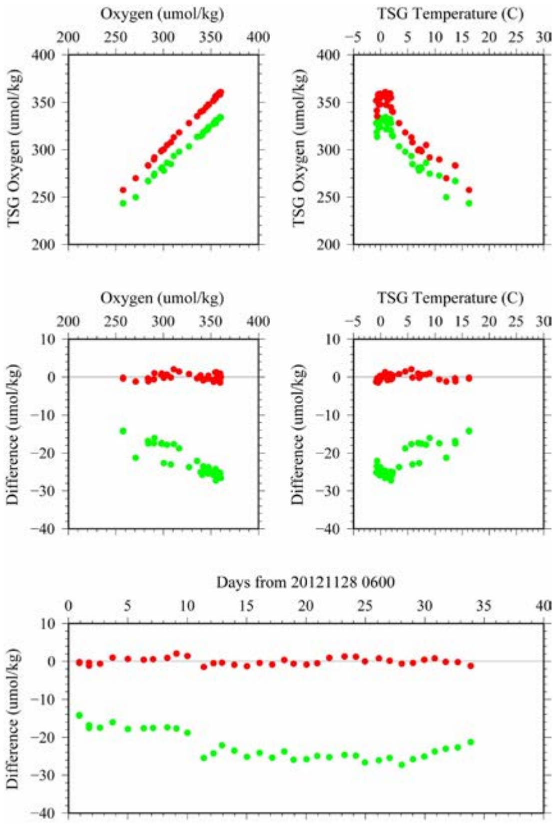

Figure 2.4.5. Same as Fig. 2.4.4, but for leg 2.

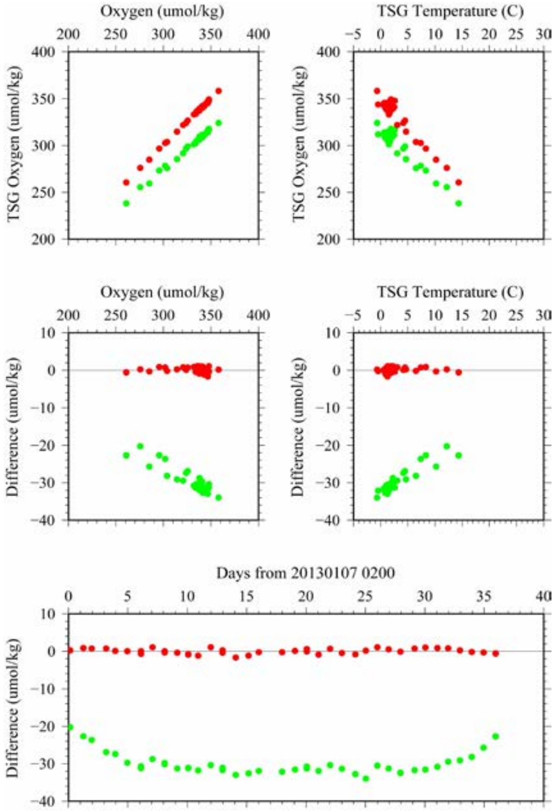

Figure 2.4.6. Same as Fig. 2.4.4, but for leg 3.

.

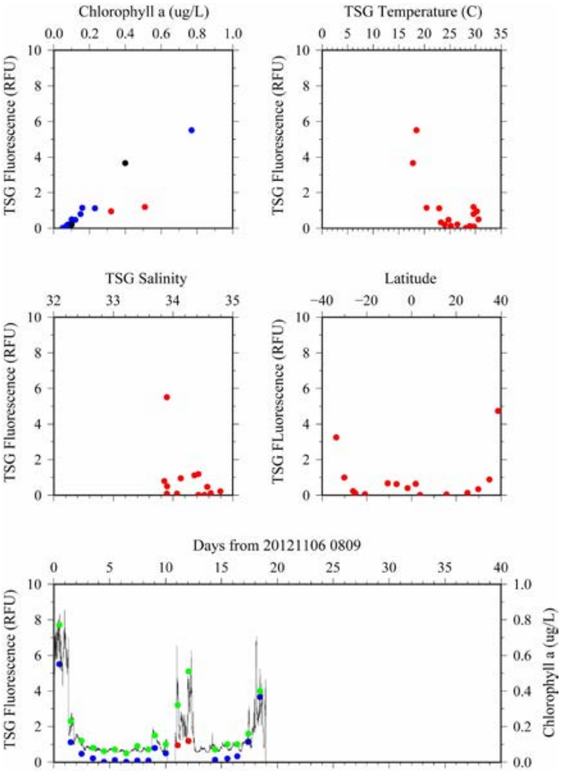

Figure 2.4.7. Comparison between TSG fluorescence and sampled chlorophyll *a* for leg 1. Black dots indicate the daytime data. For bottom panel, blue or red dots indicate fluorescence and green dots indicate water sampled chlorophyll *a*. Line indicates chlorophyll *a* estimated from fluoremeter.

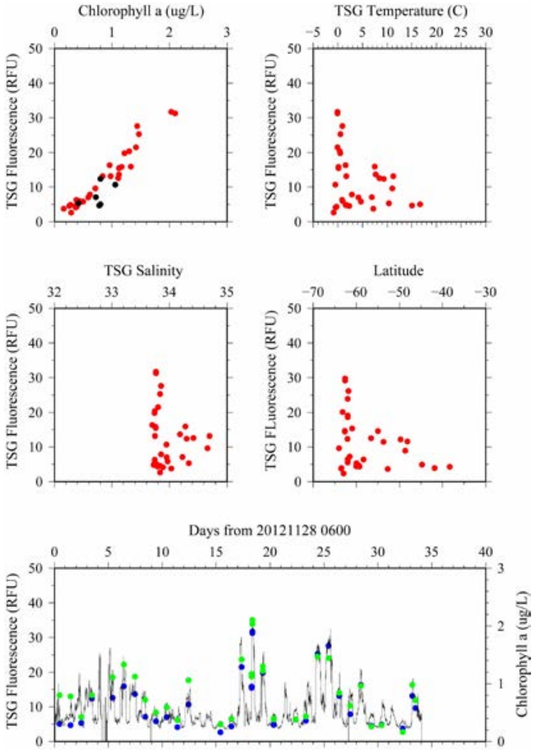

Figure 2.4.8. Same as Fig. 2.4.7, but for leg 2.

.

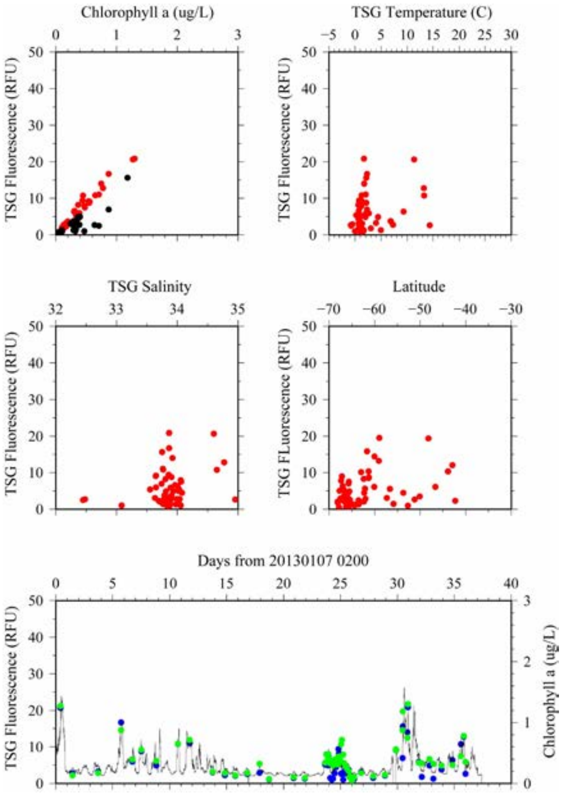

Figure 2.4.9. Same as Fig. 2.4.7, but for leg 3.

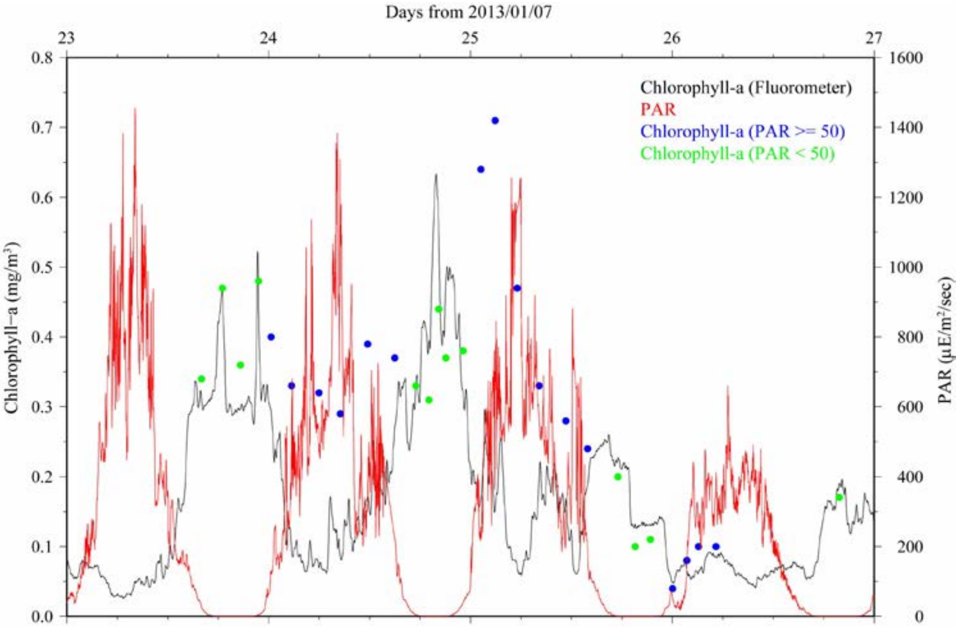

Figure 2.4.10. Diurnal variation of the chlorophyll *a* estimated from the fluorometer. Water sampled chlorophyll *a* (blue and green dots) does not show such diurnal variation.

.

2.5 pCO_2

(1) Personnel

Akihiko Murata (JAMSTEC)
Yoshiko Ishikawa (MWJ)
Atsushi Ono (MWJ)
Keisuke Obata (MWJ)

(2) Objective

Concentrations of CO_2 in the atmosphere are now increasing at a rate of about 2.0 ppmv y^{-1} owing to human activities such as burning of fossil fuels, deforestation, and cement production. It is an urgent task to estimate as accurately as possible the absorption capacity of the oceans against the increased atmospheric CO_2, and to clarify the mechanism of the CO_2 absorption, because the magnitude of the anticipated global warming depends on the levels of CO_2 in the atmosphere, and because the ocean currently absorbs 1/3 of the 6 Gt of carbon emitted into the atmosphere each year by human activities.

The Southern Ocean is one of the regions where uncertainty of uptake of anthropogenic CO_2 is large. In this cruise, therefore, we were aimed at quantifying how much anthropogenic CO_2 were absorbed in the surface ocean in the Indian sector of the Southern Ocean. For the purpose, we measured pCO_2 (partial pressure of CO_2) in the atmosphere and surface seawater along the WHP P14S and S04I lines at 174E and 65°S, respectively, in the Southern Ocean.

(3) Apparatus

Concentrations of CO_2 in the atmosphere and the sea surface were measured continuously during the cruise using an automated system with a non-dispersive infrared (NDIR) analyzer (Li-COR LI-7000). The automated system (Nippon ANS) was operated by about one and a half hour cycle. In one cycle, standard gasses, marine air and an air in a headspace of an equilibrator were analyzed subsequently. The nominal concentrations of the standard gas were 271, 331, 362 and 421 ppmv. The standard gases will be calibrated after the cruise.

The marine air taken from the bow was introduced into the NDIR by passing through a mass flow controller, which controlled the air flow rate at about 0.6 – 0.8 L/min, a cooling unit, a perma-pure dryer (GL Sciences Inc.) and a desiccant holder containing $Mg(ClO_4)_2$.

A fixed volume of the marine air taken from the bow was equilibrated with a stream of seawater that flowed at a rate of 4.0 – 5.0 L/min in the equilibrator. The air in the equilibrator was circulated with a pump at 0.7-0.8L/min in a closed loop passing through two cooling units, a perma-pure dryer (GL Science Inc.) and a desiccant holder containing $Mg(ClO_4)_2$.

(4) Results

Concentrations of CO_2 (xCO_2) of marine air and surface seawater are shown in Fig. 2.5.1, together with SST.

.

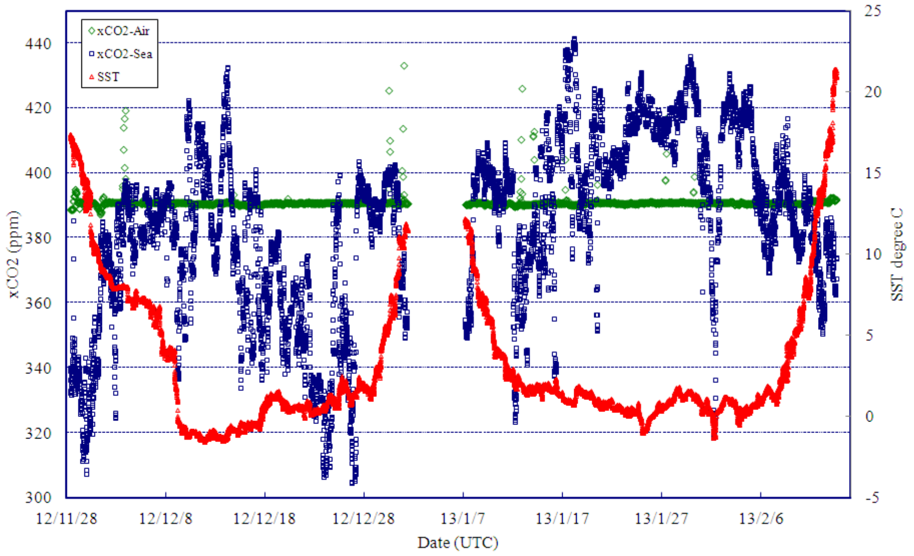

Fig. 2.5.1. Preliminary results of concentrations of CO_2 (xCO_2) in atmosphere (green) and surface seawater (blue), and SST (red) observed during (a) leg 2 and (b) leg 3 of MR12-05.

.

2.6 pCO_2 and pCH_4 by CRDS

(1) Personnel

Sohiko Kameyama (Hokkaido University/ Principal Investigator)
Hisayuki Yoshikawa-Inoue (Hokkaido University)
Masao Ishii (Meteorological Research Institute / JMA)
Daisuke Sasano (Meteorological Research Institute / JMA)
Akihiko Murata (JAMSTEC)

(2) Objective

The oceans have strong interactions with the atmosphere and are the major sinks for the increasing CO_2. Takahashi et al. (2009) estimated CO_2 sink flux over the Southern Ocean as −0.06 PgC y^{-1} and the flux is significantly smaller than that estimated on the basis of the earlier database by Takahashi et al. (2002) as −0.34 PgC y^{-1}. This is attributed primarily to the improved database. Although the Southern Ocean is one of the important regions to uptake atmospheric CO_2, the frequency of data seems not to be still enough. Furthermore, it is known that polar region face the risk of ocean acidification stronger than the other regions (Orr et al., 2005). Therefore, the highly frequent measurement of CO_2 is required to address the issues in the Southern Ocean.

Recently, a new CO_2 analyzer WS-CRDS (Picarro) was developed on the basis of Cavity Ring-Down Spectroscopy. The advantage of this analyzer is a high precision and stability. In addition, the analyzer can simultaneously measure other trace gases such as CH_4. CH_4 is the second biggest contributor to global warming. Many studies have paid attention to distribution and the production pathway of CH_4 dissolved in seawater (e.g., Oremland, 1979; Marty, 1993; Karl and Tilbrook, 1994; Sasakawa et al., 2008), however almost all of the studies obtained not continuous and real-time dataset but discrete dataset so far. In this study, we challenge to apply WS-CRDS to the underway measurements of pCO_2 and pCH_4 in the atmosphere and in surface seawater to clarify the distributions of pCO_2 and pCH_4 and their controlling mechanisms in the Southern Ocean.

(3) Parameters

CO_2 partial pressure (pCO_2) in the atmosphere and in near-surface seawater
CH_4 partial pressure (pCH_4) in the atmosphere and in near-surface seawater

(4) Instruments and Methods

We made simultaneous measurements of the CO_2 and CH_4 concentrations in the dry air equilibrated with the great excess of surface seawater during the whole cruise using an automated measuring system (Nippon ANS Co.). Seawater was taken continuously from the sea chest located ca.4.5 m below the sea level and introduced into the MRI-shower-type equilibrator (Yoshikawa-Inoue and Ishii, 2005). Wavelength-scanned cavity ring-down spectrometer (WS-CRDS, Picarro, G2301) was used as a detector. We used three standard gases with known CO_2 and CH_4 mixing ratios once a day. Corrections for the temperature-rise from the sea chest to the equilibrator are also to be made. Partial pressure of CO_2 and CH_4 will be calculated from the concentration of CO_2 and CH_4 by taking the water vapor pressure and the atmospheric pressure into account.

We also took discrete samples from the same seawater stream and Niskin bottle of 5-m depth for CH_4 concentration measurements to confirm the equilibration degree with the conventional equilibrator. Seawater was introduced into the 120-mL glass vial bottle and overflowed more than twice of the volume to avoid the contamination of CH_4 in the lab air. After sampling, a 0.5-ml saturated solution of mercuric chloride ($HgCl_2$) was added to prohibit biological activities in the bottle, then it was sealed up with rubber cap and aluminum seal immediately. The samples were stored in the fridge.

(5) Observation log

The shipboard continuous measurements were conducted during the entire cruise. The discrete samplings from both underway seawater stream and Niskin bottle were held once a day during leg. 2 of the cruise and totaled 49 samples.

(6) Data archives

These data obtained in this cruise will be analyzed by the member of JMA. The discrete CH_4 samples will be measured in the laboratory. All data will be opened within a year.

(7) References

Karl, D. M., and B. D. Tilbrook (1994) Production and transport of methane in oceanic particulate organic matter, *Nature*, *368*, 732–734.

Marty, D. G.. (1993), Methanogenic bacteria in seawater, *Limnol. Oceanogr.*, *38*, 452–456.

Oremland, R. S. (1979), Methanogenic activity in plankton samples and fish intestines: a mechanism for in situ methanogenesis in oceanic surfacewaters, *Limnol. Oceanogr.*, *24*, 1136–1141.

Orr, J. C., et al. (2005), Anthropogenic ocean acidification over the twenty first century and its impact on calcifying organisms, *Nature*,*437*, 681–686.

Sasakawa, M., U. Tsunogai, S. Kameyama, F. Nakagawa, Y. Nojiri, and A. Tsuda (2008), Carbon isotopic characterization for the origin of excess methane in subsurface seawater, *J. Geophys. Res.*, *113*, C03012.

Takahashi, T., et al. (2002), Global sea-air CO_2 flux based on climatological surface ocean pCO_2, and seasonal biological and temperature effects, *Deep Sea Res. II*, *49*, 1601–1622.

Takahashi, T., et al. (2009), Climatological mean and decadal change in surface ocean $p$$CO_2$, and net sea-air CO_2 flux over the global oceans, *Deep Sea Res. Part II*, *56*, 554–577.

Yoshikawa-Inoue, H., and M. Ishii (2005), Variations and trends of CO_2 in the surface seawater in the Southern Ocean south of Australia between 1969 and 2002, *Tellus*, *57B*, 58–69.

.

2.7 Ceilometer

(1) Personnel

Souichiro Sueyoshi	***(Global Ocean Development Inc., GODI)***	***-leg1, leg3-***
Koichi Inagaki	***(GODI)***	***-leg1, leg3-***
Kazuho Yoshida	***(GODI)***	***-leg2-***
Shinya Okumura	***(GODI)***	***-leg2-***
Masanori Murakami	***(GODI)***	***-leg2-***
Katsuhisa Maeno	***(GODI)***	***-leg3-***
Ryo Kimura	***(MIRAI Crew)***	***-leg1, leg2-***
Ryo Ohyama	***(MIRAI Crew)***	***-leg3-***

(2) Objectives

The information of cloud base height and the liquid water amount around cloud base is important to understand the process on formation of the cloud. As one of the methods to measure them, the ceilometer observation was carried out.

(3) Parameters

1. Cloud base height [m].
2. Backscatter profile, sensitivity and range normalized at 30 m resolution.
3. Estimated cloud amount [oktas] and height [m]; Sky Condition Algorithm.

(4) Methods

We measured cloud base height and backscatter profile using ceilometer (CT-25K, VAISALA, Finland). Major parameters for the measurement configuration are shown in Table 2.14-1;

Table 2.7-1 Major parameters

Laser source:	Indium Gallium Arsenide (InGaAs) Diode
Transmitting center wavelength:	905±5 nm at 25 degC
Transmitting average power:	8.9 mW
Repetition rate:	5.57 kHz
Detector:	Silicon avalanche photodiode (APD) Responsibility at 905 nm: 65 A/W
Measurement range:	0 ~ 7.5 km
Resolution:	50 ft in full range
Sampling rate:	60 sec
Sky Condition:	0, 1, 3, 5, 7, 8 oktas (9: Vertical Visibility)

(0:Sky Clear, 1:Few, 3:Scattered, 5,7:Broken, 8:Overcast)

On the archive dataset, cloud base height and backscatter profile are recorded with the resolution of 30 m (100 ft).

(5) Preliminary results

Fig.2.7-1, Fig.2.7-2 and Fig.2.7-3 show the time series of 1st, 2nd and 3rd lowest cloud base height during the cruise.

(6) Data archives

The raw data obtained during this cruise will be submitted to the Data Management Group (DMG) of JAMSTEC.

(7) Remarks (Times in UTC)

1) The following periods, the observation was carried out.

Leg1: 00:00, 05 Nov. 2012 - 15:00, 16 Nov. 2012
03:00, 17 Nov. 2012 - 07:00, 25 Nov. 2012
Leg2: 06:00, 28 Nov. 2012 - 07:00, 01 Jan. 2013
Leg3: 02:00, 07 Jan. 2013 - 12:00, 13 Feb 2013

2) The following time, the window was cleaned.

23:20, 05 Nov. 2012
23:20, 12 Nov. 2012
23:20, 18 Nov. 2012
21:28, 04 Dec. 2012
22:43, 09 Dec. 2012
22:57, 18 Dec. 2012
01:48, 10 Jan. 2013
01:58, 16 Jan. 2013
02:45, 23 Jan. 2013
01:30, 05 Feb. 2013

.

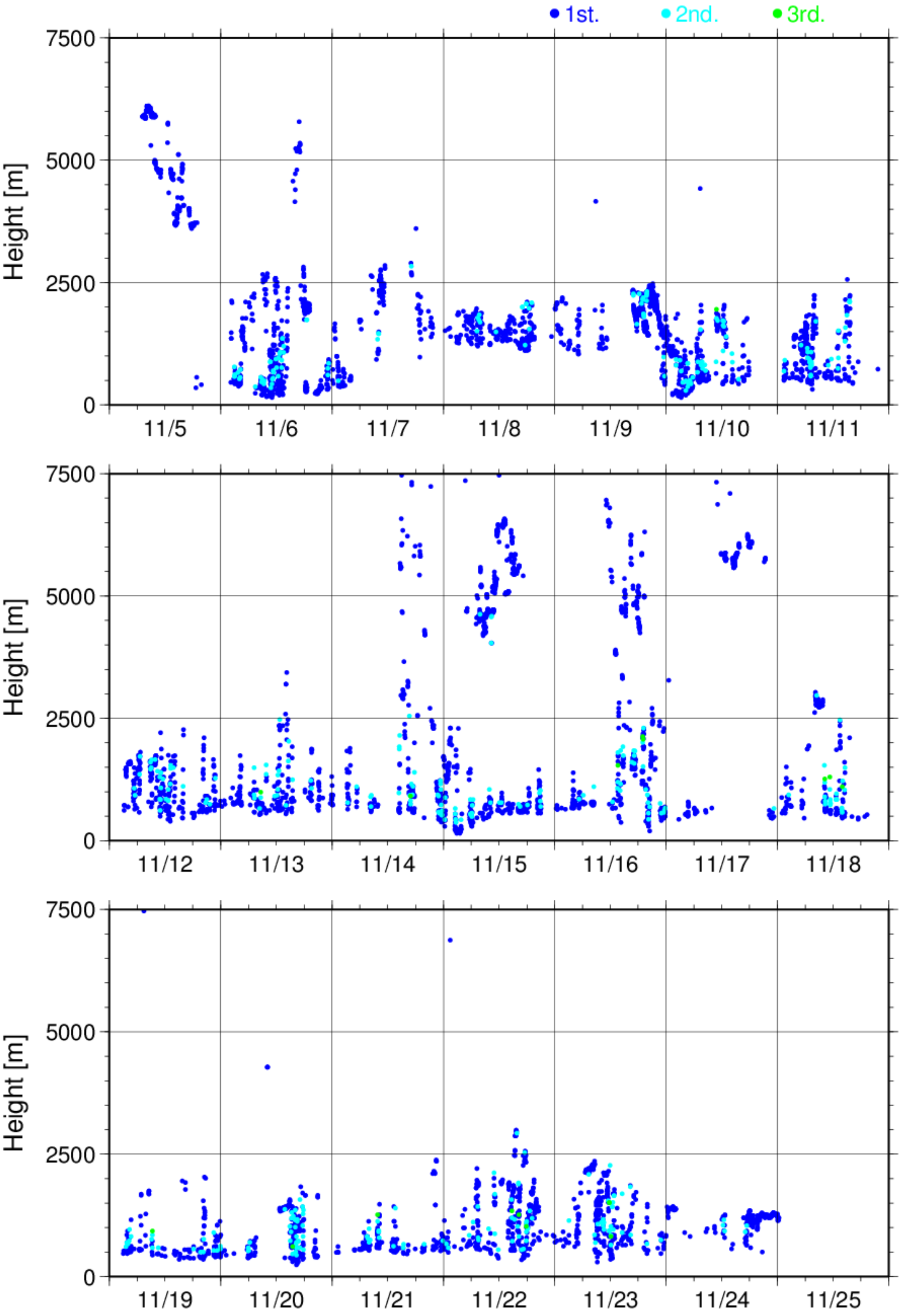

Fig. 2.7-1 1st, 2nd and 3rd lowest cloud base height during the MR12-05 leg1 cruise.

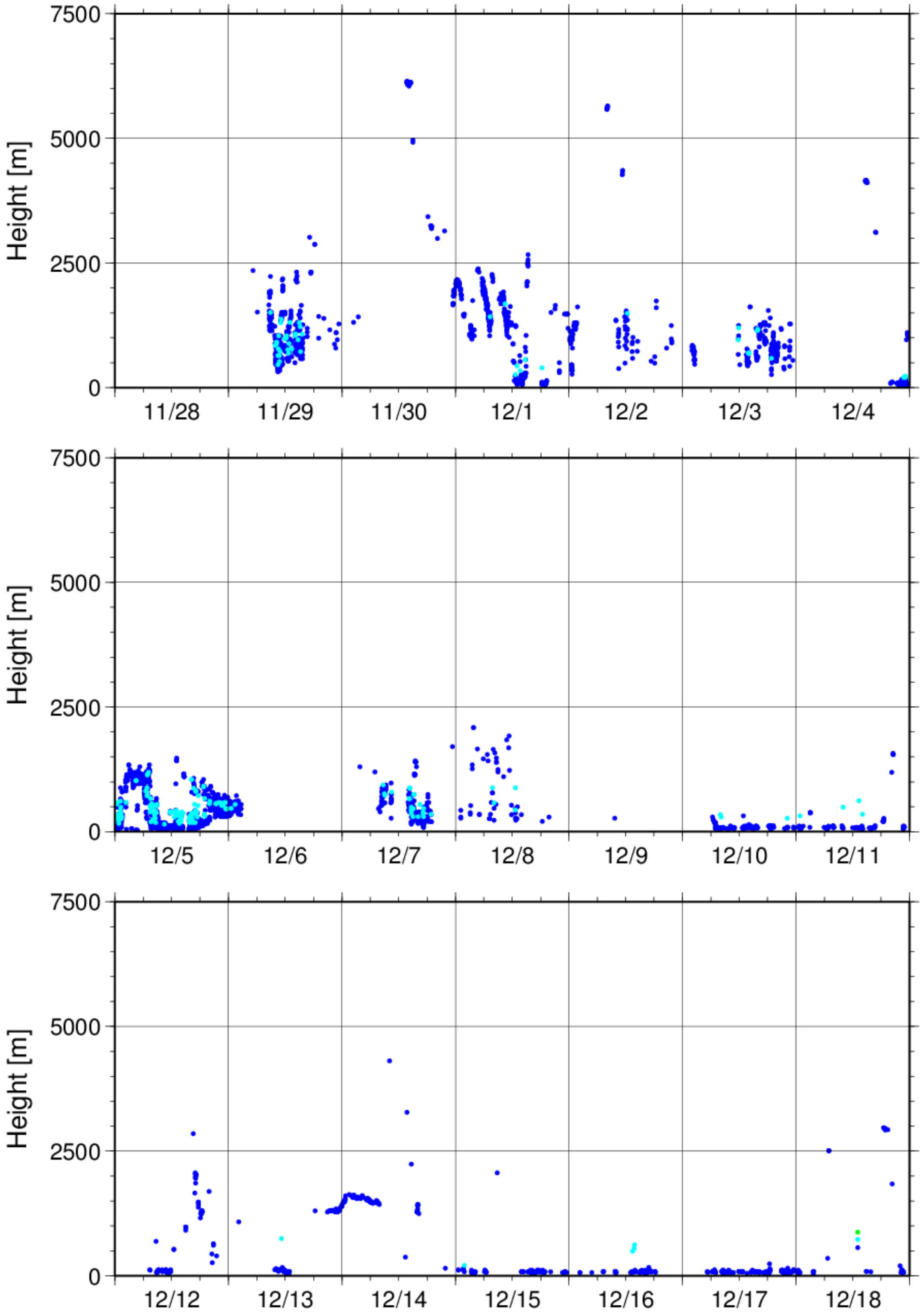

Fig. 2.7-2 1st, 2nd and 3rd lowest cloud base height during the MR12-05 leg2 cruise.

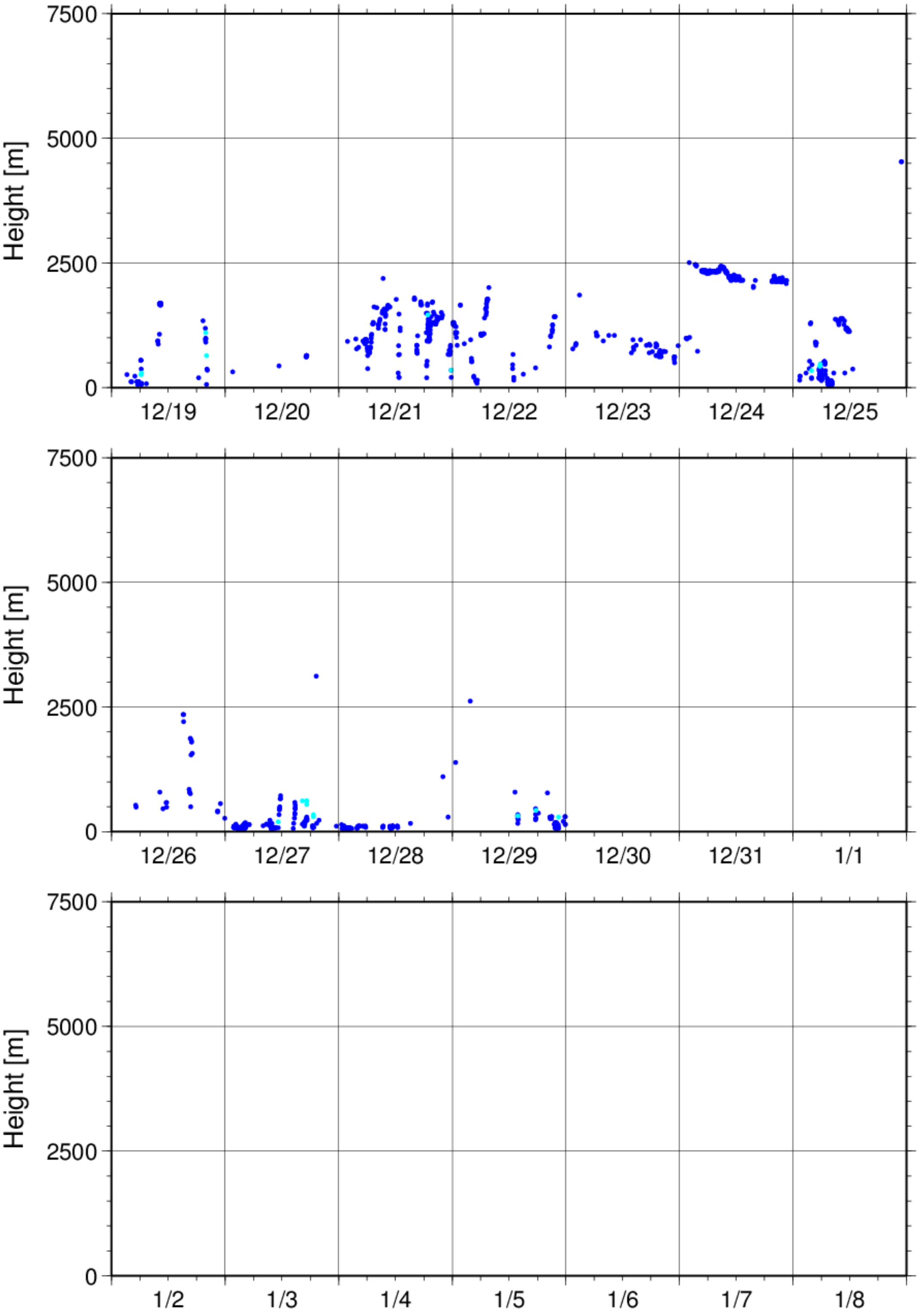

Fig. 2.7-2 (Continued)

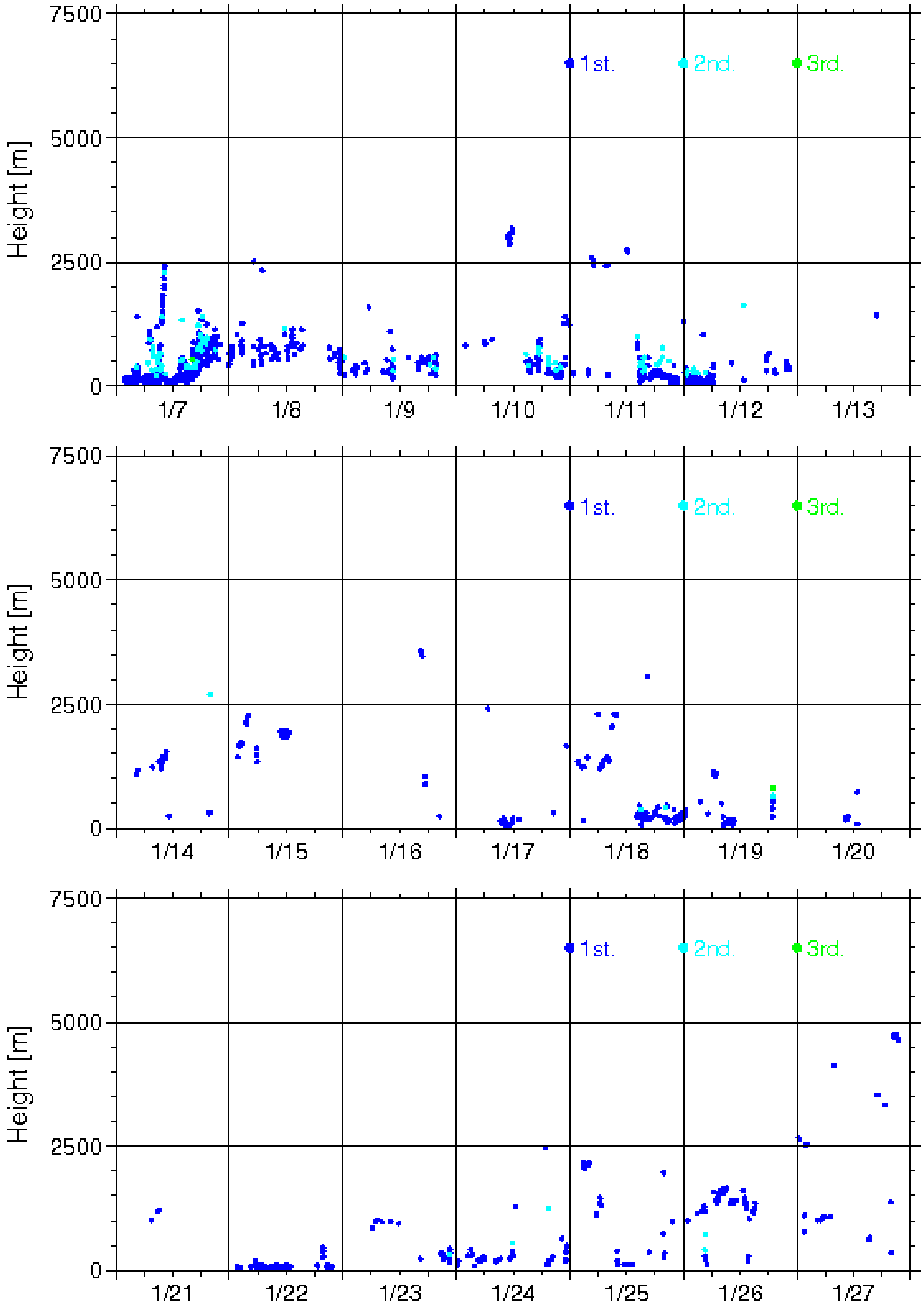

Fig. 2.7-3 1st, 2nd and 3rd lowest cloud base height during the MR12-05 leg3 cruise.

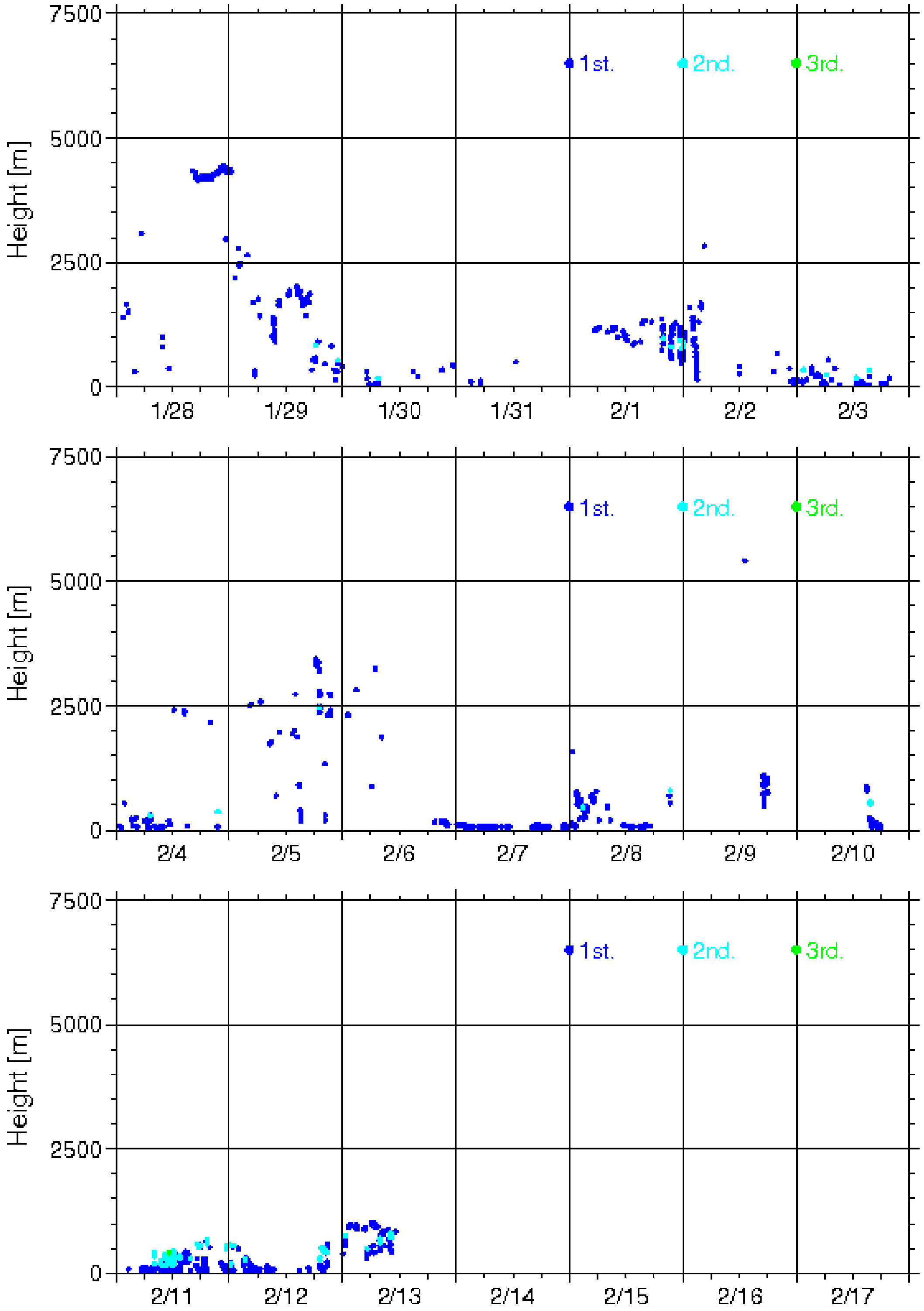

Fig. 2.7-3 (Continued)

.

2.8 Isotopes in rainfall and water vapor

(1) Personnel

Yasushi Fujiyoshi *(Hokkaido Univ./JAMSTEC)* *Principal Investigator* *（not on-board）*
Naoyuki Kurita *(JAMSTEC)*
Operator
Souichiro Sueyoshi *(Global Ocean Development Inc.: GODI)*

(2) Objective

It is well known that the variability of stable water isotopes (HDO and $H_2{}^{18}O$) reflects the integrated history of water mass exchange that occurs during transportation from the upstream region. Thus, water isotope tracer is recognized as the powerful tool to study of the hydrological cycles in the marine atmosphere. However, oceanic region is one of sparse region of the isotope data, it is necessary to fill the data to identify the moisture sources by using the isotope tracer. In this study, to fill this sparse observation area, intense water isotopes observation was conducted along the cruise track of MR12-05.

(3) Method

Following observation was carried out throughout this cruise.

- Atmospheric moisture sampling:

Water vapor isotopes in ambient air was continuously measured using the Wavelength Scanned-Cavity Ring Down Spectroscopy (WS-CRDS), manufactured by Picarro, Inc. coupled with an accessory device for the vaporization of a liquid water standard (Standard Deliver Module, SDM). The SDM is programmable from the WS-CRDS and thus this coupled system is capable of automatically conducting a calibration routine at specific intervals.

Air intake was attached at the middle level (20m above the sea level) of the mast at the compass deck and a sampling tube (20 m length of Nylon tubing (Junron A), 8mm O.D.) was connected directly to the WS-CRDS. A 1.0 μm filter with PTFE membrane was placed where the tube enters the air intake. The flow rate is less than 1 l min-1. Every 50 min, the reference water vapor was transferred into the WS-CRDS and that isotopic values were measured continuously during 10 minute. After finishing the reference gas measurement, ambient air sampling is resumed. Raw data from the analyzer is stored on the internal hard disk, and is transferred via ethernet cable. Calibration is undertaken as a post-processing step using the external computer system.

- Rainwater sampling

Rainwater samples gathered in rain/snow collector were collected just after precipitation events have ended. The collected sample was then transferred into glass bottle (6ml) immediately after the measurement of precipitation amount.

(4) Water samples for isotope analysis

Sampling of rainfall for isotope analysis is summarized in Table 2.8.1 (28 samples). Described rainfall amount is calculated from the collected amount of precipitation.

(5) Data archive

The isotopic data of water vapor can obtain from the laser based water vapor isotope analyzer on board. The archived raw observed data will be submitted to JAMSTEC Data Integration and Analysis Group (DIAG) after the cruise. As for collected water samples, isotopes (HDO, $H_2{}^{18}O$) analysis will be done at RIGC/JAMSTEC, and then analyzed isotopes data will be submitted to JAMSTEC DIAG.

Table 2.8.1 Summary of precipitation sampling for isotope analysis.

	Date	Time (UT)	Lon	Lat	Date	Time (UT)	Lon	Lat	Rain (mm)	R/S
R-01	11.5	07:00	141-14.3E	41-22.0N	11.6	21:52	142-34.0E	38-21.6N	27.1	R
R-02	11.6	21:52	142-34.0E	38-21.6N	11.7	20:28	143-18.4E	34-50.6N	2.4	R
R-03	11.7	20:28	143-18.4E	34-50.6N	11.10	00:11	145-47.3E	24-11.1N	0.7	R
R-04	11.10	00:11	145-47.3E	24-11.1N	11.11	01:03	147-30.9E	19-12.4N	4.8	R
R-05	11.11	01:03	147-30.9E	19-12.4N	11.12	03:51	149-13.1E	14-08.3N	1.9	R
R-06	11.12	03:51	149-13.1E	14-08.3N	11.12	20:00	149-46.3E	12-15.7N	0.6	R
R-07	11.12	20:00	149-46.3E	12-15.7N	11.15	00:50	149-44.1E	03-02.1N	0.8	R
R-08	11.15	00:50	149-44.1E	03-02.1N	11.15	19:38	151-20.0E	00-22.4N	10.9	R
R-09	11.17	03:00	153-51.6E	05-12.0S	11.23	17:32	169-27.8E	30-05.1S	6.9	R
R-10	11.28	06:00	176-57.8E	36-46.9S	11.29	22:23	175-38.1E	42-20.7S	5.9	R
R-15	12.6	04:15	173-58.7E	57-30.5S	12.8	20:30	172-43.9E	62-21.4S	1.8	S
R-16	12.8	20:30	172-43.9E	62-21.4S	12.13	05:24	159-26.4E	63-02.5S	23.9	S
R-17	12.13	05:24	159-26.4E	63-02.5S	12.15	20:18	146-23.1E	63-03.3S	2.2	S
R-18	12.15	20:18	146-23.1E	63-03.3S	12.23	04:19	120-01.5E	61-57.2S	9.2	S
R-19	12.23	04:19	120-01.5E	61-57.2S	12.27	23:47	118-39.5E	59-35.7S	16.3	S
R-20	12.27	23:47	118-39.5E	59-35.7S	12.30	21:42	138-00.2E	51-28.9S	5.0	R
R-21	12.30	21:42	138-00.2E	51-28.9S	1.1	06:53	143-28.9E	46-51.9S	16.2	R
R-22	1.7	02:00	143-52.9E	46-44.8S	1.7	19:48	140-24.2E	49-19.1S	18.4	R
R-23	1.7	19:48	140-24.2E	49-19.1S	1.12	12:19	109-56.3E	61-07.1S	1.1	R
R-24	1.12	12:19	109-56.3E	61-07.1S	1.17	23:16	84-01.2E	63-00.7S	19.0	S
R-25	1.17	23:16	84-01.2E	63-00.7S	1.22	07:05	64-23.9E	62-21.5S	34.7	S
R-26	1.22	07:05	64-23.9E	62-21.5S	1.31	01:03	33-39.2E	65-41.9S	33.8	S
R-27	1.31	01:03	33-39.2E	65-41.9S	2.6	02:06	70-52.0E	61-03.1S	11.0	R
R-28	2.6	02:06	70-52.0E	61-03.1S	2.13	12:02	111-12.9E	37-00.7S	8.7	R

.

2.9 Aerosol optical characteristics measured by Ship-borne Sky radiometer

(1) Personnel

Kazuma Aoki (University of Toyama) Principal Investigator / not onboard
Tadahiro Hayasaka (Tohoku University) Co-worker / not onboard
Sky radiometer operation was supported by Global Ocean Development Inc.

(2) Objectives

Objective of this observation is to study distribution and optical characteristics of marine aerosols by using a ship-borne sky radiometer (POM-01 MKII: PREDE Co. Ltd., Japan). Furthermore, collections of the data for calibration and validation to the remote sensing data were performed simultaneously.

(3) Methods and Instruments

The sky radiometer measures the direct solar irradiance and the solar aureole radiance distribution with seven interference filters (0.34, 0.4, 0.5, 0.675, 0.87, 0.94, and 1.02 μm). Analysis of these data was performed by SKYRAD.pack version 4.2 developed by Nakajima *et al.* 1996.

@ Measured parameters

- Aerosol optical thickness at five wavelengths (400, 500, 675, 870 and 1020 nm)
- Ångström exponent
- Single scattering albedo at five wavelengths
- Size distribution of volume (0.01 μm – 20 μm)

GPS provides the position with longitude and latitude and heading direction of the vessel, and azimuth and elevation angle of the sun. Horizon sensor provides rolling and pitching angles.

(4) Preliminary results

Only data collection were performed onboard. At the time of writing, the data obtained in this cruise are under post-cruise processing at University of Toyama.

(5) Data archives

Aerosol optical data are to be archived at University of Toyama (K.Aoki, SKYNET/SKY: http://skyrad.sci.u-toyama.ac.jp/) after the quality check and will be submitted to JAMSTEC.

.

2.10 Lidar

(1) Personnel

Nobuo SUGIMOTO (NIES)
Ichiro MATSUI (NIES)
Atsushi SHIMIZU (NIES)
Tomoaki NISHIZAWA (NIES)
Hajime OKAMOTO (Kyusyu University)

(Lidar operation was supported by Global Ocean Development Inc. (GODI).)

(2) Objectives

Objectives of the observations in this cruise is to study distribution and optical characteristics of ice/water clouds and marine aerosols using a two-wavelength polarization Mie lidar.

(3) Description of instruments deployed

Vertical profiles of aerosols and clouds are measured with a two-wavelength polarization Mie lidar. The lidar employs a Nd:YAG laser as a light source which generates the fundamental output at 1064nm and the second harmonic at 532nm. Transmitted laser energy is typically 30mJ per pulse at both of 1064 and 532nm. The pulse repetition rate is 10Hz. The receiver telescope has a diameter of 20 cm. The receiver has three detection channels to receive the lidar signals at 1064 nm and the parallel and perpendicular polarization components at 532nm. An analog-mode avalanche photo diode (APD) is used as a detector for 1064nm, and photomultiplier tubes (PMTs) are used for 532 nm. The detected signals are recorded with a transient recorder and stored on a hard disk with a computer. The lidar system was installed in a container which has a glass window on the roof, and the lidar was operated continuously regardless of weather. Every 10 minutes vertical profiles of four channels (532 parallel, 532 perpendicular, 1064, 532 near range) are recorded.

(4) Preliminary results

The two wavelength polarization Mie lidar worked well and succeeded in getting the lidar data during the observation period to the end of December 2012 though the laser did not work in January and February 2013. Examples of the measured data are depicted in Fig. 2-10-1. The figures indicates that the lidar can detect water clouds formed at the top of the PBL and ice clouds in the upper layer. It should be noted that the lidar could detect ice clouds (cirrus) up to very high altitude of 16km. Aerosol concentration in the PBL were possible low during the observation period since the lidar signals were very low.

.

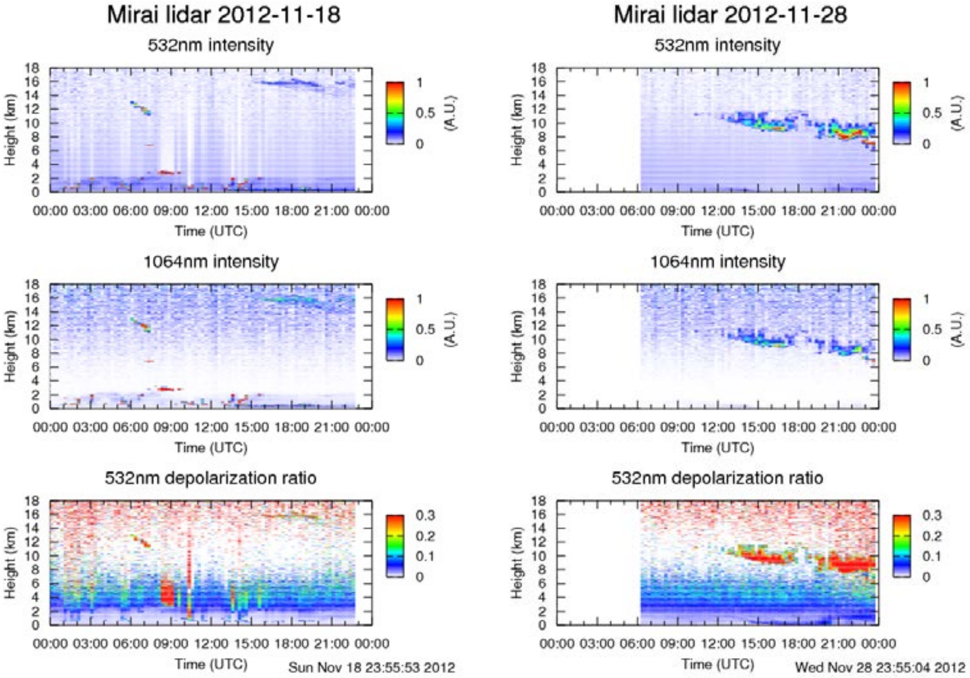

Figure 2-10-1: Time-height sections of backscatter intensities at 532nm and 1064nm and total depolarization ratios at 532nm measured on November 18 and November 28, 2012.

(5) Data archive

- Raw data

temporal resolution 10min / vertical resolution 6 m

data period (UTC): Nov. 5, 2012 ~ Dec. 30, 2012

lidar signal at 532 nm, lidar signal at 1064 nm, depolarization ratio at 532 nm

- Processed data (plan)

cloud base height, apparent cloud top height, phase of clouds (ice/water), cloud fraction

boundary layer height (aerosol layer upper boundary height),

backscatter coefficient of aerosols, particle depolarization ratio of aerosols

* Data policy and Citation

Contact NIES lidar team (nsugimot/i-matsui/shimizua/nisizawa@nies.go.jp) to utilize lidar data for productive use.

2.11 Shipboard ADCP

(1) Personnel

Shinya Kouketsu	***(JAMSTEC)***	***: Principal Investigator***
Souichiro Sueyoshi	***(Global Ocean Development Inc., GODI)***	***-leg1, leg3-***
Koichi Inagaki	***(GODI)***	***-leg1, leg3-***
Kazuho Yoshida	***(GODI)***	***-leg2-***
Shinya Okumura	***(GODI)***	***-leg2-***
Masanori Murakami	***(GODI)***	***-leg2-***
Katsuhisa Maeno	***(GODI)***	***-leg3-***
Ryo Kimura	***(MIRAI Crew)***	***-leg1, leg2-***
Ryo Ohyama	***(MIRAI Crew)***	***-leg3-***

(2) Objective

To obtain continuous measurement of the current profile along the ship's track.

(3) Methods

Upper ocean current measurements were made in the MR12-05 cruise, using the hull-mounted Acoustic Doppler Current Profiler (ADCP) system. For most of its operation the instrument was configured for water-tracking mode. Bottom-tracking mode, interleaved bottom-ping with water-ping, was made to get the calibration data for evaluating transducer misalignment angle in the shallow water. The system consists of following components;

1) R/V MIRAI has installed vessel-mount ADCP (75 kHz "Ocean Surveyor", Teledyne RD Instruments). It has a phased-array transducer with single assembly and creates 4 acoustic beams electronically.
2) For heading source, we use ship's gyro compass (Tokimec, Japan), continuously providing heading to the ADCP system directory. Also we have Inertial Navigation System (PHINS, iXSEA) which provide high-precision heading and attitude information are stored in ".N2R" data files.
3) DGPS system (Trimble SPS751 & StarFixXP) providing position fixes.
4) We used VmDas version 1.46.5 (TRDI) for data acquisition.
5) To synchronize time stamp of pinging with GPS time, the clock of the logging computer is adjusted to GPS time every 8 minutes.
6) The sound speed at the transducer does affect the vertical bin mapping and vertical velocity measurement, is calculated from temperature, salinity (constant value; 35.0 psu) and depth (6.5 m; transducer depth) by equation in Medwin (1975).

Data was configured for 8-m intervals starting 23-m below the surface. Every ping was recorded as raw ensemble data (.ENR). Also, 60 seconds and 300 seconds averaged data were recorded as short term average

(.STA) and long term average (.LTA) data, respectively. Major parameters for the measurement (Direct Command) are shown in Table 2.11-1.

(4) Preliminary results

From Fig.2.11-1 to 2.11-3 shows surface current profile along the ship's track, averaged five depth cells from the top, 43 m to 83 m with 30 minutes average.

(5) Data archive

These data obtained in this cruise will be submitted to the Data Management Group (DMG) of JAMSTEC, and will be opened to the public via JAMSTEC home page.

(6) Remarks (Times in UTC)

1) The observation was carried out within following periods

Leg1: 07:00, 05 Nov. 2012 - 15:00, 16 Nov. 2012
03:00, 17 Nov. 2012 - 07:00, 25 Nov. 2012
Leg2: 06:00, 28 Nov. 2012 - 07:00, 01 Jan. 2013
Leg3: 02:00, 07 Jan. 2013 - 12:00, 13 Feb 2013

2) RSSI (Echo Intensity) became weak deeper layers than 300m around southern part of P14S line as shown in Fig 2.6-4. The following periods, we changed temporally some of parameters (Depth cell size (WS), number of cells (WN) and blanking distance (WF)) due to trying to improve of the state.

01:30 - 01:44, 10 Dec. 2012 : WS;400[cm], WN;128, WF; 400[cm]
01:45 - 02:51, 10 Dec. 2012 : WS;400[cm], WN;128, WF; 800[cm]

3) The following periods, navigation data was invalid due to GPS position fix error.

Leg1: 23:25:06 - 23:39:07, 22 Nov. 2012 (intermittently)
Leg2: 11:47:39 - 13:41:46, 28 Dec. 2012

Table 2.11-1 Major parameters

Bottom-Track Commands

BP = 000	Pings per Ensemble (almost over 1300m depth)
	Leg1: 01:19UTC 07 Nov. 2012 – 15:00UTC 16 Nov. 2012
	03:00UTC 17 Nov. 2012 – 04:39UTC 17 Nov. 2012
	06:48UTC 17 Nov. 2012 – 09:43UTC 18 Nov. 2012
	10:59UTC 18 Nov. 2012 – 18:41UTC 22 Nov. 2012
	20:56UTC 22 Nov. 2012 – 08:09UTC 23 Nov. 2012
	09:16UTC 23 Nov. 2012 – 02:32UTC 23 Nov. 2012
	Leg2: 06:00UTC 28 Nov. 2012 – 02:31UTC 30 Nov. 2012
	17:30UTC 30 Nov. 2012 – 20:54UTC 01 Dec. 2012
	16:17UTC 03 Dec. 2012 – 07:00UTC 01 Jan. 2013
	Leg3: 17:43UTC 06 Jan. 2013 – 14:35UTC 06 Feb. 2013
	05:15UTC 07 Feb. 2013 – 12:00UTC 13 Feb. 2013
BP = 001	Pings per Ensemble (almost less than 1300m depth)
	Leg1: 04:16UTC 05 Nov. 2012 – 01:19UTC 07 Nov. 2012
	04:39UTC 17 Nov. 2012 – 06:47UTC 17 Nov. 2012
	09:43UTC 18 Nov. 2012 – 10:59UTC 18 Nov. 2012
	18:41UTC 22 Nov. 2012 – 20:56UTC 22 Nov. 2012
	08:09UTC 23 Nov. 2012 – 09:16UTC 23 Nov. 2012
	02:32UTC 23 Nov. 2012 – 07:00UTC 25 Nov. 2012
	Leg2: 02:32UTC 30 Nov. 2012 – 17:30UTC 30 Nov. 2012
	20:54UTC 01 Dec. 2012 – 16:17UTC 03 Dec. 2012
	Leg3: 06:18UTC 05 Jan. 2013 – 17:43UTC 06 Jan. 2013
	14:35UTC 06 Feb. 2013 – 05:15UTC 07 Feb. 2013

Environmental Sensor Commands

EA = +04500	Heading Alignment (1/100 deg)
EB = +00000	Heading Bias (1/100 deg)
ED = 00065	Transducer Depth (0 - 65535 dm)
EF = +001	Pitch/Roll Divisor/Multiplier (pos/neg) [1/99 - 99]
EH = 00000	Heading (1/100 deg)
ES = 35	Salinity (0-40 pp thousand)
EX = 00000	Coord Transform (Xform:Type; Tilts; 3Bm; Map)
EZ = 10200010	Sensor Source (C; D; H; P; R; S; T; U)
	C (1): Sound velocity calculates using ED, ES, ET (temp.)

D (0): Manual ED

H (2): External synchro

P (0), R (0): Manual EP, ER (0 degree)

S (0): Manual ES

T (1): Internal transducer sensor

U (0): Manual EU

Timing Commands

TE = 00:00:02.00	Time per Ensemble (hrs:min:sec.sec/100)
TP = 00:02.00	Time per Ping (min:sec.sec/100)

Water-Track Commands

WA = 255	False Target Threshold (Max) (0-255 count)
WB = 1	Mode 1 Bandwidth Control (0=Wid, 1=Med, 2=Nar)
WC = 120	Low Correlation Threshold (0-255)
WD = 111 100 000	Data Out (V; C; A; PG; St; Vsum; Vsum^2;#G;P0)
WE = 1000	Error Velocity Threshold (0-5000 mm/s)
WF = 0800	Blank After Transmit (cm)
WG = 001	Percent Good Minimum (0-100%)
WI = 0	Clip Data Past Bottom (0 = OFF, 1 = ON)
WJ = 1	Rcvr Gain Select (0 = Low, 1 = High)
WM = 1	Profiling Mode (1-8)
WN = 100	Number of depth cells (1-128)
WP = 00001	Pings per Ensemble (0-16384)
WS= 0800	Depth Cell Size (cm)
WT = 000	Transmit Length (cm) [0 = Bin Length]
WV = 0390	Mode 1 Ambiguity Velocity (cm/s radial)

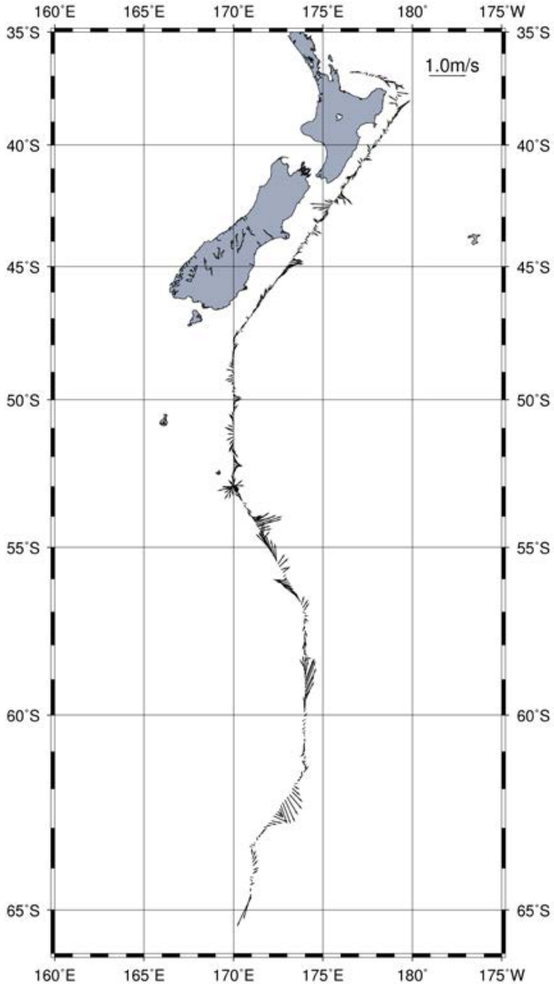

Fig 2.11-1 Current profile along the ship's track, from 43m to 83m depth, averaged every 30 minutes (Leg2).

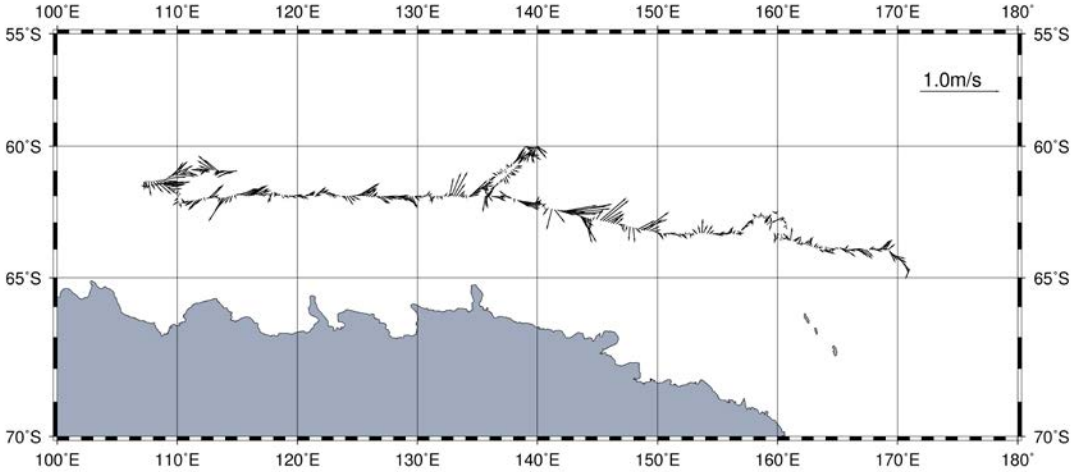

Fig 2.11-2 Current profile along the ship's track, from 43m to 83m, averaged every 30 minutes (Leg2).

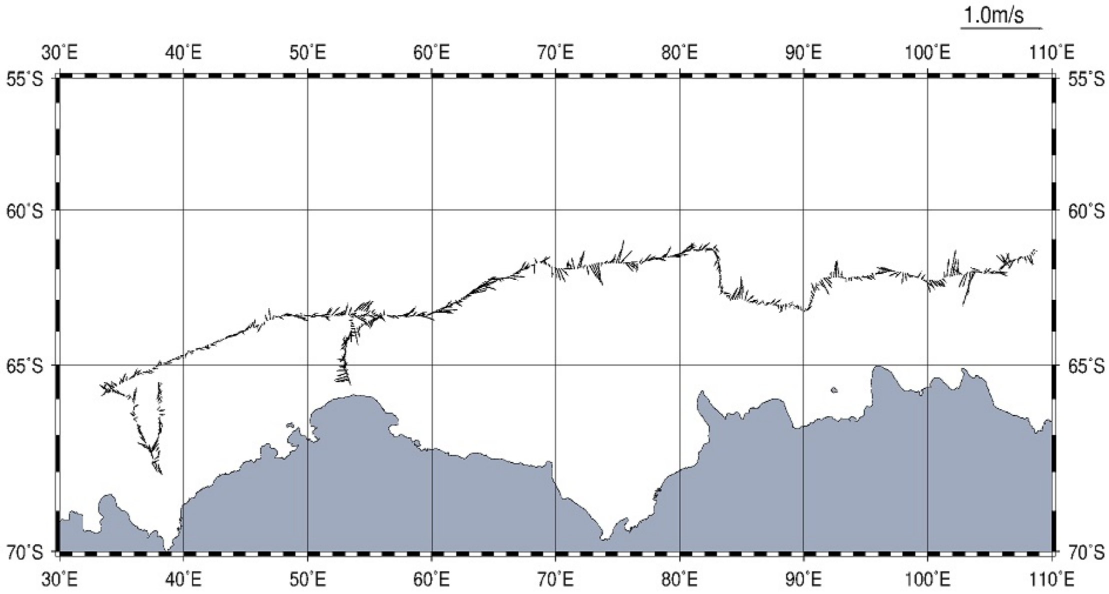

Fig 2.11-3 Current profile along the ship’s track, from 43m to 83m, averaged every 30 minutes (Leg3).

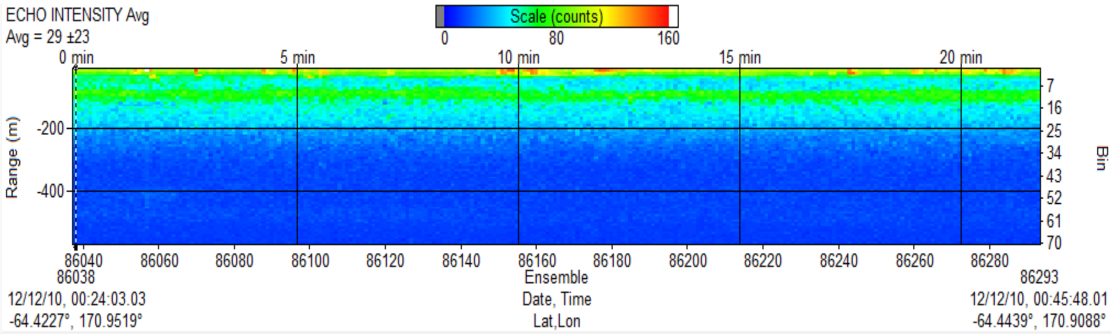

Fig 2.11-4 Time series of Echo Intensity profile between P14S-26 and P14S-27

.

2.12 Sea surface gravity

(1) Personnel

Takeshi Matsumoto (University of the Ryukyus) : Principal investigator (not on-board)
Masao Nakanishi (Chiba University) :Principal investigator (not on-board)
Souichiro Sueyoshi (Global Ocean Development Inc., GODI) -leg1, leg3-
Koichi Inagaki (GODI) -leg1, leg3-
Kazuho Yoshida (GODI) -leg2-
Shinya Okumura (GODI) -leg2-
Masanori Murakami(GODI) -leg2-
Katsuhisa Maeno (GODI) -leg3-
Ryo Kimura (MIRAI Crew) -leg1, leg2-
Ryo Ohyama (MIRAI Crew) -leg3-

(2) Introduction

The local gravity is an important parameter in geophysics and geodesy. We collected gravity data at the sea surface.

(3) Parameters

Relative Gravity [CU: Counter Unit]
[mGal] = (coef1: 0.9946) * [CU]

(5) Data Acquisition

We measured relative gravity using LaCoste and Romberg air-sea gravity meter S-116 (Micro-G LaCoste, LLC) during the MR12-05 cruise.

To convert the relative gravity to absolute one, we measured gravity, using portable gravity meter (CG-5, Scintrex), at Sekinehama as the reference point.

(6) Preliminary Results

Absolute gravity table is shown in Table 2.15-1.

Table 2.12-1. Absolute gravity table of the MR12-05 cruise

No.	Date	UTC	Port	Absolute Gravity (mGal)	Sea Level (cm)	Draft (cm)	Gravity at Sensor^{*1} (mGal)	L&R^{*2} (mGal)
1	4/Nov/2012	01:13	Sekinehama	980371.93	261	625	980372.95	12611.57
2	29/Mar/2013	02:33	Sekinehama	980371.93	323	575	980373.03	12610.35

*1: Gravity at Sensor= Absolute Gravity + Sea Level*0.3086/100 + (Draft-530)/100*0.2222

*2: Micro-g LaCoste air-sea gravity meter S-116

(6) Data Archive

Surface gravity data obtained during this cruise will be submitted to the Data Management Group (DMG) in JAMSTEC, and will be archived there.

(7) Remarks (Times in UTC)

1) The following periods, the observation was carried out.

Leg1: 07:00, 05 Nov. 2012 - 15:00, 16 Nov. 2012
03:00, 17 Nov. 2012 - 07:00, 25 Nov. 2012
Leg2: 06:00, 28 Nov. 2012 - 07:00, 01 Jan. 2013
Leg3: 02:00, 07 Jan. 2013 - 12:00, 13 Feb 2013.

2) The following periods, navigation data was invalid due to GPS position fix error.

Leg1: 23:25:06 - 23:39:07, 22 Nov. 2012(intermittently)
Leg2: 12:39:25 - 13:01:20, 28 Dec. 2012

2.13 On-board geomagnetic measurement

2.13.1 Three-component magnetometer

(1) Personnel

Takeshi Matsumoto	*(University of the Ryukyus)*	*: Principal investigator (not on-board)*
Masao Nakanishi	*(Chiba University)*	*:Principal investigator (not on-board)*
Souichiro Sueyoshi	*(Global Ocean Development Inc., GODI)*	*-leg1, leg3-*
Koichi Inagaki	*(GODI)*	*-leg1, leg3-*
Kazuho Yoshida	*(GODI)*	*-leg2-*
Shinya Okumura	*(GODI)*	*-leg2-*
Masanori Murakami	*(GODI)*	*-leg2-*
Katsuhisa Maeno	*(GODI)*	*-leg3-*
Ryo Kimura	*(MIRAI Crew)*	*-leg1, leg2-*
Ryo Ohyama	*(MIRAI Crew)*	*-leg3-*

(2) Introduction

Measurement of magnetic force on the sea is required for the geophysical investigations of marine magnetic anomaly caused by magnetization in upper crustal structure. We measured geomagnetic field using a three-component magnetometer during the MR12-05 cruise.

(3) **Principle of ship-board geomagnetic vector measurement**

The relation between a magnetic-field vector observed on-board, **H**ob, (in the ship's fixed coordinate system) and the geomagnetic field vector, **F**, (in the Earth's fixed coordinate system) is expressed as:

$$\mathbf{H}\mathrm{ob} = \tilde{\mathbf{A}}\ \tilde{\mathbf{R}}\ \tilde{\mathbf{P}}\ \tilde{\mathbf{Y}}\ \mathbf{F} + \mathbf{H}\mathrm{p} \qquad \text{(a)}$$

where $\tilde{\mathbf{R}}$, $\tilde{\mathbf{P}}$ and $\tilde{\mathbf{Y}}$ are the matrices of rotation due to roll, pitch and heading of a ship, respectively. $\tilde{\mathbf{A}}$ is a 3 x 3 matrix which represents magnetic susceptibility of the ship, and **H**p is a magnetic field vector produced by a permanent magnetic moment of the ship's body. Rearrangement of Eq. (a) makes

$$\tilde{\mathbf{R}}\ \mathbf{H}\mathrm{ob} + \mathbf{H}\mathrm{bp} = \tilde{\mathbf{R}}\ \tilde{\mathbf{P}}\ \tilde{\mathbf{Y}}\ \mathbf{F} \qquad \text{(b)}$$

where $\tilde{\mathbf{R}} = \tilde{\mathbf{A}}^{-1}$, and **H**bp = -$\tilde{\mathbf{R}}$ **H**p. The magnetic field, **F**, can be obtained by measuring $\tilde{\mathbf{R}}$, $\tilde{\mathbf{P}}$, $\tilde{\mathbf{Y}}$ and **H**ob, if $\tilde{\mathbf{R}}$ and **H**bp are known. Twelve constants in $\tilde{\mathbf{R}}$ and **H**bp can be determined by measuring variation of **H**ob with $\tilde{\mathbf{R}}$, $\tilde{\mathbf{P}}$ and $\tilde{\mathbf{Y}}$ at a place where the geomagnetic field, **F**, is known.

(4) Instruments on R/V MIRAI

A shipboard three-component magnetometer system (Tierra Tecnica SFG1214) is equipped on-board R/V MIRAI. Three-axes flux-gate sensors with ring-cored coils are fixed on the fore mast. Outputs from the sensors are digitized by a 20-bit A/D converter (1 nT/LSB), and sampled at 8 times per second. Ship's heading, pitch, and roll are measured by the Inertial Navigation System (INS) for controlling attitude of a Doppler radar. Ship's position (GPS) and speed data are taken from LAN every second.

(5) Data Archive

Surface gravity data obtained during this cruise will be submitted to the Data Management Group (DMG) in JAMSTEC, and will be archived there.

(6) Remarks (Times in UTC)

1) The following periods, the observation was carried out.

Leg1: 07:00, 05 Nov. 2012 – 15:00, 16 Nov. 2012
03:00, 17 Nov. 2012 – 07:00, 25 Nov. 2012
Leg2: 06:00, 28 Nov. 2012 – 07:00, 01 Jan. 2013
Leg3: 02:00, 07 Jan. 2013 – 12:00, 13 Feb 2013.

2) The following periods, we made a "figure-eight" turn (a pair of clockwise and anti-clockwise rotation) for calibration of the ship's magnetic effect.

Leg1: 03:59 - 04:24, 12 Nov. 2012 at 14-07N, 149-14E
20:18 - 20:46, 14 Nov. 2012 at 03-42N, 149-20E
11:17 - 11:57, 16 Nov. 2012 at 02-13S, 153-00E
05:50 - 06:18, 22 Nov. 2012 at 26-18S, 165-36E
Leg2: 20:01 - 20:25, 12 Dec. 2012 at 62-38S, 160-00E
13:15 - 13:38, 18 Dec. 2012 at 60-03S, 139-54E
05:23 - 05:42, 1 Jan. 2013 at 47-01S, 143-19E
Leg3: 11:12 – 11:37, 24 Jan. 2013 at 63-18S, 63-51E
15:24 – 15:54, 02 Feb. 2013 at 65-00S, 38-02E
00:00 – 00:30, 09 Feb. 2013 at 53-24S, 91-38E
07:02 – 07:29, 13 Feb. 2013 at 37-44S, 110-38E

3) The following periods, navigation data was invalid due to GPS position fix error.

Leg1: 23:25:06 - 23:39:07, 22 Nov. 2012 (intermittently)
Leg2: 12:14:13 - 12:21:09, 18 Dec. 2012 (intermittently)
11:47:38 - 11:52:42, 28 Dec. 2012
12:39:21 - 13:01:11, 28 Dec. 2012

4) The following periods, navigation data was not update.

Leg1: 01:01:48, 10 Nov. 2012
Leg2: 18:36:32 - 18:36:35, 19 Dec. 2012
Leg3: 04:25:13, 02 Feb. 2013
07:16:51, 03 Feb. 2013

.

02:57:15, 04 Feb. 2013

02:38:13, 06 Feb. 2013

10:59:20, 08 Feb. 2013

12:32:55 – 12:32:56, 11 Feb 2013

09:43:22, 12 Feb. 2013

2.13.2 Cesium magnetometer

(1) Personnel

Masao Nakanishi	*(Chiba University)*	*: Principal investigator (Not on-board)*
Takeshi Matsumoto	*(University of the Ryukyus)*	*: Principal investigator (Not on-board)*
Souichiro Sueyoshi	*(Global Ocean Development Inc., GODI)*	*-leg1-*
Koichi Inagaki	*(GODI)*	*-leg1-*
Ryo Kimura	*(MIRAI Crew)*	*-leg1-*

(2) Introduction

Measurement of total magnetic force on the sea is required for the geophysical investigations of marine magnetic anomaly caused by magnetization in upper crustal structure.

(3) Data Period and Sensor Rotation (Time in UTC)

19:55, 14 Nov. 2012 – 08:18, 15 Nov. 2012	Rotation = 60 degrees
21:55, 15 Nov. 2012 – 12:35, 16 Nov. 2012	Rotation = 45 degrees

(3) Specification

We measured total geomagnetic field using a cesium marine magnetometer (Geometrics Inc., G-882) and recorded by G-882 data logger (Clovertech Co., Ver.1.0.0). The G-882 magnetometer uses an optically pumped Cesium-vapor atomic resonance system. The sensor fish towed 500 m behind the vessel to minimize the effects of the ship's magnetic field. Table 2.16.2-1 shows system configuration of MIRAI cesium magnetometer system.

Table 2.13.2-1 System configuration of MIRAI cesium magnetometer.

Dynamic operating range:		20,000 to 100,000 nT
Absolute accuracy:		<±2 nT throughout range
Setting:	Cycle rate;	0.1 sec
	Sensitivity;	0.001265 nT at a 0.1 second cycle rate
	Sampling rate;	1 sec

(4) Data Archive

Total magnetic force data obtained during this cruise was submitted to the Data Management Group (DMG) of JAMSTEC, and archived there.

.

2.14 Bathymetry of the Lyra Basin

(1) Personnel

Masao Nakanishi (Graduate School of Science, Chiba University)

(2) Objectives

Lyra Basin lies west of the Ontong Java Plateau. The Lyra Basin deepens westward from 4000 m to 5000 m (Fig. 2.14.1). The Lyra Trough, crossing the Lyra Basin, is a broad and deep graben. The depth is about 6000 m. The eastern rim of the Lyra Trough is dotted seamounts. We conducted the research cruise (KR06-16) around the Lyra Trough in the Lyra Basin using R/V KAIREI, JAMSTEC, in December 2006 (Nakanishi, 2007). The bathymetric measurement revealed the topographic expression of the Lyra Trough. Elongated ridges exist in the eastern rim of the trough near the equator. The height of the ridges is more than 500 m. The strike of some ridges is parallel to the trough. The bathymetric survey was conducted in MR12-05 Leg 1 to reveal the topographic expression of the Lyra Trough in more detail.

(3) Result

Our bathymetric measurement reveals the topographic expression of the Lyra Trough (Fig. 2.14.2). The depth of the trough is around 5500 m. Elongated ridges are the predominant feature in the survey area. The height of the elongated ridges in the trench is about 500 m. The strike of some ridges is N35°W and parallel to the trough strike. That of others is N50°W and oblique to the trough strike. The length of the lineated ridges is around 20 km.

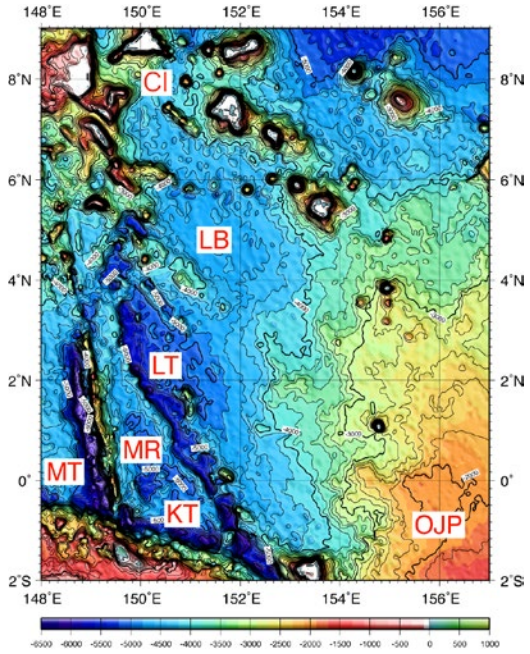

Fig. 2.14.1. Bathymetric map of the Lyra Basin Plateau. Contour interval is 100 m. Abbreviations are CI: Caroline Islands, OJP: Ontong Java Plateau, LB: Lyra Basin, LT: Lyra Trough, KT: Kilinailau Trench, MR: Mussau Ridge, MT: Mussau Trench.

Fig. 2.14.2. Bathymetric map of the Lyra Trough made using the bathymetric data obtained during MR12-05 Leg1 illuminated from the northeast. Contour interval is 200 m.

References

Nakanishi, M. (Ed.), Cruise Report R/V KAIREI KR06-16, Tectonic history of Lyra Basin west of the Ontong Java Plateau, 80 pp., JAMSTEC, 2007.

Nakanishi, M., Sano, T., and Shimizu, K. (2007) Tectonic setting of the Lyra Basin, west of the Ontong Java Plateau: EOS Transactions, American Geophysical Union, v. 12, p. T13A-1122.

.

2.15. Photosynthetically Available Radiation (PAR)

(1) Personnel

Hiroshi Uchida (JAMSTEC)

(2) Objectives

The PAR sensor is used to measure surface Photosynthetically Available Radiation (PAR) continuously along the cruise track for a study of primary production.

(3) Instrument and method

The PAR is measured by a PUV-510B (Biospherical Instruments Inc., San Diego, CA, USA) at one minute intervals. The PAR sensor was installed on the roof top of the anti-rolling system by looking upward. The PAR sensor was calibrated before the cruise by the K-Engineering Co., Ltd., Japan.

Serial no.: 19209
Date of calibration: September 28, 2012
Slope: –6.220
Offset: 0.000109 μE/(cm^2 sec)

(4) Comparison with another PAR sensor

Data measured by a PUV-510B were compared with the data measured by another PAR sensor (Serial no.: 049, Satlantic LP, Halifax, NS, Canada) used in the CTD profiler measurement. The Satlantic's PAR sensor was attached to the body of the surface PAR (PUV-510B) sensor and the PAR data were compared for four hours of daytime (2:54-6:53 [UTC], February 9, 2013) (Figure 2.15.1).

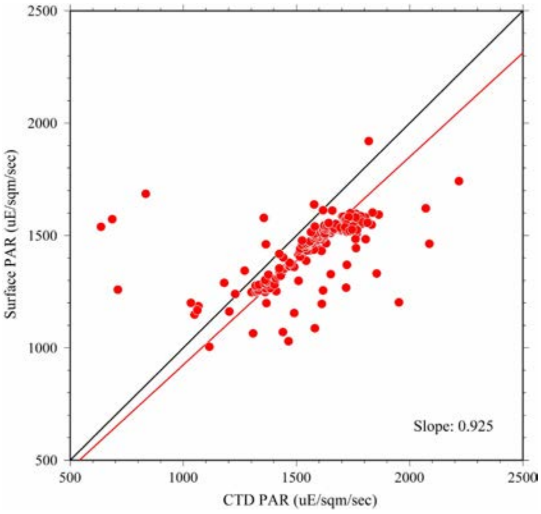

Figure 2.15.1. Comparison of two PAR sensors used for the surface PAR measurement and the CTD profiler measurement.

.

3. Station Observation

3.1 CTDO$_2$ Measurements

(1) Personnel

Hiroshi Uchida (JAMSTEC)
Shinsuke Toyoda (MWJ) (legs 1, 2)
Tomohide Noguchi (MWJ) (leg 2)
Tomoyuki Takamori (MWJ) (leg 2)
Shungo Oshitani (MWJ) (leg 2)
Naoko Miyamoto (MWJ) (leg 3)
Satoshi Ozawa (MWJ) (leg 3)
Hiroshi Matsunaga (MWJ) (leg 3)
Takami Mori (MWJ) (leg 3)

(2) Winch arrangements

The CTD package was deployed by using 4.5 Ton Traction Winch System (Dynacon, Inc., Bryan, Texas, USA), which was installed on the R/V Mirai in April 2001 (Fukasawa et al., 2004). Primary system components include a complete CTD Traction Winch System with up to 8000 m of 9.53 mm armored cable (Ocean Cable and Communications Co., Yokohama, Kanagawa, Japan).

(3) Overview of the equipment

The CTD system was SBE 911plus system (Sea-Bird Electronics, Inc., Bellevue, Washington, USA). The SBE 911plus system controls 36-position SBE 32 Carousel Water Sampler. The Carousel accepts 12-litre Niskin-X water sample bottles (General Oceanics, Inc., Miami, Florida, USA). The SBE 9plus was mounted horizontally in a 36-position carousel frame. SBE's temperature (SBE 3) and conductivity (SBE 4) sensor modules were used with the SBE 9plus underwater unit. The pressure sensor is mounted in the main housing of the underwater unit and is ported to outside through the oil-filled plastic capillary tube. A modular unit of underwater housing pump (SBE 5T) flushes water through sensor tubing at a constant rate independent of the CTD's motion, and pumping rate (3000 rpm) remain nearly constant over the entire input voltage range of 12-18 volts DC. Flow speed of pumped water in standard TC duct is about 2.4 m/s. Two sets of temperature and conductivity modules were used. An SBE's dissolved oxygen sensor (SBE 43) was placed between the primary conductivity sensor and the pump module. Auxiliary sensors, a Deep Ocean Standards Thermometer (SBE 35), an altimeter (PSA-916T; Teledyne Benthos, Inc., North Falmous, Massachusetts, USA), two oxygen optodes (RINKO-III; JFE Alec Co., Ltd, Kobe Hyogo, Japan), two fluorometers (Seapoint sensors, Inc., Kingston, New Hampshire, USA), a transmissometer (C-Star Transmissometer; WET Labs, Inc., Philomath, Oregon, USA), and a Photosynthetically Active Radiation (PAR) sensor (Satlantic, LP, Halifax, Nova Scotia, Canada) were also used with the SBE 9plus underwater unit. To minimize rotation of the CTD package, a heavy stainless frame (total weight of the CTD package without sea water in the bottles is about 1000 kg) was used with an aluminum plate (54 × 90 cm).

.

Summary of the system used in this cruise

Deck unit:

SBE 11plus, S/N 0272 (leg 1, leg 2 stations from 001_1 to 076_1)

SBE 11plus, S/N 0344 (leg 2 stations from 076_2 to 503_1, leg 3)

Under water unit:

SBE 9plus, S/N 117457 (Pressure sensor: S/N 1027)

Temperature sensor:

SBE 3plus, S/N 4815 (primary)

SBE 3plus, S/N 1464 (secondary)

Conductivity sensor:

SBE 4, S/N 2854 (leg 1 primary, legs 2 and 3 secondary)

SBE 4, S/N 2435 (leg 1 secondary, legs 2 and 3 primary)

Oxygen sensor:

SBE 43, S/N 2211 (legs 2 and 3)

SBE 43, S/N 0949 (leg 3)

JFE Advantech RINKO-III, S/N 0024 (foil batch no. 144002A) (primary)

JFE Advantech RINKO-III, S/N 0079 (foil batch no. 160002A) (secondary: legs 1 and 2)

JFE Advantech RINKO-III, S/N 0037 (foil batch no. 160005A) (secondary: leg 3)

Pump:

SBE 5T, S/N 4598 (primary)

SBE 5T, S/N 4595 (secondary)

Altimeter:

PSA-916T, S/N 1100

Deep Ocean Standards Thermometer:

SBE 35, S/N 0022

Fluorometer:

Seapoint Sensors, Inc., S/N 3054 (measurement range: 0-5 ug/L)

Seapoint Sensors, Inc., S/N 3497 (measurement range: 0-15 ug/L)

Transmissometer:

C-Star, S/N CST-1363DR

PAR:

Satlantic LP, S/N 0049

Carousel Water Sampler:

SBE 32, S/N 0278

Water sample bottle:

12-litre Niskin-X model 1010X (no TEFLON coating)

(4) Pre-cruise calibration

.

i. Pressure

The Paroscientific series 4000 Digiquartz high pressure transducer (Model 415K: Paroscientific, Inc., Redmond, Washington, USA) uses a quartz crystal resonator whose frequency of oscillation varies with pressure induced stress with 0.01 per million of resolution over the absolute pressure range of 0 to 15000 psia (0 to 10332 dbar). Also, a quartz crystal temperature signal is used to compensate for a wide range of temperature changes at the time of an observation. The pressure sensor has a nominal accuracy of 0.015 % FS (1.5 dbar), typical stability of 0.0015 % FS/month (0.15 dbar/month), and resolution of 0.001 % FS (0.1 dbar). Since the pressure sensor measures the absolute value, it inherently includes atmospheric pressure (about 14.7 psi). SEASOFT subtracts 14.7 psi from computed pressure automatically.

Pre-cruise sensor calibrations for linearization were performed at SBE, Inc.

S/N 1027, 4 February 2011

The time drift of the pressure sensor is adjusted by periodic recertification corrections against a dead-weight piston gauge (Model 480DA, S/N 23906; Piston unit, S/N 079K; Weight set, S/N 3070; Bundenberg Gauge Co. Ltd., Irlam, Manchester, UK). The corrections are performed at JAMSTEC, Yokosuka, Kanagawa, Japan by Marine Works Japan Ltd. (MWJ), Yokohama, Kanagawa, Japan, usually once in a year in order to monitor sensor time drift and linearity.

S/N 1027, 23 August 2012

slope = 1.00003946

offset = –0.42611

ii. Temperature (SBE 3)

The temperature sensing element is a glass-coated thermistor bead in a stainless steel tube, providing a pressure-free measurement at depths up to 10500 (6800) m by titanium (aluminum) housing. The SBE 3 thermometer has a nominal accuracy of 1 mK, typical stability of 0.2 mK/month, and resolution of 0.2 mK at 24 samples per second. The premium temperature sensor, SBE 3plus, is a more rigorously tested and calibrated version of standard temperature sensor (SBE 3).

Pre-cruise sensor calibrations were performed at SBE, Inc.

S/N 4815, 1 March 2012

S/N 1464, 20 September 2012

Pressure sensitivities of SBE 3s were corrected according to a method by Uchida et al. (2007), for the following sensors.

S/N 4815, –3.45974716e–7 [°C/dbar]

S/N 1464, –7.75293156e–9 [°C/dbar]

iii. Conductivity (SBE 4)

The flow-through conductivity sensing element is a glass tube (cell) with three platinum electrodes to provide in-situ measurements at depths up to 10500 (6800) m by titanium (aluminum) housing. The SBE 4 has a nominal accuracy of 0.0003 S/m, typical stability of 0.0003 S/m/month, and resolution of 0.00004 S/m at 24 samples per second. The conductivity cells have been replaced to newer style cells for deep ocean measurements.

.

Pre-cruise sensor calibrations were performed at SBE, Inc.

S/N 2854, 21 September 2012

S/N 2435, 21 September 2012

The value of conductivity at salinity of 35, temperature of 15 °C (IPTS-68) and pressure of 0 dbar is 4.2914 S/m.

iv. Oxygen (SBE 43)

The SBE 43 oxygen sensor uses a Clark polarographic element to provide in-situ measurements at depths up to 7000 m. The range for dissolved oxygen is 120 % of surface saturation in all natural waters, nominal accuracy is 2 % of saturation, and typical stability is 2 % per 1000 hours.

Pre-cruise sensor calibration was performed at SBE, Inc.

S/N 2211, 19 October 2012

S/N 0949, 18 September 2012

v. Deep Ocean Standards Thermometer

Deep Ocean Standards Thermometer (SBE 35) is an accurate, ocean-range temperature sensor that can be standardized against Triple Point of Water and Gallium Melt Point cells and is also capable of measuring temperature in the ocean to depths of 6800 m. The SBE 35 was used to calibrate the SBE 3 temperature sensors in situ (Uchida et al., 2007).

Pre-cruise sensor linearization was performed at SBE, Inc.

S/N 0022, 4 March 2009

Then the SBE 35 is certified by measurements in thermodynamic fixed-point cells of the TPW (0.01 °C) and GaMP (29.7646 °C). The slow time drift of the SBE 35 is adjusted by periodic recertification corrections. Pre-cruise sensor calibration was performed at SBE, Inc. From the end of 2011, the SBE has been applying a NIST correction to the fixed-point cells used for the calibration.

S/N 0022, 6 March 2012 (slope and offset correction)

Slope = 1.000012

Offset = –0.000023

The time required per sample = 1.1 × NCYCLES + 2.7 seconds. The 1.1 seconds is total time per an acquisition cycle. NCYCLES is the number of acquisition cycles per sample and was set to 4. The 2.7 seconds is required for converting the measured values to temperature and storing average in EEPROM.

vi. Altimeter

Benthos PSA-916T Sonar Altimeter (Teledyne Benthos, Inc.) determines the distance of the target from the unit by generating a narrow beam acoustic pulse and measuring the travel time for the pulse to bounce back from the target surface. It is rated for operation in water depths up to 10000 m. The PSA-916T uses the nominal speed of sound of 1500 m/s.

vii. Oxygen optode (RINKO)

.

RINKO (JFE Alec Co., Ltd.) is based on the ability of selected substances to act as dynamic fluorescence quenchers. RINKO model III is designed to use with a CTD system which accept an auxiliary analog sensor, and is designed to operate down to 7000 m.

Data from the RINKO can be corrected for the time-dependent, pressure-induced effect by means of the same method as that developed for the SBE 43 (Edwards et al., 2010). The calibration coefficients, H1 (amplitude of hysteresis correction), H2 (curvature function for hysteresis), and H3 (time constant for hysteresis) were determined empirically as follows.

H1 = 0.007 (for S/N 0024)

H1 = 0.008 (for S/N 0079 and 0037)

H2 = 5000 dbar

H3 = 2000 seconds

Outputs from RINKO are the raw phase shift data. The RINKO can be calibrated by the Stern-Volmer equation, according to a method by Uchida et al. (2010):

O_2 (μmol/l) = $[(V_0 / V) – 1] / K_{sv}$

where V is voltage, V_0 is voltage in the absence of oxygen and K_{sv} is Stern-Volmer constant. The V_0 and the K_{sv} are assumed to be functions of temperature as follows.

$K_{sv} = C_0 + C_1 \times T + C_2 \times T^2$

$V_0 = 1 + C_3 \times T$

$V = C_4 + C_5 \times V_b$

where T is CTD temperature (°C) and V_b is raw output (volts). V_0 and V are normalized by the output in the absence of oxygen at 0°C. The oxygen concentration is calculated using accurate temperature data from the CTD temperature sensor instead of temperature data from the RINKO. The pressure-compensated oxygen concentration O_{2c} can be calculated as follows.

$O_{2c} = O_2 (1 + C_p p / 1000)^{1/3}$

where p is CTD pressure (dbar) and C_p (0.013 for S/N0024) is the compensation coefficient.

Since the sensing foil of the optode is permeable only to gas and not to water, the optode oxygen must be corrected for salinity. The salinity-compensated oxygen can be calculated by multiplying the factor of the effect of salt on the oxygen solubility. The coefficients of the equation by García and Gordon (1992) were modified based on the laboratory experiment (Uchida et al., in prep.) and used for the compensation (B0 = –6.33568e–3, B1 = –6.84389e–3, B2 = –1.18326e–2, B3 = –5.51960e–2, C0 = 3.40543e–6).

Pre-cruise sensor calibrations were performed at RIGC/JAMSTEC.

S/N 0024, 21 May 2012

S/N 0079, 21 May 2012

S/N 0037, 18 September 2012

viii. Fluorometer

The Seapoint Chlorophyll Fluorometer (Seapoint Sensors, Inc., Kingston, New Hampshire, USA) provides in-situ measurements of chlorophyll-a at depths up to 6000 m. The instrument uses modulated blue LED lamps and a blue

.

excitation filter to excite chlorophyll-a. The fluorescent light emitted by the chlorophyll-a passes through a red emission filter and is detected by a silicon photodiode. The low level signal is then processed using synchronous demodulation circuitry, which generates an output voltage proportional to chlorophyll-a concentration.

ix. Transmissometer

The C-Star Transmissometer (WET Labs, Inc., Philomath, Oregon, USA) measures light transmittance at a single wavelength (650 nm) over a know path (25 cm). In general, losses of light propagating through water can be attributed to two primary causes: scattering and absorption. By projecting a collimated beam of light through the water and placing a focused receiver at a known distance away, one can quantify these losses. The ratio of light gathered by the receiver to the amount originating at the source is known as the beam transmittance. Suspended particles, phytoplankton, bacteria and dissolved organic matter contribute to the losses sensed by the instrument. Thus, the instrument provides information both for an indication of the total concentrations of matter in the water as well as for a value of the water clarity.

Light transmission T_r (in %) and beam attenuation coefficient c_p are calculated from the sensor output (V in volt) as follows.

$T_r = c_0 + c_1 V$

$c_p = -(1 / 0.25) \ln(T_r / 100)$

The calibration coefficients were determined by using the data obtained in the R/V Mirai MR12-02 cruise.

c0 = –0.0251

c1 = 20.8982

x. PAR

Satlantic’s Photosynthetically Active Radiation (PAR) sensors provide highly accurate measurements of PAR (400 – 700 nm) for a wide range of aquatic and terrestrial applications. The ideal spectral response for a PAR sensor is one that gives equal emphasis to all photons between 400 – 700 nm. Satlantic PAR sensors use a high quality filtered silicon photodiode to provide a near equal spectral response across the entire wavelength range of the measurement.

Pre-cruise sensor calibration was performed at Satlantic, LP.

S/N 0049, 22 January 2009

(5) Data collection and processing

i. Data collection

CTD system was powered on at least 20 minutes in advance of the data acquisition to stabilize the pressure sensor and was powered off at least two minutes after the operation in order to acquire pressure data on the ship’s deck.

The package was lowered into the water from the starboard side and held 10 m beneath the surface in order to activate the pump. After the pump was activated, the package was lifted to the surface and lowered at a rate of 1.0 m/s to 200 m (or 300 m when significant wave height was high) then the package was stopped to operate the heave compensator of the crane. The package was lowered again at a rate of 1.2 m/s to the bottom. For the up cast, the package was lifted at a rate of 1.1 m/s except for bottle firing stops. As a rule, the bottle was fired after waiting from the stop for 30 seconds and the package was stayed at least 5 seconds for measurement of the SBE 35 at each bottle firing stops. For depths where vertical gradient of water properties were expected to be large, the bottle was exceptionally fired after waiting from the stop for 60 seconds to enhance exchanging the water between inside and outside of the bottle (depths ≤ 500 dbar for station from C01_1 to C03_1, depths ≤ 100 dbar for station from 063_1 to 068_1, depths ≤ 200 dbar for station from C04_1 to 073_1, depths ≤ 250 dbar for station from 074_1 to 166_1). At 200 m (or 300 m) from the surface, the package was stopped to stop the heave compensator of the crane.

Water samples were collected using a 36-bottle (or 12-bottles) SBE 32 Carousel Water Sampler with 12-litre Niskin-X bottles. Before a cast taken water for CFCs, the bottle frame and Niskin-X bottles were wiped with acetone.

Data acquisition software

SEASAVE-Win32, version 7.22

ii. Data collection problems

(a) Miss trip and miss fire

Niskin bottles did not trip correctly at the following stations.

Miss trip	Miss fire
None	None

iii. Data processing

SEASOFT consists of modular menu driven routines for acquisition, display, processing, and archiving of oceanographic data acquired with SBE equipment. Raw data are acquired from instruments and are stored as unmodified data. The conversion module DATCNV uses instrument configuration and calibration coefficients to create a converted engineering unit data file that is operated on by all SEASOFT post processing modules. The following are the SEASOFT and original software data processing module sequence and specifications used in the reduction of CTD data in this cruise.

Data processing software

SBEDataProcessing-Win32, version 7.22

DATCNV converted the raw data to engineering unit data. DATCNV also extracted bottle information where scans were marked with the bottle confirm bit during acquisition. The duration was set to 4.4 seconds, and the offset was set to 0.0 second. The hysteresis correction for the SBE 43 data (voltage) was applied for both profile and bottle information data.

TCORP (original module, version 1.1) corrected the pressure sensitivity of the SBE 3 for both profile and bottle information data.

RINKOCOR (original module, version 1.0) corrected the time-dependent, pressure-induced effect (hysteresis) of the RINKO for both profile data.

RINKOCORROS (original module, version 1.0) corrected the time-dependent, pressure-induced effect (hysteresis) of the RINKO for bottle information data by using the hysteresis-corrected profile data.

BOTTLESUM created a summary of the bottle data. The data were averaged over 4.4 seconds (or 1 second for the bottle fired without stop).

ALIGNCTD converted the time-sequence of sensor outputs into the pressure sequence to ensure that all calculations were made using measurements from the same parcel of water. For a SBE 9plus CTD with the ducted temperature and conductivity sensors and a 3000-rpm pump, the typical net advance of the conductivity relative to the temperature is 0.073 seconds. So, the SBE 11plus deck unit was set to advance the primary and the secondary conductivity for 1.73 scans (1.75/24 = 0.073 seconds). Oxygen data are also systematically delayed with respect to depth mainly because of the long time constant of the oxygen sensor and of an additional delay from the transit time of water in the pumped plumbing line. This delay was compensated by 6 seconds advancing the SBE 43 oxygen sensor output (voltage) relative to the temperature data. Delay of the RINKO data was also compensated by 1 second advancing sensor output (voltage) relative to the temperature data. Delay of the transmissometer data was also compensated by 2 seconds advancing sensor output (voltage) relative to the temperature data.

WILDEDIT marked extreme outliers in the data files. The first pass of WILDEDIT obtained an accurate estimate of the true standard deviation of the data. The data were read in blocks of 1000 scans. Data greater than 10 standard deviations were flagged. The second pass computed a standard deviation over the same 1000 scans excluding the flagged values. Values greater than 20 standard deviations were marked bad. This process was applied to pressure, temperature, conductivity, SBE 43, and RINKO output.

CELLTM used a recursive filter to remove conductivity cell thermal mass effects from the measured conductivity. Typical values used were thermal anomaly amplitude alpha = 0.03 and the time constant 1/beta = 7.0.

FILTER performed a low pass filter on pressure with a time constant of 0.15 seconds. In order to produce zero phase lag (no time shift) the filter runs forward first then backwards.

WFILTER performed as a median filter to remove spikes in fluorometer and transmissometer data. A median value was determined by 49 scans of the window.

SECTIONU (original module, version 1.1) selected a time span of data based on scan number in order to reduce a file size. The minimum number was set to be the start time when the CTD package was beneath the sea-surface after activation of the pump. The maximum number was set to be the end time when the depth of the package was 1 dbar below the surface. The minimum and maximum numbers were automatically calculated in the module.

LOOPEDIT marked scans where the CTD was moving less than the minimum velocity of 0.0 m/s (traveling backwards due to ship roll).

DESPIKE (original module, version 1.0) removed spikes of the data. A median and mean absolute deviation was calculated in 1-dbar pressure bins for both down- and up-cast, excluding the flagged values. Values greater than 4 mean absolute deviations from the median were marked bad for each bin. This process was performed 2 times for temperature, conductivity, SBE 43, and RINKO output.

DERIVE was used to compute oxygen (SBE 43).

BINAVG averaged the data into 1-dbar pressure bins. The center value of the first bin was set equal to the bin size. The bin minimum and maximum values are the center value plus and minus half the bin size. Scans with pressures greater than the minimum and less than or equal to the maximum were averaged. Scans were interpolated so that a data record exist every dbar.

DERIVE was re-used to compute salinity, potential temperature, and density (σ_θ).

SPLIT was used to split data into the down cast and the up cast.

Remaining spikes in the CTD data were manually eliminated from the 1-dbar-averaged data. The data gaps resulting

.

from the elimination were linearly interpolated with a quality flag of 6.

(6) Post-cruise calibration

i. Pressure

The CTD pressure sensor offset in the period of the cruise was estimated from the pressure readings on the ship deck. For best results the Paroscientific sensor was powered on for at least 20 minutes before the operation. In order to get the calibration data for the pre- and post-cast pressure sensor drift, the CTD deck pressure was averaged over first and last one minute, respectively. Then the atmospheric pressure deviation from a standard atmospheric pressure (14.7 psi) was subtracted from the CTD deck pressure to check the pressure sensor time drift. The atmospheric pressure was measured at the captain deck (20 m high from the base line) and sub-sampled one-minute interval as a meteorological data. Time series of the CTD deck pressure is shown in Fig. 3.1.1. The CTD pressure sensor offset was estimated from the deck pressure. Mean of the pre- and the post-casts data over the whole period gave an estimation of the pressure sensor offset (–0.01 dbar) from the pre-cruise calibration. The post-cruise correction of the pressure data is not deemed necessary for the pressure sensor.

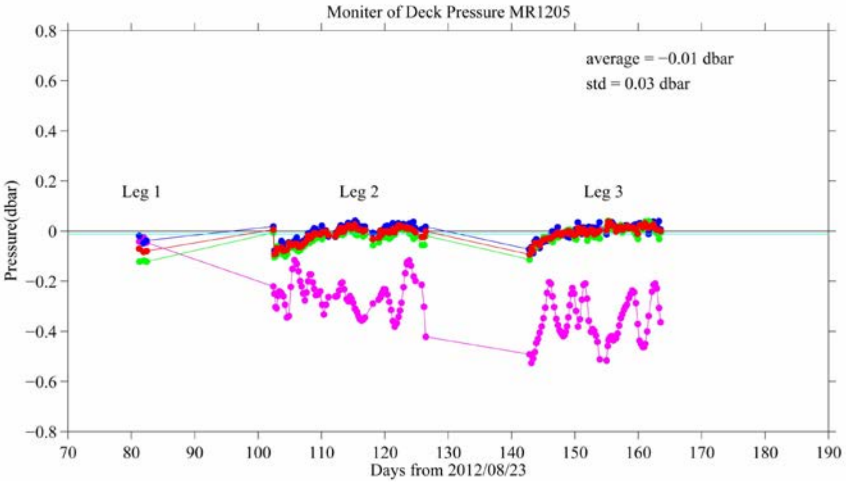

Fig. 3.1.1 Time series of the CTD deck pressure. Atmospheric pressure deviation (magenta dots) from a standard atmospheric pressure was subtracted from the CTD deck pressure. Blue and green dots indicate pre- and post-cast deck pressures, respectively. Red dots indicate averages of the pre- and the post-cast deck pressures.

ii. Temperature

The CTD temperature sensors (SBE 3) were calibrated with the SBE 35 under the assumption that discrepancies between SBE 3 and SBE 35 data were due to pressure sensitivity, the viscous heating effect, and time drift of the SBE 3, according to a method by Uchida et al. (2007).

Post-cruise sensor calibration for the SBE 35 will be performed at SBE, Inc in August 2013.

The CTD temperature was preliminary calibrated as

Calibrated temperature = $T - (c_0 \times P + c_1 \times t + c_2)$

where T is CTD temperature in °C, P is pressure in dbar, t is time in days from pre-cruise calibration date of the CTD temperature and c_0, c_1, and c_2 are calibration coefficients. The coefficients were determined using the data for the depths deeper than 950 dbar.

The primary temperature data were basically used for the post-cruise calibration. The secondary temperature sensor was also calibrated and used instead of the primary temperature data when the data quality of the primary temperature data was bad. The calibration coefficients are listed in Table 3.1.1. The results of the post-cruise calibration for the CTD temperature are summarized in Table 3.1.2 and shown in from Fig. 3.1.2 to Fig. 3.1.6.

Table 3.1.1 Calibration coefficients for the CTD temperature sensors.

Leg	Serial number	c_0 (°C/dbar)	c_1 (°C/day)	c_2 (°C)	Station
1	4815	-	-	0.0009	
2	4815	–1.54321e–8	2.87072e-5	–0.0071	~025
		1.72901e-8	–8.25355e-6	0.0035	026~
2	1464	9.52754e-8	7.92269e-5	–0.0057	~025
		1.09093e-7	–3.12326e-6	0.0011	026~
3	4815	–4.63955e-9	3.34095e-6	0.0001	
3	1464	7.28496e-8	1.32368e-5	–0.0006	

Table 3.1.2 Difference between the CTD temperature and the SBE 35 after the post-cruise calibration. Mean and standard deviation (Sdev) are calculated for the data below and above 950 dbar. Number of data used is also shown.

Leg	Serial number	Pressure ≥ 950 dbar			Pressure < 950 dbar		
		Number	Mean (mK)	Sdev (mK)	Number	Mean (mK)	Sdev (mK)
1	4815	18	0.0	0.5	45	1.2	6.9
2	4815	1056	0.0	0.2	1295	0.4	5.3
2	1464	1054	0.0	0.2	1306	–0.0	4.8
3	4815	1010	–0.0	0.2	1246	0.3	4.7
3	1525	1002	0.0	0.3	1251	–0.6	4.4

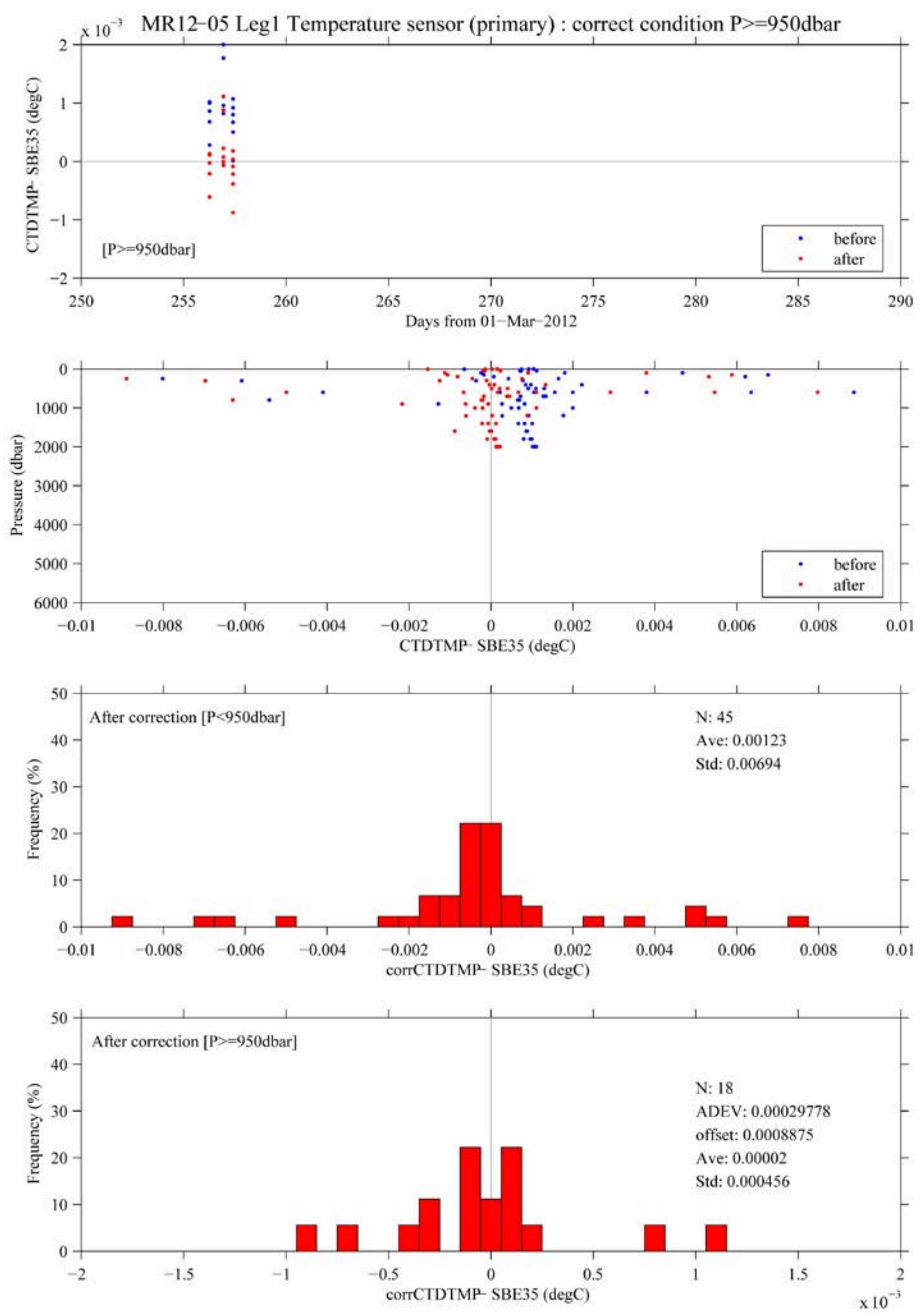

Fig. 3.1.2 Difference between the CTD temperature (primary) and the SBE 35 for leg 1. Blue and red dots indicate before and after the post-cruise calibration using the SBE 35 data, respectively. Lower two panels show histogram of the difference after the calibration.

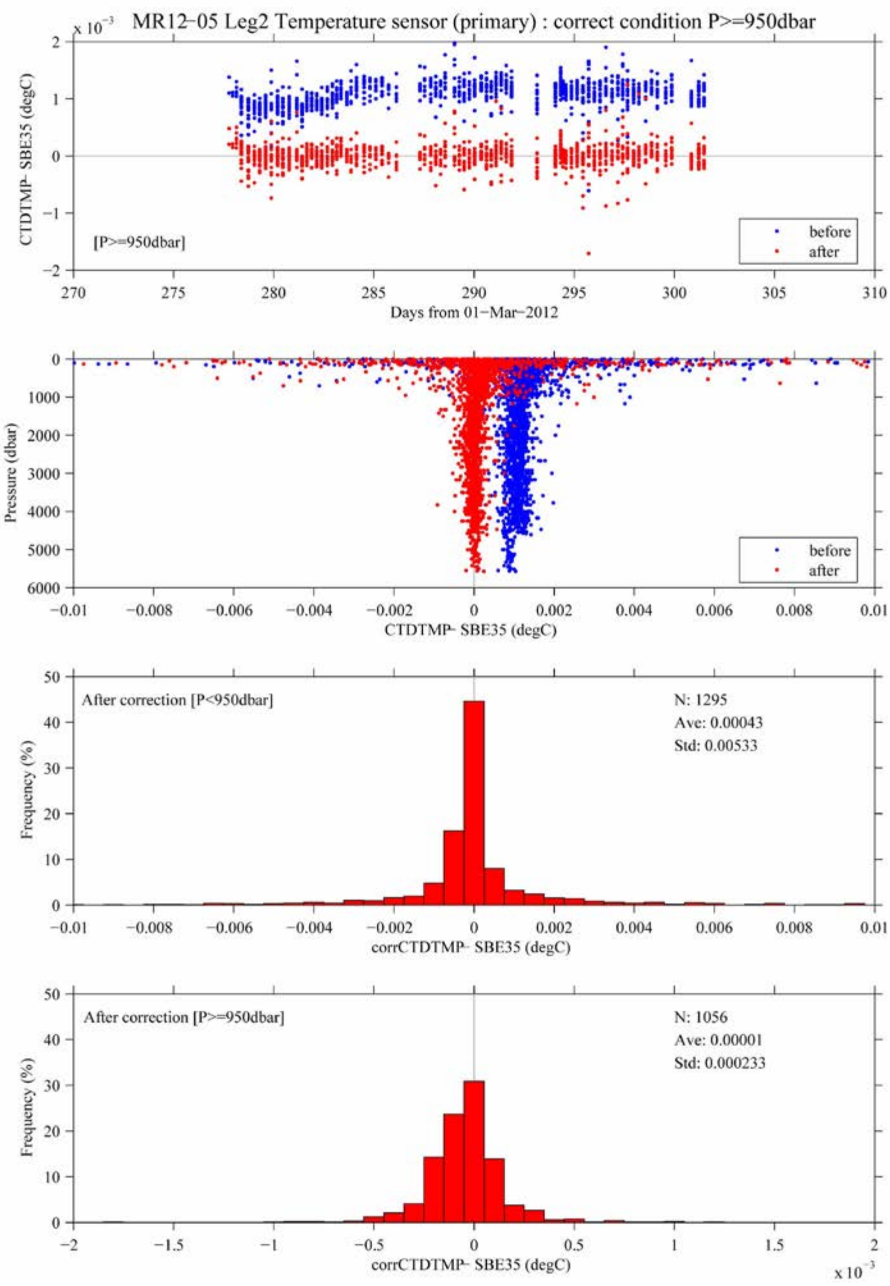

Fig. 3.1.3 Same as Fig. 3.1.2, but for 2.

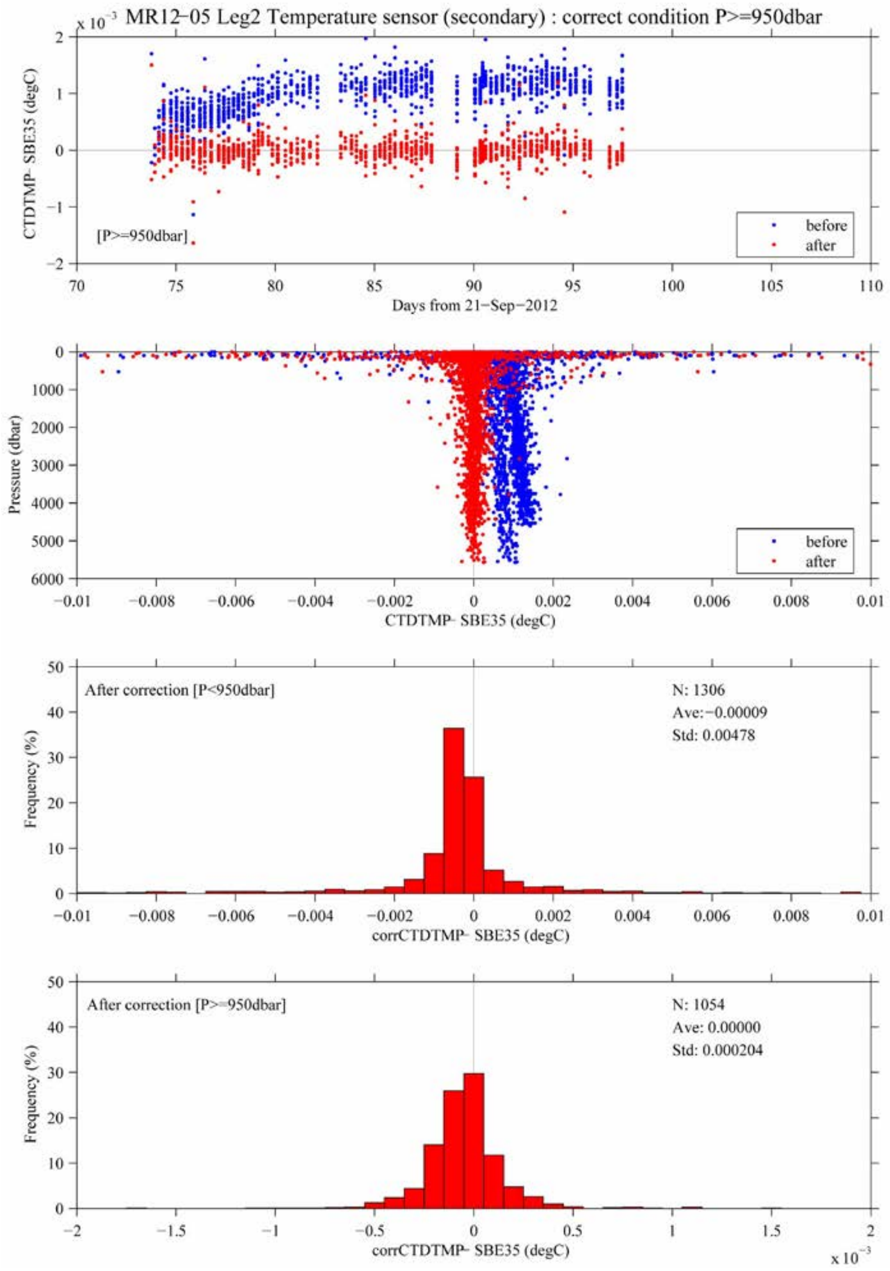

Fig. 3.1.4 Same as Fig. 3.1.2, but for secondary temperature sensor for leg 2.

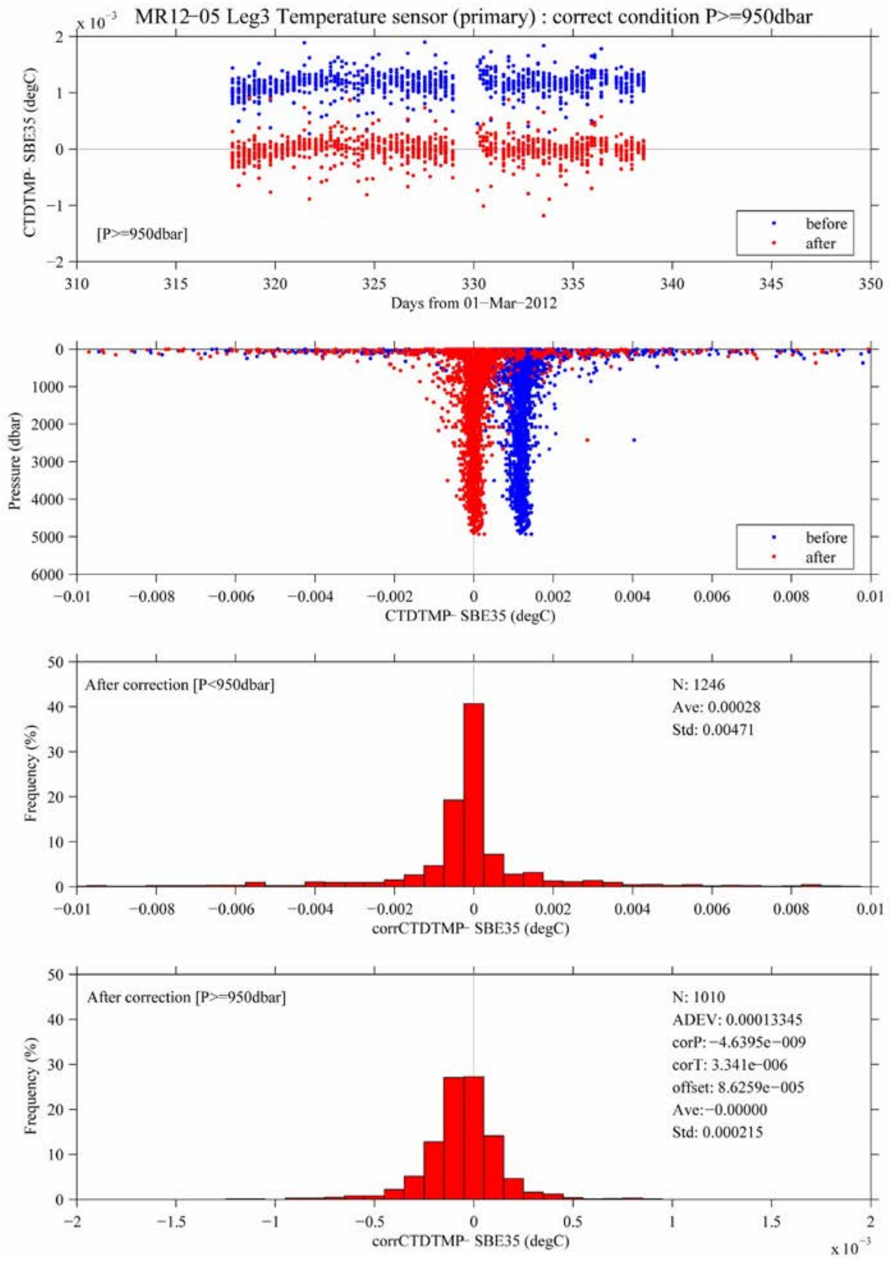

Fig. 3.1.5 Same as Fig. 3.1.2, but for leg 3.

.

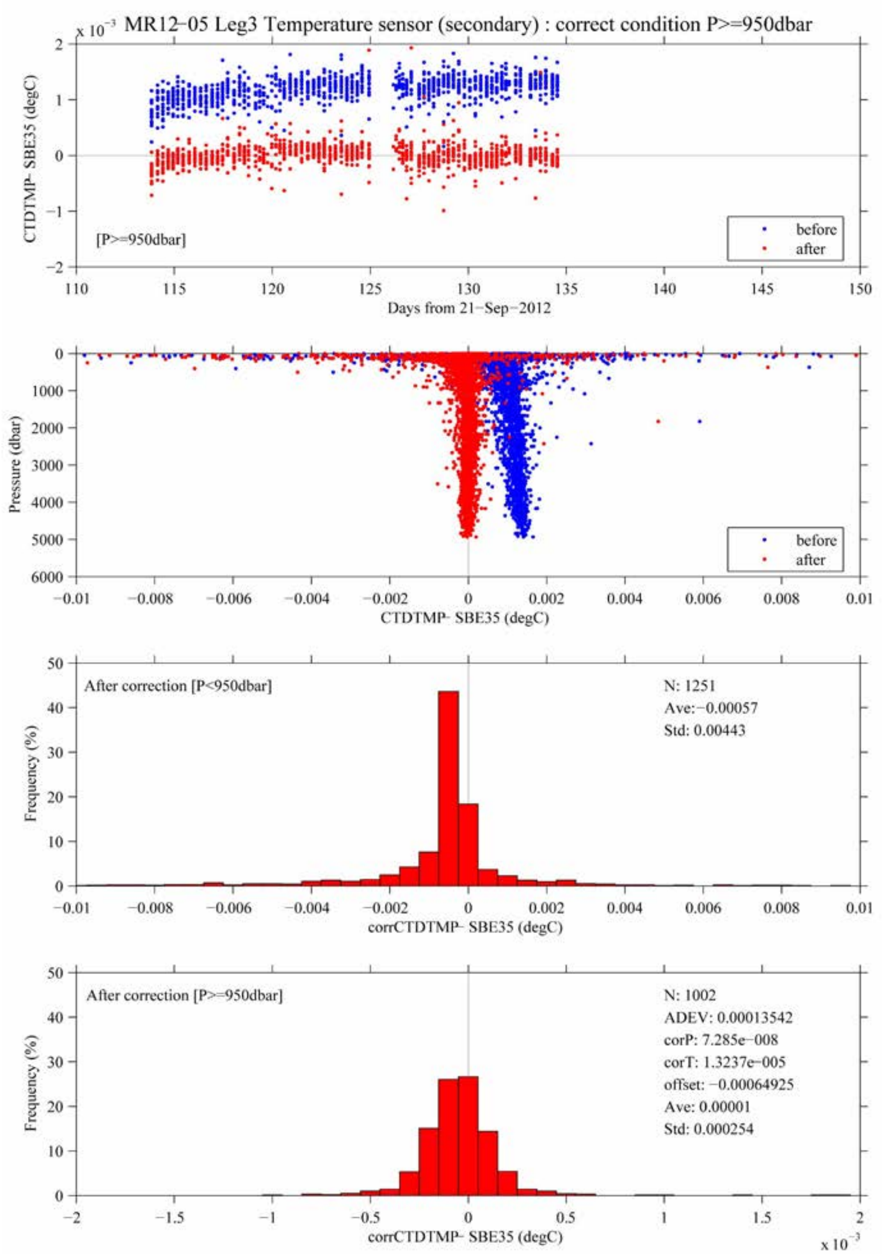

Fig. 3.1.6 Same as Fig. 3.1.2, but for secondary temperature sensor for leg 3.

iii. Salinity

The discrepancy between the CTD conductivity and the conductivity calculated from the bottle salinity data with the CTD temperature and pressure data is considered to be a function of conductivity, pressure and time. The CTD conductivity was calibrated as

$$\text{Calibrated conductivity} = c_0 \times C + c_1 \times P + c_2 \times C \times P + c_3 \times t + c_4$$

where C is CTD conductivity in S/m, P is pressure in dbar, t is time in days from 14 April 2009 and c_0, c_1, c_2, c_3 and c_4 are calibration coefficients. The best fit sets of coefficients were determined by a least square technique to minimize the deviation from the conductivity calculated from the bottle salinity data.

.

The primary conductivity data created by the software module ROSSUM were basically used after the post-cruise calibration for the temperature data. The secondary conductivity sensor was also calibrated and used instead of the primary conductivity data when the data quality of the primary temperature or conductivity data was bad. The coefficients were determined for each leg. The calibration coefficients are listed in Table 3.1.3. The results of the post-cruise calibration for the CTD salinity are summarized in Table 3.1.4 and shown in from Fig. 3.1.7 to Fig. 3.1.11.

Table 3.1.3 Calibration coefficients for the CTD conductivity sensors.

Leg	Serial Number	c_0	c_1 [S/(m dbar)]	c_2 (1/dbar)	c_3 [S/(m day)]	c_4 (S/m)	Station
1	2854	–7.70527e–5	1.39303e–6	–4.83208e–7	–4.97522e–5	5.04388e–4	
2	2435	1.31818e–4	4.00954e–7	–1.14786e–7	–6.09242e–6	–5.06603e–4	
2	2854	1.02000e–4	1.61048e–7	–4.41938e–8	–4.80557e–6	–4.38375e–4	
3	2435	3.18511e–4	1.06019e–6	–3.37484e–7	–2.48779e–5	–1.11175e–3	~110
		2.04845e–4	5.84160e–7	–1.79325e–7	–4.40484e–6	–8.93388e–4	111~
3	2854	1.96052e–4	8.09425e–7	–2.62172e–7	–3.45533e–5	–6.80743e–4	
		8.92585e–5	–9.12391e–8	3.75737e–8	–7.47841e–7	–5.49522e–4	

Table 3.1.4 Difference between the CTD salinity and the bottle salinity after the post-cruise calibration. Mean and standard deviation (Sdev) (in 10^{-3}) are calculated for the data below and above 950 dbar. Number of data used is also shown.

Leg	Serial number	Pressure ≥ 950 dbar			Pressure < 950 dbar		
		Number	Mean	Sdev	Number	Mean	Sdev
1	2854	18	0.1	0.3	39	1.3	7.5
2	2435	989	0.0	0.4	1156	–0.5	3.6
2	2854	987	–0.0	0.4	1167	–0.2	3.6
3	2435	1006	–0.0	0.4	1225	–0.0	5.5
3	2854	996	–0.0	0.4	1230	0.1	5.8

.

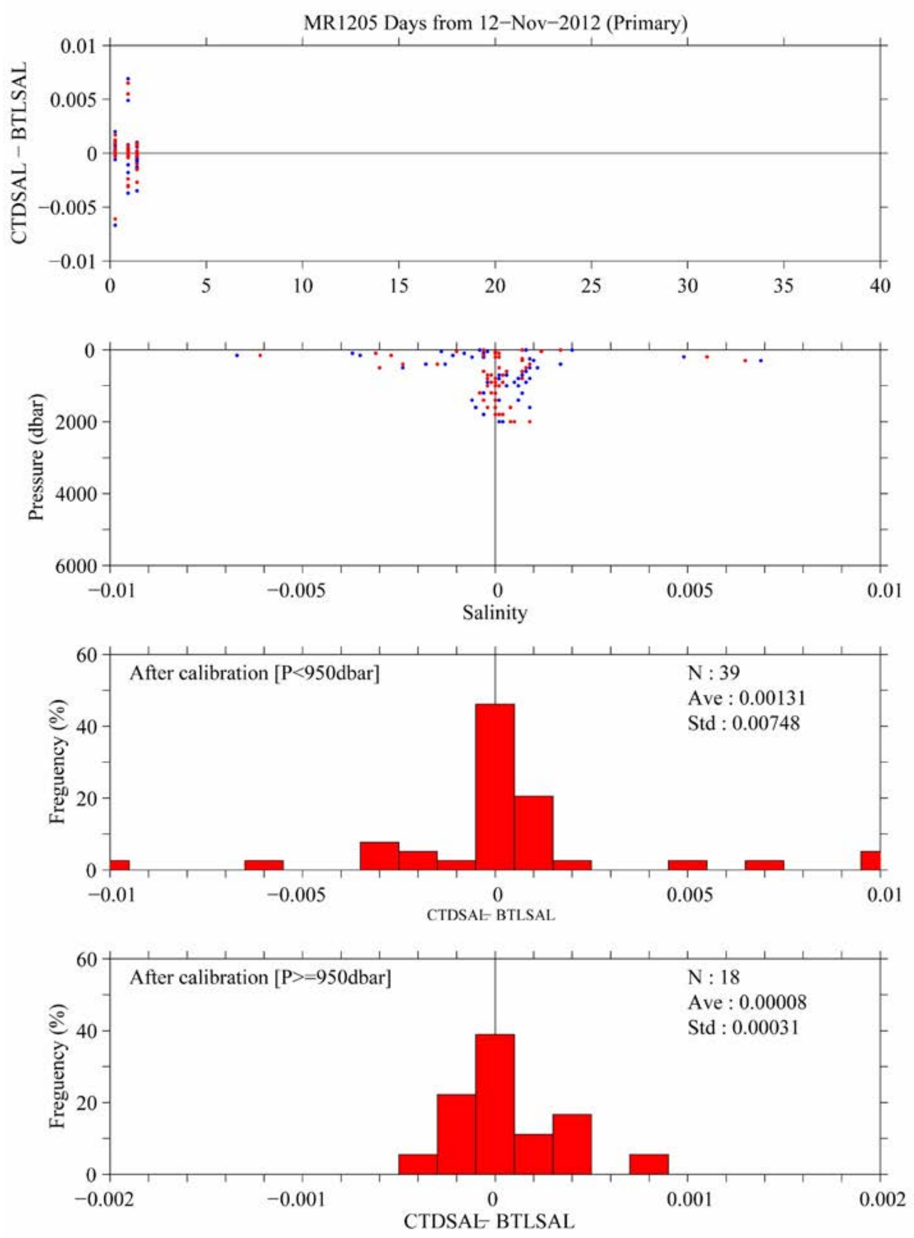

Fig. 3.1.7 Difference between the CTD salinity (primary) and the bottle salinity for leg 1. Blue and red dots indicate before and after the post-cruise calibration, respectively. Lower two panels show histogram of the difference after the calibration.

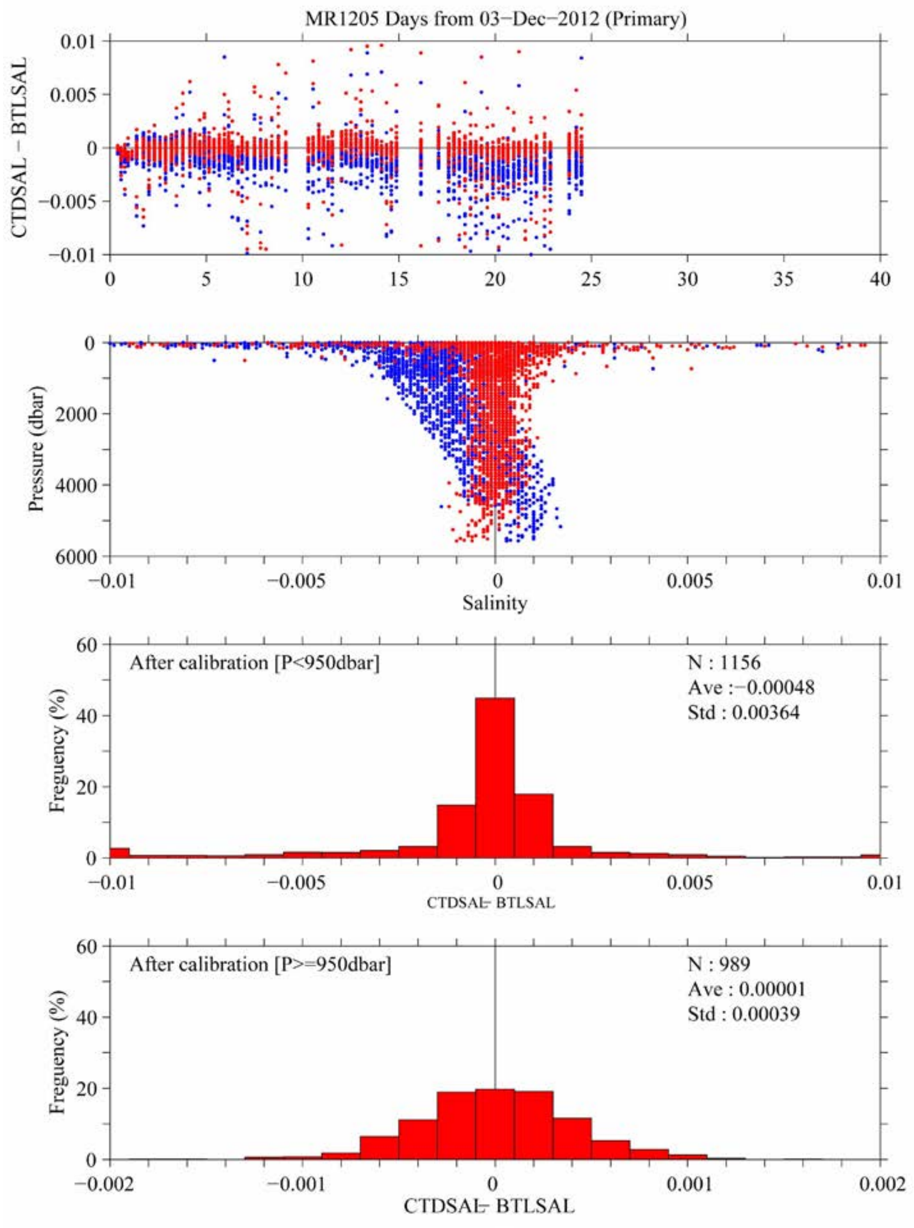

Fig. 3.1.8 Same as Fig. 3.1.7, but for leg 2.

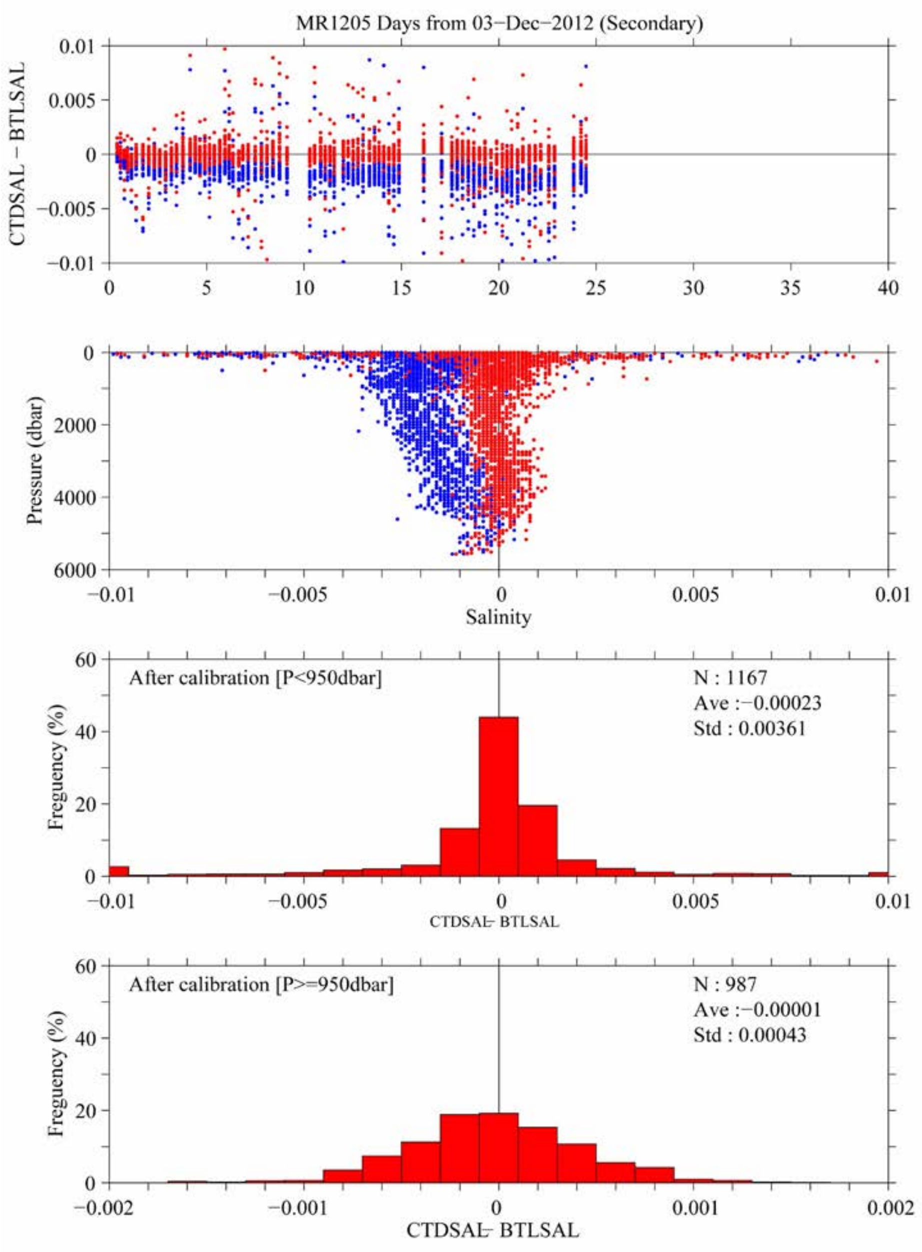

Fig. 3.1.9 Same as Fig. 3.1.7, but for secondary salinity data for leg 2.

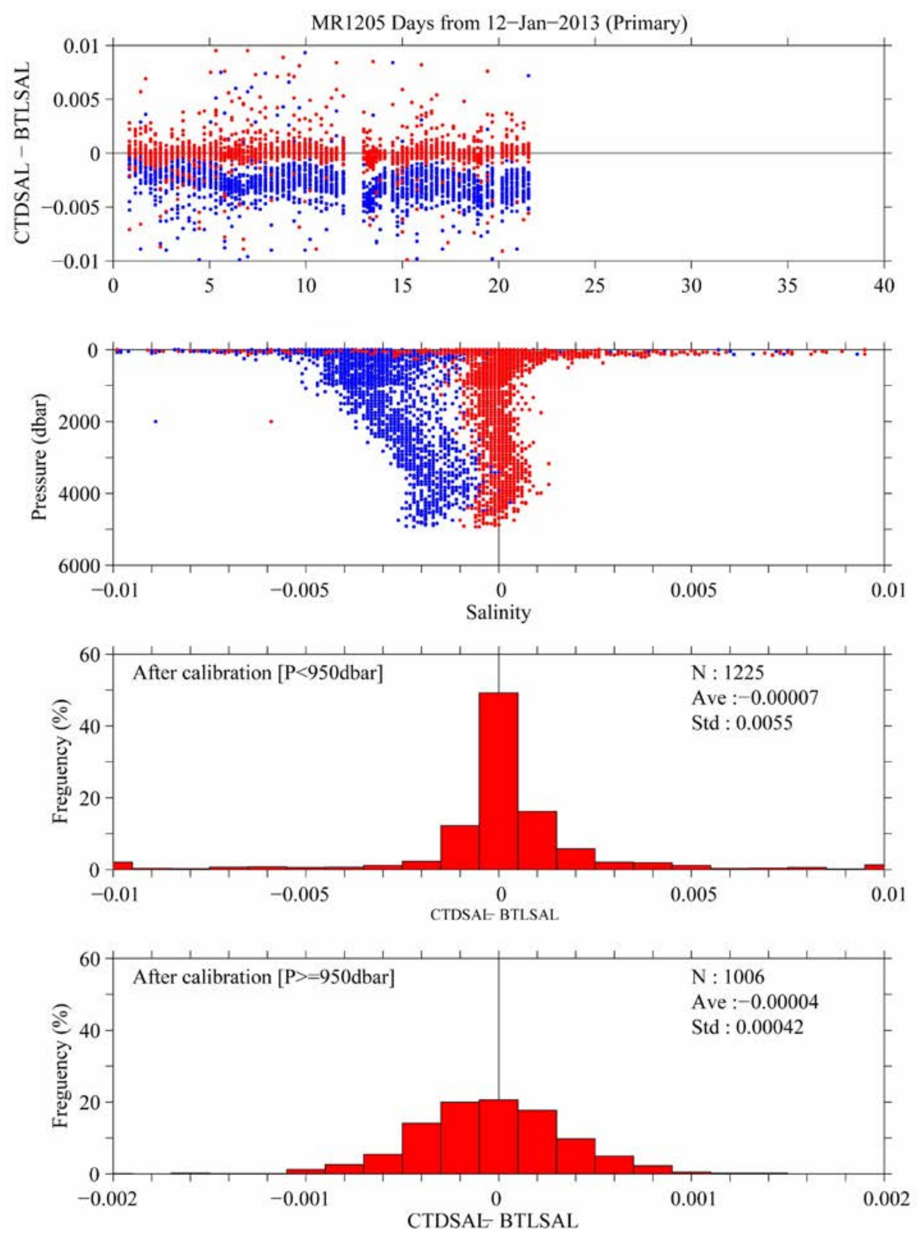

Fig. 3.1.10 Same as Fig. 3.1.7, but for leg 3.

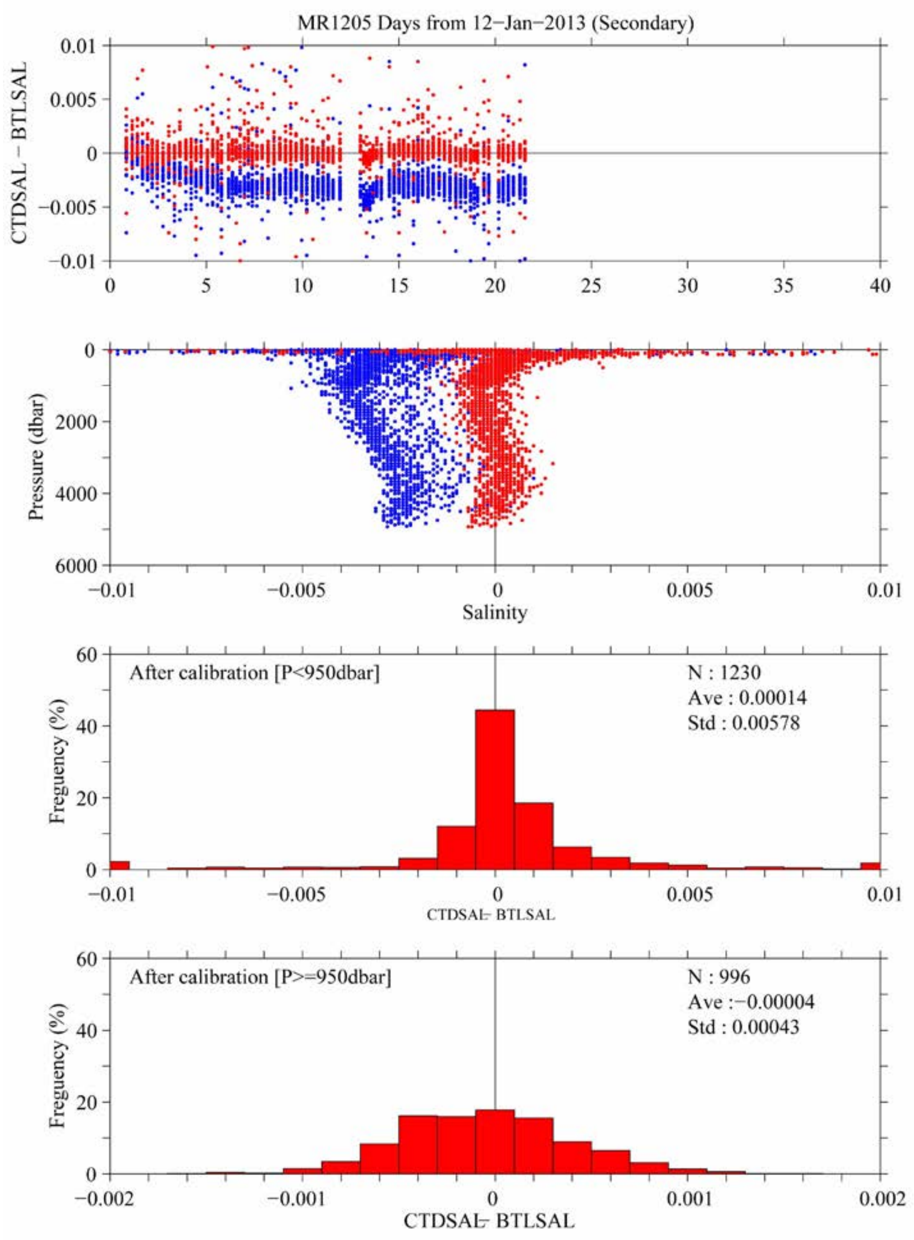

Fig. 3.1.11 Same as Fig. 3.1.7, but for secondary salinity data for leg 3.

iv. Oxygen

The RINKO oxygen optode (S/N 0024) was calibrated and used as the CTD oxygen data, since the RINKO has a fast time response. The pressure-hysteresis corrected RINKO data was calibrated by the modified Stern-Volmer equation, basically according to a method by Uchida et al. (2010) with slight modification:

$$[O_2]\ (\mu mol/l) = [(V_0 / V)^{1.2} - 1] / K_{sv}$$

and

$$K_{sv} = C_0 + C_1 \times T + C_2 \times T^2$$

$$V_0 = 1 + C_3 \times T$$

$$V = C_4 + C_5 \times V_b + C_6 \times t + C_7 \times t \times V_b$$

where V_b is the RINKO output (voltage), V_0 is voltage in the absence of oxygen, T is temperature in °C, and t is exciting time (days) integrated from the first CTD cast for each leg. Time drift of the RINKO output was corrected. The calibration coefficients were determined by minimizing the sum of absolute deviation with a weight from the bottle oxygen data. The revised quasi-Newton method (DMINF1) was used to determine the sets.

The post-cruise calibrated temperature and salinity data were used for the calibration. The calibration coefficients are listed in Table 3.1.4. The results of the post-cruise calibration for the RINKO oxygen are summarized in Table 3.1.5 and shown in from Fig. 3.1.12 to Fig. 3.1.14.

Table 3.1.4 Calibration coefficients for the RINKO oxygen sensors.

Leg	c_0	c_1	c_2	c_3	c_4	c_5
1	4.733362e-3	1.729522e-4	2.164708e-6	-1.431144e-3	-7.402308e-2	3.205825e-1
2	5.644516e-3	2.046661e-4	2.784686e-6	-3.090264e-3	-0.1119851	0.3162570
3	4.729148e-3	2.002866e-4	3.871103e-6	8.659935e-4	-9.234123e-2	0.3306834

Table 3.1.4 Continue.

Leg	c_6	c_7
1	-	-
2	-1.036494e-4	2.598641e-4
3	-2.497366e-4	2.824747e-4

Table 3.1.5 Difference between the RINKO oxygen and the bottle ooxygen after the post-cruise calibration. Mean and standard deviation (Sdev) are calculated for the data below and above 950 dbar. Number of data used is also shown.

Leg	Serial number	Pressure ≥ 950 dbar			Pressure < 950 dbar		
		Number	Mean [μmol/kg]	Sdev	Number	Mean [μmol/kg]	Sdev
1	0024	52	0.00	0.11	40	0.02	0.45
2	0024	987	–0.01	0.29	1157	0.09	1.00
3	0024	1009	–0.04	0.29	1245	–0.02	0.90

.

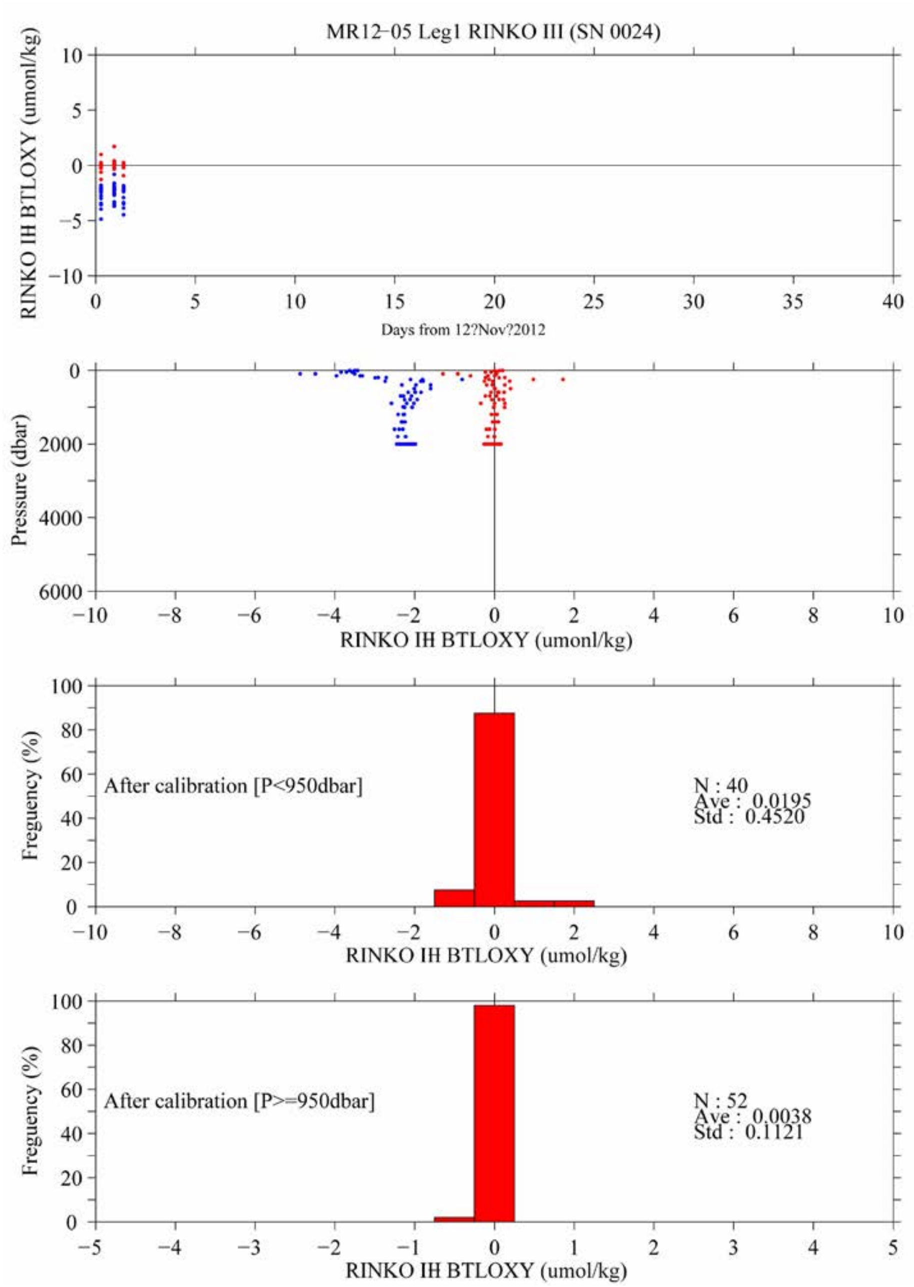

Fig. 3.1.12 Difference between the CTD oxygen and the bottle oxygen for leg 1. Blue and red dots indicate before and after the post-cruise calibration, respectively. Lower two panels show histogram of the difference after the calibration.

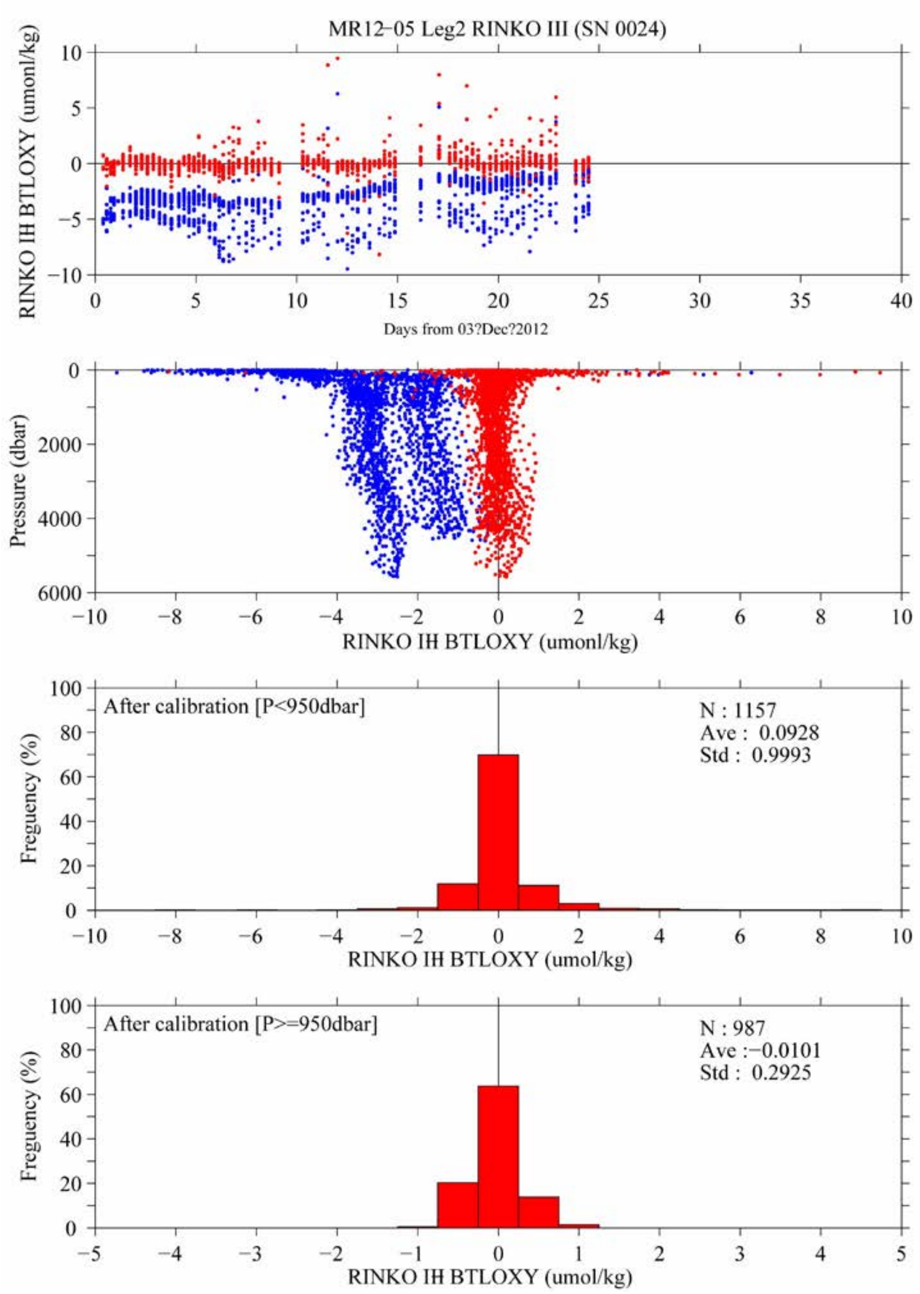

Fig. 3.1.13 Same as Fig. 3.1.12, but for leg 2.

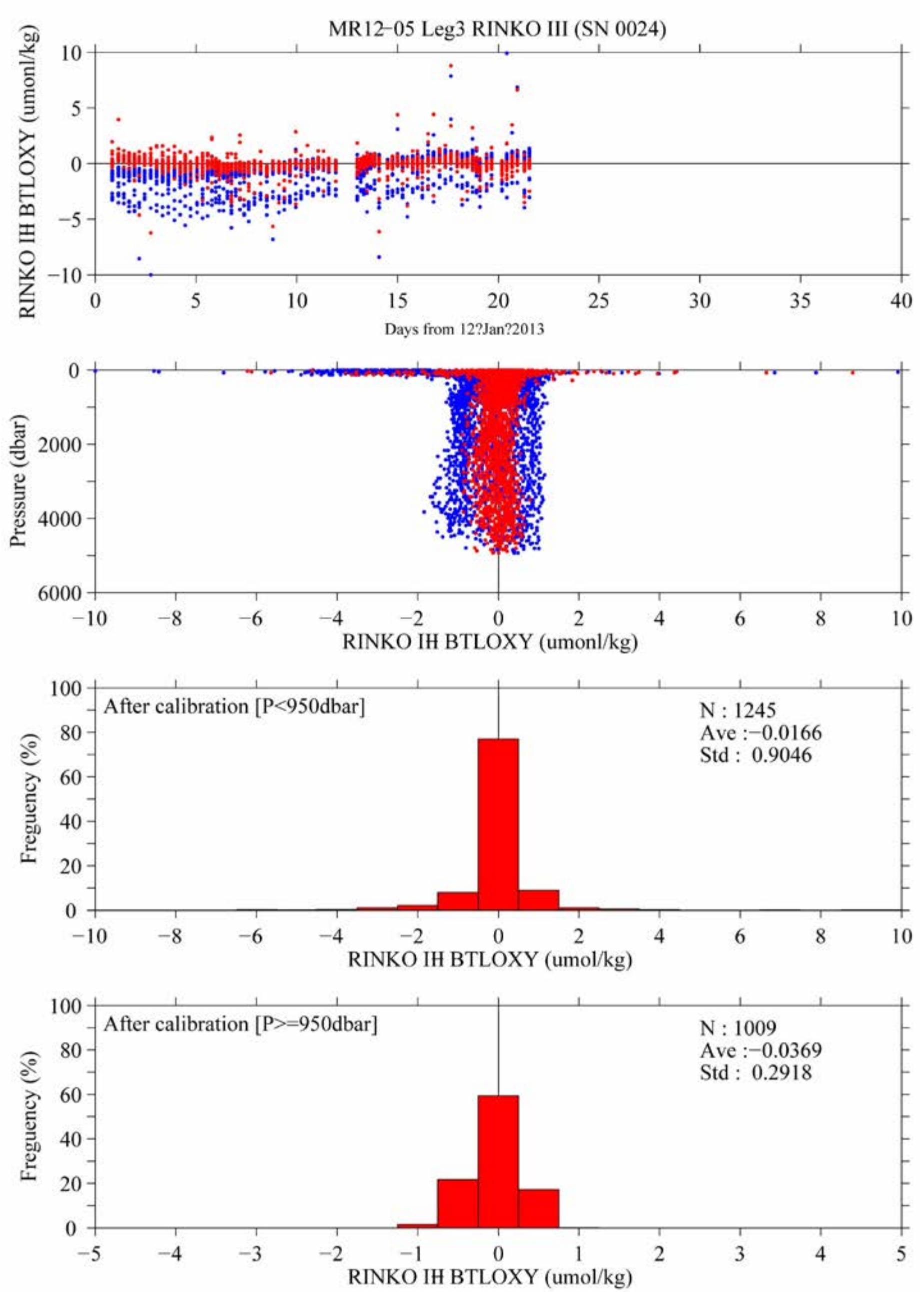

Fig. 3.1.14 Same as Fig. 3.1.12, but for leg 3.

v. Fluorometer

(in preparation)

vi. Transmissometer

(in preparation)

vii. PAR

(in preparation)

.

References

Edwards, B., D. Murphy, C. Janzen and N. Larson (2010): Calibration, response, and hysteresis in deep-sea dissolved oxygen measurements, *J. Atmos. Oceanic Technol.*, 27, 920–931.

Fukasawa, M., T. Kawano and H. Uchida (2004): Blue Earth Global Expedition collects CTD data aboard Mirai, BEAGLE 2003 conducted using a Dynacon CTD traction winch and motion-compensated crane, *Sea Technology*, 45, 14–18.

García, H. E. and L. I. Gordon (1992): Oxygen solubility in seawater: Better fitting equations. *Limnol. Oceanogr.*, 37 (6), 1307–1312.

Uchida, H., G. C. Johnson, and K. E. McTaggart (2010): CTD oxygen sensor calibration procedures, The GO-SHIP Repeat Hydrography Manual: A collection of expert reports and guidelines, IOCCP Rep., No. 14, ICPO Pub. Ser. No. 134.

Uchida, H., K. Ohyama, S. Ozawa, and M. Fukasawa (2007): In situ calibration of the Sea-Bird 9plus CTD thermometer, *J. Atmos. Oceanic Technol.*, 24, 1961–1967.

.

3.2 Bottle Salinity

(1) Personnel

Hiroshi Uchida (JAMSTEC)
Tatsuya Tanaka (MWJ) (Legs 1 and 2)
Hiroki Ushiromura (MWJ) (Leg 3)
Tamami Ueno (MWJ) (Leg 3)
Keisuke Tsubata (MWJ) (Leg 2)

(2) Objectives

Bottle salinities were measured to calibrate CTD salinity data.

(3) Instrument and Method

Salinity measurement was conducted basically based on a method by Kawano (2010).

i. Salinity Sample Collection

The bottles in which the salinity samples were collected and stored were 250 ml Phoenix brown glass bottles with screw caps. Each bottle was rinsed three times with sample water and was filled to the shoulder of the bottle. The caps were also thoroughly rinsed. Salinity samples were stored more than 24 hours in the same laboratory as the salinity measurement was made.

ii. Instruments and Methods

Salinity of water samples was measured with two salinometers (Autosal model 8400B; Guildline Instruments Ltd., Ontario, Canada; S/N 62556 for leg 1 and S/N 62827 for legs 2 and 3), which was modified by adding an peristaltic-type intake pump (Ocean Scientific International Ltd., Hampshire, UK) and two platinum thermometers (Guildline Instruments Ltd., model 9450). One thermometer monitored an ambient temperature and the other monitored a salinometer’s bath temperature. The resolution of the thermometers was 0.001 °C. The measurement system was almost same as Aoyama et al. (2002). The salinometer was operated in the air-conditioned laboratory of the ship at a bath temperature of 24 °C.

The ambient temperature varied from approximately 20 to 24 °C, while the bath temperature was stable and varied within ±0.002 °C. A measure of a double conductivity ratio of a sample was taken as a median of 31 readings. Data collection was started after 10 seconds and it took about 10 seconds to collect 31 readings by a personal computer. Data were sampled for the sixth and seventh filling of the cell. In case where the difference between the double conductivity ratio of this two fillings was smaller than 0.00002, the average value of the two double conductivity ratios was used to calculate the bottle salinity with the algorithm for practical salinity scale, 1978 (UNESCO, 1981). When the difference was grater than or equal to the 0.00003, we measured another additional filling of the cell. In case where the double conductivity ratio of the additional filling did not satisfy the criteria above, we measured other additional fillings of the cell within 10 fillings in total. In case where the number of fillings was 10 and those fillings did not satisfy the criteria above, the median of the double conductivity ratios of five fillings were used to calculate the bottle salinity.

The measurement was conducted about from 6 to 23 hours per day and the cell was cleaned with soap after the measurement for each day. A total of about 5700 water samples were measured during the cruise.

(4) Results

i. Standard Seawater

Standardization control was set to 688 (leg 1), 509 (leg 2), and 514 (leg 3). The value of STANDBY was 5197±0001 (leg 1), 5432±0002 (leg 2), and 5438±0002 (leg 3), and that of ZERO was 0.00000 or -0.00001 for all legs. We used IAPSO Standard Seawater batch P154 whose conductivity ratio is 0.99990 (double conductivity ratio is 1.99980) as the standard for salinity measurement. We measured 8 (leg 1), 98 (leg 2), and 115 (leg 3) bottles of the Standard Seawater during the cruise. Histories of double conductivity ratio measurement of the Standard Seawater are shown in Figs. 3.2.1 (leg 1), 3.2.2 (leg 2), and 3.2.3 (leg 3).

Time drift of the salinometer was corrected by using the Standard Seawater measurements. For leg 1, offset of the salinometer was estimated from the average of the Standard Seawater measurement for each day because number of data was small. For legs 2 and 3, linear time drift of the salinometer was estimated from the Standard Seawater measurement by using the least square method (thin black lines in Figs. 3.2.2 and 3.2.3). For leg 2, linear time drift was calculated for two periods before and after December 15, 2013, because tendency of the time drift was changed during the cruise. The average of double conductivity ratio was 1.99980 and the standard deviation was 0.00001, which is equivalent to 0.0002 in salinity after the time drift correction.

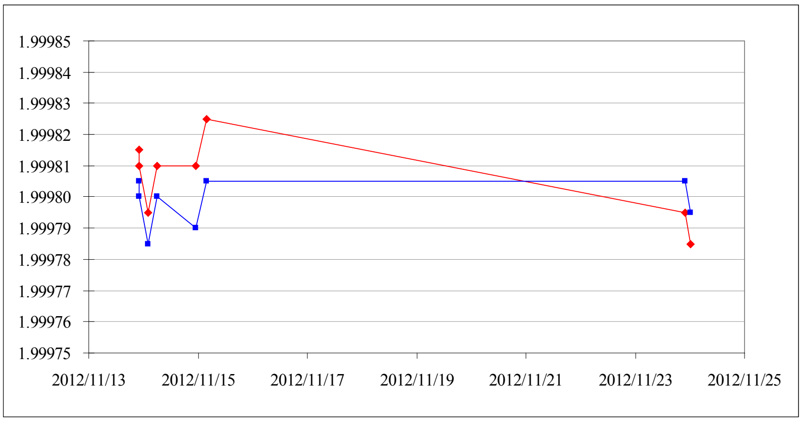

Fig. 3.2.1. History of double conductivity ratio measurement of the Standard Seawater (P154) during leg1. Horizontal and vertical axes represents date and double conductivity ratio, respectively. Blue dots indicate raw data and red dots indicate corrected data.

.

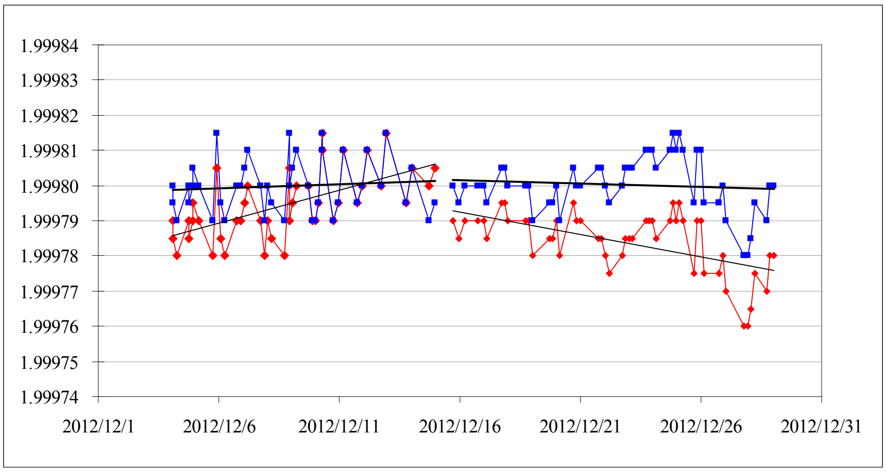

Fig. 3.2.2. Same as Fig. 3.2.1, but for leg 2.

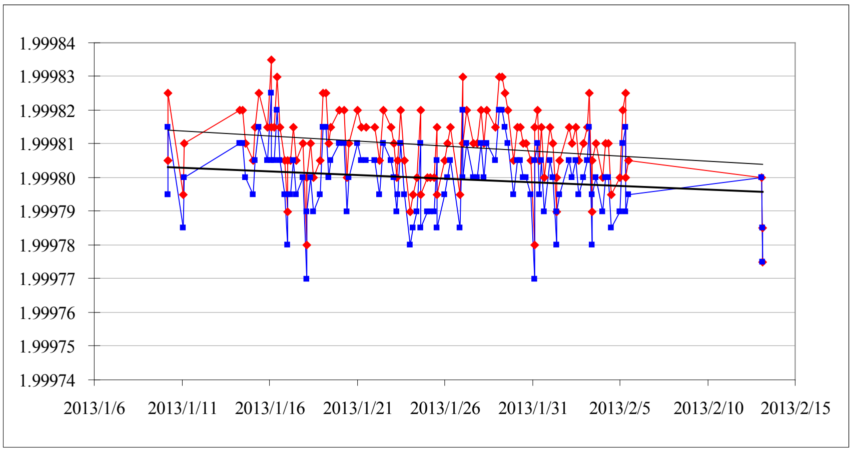

Fig. 3.2.3. Same as Fig. 3.2.1, but for leg 3.

ii. Sub-Standard Seawater

We also used sub-standard seawater which was deep-sea water filtered by pore size of 0.45 μm and stored in a 20 liter cubitainer made of polyethylene and stirred for at least 24 hours before measuring. It was measured every 6 samples in order to check the possible sudden drift of the salinometer. During the whole measurements, there was no detectable sudden drift of the salinometer.

iii. Replicate Samples

We took 12 (leg 1), 419 (leg 2), and 437 (leg 3) pairs of replicate samples during the cruise. Histograms of the absolute difference between replicate samples are shown in Figs. 3.2.4 (leg 1), 3.2.5 (leg 2), and 3.2.6 (leg 3). The root-mean-squares of the absolute deference were 0.00015 (leg 1), 0.00018 (leg 2), and 0.00020 (leg 3).

.

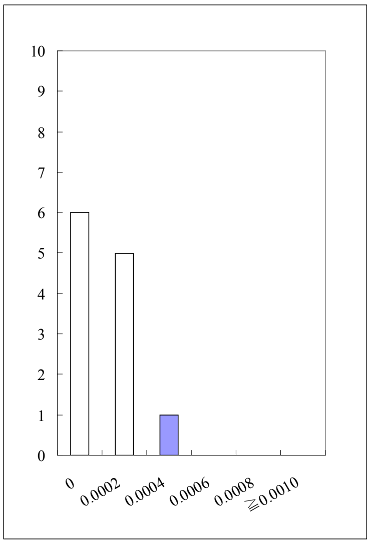

Fig.3.2.4. Histogram of the absolute difference between replicate samples for leg 1. Horizontal axis is absolute difference in salinity and vertical axis is frequency.

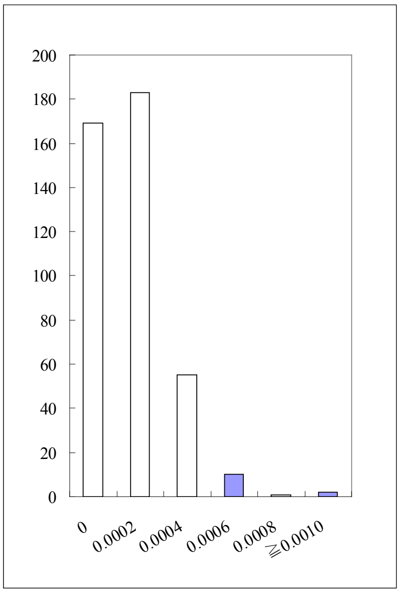

Fig. 3.2.5. Same as Fig. 3.2.4, but for leg 2.

.

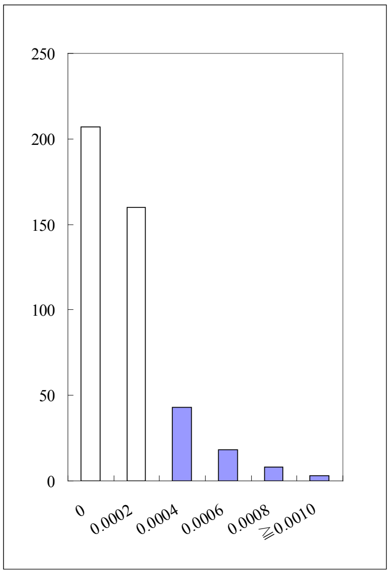

Fig. 3.2.6. Same as Fig. 3.2.4, but for leg 3.

(5) References

Aoyama, M., T. Joyce, T. Kawano and Y. Takatsuki (2002): Standard seawater comparison up to P129. Deep-Sea Research, I, Vol. 49, 1103-1114.

Kawano (2010): Salinity. The GO-SHIP Repeat Hydrography Manual: A collection of Expert Reports and Guidelines, IOCCP Report No. 14, ICPO Publication Series No. 134, Version 1.

UNESCO (1981): Tenth report of the Joint Panel on Oceanographic Tables and Standards. UNESCO Tech. Papers in Mar. Sci., 36, 25 pp.

3.3 Density

(1) Personnel

Hiroshi Uchida (JAMSTEC)

(2) Objectives

The objective of this study is to collect absolute salinity (also called “density salinity”) data, and to evaluate an algorithm to estimate absolute salinity provided along with TEOS-10 (the International Thermodynamic Equation of Seawater 2010) (IOC et al., 2010).

(3) Materials and methods

Seawater densities were measured during the cruise and a part of the seawater samples will be measured in a laboratory in the Japan Agency for Marine-Earth Science and Technology, Yokosuka, Japan, after the cruise with an oscillation-type density meter (DMA 5000M, serial no. 80570578, Anton-Paar GmbH, Graz, Austria) with a sample changer (Xsample 122, serial no. 80548492, Anton-Paar GmbH). The sample changer was used to load samples automatically from up to ninety-six 12-mL glass vials. AC power was supplied to the density meter through a frequency conversion AC power supply unit (AA500F, Takasago, Ltd., Japan).

The water samples were collected in 100-mL aluminum bottles (Mini Bottle Can, Daiwa Can Company, Japan). The bottles were stored at room temperature (~20 ºC) upside down. Densities of the samples were measured at 20 ºC by the density meter from two to several times for each bottle. The bottles were warmed up in a water bath (~30 ºC) for about one hour before measurement.

Time drift of the density meter was monitored by periodically measuring the density of ultra-pure water (Milli-Q water, Millipore, Billerica, Massachusetts, USA) prepared from Yokosuka (Japan) tap water in October 2012. The true density at 20 ºC of the Milli-Q water was estimated to be 998.2042 kg m^{-3} from the isotopic composition ($\delta D = -8.76$ ‰, $\delta^{18}O = -56.86$ ‰) and International Association for the Properties of Water and Steam (IAPWS)-95 standard. An offset correction was applied to the measured density by using the Milli-Q water measurements ($\rho_{\text{Milli-Q}}$) with a slight modification of the density dependency (Uchida et al., 2011). The offset (ρ_{offset}) of the measured density (ρ) was estimated from the following equation:

$$\rho_{\text{offset}} = (\rho_{\text{Milli-Q}} - 998.2042) - (\rho - 998.2042) \times 0.000241 \text{ [kg m}^{-3}\text{]}.$$

The offset correction was verified by measuring Reference Material for Density in Seawater (prototype Dn-RM1) developing with Marine Works Japan, Ltd., Kanagawa, Japan, and produced by Kanso Technos Co., Ltd., Osaka, Japan, and Reference Material for Nutrients in Seawater (RMNS) lot BF (Kanso Technos Co., Ltd.) along with the Milli-Q water. Density salinity can be back calculated from measured density and temperature with TEOS-10.

(4) Reference

IOC, SCOR and IAPSO (2010): The international thermodynamic equation of seawater – 2010: Calculation and use of thermodynamic properties. Intergovernmental Oceanographic Commission, Manuals and Guides No. 56, United Nations Educational, Scientific and Cultural Organization (English), 196 pp.

Uchida, H., T. Kawano, M. Aoyama and A. Murata (2011): Absolute salinity measurements of standard seawaters for conductivity and nutrients. *La mer*, 49, 237-244.

.

3.4 Oxygen

April 19, 2013

Yuichiro Kumamoto
Japan Agency for Marine-Earth Science and Technology

(1) Personnel

Yuichiro Kumamoto (JAMSTEC)
Misato Kuwahara (Marine Works Japan Co. Ltd, MWJ)
Kanako Yoshida (MWJ)
Keitaro Matsumoto (MWJ)
Takuhiro Osumi (MWJ)

(2) Objectives

Dissolved oxygen is one of good tracers for the ocean circulation. Climate models predict a decline in oceanic dissolved oxygen concentration and a consequent expansion of the oxygen minimum layers under global warming conditions, which results mainly from decreased interior advection and ongoing oxygen consumption by remineralization. The mechanism of the decrease, however, is still unknown. During MR12-05 cruise, we measured dissolved oxygen concentration from surface to bottom layers at all the hydrocast stations in the western Pacific and Southern Oceans. Most of the stations reoccupied the WOCE Hydrographic Program P14S and S4 stations in the 1990s. Our purpose is to evaluate temporal change in dissolved oxygen concentration in the western Pacific and Southern Oceans between the 1990s and 2012/13.

(3) Reagents

Pickling Reagent I: Manganous chloride solution (3M)
Pickling Reagent II: Sodium hydroxide (8M) / sodium iodide solution (4M)
Sulfuric acid solution (5M)
Sodium thiosulfate (0.025M)
Potassium iodate (0.001667M): Wako Pure Chemical Industries, Ltd., volumetric standard, reference material for iodometry, Lot No.EPR3227, Purity: 99.96±0.01%
CSK standard of potassium iodate: Lot DCE2131, Wako Pure Chemical Industries Ltd., 0.0100N

(4) Instruments

Burette for sodium thiosulfate and potassium iodate;
APB-620 and APB-510 manufactured by Kyoto Electronic Co. Ltd. / 10 cm^3 of titration vessel
Detector;
Automatic photometric titrator, DOT-01X manufactured by Kimoto Electronic Co. Ltd.

(5) Seawater sampling

Following procedure is based on a determination method in the WHP Operations Manual (Dickson, 1996). Seawater samples were collected from 12-liters Niskin sampler bottles attached to the CTD-system. Seawater for bottle oxygen measurement was transferred from the Niskin sampler bottle to a volume calibrated glass flask (ca. 100 cm^3). Three times volume of the flask of seawater was overflowed. Sample temperature was measured by a thermometer during the overflowing. Then two reagent solutions (Reagent I, II) of 0.5 cm^3 each were added immediately into the sample flask and the stopper was inserted carefully into the flask. The sample flask was then shaken vigorously to mix the contents and to disperse the precipitate finely throughout. After the precipitate has settled at least halfway down the flask, the flask was shaken again to disperse the precipitate. The sample flasks containing pickled samples were stored in a laboratory until they were titrated.

(6) Sample measurement

At least two hours after the re-shaking, the pickled samples were measured on board. A magnetic stirrer bar and 1 cm^3 sulfuric acid solution were added into the sample flask and stirring began. Samples were titrated by sodium thiosulfate solution whose molarity was determined by potassium iodate solution. Temperature of sodium thiosulfate during titration was recorded by a thermometer. We measured dissolved oxygen concentration using two sets of the titration apparatus, named DOT-7 and DOT-8. Dissolved oxygen concentration (μmol kg^{-1}) was calculated by the sample temperature during the sampling, bottle salinity, flask volume, and titrated volume of the sodium thiosulfate solution. When the bottle salinity data is flagged to be 3 (questionable), 4 (bad), or 5 (missing), CTD salinity (primary) data is referred in the calculation alternatively.

(7) Standardization

Concentration of sodium thiosulfate titrant (ca. 0.025M) was determined by potassium iodate solution. Pure potassium iodate was dried in an oven at 130°C. 1.7835 g potassium iodate weighed out accurately was dissolved in deionized water and diluted to final volume of 5 dm^3 in a calibrated volumetric flask (0.001667M). 10 cm^3 of the standard potassium iodate solution was added to a flask using a volume-calibrated dispenser. Then 90 cm^3 of deionized water, 1 cm^3 of sulfuric acid solution, and 0.5 cm^3 of pickling reagent solution II and I were added into the flask in order. Amount of titrated volume of sodium thiosulfate (usually 5 times measurements average) gave the molarity of the sodium thiosulfate titrant. Table 3.4.1 shows result of the standardization during this cruise. Coefficient of variation (C.V.) for the standardizations was 0.02±0.01 % (n = 67), c.a. 0.05 μmol kg^{-1}.

(8) Determination of the blank

The oxygen in the pickling reagents I (0.5 cm^3) and II (0.5 cm^3) was assumed to be 3.8 × 10^{-8} mol (Murray *et al.*, 1968). The blank from the presence of redox species apart from oxygen in the reagents (the pickling reagents I, II, and the sulfuric acid solution) was determined as follows. 1 and 2 cm^3 of the standard potassium iodate solution were added to two flasks respectively. Then 100 cm^3 of deionized water, 1 cm^3 of sulfuric acid solution, and 0.5 cm^3 of pickling reagent solution II and I each were added into the two flasks in order. The blank was determined by difference between the two times of the first (1 cm^3 of KIO_3) titrated volume of the sodium thiosulfate and the second (2 cm^3 of KIO_3) one. The results of 3 times blank determinations were averaged (Table 3.4.1). The averaged blank values for DOT-7 and

DOT-8 were 0.003±0.001 (standard deviation, S.D., n=34) and 0.001±0.001 (S.D., n=33) cm^3, respectively.

Table 3.4.1 Results of the standardization (End point, E.P.) and the blank determinations (cm^3).

(9)

Date	KIO$_3$ No.		Na$_2$S$_2$O$_3$ No.	DOT-7		DOT-8		Stations
(UTC)	#	ID No.		E.P.	blank	E.P.	blank	
2012/11/06	03	20120417-03-03	20120615-16	3.970	0.003	3.964	0.002	C01,C02,C03
2012/12/04		20120417-03-11	20120615-16	3.972	0.003	3.967	0.001	008-011
2012/12/06		20120417-03-09	20120615-17	3.969	0.004	3.965	0.001	012-022
2012/12/09		20120417-03-06	20120615-17	3.967	0.002	3.963	0.001	023-027,402,404,406
2012/12/11		20120417-03-10	20120615-18	3.968	0.003	3.964	-0.001	408,410,050-054
2012/12/14	04	20120419-04-01	20120615-18	3.966	0.001	3.962	0.002	055-062
2012/12/16		20120419-04-09	20120615-19	3.969	0.002	3.965	0.001	063-068,C04,069-071
2012/12/21		20120419-04-07	20120615-19	3.966	0.002	3.962	0.001	072-078
2012/12/23		20120419-04-08	20120615-20	3.968	0.002	3.964	0.001	079-085
2012/12/25		20120419-04-03	20120615-20	3.966	0.003	3.962	0.002	086-088,501,502,503
2013/01/08		20120419-04-05	20120615-21	3.970	0.003	3.966	0.001	088-091
2013/01/14		20120419-04-06	20120615-21	3.970	0.002	3.966	0.002	092-102
2013/01/17		20120419-04-02	20120615-22	3.970	0.002	3.967	0.000	103-116
2013/01/20	05	20120419-05-01	20120615-22	3.969	0.003	3.966	0.000	117-122
2013/1/21		20120419-05-02	20120615-23	3.970	0.002	3.966	0.001	123-130,140,139,138,137
2013/1/25		20120419-05-03	20120615-23	3.969	0.004	3.966	0.003	136,135,134,131,132,133
2013/1/27		20120419-05-05	20120615-24	3.975	0.002	3.971	0.000	141-150
2013/1/29		20120419-05-04	20120615-24	3.970	0.001	3.967	0.000	151-158
2013/2/1		20120419-05-07	20120615-25	3.967	0.002	3.962	0.001	162-165,167,166

Replicate sample measurement

From a routine CTD cast at all the stations, a pair of replicate samples was collected at four layers of 25, 400, 1500, and 3500 dbars. In order to estimate uncertainty including instrumental error, two samples of a replicate pair were measured using DOT-7 and DOT-8 separately. The total number of the replicate sample pairs in good measurement (flagged 2) was 550 (Fig. 3.4.1). The standard deviation of the replicate measurement was 0.09 µmol kg^{-1} calculated by a procedure (SOP23) in DOE (1994). In the hydrographic data sheet, a mean of replicate sample pairs is listed with the flag 2 (see section 12).

.

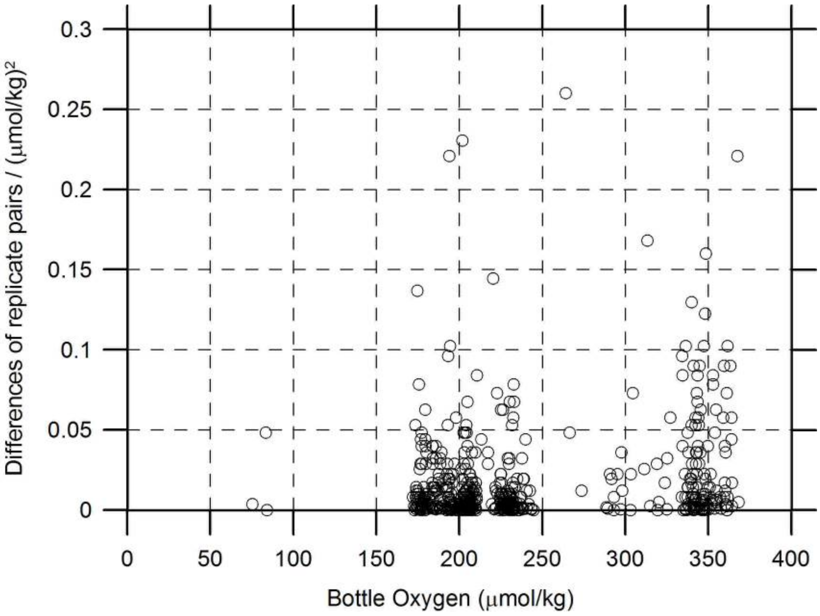

Figure 3.4.1 Oxygen difference between measurements of a replicate pair against oxygen concentration.

(10) Duplicate sample measurement

During the leg-1 duplicate samples were taken from 18 Niskin bottles at stations C01 and C02 each (Table 3.4.2). The duplicate samples were measured using both DOT-7 and DOT-8 in order to estimate uncertainty due to the apparatus. The standard deviation of the duplicate measurements at stations C01 and C02 were calculated to be 0.12 and 0.07 μmol kg^{-1}, respectively, which were equivalent with that of the replicate measurements (0.09 μmol kg^{-1}, see section 9).

(11) CSK standard measurements

The CSK standard is a commercial potassium iodate solution (0.0100 N) for analysis of dissolved oxygen. We titrated the CSK standard solutions (Lot DCE2131) against our KIO_3 standards as samples before and before and during the cruises (Table 3.4.3). A good agreement among them confirms that there was no systematic shift in our oxygen analyses between preparation of our KIO_3 standards onshore and the sample measurements on board.

(12) Quality control flag assignment

Quality flag values were assigned to oxygen measurements using the code defined in Table 0.2 of WHP Office Report WHPO 91-1 Rev.2 section 4.5.2 (Joyce *et al.*, 1994). Measurement flags of 2 (good), 3 (questionable), 4 (bad), and 5 (missing) have been assigned (Table 3.4.4). The replicate data were averaged and flagged 2 if both of them were flagged 2. If either of them was flagged 3 or 4, a datum with "younger" flag was selected. Thus we did not use flag of 6 (replicate measurements). For the choice between 2, 3, or 4, we basically followed a flagging procedure as listed below:

Table 3.4.2 Results of the duplicate sample measurements.

	Leg	Stations	Pressure (dbar)	Niskins		Apparatus	Oxygen [umol/kg]
1	1	C01	2001.9	18	X12J18	DOT-8	107.29
2	1	C01	2001.6	17	X12J17	DOT-8	107.42

3	1	C01	2001.2	16	X12J16	DOT-8	107.41
4	1	C01	2001.1	15	X12J15	DOT-8	107.56
5	1	C01	2001.0	14	X12J14	DOT-8	107.48
6	1	C01	2000.8	13	X12J13	DOT-8	107.45
7	1	C01	2000.5	12	X12J12	DOT-8	107.45
8	1	C01	2000.6	11	X12J11	DOT-8	107.47
9	1	C01	2000.4	10	X12J10	DOT-8	107.34
10	1	C01	2000.6	9	X12J09	DOT-7	107.23
11	1	C01	2000.4	8	X12J08	DOT-7	107.16
12	1	C01	2000.4	7	X12J07	DOT-7	107.23
13	1	C01	2000.6	6	X12J06	DOT-7	107.21
14	1	C01	2000.4	5	X12J05	DOT-7	107.27
15	1	C01	2000.6	4	X12J04	DOT-7	107.18
16	1	C01	2001.1	3	X12J03	DOT-7	107.32
17	1	C01	2000.4	2	X12J02	DOT-7	107.38
18	1	C01	2001.0	1	X12J01	DOT-7	107.33
19	1	C02	2003.6	36	X12J36	DOT-8	110.46
20	1	C02	2003.2	35	X12J35	DOT-8	110.35
21	1	C02	2003.5	34	X12J34	DOT-8	110.43
22	1	C02	2003.8	33	X12J33	DOT-8	110.51
23	1	C02	2003.3	32	X12J32	DOT-8	110.51
24	1	C02	2003.3	31	X12J31	DOT-8	110.47
25	1	C02	2003.2	30	X12J30	DOT-8	110.43
26	1	C02	2003.1	29	X12J29	DOT-8	110.50
27	1	C02	2002.7	28	X12J28	DOT-8	110.44
28	1	C02	2002.5	27	X12J27	DOT-7	110.43
29	1	C02	2003.0	26	X12J26	DOT-7	110.36
30	1	C02	2002.8	25	X12J25	DOT-7	110.41
31	1	C02	2002.3	24	X12J24	DOT-7	110.34
32	1	C02	2002.1	23	X12J23	DOT-7	110.40
33	1	C02	2002.4	22	X12J22	DOT-7	110.31
34	1	C02	2002.4	21	X12J21	DOT-7	110.41
35	1	C02	2001.6	20	X12J20	DOT-7	110.30
36	1	C02	2001.4	19	X12J19	DOT-7	110.34

Table 3.4.3 Results of the CSK standard (Lot DCE2131) measurements.

.

Date (UTC)	KIO_3 ID No.	DOT-1		-		Remarks
		Conc. (N)	error (N)	-	-	
2012/4/25	20120419-04-10	0.010004	0.000002	-	-	Onshore lab.
2012/4/25	20120419-05-10	0.010011	0.000004	-	-	Onshore lab.
		DOT-7		DOT-8		
		Conc. (N)	error (N)	Conc. (N)	error (N)	
2012/10/6	20120417-03-01	0.009997	0.000004	0.010000	0.000003	MR12-E03
2012/12/14	20120419-04-01	0.009996	0.000003	0.009999	0.000004	MR12-05 Leg-2
2013/01/20	20120419-05-01	0.010012	0.000004	0.010009	0.000004	MR12-05 Leg-3

a. Bottle oxygen concentration at the sampling layer was plotted against sampling pressure. Any points not lying on a generally smooth trend were noted.

b. Difference between bottle oxygen and CTD oxygen (RINKO sensor) was then plotted against sampling pressure. If a datum deviated from a group of plots, it was flagged 3.

c. Vertical sections against pressure and potential density were drawn. If a datum was anomalous on the section plots, datum flag was degraded from 2 to 3, or from 3 to 4.

d. If there was problem in the measurement, the datum was flagged 4.

e. If the bottle flag was 4 (did not trip correctly), a datum was flagged 4 (bad). In case of the bottle flag 3 (leaking) or 5 (unknown problem), a datum was flagged based on steps a, b, c, and d.

Table 3.4.4 Summary of assigned quality control flags.

Flag	Definition	
2	Good	5657
3	Questionable	4
4	Bad	0
5	Not report (missing)	0
	Total	5661

References

Dickson, A. (1996) Determination of dissolved oxygen in sea water by Winkler titration, in WHPO Pub. 91-1 Rev. 1, November 1994, Woods Hole, Mass., USA.

DOE (1994) Handbook of methods for the analysis of the various parameters of the carbon dioxide system in sea water; version 2. A.G. Dickson and C. Goyet (eds), ORNL/CDIAC-74.

Joyce, T., and C. Corry, eds., C. Corry, A. Dessier, A. Dickson, T. Joyce, M. Kenny, R. Key, D. Legler, R. Millard, R. Onken, P. Saunders, M. Stalcup (1994) Requirements for WOCE Hydrographic Programme Data Reporting, WHPO Pub. 90-1 Rev. 2, May 1994 Woods Hole, Mass., USA.

Murray, C.N., J.P. Riley, and T.R.S. Wilson (1968) The solubility of oxygen in Winkler reagents used for determination of dissolved oxygen, Deep-Sea Res., 15, 237-238.

.

3.5. Nutrients

(1) Personnel

Michio AOYAMA (Meteorological Research Institute / Japan Meteorological Agency, Principal Investigator)
LEG 2
Minoru KAMATA (Department of Marine Science, Marine Works Japan Ltd.)
Yasuhiro ARII (Department of Marine Science, Marine Works Japan Ltd.)
Kohei MIURA(Department of Marine Science, Marine Works Japan Ltd.)
LEG 3
Minoru KAMATA (Department of Marine Science, Marine Works Japan Ltd.)
Masanori ENOKI (Department of Marine Science, Marine Works Japan Ltd.)
Elena HAYASHI (Department of Marine Science, Marine Works Japan Ltd.)

(2) Objectives

The objectives of nutrients analyses during the R/V Mirai MR1205 cruise, WOCE P14S, S04 and S04I revisited cruise in 2012/2013, in the Southern Ocean are as follows;

- Describe the present status of nutrients concentration with excellent comparability.
- The determinants are nitrate, nitrite, silicate and phosphate.
- Study the temporal and spatial variation of nutrients concentration based on the previous high quality experiments data of WOCE previous P14S, S04 and S04I cruises in 1993 and 2005, GOESECS, IGY and so on.
- Study of temporal and spatial variation of nitrate: phosphate ratio, so called Redfield ratio.
- Obtain more accurate estimation of total amount of nitrate, silicate and phosphate in the interested area.
- Provide more accurate nutrients data for physical oceanographers to use as tracers of water mass movement.

(3) Summary of nutrients analysis

We made 142 QuAAtro 2-HR runs for the samples at 145 stations in MR1205. The total amount of layers of the seawater sample reached up to 4292 for MR1205. We made duplicate measurement at all layers.

(4) Instrument and Method

(4.1) Analytical detail using QuAAtro 2-HR systems (BL-Tech)

Nitrate + nitrite and nitrite were analyzed according to the modification method of Grasshoff (1970). The sample nitrate was reduced to nitrite in a cadmium tube inside of which was coated with metallic copper. The sample streamed with its equivalent nitrite was treated with an acidic, sulfanilamide reagent and the nitrite forms nitrous acid which reacted with the sulfanilamide to produce a diazonium ion. N-1-Naphthylethylene-diamine added to the sample stream then coupled with the diazonium ion to produce a red, azo dye. With reduction of the nitrate to nitrite, both nitrate and nitrite reacted and were measured; without reduction, only nitrite reacted. Thus, for the nitrite analysis, no reduction was performed and the alkaline buffer was not necessary. Nitrate was computed by difference.

The silicate method was analogous to that described for phosphate. The method used was essentially that of Grasshoff et al. (1983), wherein silicomolybdic acid was first formed from the silicate in the sample and added molybdic acid; then the silicomolybdic acid was reduced to silicomolybdous acid, or "molybdenum blue" using ascorbic acid as the

.

reductant. The analytical methods of the nutrients, nitrate, nitrite, silicate and phosphate, during this cruise were same as the methods used in (Kawano et al. 2009).

The phosphate analysis was a modification of the procedure of Murphy and Riley (1962). Molybdic acid was added to the seawater sample to form phosphomolybdic acid which was in turn reduced to phosphomolybdous acid using L-ascorbic acid as the reductant.

The details of modification of analytical methods used in this cruise are also compatible with the methods described in nutrients section in GO-SHIP repeat hydrography manual (Hydes et al., 2010). The flow diagrams and reagents for each parameter are shown in Figures 3.5.1 to 3.5.4.

(4.2) Nitrate Reagents

Imidazole (buffer), 0.06 M (0.4 % w/v)
Dissolve 4 g imidazole, $C_3H_4N_2$, in ca. 1000 ml DIW; add 2 ml concentrated HCl. After mixing, 1 ml Triton(R)X-100 (50 % solution in ethanol) is added.

Sulfanilamide, 0.06 M (1 % w/v) in 1.2 M HCl
Dissolve 10 g sulfanilamide, 4-$NH_2C_6H_4SO_3H$, in 900 ml of DIW, add 100 ml concentrated HCl. After mixing, 2 ml Triton(R)X-100 (50 %f solution in ethanol) is added.

N-1-Napthylethylene-diamine dihydrochloride, 0.004 M (0.1 %f w/v)
Dissolve 1 g NEDA, $C_{10}H_7NHCH_2CH_2NH_2 \cdot 2HCl$, in 1000 ml of DIW and add 10 ml concentrated HCl. After mixing, 1 ml Triton(R)X-100 (50 %f solution in ethanol) is added.
Stored in a dark bottle.

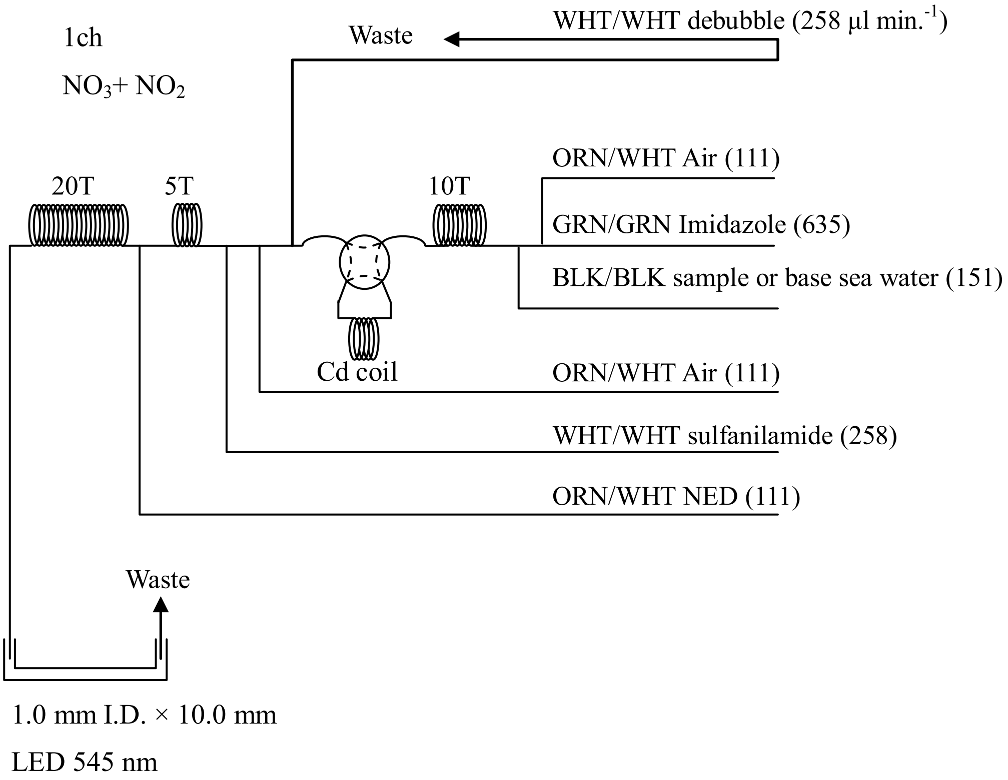

Figure 3.5.1 $NO_3 + NO_2$ (1ch.) Flow diagram.

(4.3) Nitrite Reagents

Sulfanilamide, 0.06 M (1 % w/v) in 1.2 M HCl

Dissolve 10 g sulfanilamide, 4-$NH_2C_6H_4SO_3H$, in 900 ml of DIW, add 100 ml concentrated HCl. After mixing, 2 ml Triton(R)X-100 (50 % solution in ethanol) is added.

N-1-Napthylethylene-diamine dihydrochloride, 0.004 M (0.1 % w/v)

Dissolve 1 g NEDA, $C_{10}H_7NHCH_2CH_2NH_2 \cdot 2HCl$, in 1000 ml of DIW and add 10 ml concentrated HCl. After mixing, 1 ml Triton(R)X-100 (50 %f solution in ethanol) is added. This reagent was stored in a dark bottle.

.

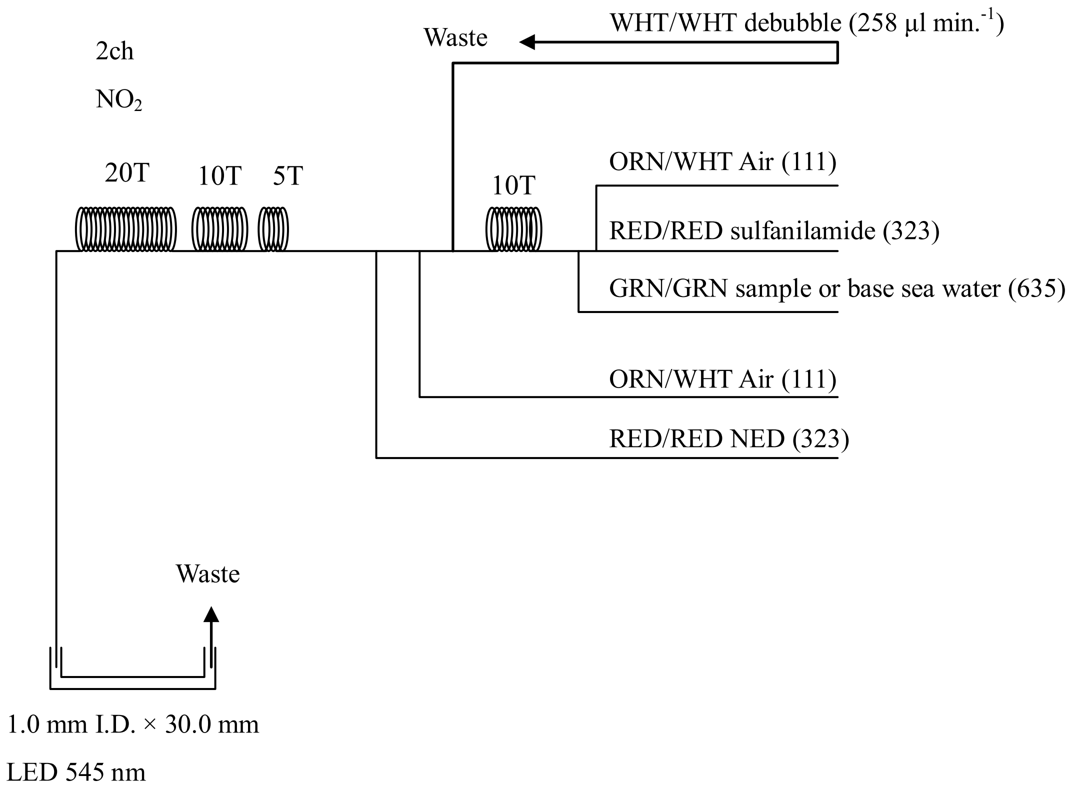

Figure 3.5.2 NO_2 (2ch.) Flow diagram.

(4.4) Silicate

Reagents

Molybdic acid, 0.06 M (2 % w/v)

Dissolve 15 g disodium Molybdate (VI) dihydrate, $Na_2M_oO_4 \cdot 2H_2O$, in 980 ml DIW, add 8 ml concentrated H_2SO_4. After mixing, 20 ml sodium dodecyl sulphate (15 % solution in water) is added.

Oxalic acid, 0.6 M (5 % w/v)

Dissolved 50 g oxalic acid anhydrous, HOOC: COOH, in 950 ml of DIW.

Ascorbic acid, 0.01 M (3 % w/v)

Dissolved 2.5g L (+)- ascorbic acid, $C_6H_8O_6$, in 100 ml of DIW. This reagent was freshly prepared before every measurement.

(4.4) Silicate Reagents

Molybdic acid, 0.06 M (2 % w/v)

Dissolve 15 g disodium Molybdate (VI) dihydrate, $Na_2M_oO_4 \cdot 2H_2O$, in 980 ml DIW, add 8 ml concentrated H_2SO_4. After mixing, 20 ml sodium dodecyl sulphate (15 % solution in water) is added.

Oxalic acid, 0.6 M (5 % w/v)

.

Dissolved 50 g oxalic acid anhydrous, HOOC: COOH, in 950 ml of DIW.

Ascorbic acid, 0.01 M (3 % w/v)

Dissolved 2.5g L (+)- ascorbic acid, $C_6H_8O_6$, in 100 ml of DIW. This reagent was freshly prepared before every measurement.

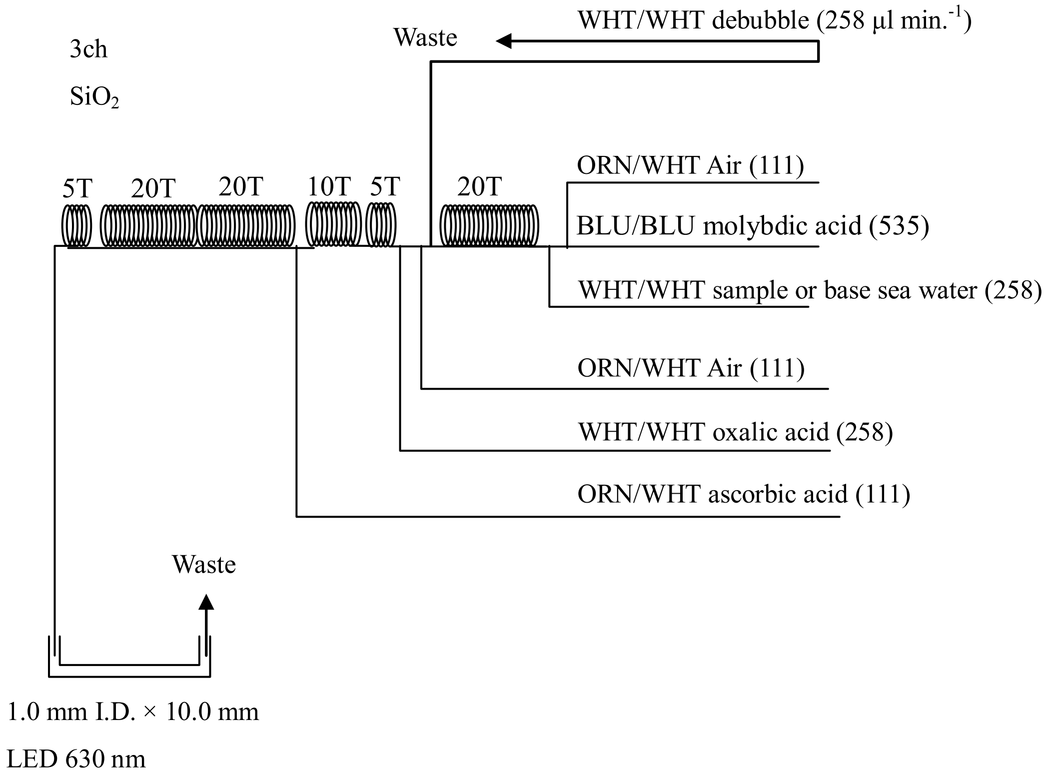

Figure 3.5.3 SiO_2 (3ch.) Flow diagram.

(4.5) Phosphate Reagents

Stock molybdate solution, 0.03 M (0.8 % w/v)

Dissolved 8 g disodium molybdate(VI) dihydrate, $Na_2M_0O_4•2H_2O$, and 0.17 g antimony potassium tartrate, $C_8H_4K_2O_{12}Sb_2•3H_2O$, in 950 ml of DIW and added 50 ml concentrated H_2SO_4.

Mixed Reagent

Dissolved1.2 g L (+)-ascorbic acid, $C_6H_8O_6$, in 150 ml of stock molybdate solution. After mixing, 3 ml sodium dodecyl sulphate (15 % solution in water) was added in leg3 of this cruise, 4 mL sodium dodecyl sulphate (15 % solution in water) was added in leg2 because to reduce relatively noisy signals. This reagent was freshly prepared before every measurement.

.

Reagent for sample dilution

Dissolved sodium chloride, NaCl, 10 g in ca. 950 ml of DIW, added 50 ml acetone and 4 ml concentrated H_2SO_4. After mixing, 5 ml sodium dodecyl sulphate (15 % solution in water) was added.

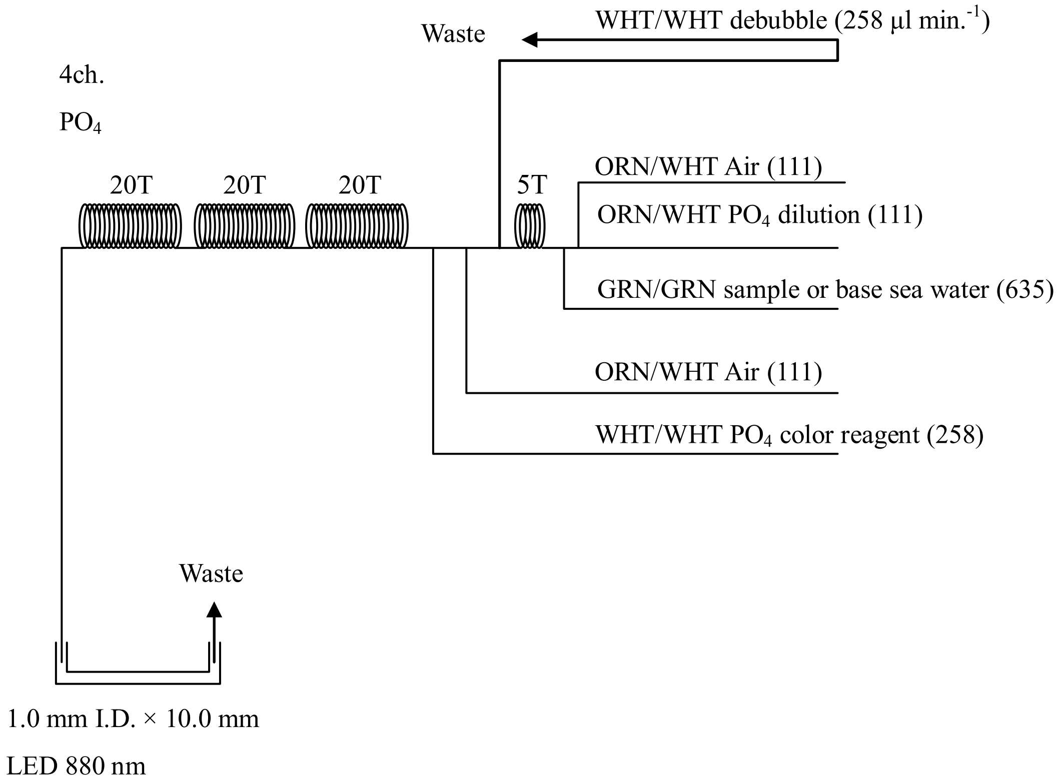

Figure 3.5.4 PO_4 (4ch.) Flow diagram.

(4.6) Sampling procedures

Sampling of nutrients followed that oxygen, salinity and trace gases. Samples were drawn into two of virgin 10 ml polyacrylates vials without sample drawing tubes. These were rinsed three times before filling and vials were capped immediately after the drawing. The vials were put into water bath adjusted to ambient temperature, 24 ± 2 deg. C, in about 30 minutes before use to stabilize the temperature of samples in MR1205.

No transfer was made and the vials were set an auto sampler tray directly. Samples were analyzed after collection basically within 24 hours in MR1205.

(4.7) Data processing

Raw data from QuAAtro 2-HR was treated as follows:

- Checked baseline shift.
- Checked the shape of each peak and positions of peak values taken, and then changed the positions of peak values taken

.

if necessary.

- Carry-over correction and baseline drift correction were applied to peak heights of each samples followed by sensitivity correction.
- Baseline correction and sensitivity correction were done basically using liner regression.
- Loaded pressure and salinity from CTD data to calculate density of seawater.
- Calibration curves to get nutrients concentration were assumed second order equations.

(5) Nutrients standards

(5.1) Volumetric laboratory ware of in-house standards

All volumetric glass ware and polymethylpentene (PMP) ware used were gravimetrically calibrated. Plastic volumetric flasks were gravimetrically calibrated at the temperature of use within 0 to 4 K.

Volumetric flasks

Volumetric flasks of Class quality (Class A) are used because their nominal tolerances are 0.05 % or less over the size ranges likely to be used in this work. Class A flasks are made of borosilicate glass, and the standard solutions were transferred to plastic bottles as quickly as possible after they are made up to volume and well mixed in order to prevent excessive dissolution of silicate from the glass. High quality plastic (polymethylpentene, PMP, or polypropylene) volumetric flasks were gravimetrically calibrated and used only within 0 to 4 K of the calibration temperature.

The computation of volume contained by glass flasks at various temperatures other than the calibration

temperatures were done by using the coefficient of linear expansion of borosilicate crown glass.

Because of their larger temperature coefficients of cubical expansion and lack of tables constructed for these materials, the plastic volumetric flasks were gravimetrically calibrated over the temperature range of intended use and used at the temperature of calibration within 0 to 4 K. The weights obtained in the calibration weightings were corrected for the density of water and air buoyancy.

Pipettes and pipettors

All pipettes have nominal calibration tolerances of 0.1 % or better. These were gravimetrically calibrated in order to verify and improve upon this nominal tolerance.

(5.2) Reagents, general considerations

Specifications

For nitrate standard, “potassium nitrate 99.995 suprapur®” provided by Merck, CAS No. : 7757-91-1, was used.

For nitrite standard, “sodium nitrate” provided by Wako, CAS No. : 7632-00-0, was used. The assay of nitrite salts was determined according JIS K8019 were 98.73 %. We use that value to adjust the weights taken.

For the silicate standard, we use “Silicon standard solution SiO_2in NaOH 0.5 mol/l CertiPUR®” provided by Merck, CAS No. : 1310-73-2, of which lot number is HC097572 is used. The silicate concentration is certified by

NIST-SRM3150 with the uncertainty of 0.5 %. Factor of HC097572 was signed 1.000, however we reassigned the factor as 0.976 from the result of comparison among RMNS in MR11E02 cruise. A history of assigned factor of Merck solutions are shown in Table 3.5.1.

For phosphate standard, “potassium dihydrogen phosphate anhydrous 99.995 suprapur®” provided by Merck, CAS No. : 7778-77-0, was used.

Table 3.5.1 A history of assigned factor of Merck solutions

Lot	Factor	Date	Reference
Merck OC551722	**1.001**	**2006/5/24**	
Merck HC623465	**1.000**		
Merck HC751838	**0.998**	**2007/4/13**	
Merck HC814662	**0.999**	**2008/8/27**	
Merck HC074650	**0.975**		
Merck HC097572	**0.976**	**MR11-E02** **(2011/06/20)**	**RMNS_BA, AY, BD, BE, BF**

Ultra pure water

Ultra pure water (MilliQ water) freshly drawn was used for preparation of reagents, standard solutions and for measurement of reagent and system blanks.

Low-Nutrient Seawater (LNSW)

Surface water having low nutrient concentration was taken and filtered using 0.45 μm pore size membrane filter. This water is stored in 20 liter cubitainer with paper box. The concentrations of nutrient of this water were measured carefully in Aug 2012.

Treatment of silicate standard due to high alkalinity

Since the silicon standard solution Merck CertiPUR® is in NaOH 0.5 mol/l, we need to dilute and neutralize to avoid make precipitation of $MgOH_2$ etc. When we make B standard, silicon standard solution is diluted by factor 12 with pure water and neutralized by HCl 1.0 mol/l to be about 7. After that B standard solution is used to prepare C standards.

(5.3) Concentrations of nutrients for A, B and C standards

Concentrations of nutrients for A, B and C standards are set as shown in Table 3.5.2. The C standard is prepared according recipes as shown in Table 3.5.3. All volumetric laboratory tools were calibrated prior the cruise as stated in chapter (i). Then the actual concentration of nutrients in each fresh standard was calculated based on the ambient, solution temperature and determined factors of volumetric lab. wares.

The calibration curves for each run were obtained using 6 levels, C-1, C-2, C-3, C-4, C-5 and C-6.

Table 3.5.2 Nominal concentrations of nutrients for A, B and C standards.

	A	B	C-1	C-2	C-3	C-4	C-5	C-6

NO_3(µM)	**22500**	**900**	**BS**	**BU**	**BT**	**BD**	**BF**	**45**
NO_2(µM)	**4000**	**20**	**BS**	**BU**	**BT**	**BD**	**BF**	**1.0**
SiO_2(µM)	**36000**	**2160**	**BS**	**BU**	**BT**	**BD**	**BF**	**105**
PO_4(µM)	**3000**	**60**	**BS**	**BU**	**BT**	**BD**	**BF**	**3.0**

Table 3.5.3 Working calibration standard recipes.

C Std.	B-1 Std.	B-2 Std.
C-6	25 ml	25 ml

B-1 Std.: Mixture of nitrate, silicate and phosphate

B-2 Std.: Nitrite

(5.4) Renewal of in-house standard solutions.

In-house standard solutions as stated in (iii) were renewed as shown in Table 3.5.4 (a) to (c).

Table 3.5.4(a) Timing of renewal of in-house standards.

NO_3, NO_2, SiO_2, PO_4	Renewal
A-1 Std. (NO_3)	maximum 1 month
A-2 Std. (NO_2)	maximum 1 month
A-3 Std. (SiO_2)	commercial prepared solution
A-4 Std. (PO_4)	maximum 1 month
B-1 Std. (mixture of NO_3, SiO_2, PO_4)	8 days
B-2 Std. (NO_2)	8 days

Table 3.5.4(b) Timing of renewal of in-house standards.

Working standards	Renewal
C-6 Std. (mixture of B-1 and B-2 Std.)	24 hours

Table 3.5.4(c) Timing of renewal of in-house standards for reduction estimation.

Reduction estimation	Renewal
D-1 Std.(3600 µM NO_3)	8 days
43 µM NO_3	when C Std. renewed
39 µM NO_2	when C Std. renewed

(6) Reference material of nutrients in seawater

To get the more accurate and high quality nutrients data to achieve the objectives stated above, huge numbers of the bottles of the reference material of nutrients in seawater (hereafter RMNS) are prepared (Aoyama et al., 2006, 2007, 2008, 2009). In the previous worldwide expeditions, such as WOCE cruises, the higher reproducibility and precision of nutrients measurements were required (Joyce and Corry, 1994). Since no standards were available for the measurement of nutrients in seawater at that time, the requirements were described in term of reproducibility. The required reproducibility was 1 %, 1 to 2 %, 1 to 3 % for nitrate, phosphate and silicate, respectively. Although nutrient data from the WOCE one-time survey was of unprecedented quality and coverage due to much care in sampling and measurements, the differences of nutrients concentration at crossover points are still found among the expeditions (Aoyama and Joyce, 1996, Mordy et al., 2000, Gouretski and Jancke, 2001). For instance, the mean offset of nitrate concentration at deep waters was 0.5 μmol kg^{-1} for 345 crossovers at world oceans, though the maximum was 1.7 μmol kg^{-1} (Gouretski and Jancke, 2001). At the 31 crossover points in the Pacific WHP one-time lines, the WOCE standard of reproducibility for nitrate of 1 % was fulfilled at about half of the crossover points and the maximum difference was 7 % at deeper layers below 1.6 deg. C in potential temperature (Aoyama and Joyce, 1996).

During the period from 2003 to 2010, RMNS were used to keep comparability of nutrients measurement among the 8 cruises of CLIVAR project (Sato et al., 2010), MR1005 cruise for Arctic research (Aoyama et al., 2010) and MR1006 cruise for “Change in material cycles and ecosystem by the climate change and its feedback” (Aoyama et al., 2011).

(6.1) RMNSs for this cruise

RMNS lots BS, BU, BT, BD and BF, which cover full range of nutrients concentrations in the Southern Ocean are prepared. 82 sets of BS, BU, BT, BD and BF are prepared.

One hundred seventy bottles of RMNS lot BV are prepared for MR1205. Lot BV was used all stations. These RMNS assignment were completely done based on random number. The RMNS bottles were stored at a room in the ship, REAGENT STORE, where the temperature was maintained around 15 – 33 deg. C.

(6.2) Assigned concentration for RMNSs

We assigned nutrients concentrations for RMNS lots BS, BU, BT, BD, BV, and BF as shown in Table 3.5.4.

Table 3.5.4 Assigned concentration of RMNSs.

unit: µmol kg^{-1}

	Nitrate	Phosphate	Silicate	Nitrite
BS*	**0.07**	**0.063**	**1.61**	**0.02**
BU*	**3.96**	**0.378**	**20.27**	**0.07**
BT*	**18.18**	**1.318**	**40.94**	**0.47**
BD*	**29.82**	**2.191**	**64.30**	**0.05**
BV**	**35.32**	**2.541**	**99.55**	**0.06**
BF***	**41.39**	**2.809**	**149.71†**	**0.02**

* The values are assigned for this cruise on 27 July 2011.

** The values are assigned for this cruise on 4 April 2009 (Table 3.4.4 in WHP P21 REVISIT DATA BOOK).

*** The values are assigned for this cruise on 21 August 2012.

† This value is changed for MR1205 cruise.

(6.3) The homogeneity of RMNSs

The homogeneity of lot BV used in MR1205 cruise and analytical precisions are shown in Table 3.5.6. These are for the assessment of the magnitude of homogeneity of the RMNS bottles those are used during the cruise. As shown in Table 3.5.6 homogeneity of RMNS lot BV for nitrate, phosphate and silicate are the same magnitude of analytical precision derived from fresh raw seawater in January 2009.

Table 3.5.6 Homogeneity of lot BV derived from simultaneous 298 samples measurements and analytical precision onboard R/V Mirai in MR1205.

	Nitrate	Phosphate	Silicate
	CV %	**CV %**	**CV %**
BV	**0.13**	**0.19**	**0.15**
Precision	**0.10**	**0.16**	**0.11**

BV: N=298

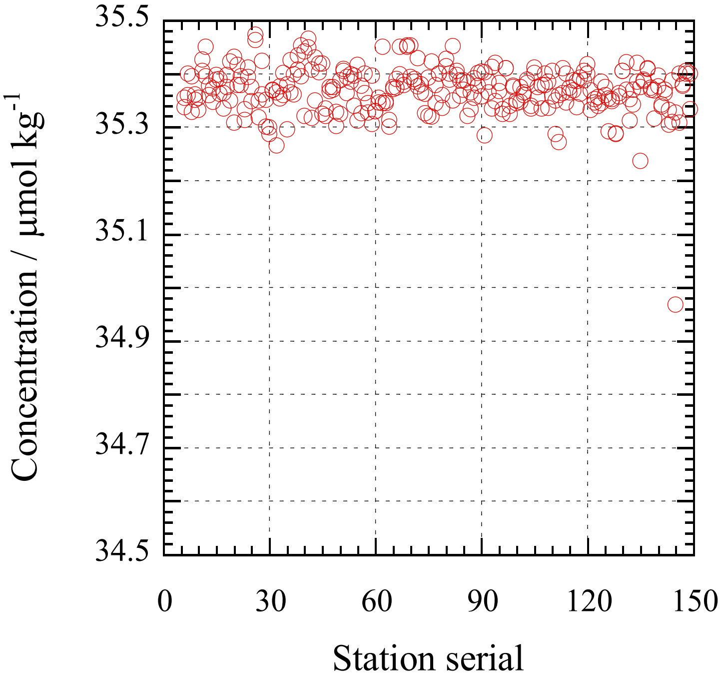

Figure3.5.5 Time series of RMNS-BV of nitrate for MR1205.

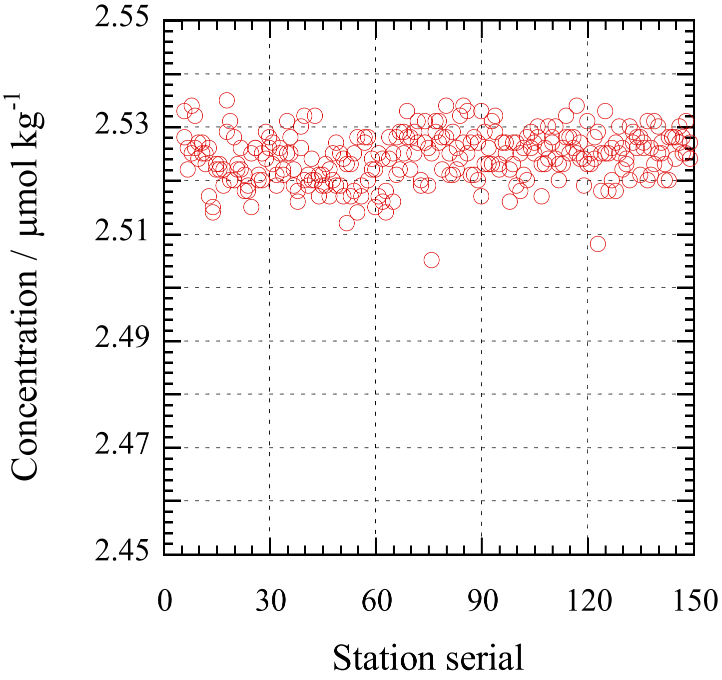

Figure 3.5.6 Time series of RMNS-BV of phosphate for MR1205.

.

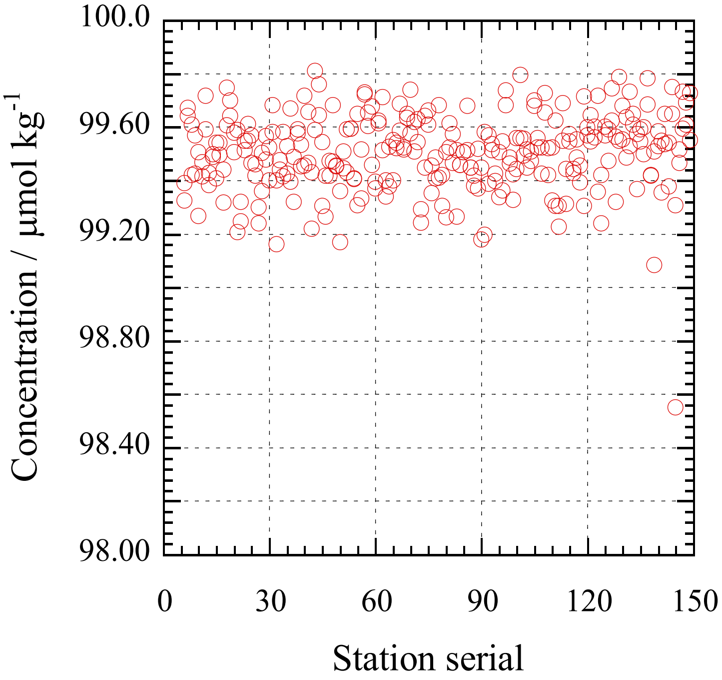

Figure 3.5.7 Time series of RMNS-BV of silicate for MR1205.

(6.4) Comparability of RMNSs during the periods from 2003 to 2011

Cruise-to-cruise comparability has examined based on the results of the previous results of RMNSs measurements obtained among cruises and RMNS international comparison experiments in 2003 and 2009. The uncertainties for each value were obtained similar method described in 7.1 in this chapter at the measurement before each cruise and inter-comparison study, shown as precruise and intercomparison, and mean of uncertainties during each cruise, only shown cruise code, respectively. As shown in Table 3.5.7, the nutrients concentrations of RMNSs were in good agreement among the measurements during the period from 2003 to 2011. For the silicate measurements, we show lot numbers and chemical company names of each cruise/measurement in the footnote. As shown in Table 3.4.7, there shows less comparability among the measurements due to less comparability among the standard solutions provided by chemical companies in the silicate measurements.

Table 3.5.7 (a) Comparability for nitrate.

unit: µmol kg^{-1}

Cruise	RM Lots											
	BS	unc.	BU	unc.	BT	unc.	BD	unc.	BV	unc.	BF	unc.
						Nitrate						
MR07-04											41.34	0.083
MR10-05							29.80	0.097				
MR10-06							29.81	0.053			41.41	0.036
MR11-02							29.83	0.047			41.39	0.058
MR11-03					18.11	0.073	29.80	0.053			41.39	0.051

MR11-05					18.04	0.025	29.89	0.073			41.40	0.075
MR11-08	0.10	0.031	3.97	0.031	18.19	0.054	29.85	0.082			41.45	0.082
MR12-E03	0.08	0.012	3.97	0.017	18.23	0.030	29.86	0.054				
MR12-05	0.07	0.011	3.96	0.012	18.19	0.039	29.82	0.043	35.37	0.046	41.40	0.042

Table 3.5.7 (b) Comparability for Phosphate.

unit: µmol kg^{-1}

Cruise	RM Lots											
	BS	unc.	BU	unc.	BT	unc.	BD	unc.	BV	unc.	BF	unc.
	Phosphate											
MR07-04											2.803	0.006
MR10-05							2.184	0.011				
MR10-06							2.182	0.006			2.807	0.007
MR11-02							2.187	0.003			2.810	0.006
MR11-03					1.316	0.011	2.187	0.004			2.815	0.007
MR11-05					1.313	0.009	2.183	0.007			2.808	0.007
MR11-08	0.064	0.010	0.377	0.007	1.317	0.010	2.190	0.011			2.821	0.009
MR12-E03	0.070	0.007	0.385	0.006	1.331	0.007	2.211	0.007				
MR12-05	0.063	0.003	0.377	0.003	1.319	0.004	2.190	0.004	2.524	0.005	2.818	0.005

Table 3.5.7 (C) Comparability for Silicate.

unit: µmol kg^{-1}

Cruise	RM Lots											
	BS	unc.	BU	unc.	BT	unc.	BD	unc.	BV	unc.	BF	unc.
	Silicate											
MR07-04$^{\$\$}$											150.69	1.02
MR10-05							64.40	0.10				
MR10-06							64.47	0.07			150.40	0.17
MR11-02							64.40	0.11			150.12	0.33
MR11-03					40.97	0.16	64.43	0.11			150.14	0.16
MR11-05					40.96	0.09	64.40	0.07			150.18	0.13
MR11-08^{++}	1.46	0.15	20.24	0.13	41.02	0.16	64.38	0.19			149.97	0.32
MR12-E03	1.61	0.04	20.25	0.08	40.89	0.12	64.11	0.18				
MR12-05	1.58	0.08	20.23	0.07	40.88	0.10	64.13	0.13	99.50	0.15	149.64	0.26

List of lot numbers: $$: Merck HC623465; ++: HC097572

(7) Quality control

(7.1) Precision of nutrients analyses during the cruise

Precision of nutrients analyses during the cruise was evaluated based on the 9 to 11 measurements, which are measured every 10 to 12 samples, during a run at the concentration of C-6 std. Summary of precisions are shown as shown in Table 3.5.8 and Figures 3.5.8 to 3.5.10, the precisions for each parameter are generally good considering the analytical precisions during the Mirai cruses conducted in 2009 − 2012. During this cruise, analytical precisions were 0.10 % for nitrate, 0.16 % for phosphate and 0.11 % for silicate in terms of median of precision, respectively.

Table 3.5.8 Summary of precision based on the replicate analyses.

	Nitrate	**Phosphate**	**Silicate**
	CV %	**CV %**	**CV %**
Median	**0.10**	**0.11**	**0.16**
Mean	**0.10**	**0.11**	**0.18**
Maximum	**0.23**	**0.24**	**0.40**
Minimum	**0.04**	**0.03**	**0.08**
N	**144**	**144**	**144**

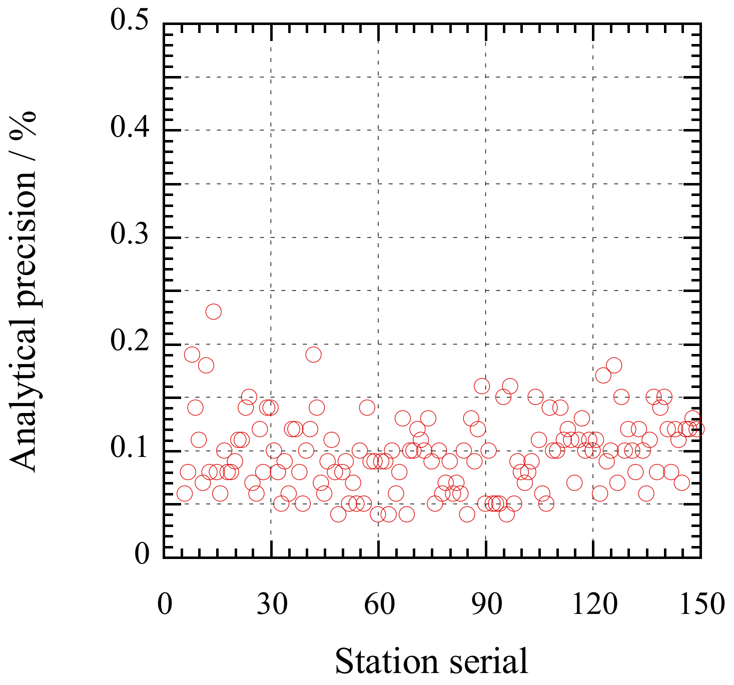

Figure 3.5.8 Time series of precision of nitrate for MR1205.

.

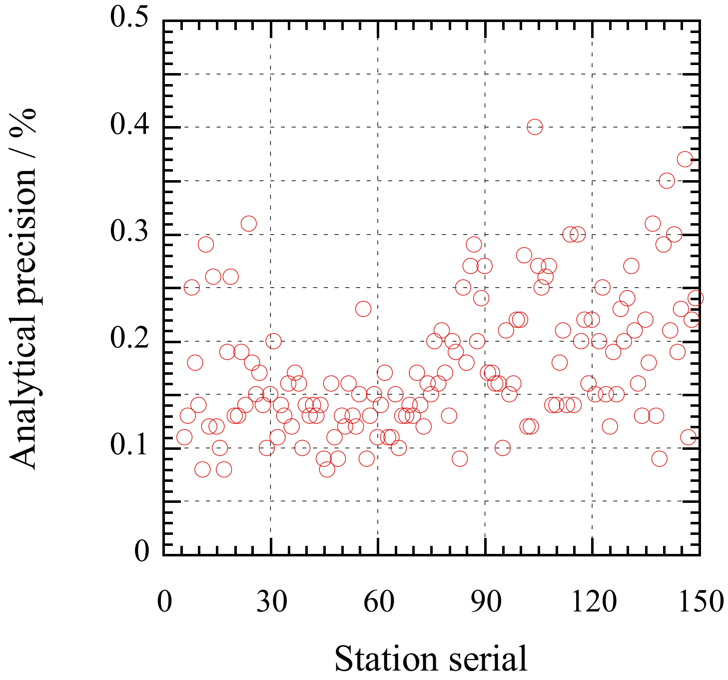

Figure 3.5.9 Time series of precision of phosphate for MR1205.

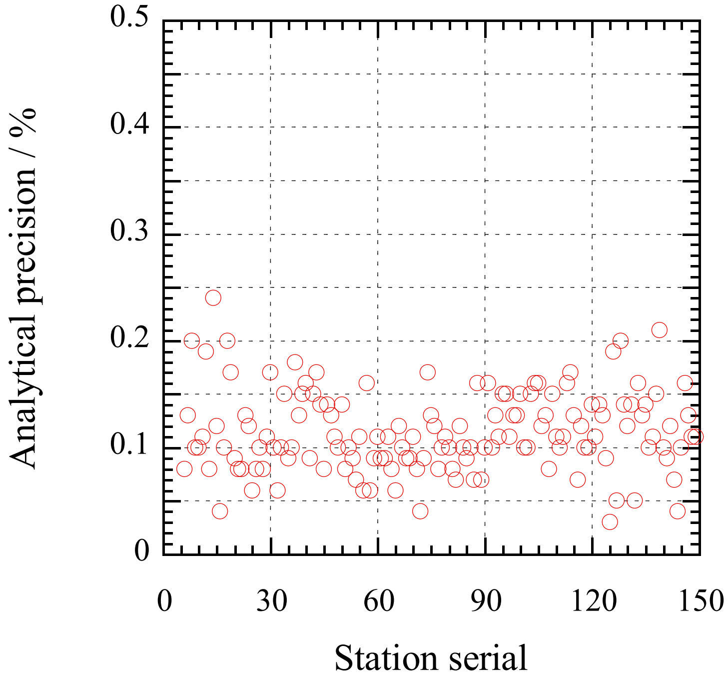

Figure 3.5.10 Time series of precision of silicate for MR1205.

(7.2) Carry over

We also summarize the magnitudes of carry over throughout the cruise. These are small enough within acceptable

.

levels as shown in Table 3.5.9 and Figures 3.5.11 – 3.5.13.

Table 3.5.9 Summary of carry over throughout MR1205 cruise.

	Nitrate **CV %**	**Phosphate** **CV %**	**Silicate** **CV %**
Median	**0.14**	**0.20**	**0.34**
Mean	**0.14**	**0.20**	**0.39**
Maximum	**0.23**	**0.37**	**0.95**
Minimum	**0.03**	**0.08**	**0.01**
N	**144**	**144**	**144**

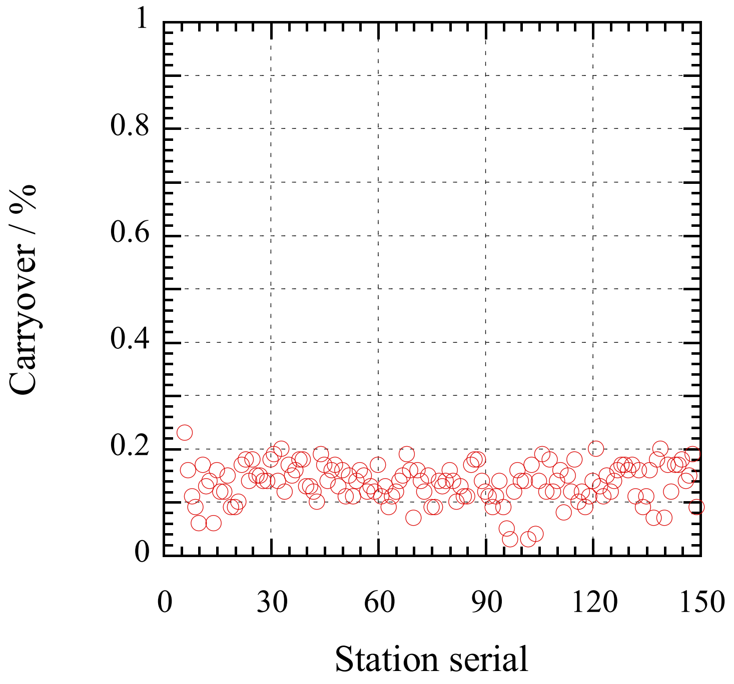

Figure 3.5.11 Time series of carryover of nitrate for MR1205.

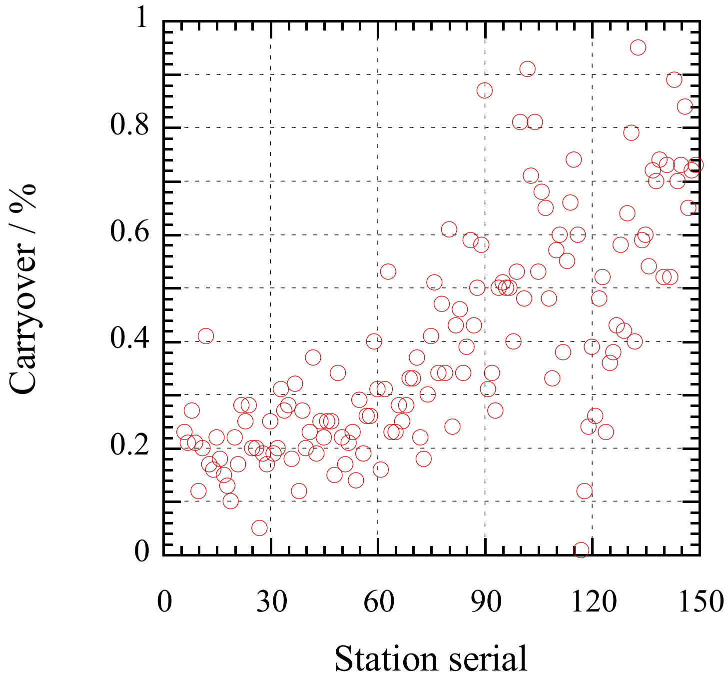

Figure 3.5.12 Time series of carryover of phosphatefor MR1205.

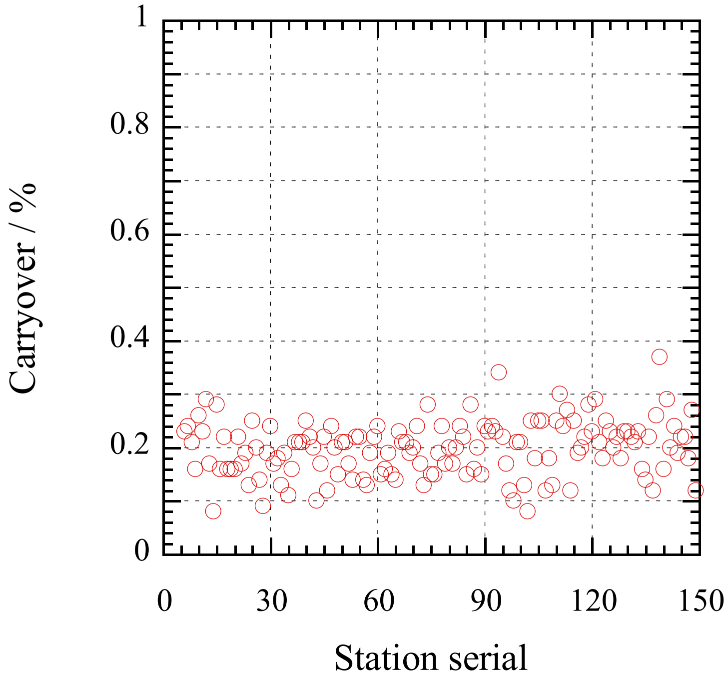

Figure 3.5.13 Time series of carryover of silicate for MR1205.

(7.2) Estimation of uncertainty of phosphate, nitrate and silicate concentrations

Empirical equations, eq. (1), (2) and (3) to estimate uncertainty of measurement of phosphate, nitrate and silicate are

.

used based on measurements of 72sets of RMNSs during the this cruise. These empirical equations are as follows, respectively.

Phosphate Concentration Cp in µmol kg^{-1}:
Uncertainty of measurement of phosphate (%) =
0.05668 + 0.3158 / Cp --- (1)
where Cp is phosphate concentration of sample.

Nitrate Concentration Cn in µmol kg^{-1}:
Uncertainty of measurement of nitrate (%) =
0.09216 + 1.0861 / Cn --- (2)
where Cn is nitrate concentration of sample.

Silicate Concentration Cs in µmol kg^{-1}:
Uncertainty of measurement of silicate (%) =
0.06383 + 7.436 / Cs --- (3)
where Cs is silicate concentration of sample.

(8) Problems/improvements occurred and solutions.

During this cruise we observed relatively large carryover of phosphate measurement especially in leg 3 as shown in figure 3.5.12. We washed assemblies and a flow cell of phosphate channel a few times in leg 3, however relatively large carry over did not changed.

We also found that carry over correction on the raw data was considered only “High to Low”. A equation of carry over correction is as below

A(i)corrected A(i) - A(i-1) x k --- (4)

Where A(i) is absorbance of sample I, k is carry over coefficient.

Although this carryover correction method is adopted in AACE software ver 6.07, this might make systematic underestimate on the nutrient concentration. A magnitude might depend a gradient of nutrient concentration and in case of phosphate it is estimated to be about 0.002 µmol kg^{-1} at 0.005 µmol kg^{-1} m^{-1}.

(9) Data archive

All data will be submitted to JAMSTEC Data Management Office (DMO) and is currently under its control.

References

Aminot, A. and Kerouel, R. 1991. Autoclaved seawater as a reference material for the determination of nitrate and phosphate in seawater. Anal. Chim. Acta, 248: 277-283.

Aminot, A. and Kirkwood, D.S. 1995. Report on the results of the fifth ICES intercomparison exercise for nutrients in sea water, ICES coop. Res. Rep. Ser., 213.

.

Aminot, A. and Kerouel, R. 1995. Reference material for nutrients in seawater: stability of nitrate, nitrite, ammonia and phosphate in autoclaved samples. Mar. Chem., 49: 221-232.

Aoyama M., and Joyce T.M. 1996, WHP property comparisons from crossing lines in North Pacific. In Abstracts, 1996 WOCE Pacific Workshop, Newport Beach, California.

Aoyama, M., 2006: 2003 Intercomparison Exercise for Reference Material for Nutrients in Seawater in a Seawater Matrix, Technical Reports of the Meteorological Research Institute No.50, 91pp, Tsukuba, Japan.

Aoyama, M., Susan B., Minhan, D., Hideshi, D., Louis, I. G., Kasai, H., Roger, K., Nurit, K., Doug, M., Murata, A., Nagai, N., Ogawa, H., Ota, H., Saito, H., Saito, K., Shimizu, T., Takano, H., Tsuda, A., Yokouchi, K., and Agnes, Y. 2007. Recent Comparability of Oceanographic Nutrients Data: Results of a 2003 Intercomparison Exercise Using Reference Materials. Analytical Sciences, 23: 1151-1154.

Aoyama M., J. Barwell-Clarke, S. Becker, M. Blum, Braga E. S., S. C. Coverly,E. Czobik, I. Dahllof, M. H. Dai, G. O. Donnell, C. Engelke, G. C. Gong, Gi-Hoon Hong, D. J. Hydes, M. M. Jin, H. Kasai, R. Kerouel, Y. Kiyomono, M. Knockaert, N. Kress, K. A. Krogslund, M. Kumagai, S. Leterme, Yarong Li, S. Masuda, T. Miyao, T. Moutin, A. Murata, N. Nagai, G.Nausch, M. K. Ngirchechol, A. Nybakk, H. Ogawa, J. van Ooijen, H. Ota, J. M. Pan, C. Payne, O. Pierre-Duplessix, M. Pujo-Pay, T. Raabe, K. Saito, K. Sato, C. Schmidt, M. Schuett, T. M. Shammon, J. Sun, T. Tanhua, L. White, E.M.S. Woodward, P. Worsfold, P. Yeats, T. Yoshimura, A.Youenou, J. Z. Zhang, 2008: 2006 Intercomparison Exercise for Reference Material for Nutrients in Seawater in a Seawater Matrix, Technical Reports of the Meteorological Research Institute No. 58, 104pp.

Aoyama, M., Nishino, S., Nishijima, K., Matsushita, J., Takano, A., Sato, K., 2010a. Nutrients, In: R/V Mirai Cruise Report MR10-05. JAMSTEC, Yokosuka, pp. 103-122.

Aoyama, M., Matsushita, J., Takano, A., 2010b. Nutrients, In: MR10-06 preliminary cruise report. JAMSTEC, Yokosuka, pp. 69-83

Gouretski, V.V. and Jancke, K. 2001. Systematic errors as the cause for an apparent deep water property variability: global analysis of the WOCE and historical hydrographic data・REVIEW ARTICLE, Progress In Oceanography, 48: Issue 4, 337-402.

Grasshoff, K., Ehrhardt, M., Kremling K. et al. 1983. Methods of seawater anylysis. 2nd rev. Weinheim: VerlagChemie, Germany, West.

Hydes, D.J., Aoyama, M., Aminot, A., Bakker, K., Becker, S., Coverly, S., Daniel, A., Dickson, A.G., Grosso, O., Kerouel, R., Ooijen, J. van, Sato, K., Tanhua, T., Woodward, E.M.S., Zhang, J.Z., 2010. Determination of Dissolved Nutrients (N, P, Si) in Seawater with High Precision and Inter-Comparability Using Gas-Segmented Continuous Flow Analysers, In: GO-SHIP Repeat Hydrography Manual: A Collection of Expert Reports and Guidelines. IOCCP Report No. 14, ICPO Publication Series No 134.

Joyce, T. and Corry, C. 1994. Requirements for WOCE hydrographic programmed data reporting. WHPO Publication, 90-1, Revision 2, WOCE Report No. 67/91.

Kawano, T., Uchida, H. and Doi, T. WHP P01, P14 REVISIT DATA BOOK, (Ryoin Co., Ltd., Yokohama, 2009).

Kirkwood, D.S. 1992. Stability of solutions of nutrient salts during storage. Mar. Chem., 38 : 151-164.

Kirkwood, D.S. Aminot, A. and Perttila, M. 1991. Report on the results of the ICES fourth intercomparison exercise for nutrients in sea water. ICES coop. Res. Rep. Ser., 174.

.

Mordy, C.W., Aoyama, M., Gordon, L.I., Johnson, G.C., Key, R.M., Ross, A.A., Jennings, J.C. and Wilson. J. 2000. Deep water comparison studies of the Pacific WOCE nutrient data set. Eos Trans-American Geophysical Union. 80 (supplement), OS43.

Murphy, J., and Riley, J.P. 1962. Analyticachim. Acta 27, 31-36.

Sato, K., Aoyama, M., Becker, S., 2010. RMNS as Calibration Standard Solution to Keep Comparability for Several Cruises in the World Ocean in 2000s. In: Aoyama, M., Dickson, A.G., Hydes, D.J., Murata, A., Oh, J.R., Roose, P., Woodward, E.M.S., (Eds.), Comparability of nutrients in the world's ocean. Tsukuba, JAPAN: MOTHER TANK, pp 43-56.

Uchida, H. &Fukasawa, M. WHP P6, A10, I3/I4 REVISIT DATA BOOK Blue Earth Global Expedition 2003 1, 2, (Aiwa Printing Co., Ltd., Tokyo, 2005).

3.6 Chlorofluorocarbons and Sulfur hexafluoride

(1) Personnel

Ken'ichi Sasaki (Mutsu Institute for Oceanography, JAMSTEC)
Hironori Satoh (Marine Works Japan Co. Ltd, MWJ)
Hideki Yamamoto (MWJ)
Katsunori Sagishima (MWJ)
Shoko Tatamisashi (MWJ)
Masahiro Orui (MWJ)

(2) Objectives

Chlorofluorocarbons (CFCs) and sulfur hexafluoride (SF_6) are man-made stable gases. These atmospheric gases can slightly dissolve in sea surface water by air-sea gas exchange and then are spread into the ocean interior. So dissolved these gases could be used as chemical tracers for the ocean circulation. We measured concentrations of three chemical species of CFCs, CFC-11 (CCl_3F), CFC-12 (CCl_2F_2), and CFC-113 ($C_2Cl_3F_3$), and SF_6 in seawater on board.

(3) Apparatus

We use three measurement systems. One of them is CFCs analyzing system. Other two are SF_6/CFCs simultaneous analyzing system. Both systems are basically purging and trapping gas chromatography.

Table 3-5-1 Instruments

SF_6/CFCs simultaneous analyzing system	
Gas Chromatograph:	GC-14B (Shimadzu Ltd.)
Detector 1:	ECD-14 (Shimadzu Ltd)
Detector 2:	ECD-14 (Shimadzu Ltd)
Analytical Column:	
Pre-column:	Silica Plot capillary column [i.d.: 0.32 mm, length: 10 m, film thickness: 4 µm]
Main column 1:	Connected two columns (MS 5A packed column [1/16" OD, 10 cm length stainless steel tubing packed the section of 7 cm with 80/100 mesh Molecular Sieve 5A] followed by Gas Pro [i.d.: 0.32 mm, length: 30m])
Main culumn2:	Silica Plot capillary column [i.d.: 0.32mm, length: 30 m, film thickness: 4 µm]
Purging & trapping:	Developed in JAMSTEC. Cold trap columns are 30 cm length stainless steel tubing packed the section of 5cm with 100/120 mesh Porapak T and followed by the section of 5cm of 100/120 mesh Carboxen 1000. Outer diameters of the main and focus trap columns are 1/8" and 1/16", respectively.
CFCs analyzing system	
Gas Chromatograph:	GC-14B (Shimadzu Ltd.)

Detector:	ECD-14 (Shimadzu Ltd)
Analytical Column:	
Pre-column:	Silica Plot capillary column [i.d.: 0.53mm, length: 6 m, film thickness: 6μm]
Main column:	Connected two capillary columns (Pola Bond-Q [i.d.: 0.53mm, length: 9 m, film thickness: 10μm] followed by Silica Plot [i. d.: 0.53mm, length: 18 m, film thickness: 6μm])
Purging & trapping:	Developed in JAMSTEC. Cold trap columns are 1/16” SUS tubing packed with Porapak T.

(3) Procedures

i. Sampling

Seawater sub-samples were collected from 12 litter Niskin bottles to 450 ml of glass bottles. The bottles were filled by nitrogen gas before sampling. Two times of the bottle volume of seawater sample were overflowed. The seawater samples were kept in water bathes controlled at 7ºC. The samples were taken to determination as soon as possible after sampling (usually within 12 hours).

In order to confirm CFC/SF$_6$ concentrations of standard gases and their stabilities and also to check saturation levels in sea surface water, mixing ratios in background air were periodically analyzed. Air samples were continuously led into laboratory by 10 mm OD Dekaron tubing. The end of the tubing was put on a head of the compass deck and another end was connected onto an air pump in the laboratory. The tubing was relayed by a T-type union which had a small stop cock. Air sample was collected from the flowing air into a 200ml glass cylinder attached on the cock.

ii. Analysis

SF$_6$/CFCs simultaneous analyzing system

Constant volume of sample water (200 ml) is taken into a sample loop. The sample is send into stripping chamber and dissolved SF$_6$ and CFCs are de-gassed by N$_2$ gas purging for 8 minutes. The gas sample is dried by magnesium perchlorate desiccant and concentrated on a main trap column cooled down to -80 ºC. Stripping efficiencies are frequently confirmed by re-stripping of surface layer samples and more than 99 % of dissolved SF$_6$ and CFCs are extracted on the first purge. Following purging & trapping, the main trap column is isolated and electrically heated to 175 ºC. After 1 minute, the desorbed gases are sent onto focus trap cooled down to -80 ºC for 30 seconds. Gaseous sample on the focus trap are desorbed by same manner of the main trap, and lead into the pre-column. Sample gases are roughly separated on the pre-column. SF$_6$ and CFC-12 are sent onto main column 1 (MC 1) and CFC-11 and CFC-113 still remain on the pre-column. Main column connected on pre-column is switched to the main column 2 (MC 2). Another carrier gas line is connected to MC 1 and SF6 and CFC-12 are further separated and detected by an electron capture detector, ECD 1. CFC-11 and CFC-113 lead to MC 2 are detected by ECD 2. When CFC-113 eluted from pre-column onto MC 2, the pre-column is switched onto another line and flushed by counter flow of pure nitrogen gas.

CFCs analyzing system

Constant volume of sample water (50 ml) is taken into a sample loop. The sample is send into stripping chamber and dissolved CFCs are de-gassed by N_2 gas purging for 8 minutes. The gas sample is dried by magnesium perchlorate desiccant and concentrated on a main trap column cooled down to -55 ºC. Stripping efficiencies are frequently confirmed by re-stripping of surface layer samples and more than 99.5 % of dissolved CFCs are extracted on the first purge. Following purging & trapping, the trap column is isolated and electrically heated to 140 ºC. The desorbed gases are lead into the pre-column. Sample gases are roughly separated in the pre-column. When CFC-113 eluted from pre-column onto main column, the pre-column is switched onto another line and flushed by counter flow of pure nitrogen gas.

Nitrogen gases used in these system was filtered by gas purifier tube packed with Molecular Sieve 13X (MS-13X).

Table 3-5-2 Analytical conditions

SF_6/CFCs simultaneous analyses

Temperature

Analytical Column: 95 ºC
Detector (ECD): 300 ºC
Trap column: -80 ºC (at adsorbing) & 175 ºC (at desorbing)

Mass flow rate of nitrogen gas (99.99995%)

Carrier gas 1: 5 ml/min
Carrier gas 2: 5 ml/min
Detector make-up gas 1: 30 ml/min
Detector make-up gas 2: 30 ml/minm
Back flush gas: 7 ml/min
Sample purge gas: 230 ml/min

CFCs analyses

Temperature

Analytical Column: 95 ºC
Detector (ECD): 240 ºC
Trap column: -50 ºC (at adsorbing) & 140 ºC (at desorbing)

Mass flow rate of nitrogen gas (99.99995%)

Carrier gas : 13 ml/min
Detector make-up gas : 24 ml/min

.

Back flush gas: 20 ml/min
Sample purge gas: 130 ml/min

Standard gas (Japan Fine Products co. ltd.)

Cylinder No.	Base gas	CFC-11	CFC-12	CFC113	SF_6	remarks
		ppt	ppt	ppt	ppt	
CPB26845	Air	1304	649	130	9.99	SF_6/CFC, Leg 2
CPB25863	Air	1301	649	130	10.00	SF_6/CFC, Leg 2,3
CPB17252	Air	1304	652	130	9.93	SF_6/CFC, Leg 3
CPB30572	Air	1301	651	130	9.98	SF_6/CFC, Leg 3
CPB07911	N_2	302	159	30.0	0.0	CFC, Leg 2,3
CPB15651	N_2	299	159	30.2	0.0	CFC, Reference

iii. Performance

The analytical precisions are estimated from replicate sample analyses. The estimated preliminary precisions were ± 0.013 pmol/kg (n = 527), ± 0.007 pmol/kg (n = 529), ± 0.005 pmol/kg (n = 528), and ± 0.03 fmol/kg (n = 352) for CFC-11, CFC-12, CFC-113, and SF6, respectively.

(4) Data archive

All data will be submitted to JAMSTEC Data Management office (DMO) and under its control.

.

3.7 Carbon items

(1) Personnel

Akihiko Murata (JAMSTEC)
Sohiko Kameyama (Hokkaido Univ.)
Yoshiko Ishikawa (MWJ)
Tomonori Watai (MWJ)
Emi Deguchi (MWJ)
Atsushi Ono (MWJ)
Keisuke Tsubata (MWJ)

(2) Objectives

Concentrations of CO_2 in the atmosphere are now increasing at a rate of about 2.0 ppmv y^{-1} owing to human activities such as burning of fossil fuels, deforestation, and cement production. It is an urgent task to estimate as accurately as possible the absorption capacity of the oceans against the increased atmospheric CO_2, and to clarify the mechanism of the CO_2 absorption, because the magnitude of the anticipated global warming depends on the levels of CO_2 in the atmosphere, and because the ocean currently absorbs 1/3 of the 6 Gt of carbon emitted into the atmosphere each year by human activities.

The Southern Ocean is one of the regions where uncertainty of uptake of anthropogenic CO_2 is large. In this cruise, therefore, we were aimed at quantifying how much anthropogenic CO_2 were absorbed in the surface ocean in the Indian sector of the Southern Ocean. For the purpose, we measured CO_2-system parameters such as dissolved inorganic carbon (C_T), total alkalinity (A_T) and pH along the WHP P14S and S04I lines at 174E and 65°S, respectively, in the Southern Ocean.

(3) Apparatus

i. C_T

Measurement of C_T was made with two total CO_2 measuring systems (called as Systems C and D, respectively; Nippon ANS, Inc.), which were slightly different from each other. The systems comprised of a seawater dispensing system, a CO_2 extraction system and a coulometer. In this cruise, we used coulometers, Seacat2000 and Model23000 for Systems C and D, respectively, both of which were constructed by Nippon ANS. Each of the two systems had almost a same specification as follows:

> The seawater dispensing system has an auto-sampler (6 ports), which dispenses seawater from a 300 ml borosilicate glass bottle into a pipette of about 15 ml volume by PC control. The pipette is kept at 20 °C by a water jacket, in which water from a water bath set at 20 °C is circulated. CO_2 dissolved in a seawater sample is extracted in a stripping chamber of the CO_2 extraction system by adding phosphoric acid (~ 10 % v/v) of about 2 ml. The stripping chamber is approx. 25 cm long and has a fine frit at the bottom. The acid is added to the stripping chamber from the bottom of the chamber by pressurizing an acid bottle for a given time to push out the right amount of acid. The pressurizing is made with nitrogen gas (99.9999 %). After the acid is

transferred to the stripping chamber, a seawater sample kept in a pipette is introduced to the stripping chamber by the same method as in adding an acid. The seawater reacted with phosphoric acid is stripped of CO_2 by bubbling the nitrogen gas through a fine frit at the bottom of the stripping chamber. The CO_2 stripped in the chamber is carried by the nitrogen gas (flow rates is 140 ml min^{-1}) to the coulometer through a dehydrating module. The modules of Systems C and D consist of two electric dehumidifiers (kept at ~4 °C) and a chemical desiccant ($Mg(ClO_4)_2$).

The measurement sequence such as system blank (phosphoric acid blank), 1.865 % CO_2 gas in a nitrogen base, sea water samples (6) is programmed to repeat. The measurement of 1.865 % CO_2 gas is made to monitor response of coulometer solutions purchased from UIC, Inc. or laboratory-made.

ii. A_T

Measurement of A_T was made based on spectrophotometry using a custom-made system (Nippon ANS, Inc.). The system comprises of a water dispensing unit, an auto-burette (765 Dosimat, Metrohm), and a spectrophotometer (Carry 50 Scan, Varian), which are automatically controlled by a PC. The water dispensing unit has a water-jacketed pipette and a water-jacketed titration cell. The spectrophotometer has a water-jacketed quartz cell, length and volume of which are 8 cm and 13 ml, respectively. To circulate sample seawater between the titration and the quartz cells, PFA tubes are connected to the cells.

A seawater of approx. 42 ml is transferred from a sample bottle (borosilicate glass bottle; 130 ml) into the water-jacketed (25 ºC) pipette by pressurizing the sample bottle (nitrogen gas), and is introduced into the water-jacketed (25 ºC) titration cell. The seawater is circulated between the titration and the quartz cells by a peristaltic pump to rinse the route. Then, Milli-Q water is introduced into the titration cell, and is circulated in the route twice to rinse the route. Next, a seawater of approx. 42 ml is weighted again by the pipette, and is transferred into the titration cell. The weighted seawater is introduced into the quartz cell. Then, absorbance at three wavelengths (750, 616 and 444 nm) is measured for seawater blank. After the measurement, an acid titrant, which is a mixture of approx. 0.05 M HCl in 0.65 M NaCl and bromocresol green (BCG) is added (about 2 ml) into the titration cell. The seawater + acid titrant solution is circulated for 6 minutes between the titration and the quartz cells, with stirring by a stirring tip and bubbling by wet nitrogen gas in the titration cell. Then, absorbance at the three wavelengths is measured again.

Calculation of A_T is made by the following equation:

$$A_T = (-[H^+]_T V_{SA} + M_A V_A) / V_S,$$

where M_A is the molarity of the acid titrant added to the seawater sample, $[H^+]_T$ is the total excess hydrogen ion concentration in the seawater, and V_S, V_A and V_{SA} are the initial seawater volume, the added acid titrant volume, and the combined seawater plus acid titrant volume, respectively. $[H^+]_T$ is calculated from the measured absorbances based on the following equation (Yao and Byrne, 1998):

.

$$pH_T = -\log[H^+]_T = 4.2699 + 0.002578(35 - S) + \log((R - 0.00131)/(2.3148 - 0.1299R)) \\ - \log(1 - 0.001005S),$$

where S is the sample salinity, and R is the absorbance ratio calculated as:

$$R = (A_{616} - A_{750})/(A_{444} - A_{750}),$$

where A_i is the absorbance at wavelength *i* nm.

The HCl in the acid titrant is standardized on land. The concentrations of BCG were estimated to be approx. 2.0×10^{-6} M in the sample seawater, respectively.

iii. pH

Measurement of pH was made by a pH measuring system (Nippon ANS, Inc.). For the detection of pH, spectrophotometry was adopted. The system comprises of a water dispensing unit and a spectrophotometer (Bio 50 Scan, Varian). For an indicator, *m*-cresol purple (2 mM) was used.

Seawater is transferred from borosilicate glass bottle (300 ml) to a sample cell in the spectrophotometer. The length and volume of the cell are 8 cm and 13 ml, respectively, and the sample cell is kept at 25.00 ± 0.05 ºC in a thermostated compartment. First, absorbance of seawater only is measured at three wavelengths (730, 578 and 434 nm). Then the indicator is injected and circulated for about 4 minutes to mix the indicator and seawater sufficiently. After the pump is stopped, the absorbance of seawater + indicator is measured at the same wavelengths. The pH is calculated based on the following equation (Clayton and Byrne, 1993):

$$pH = pK_2 + \log\left(\frac{A_1/A_2 - 0.00691}{2.2220 - 0.1331(A_1/A_2)}\right),$$

where A_1 and A_2 indicate absorbance at 578 and 434 nm, respectively, and pK_2 is calculated as a function of water temperature and salinity.

(4) Performances

i. C_T

The two systems worked well without a major malfunction. During the cruise, we analyzed certified reference materials (CRM, Batch No. 121, Certified value: 2039.26 ± 0.38μmol kg^{-1}) provided by Prof. A. Dickson, Scripps Institution of Oceanography, USA. In leg 2, the analyzed values were 2038.3 ± 1.6 (n=10) and 2038.5 ± 1.7 μmol kg^{-1} (n=16) for Systems C and D, respectively, while in leg 3, they were 2041.1 ± 2.3 (n=12) and 2037.6 ± 1.8μmol kg^{-1} (n=14), respectively.

.

ii. A_T

The system worked well during the cruise, and showed a very good precision of < 0.5 μmol kg^{-1}. The analyzed values of CRM (Batch No. 121), certified value of which is 2225.01 ± 0.96 μmol kg^{-1}, were 2225.0 ± 0.9 (n=55) and 2225.0 ± 1.3 μmol kg^{-1} (n=51) for legs 2 and 3, respectively.

iii. pH

The system worked well with no troubles. The estimated analytical precision was ~0.0005 pH unit.

(5) Results

Cross sections of C_T, pH, and A_T along WOCE S04I line are illustrated in Figs. 3.7.1, 3.7.2 and 3.7.3, respectively.

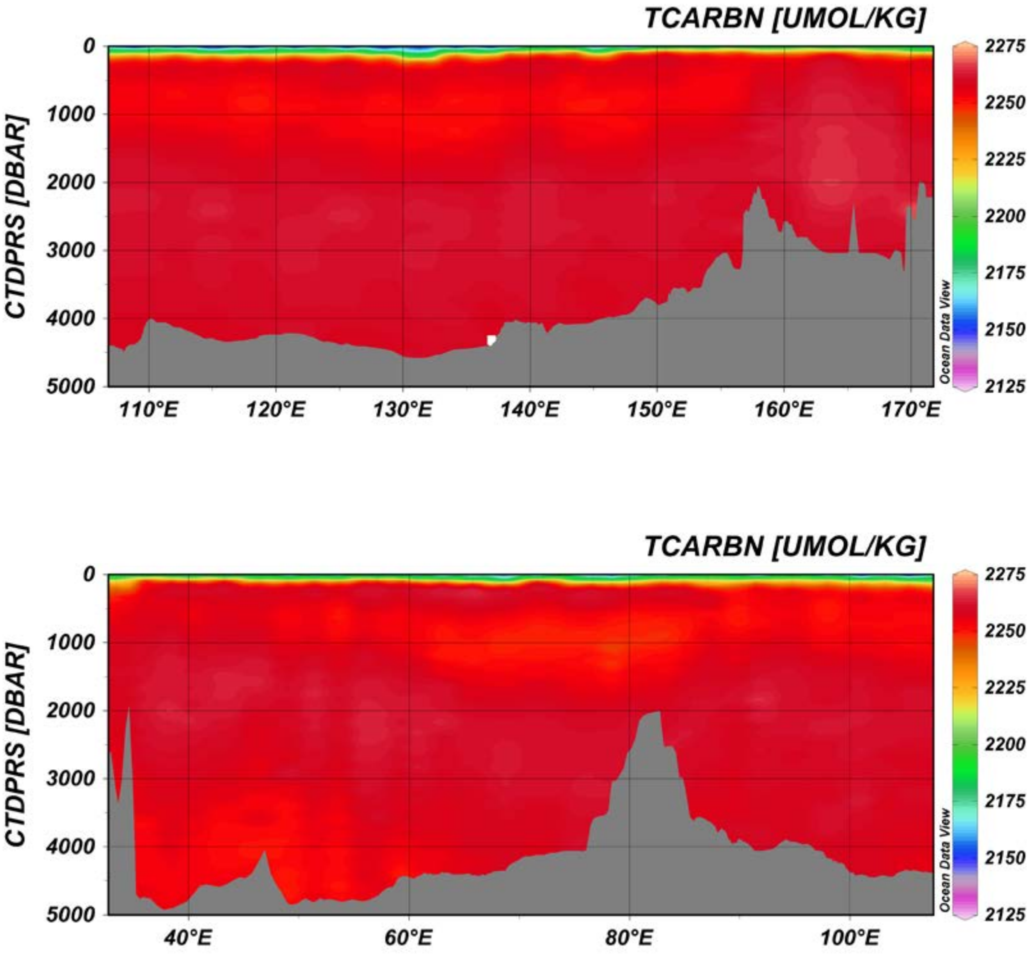

Fig. 3.7.1. Distributions of C_T along the S04I line for legs 2 (upper) and 3 (lower).

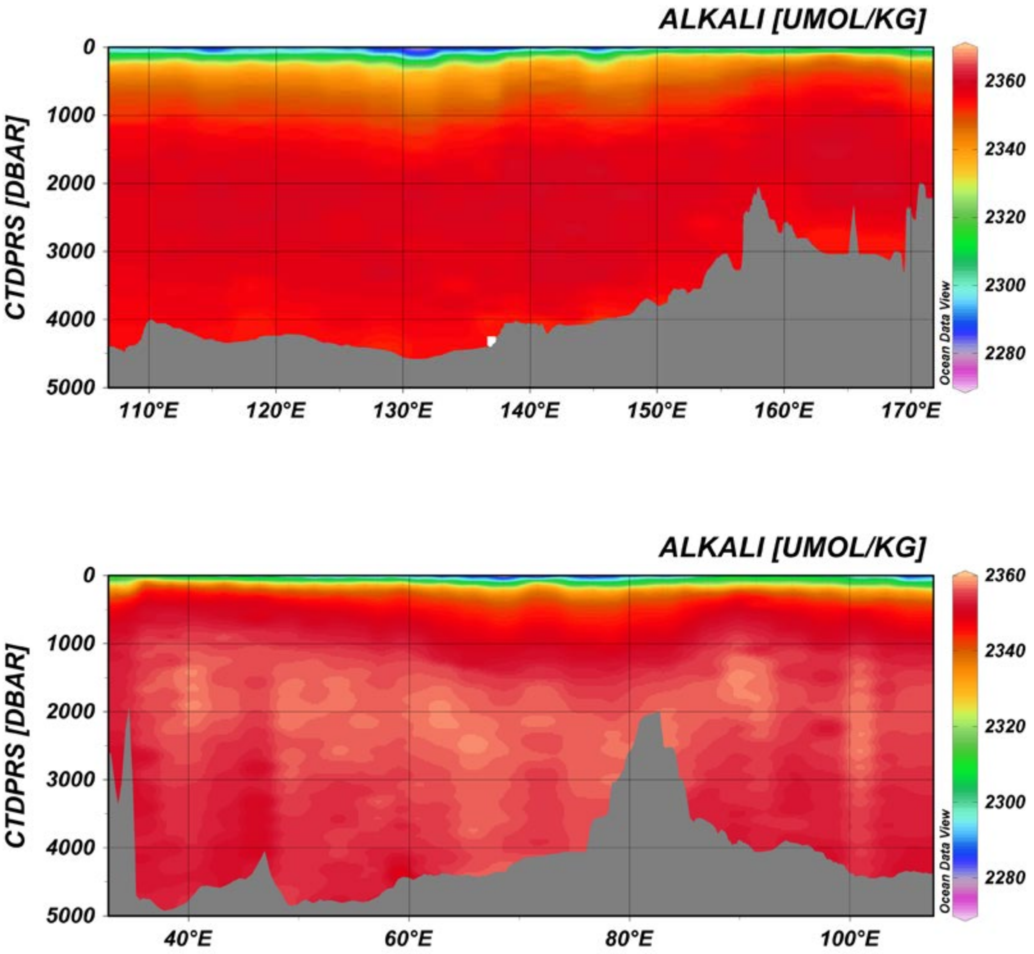

Fig. 3.7.2. Distributions of A_T along the S04I line for legs 2 (upper) and 3 (lower).

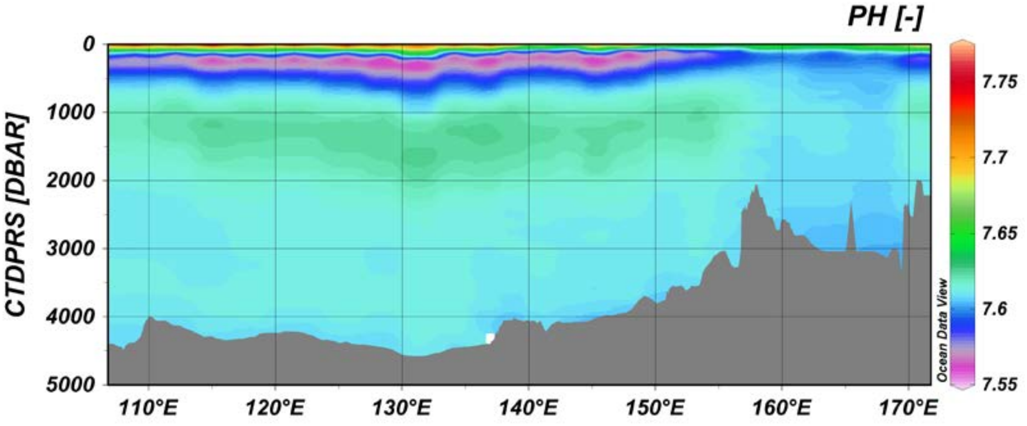

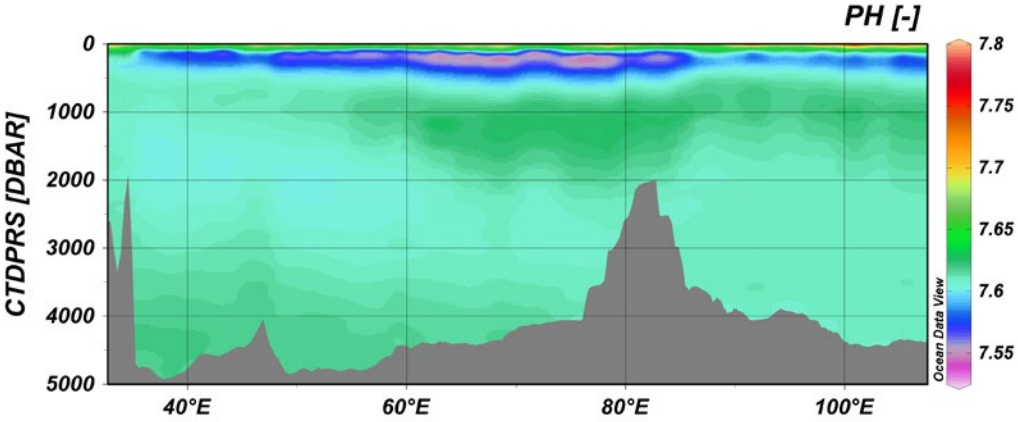

Fig. 3.7.3. Distributions of pH along the S04I line legs 2 (upper) and 3 (lower).

References

Clayton T.D. and R.H. Byrne (1993) Spectrophotometric seawater pH measurements: total hydrogen ion concentrtaion scale calibration of m-cresol purple and at-sea results. Deep-Sea Research 40, 2115-2129.

Yao W. and R. H. Byrne (1998) Simplified seawater alkalinity analysis: Use of linear array spectrometers. Deep-Sea Research I 45, 1383-1392.

.

3.8 DMS and isoprene

(1) Personnel

Sohiko Kameyama (Hokkaido University/ Principal Investigator)

Hisayuki Yoshikawa-Inoue (Hokkaido University)

(2) Objective

Air–sea exchange of volatile organic compounds (VOCs) plays an important role in the earth's biogeochemical cycles and in the chemistry of the atmosphere. It is known that the Southern Ocean is one of the high-productivity regions in the world oceans. The variability of phytoplankton activity is large there; therefore, distribution of biogenic VOCs including dimethyl sulfide (DMS) and isoprene should be variable. DMS and isoprene is known as a precursor of cloud condensation nuclei (CCN) over the ocean (Andreae and Raemdonck, 1983; Grenfell et al., 1999), but the degree of its contribution to formation of cloud is still uncertain. In order to investigate the factor controlling the distribution of DMS and isoprene in surface water column we took seawater samples and measured the concentrations during the cruise. Samples for the measurements of dimethylsulfoniopropionate (DMSP), one of the major precursors of DMS, were also taken.

(3) Parameters

DMS, dissolved and particulate DMSP concentration in seawater

Isoprene concentration in seawater

(4) Instruments and Methods

The surface water samplings (5-m depth) were basically held once a day. Depth samples to 300-m depth were taken a half and a quarter frequency of surface water sampling for DMS and isoprene, respectively. Seawater sample for DMS measurement was subsampled to glass vial bottle with filtration by the GF/F filter and stored at 4˚C until the measurement. Samples for isoprene and DMSP were taken without the filter and overflowed for the twice volume of the sample to avoid contamination. For dissolved DMSP sample, we made gravity filtering in the laboratory according to the method of Kiene and Slezak (2006). Both dissolved and particulate DMSP samples were stored at −80˚C.

All samples were measured by gas chromatography (GC) coupling with conventional purge and trap extraction system. Briefly, seawater sample was introduced into a purge bottle and extracted by pure N_2 carrier gas for 14 minutes. Extracted gas stream including DMS and isoprene passed through cold dehydration trap (dry ice/ethanol cooled hollow U-shaped glass tube) and concentrated on the cold trap (dry ice/ethanol temperature) with TENAX TA. Concentrated gas was eliminated by replacing the Dewar bottle of from dry ice/ethanol refrigerant to boiled water. Eliminated gas was introduced to GC (GC-2014, Shimadzu) with Flame Photometric Detector (FPD) for DMS and Flame Ionization Detector (FID) for isoprene**.** Isoprene samples were immediately measured after sampling. DMS samples were measured after isoprene measurements because we confirmed that DMS could be preserved for 2 days at least. For DMSP measurements, alkali treatment permits the cleavage of DMSP into gaseous DMS. After the alkali treatment, the sample bottles were stored at 4°C for at least 24 h to complete the cleavage before analyses. The cleaved DMS were analyzed by the same manner of DMS measurement.

.

(5) Preliminary results

Figures 3-8-1 and 3-8-2 shows vertical profiles of DMS and isoprene concentration during the leg. 2 cruise, respectively. All profiles show gradual decrease along a depth with the maximum at the subsurface (25–50 m) where phytoplankton abundance often reach maximum. We could also find large variability for profiles of all species and it should be comparable with the biological activities. Further data analysis after the measurements of other biological parameters is required to address the controlling factors of the distributions.

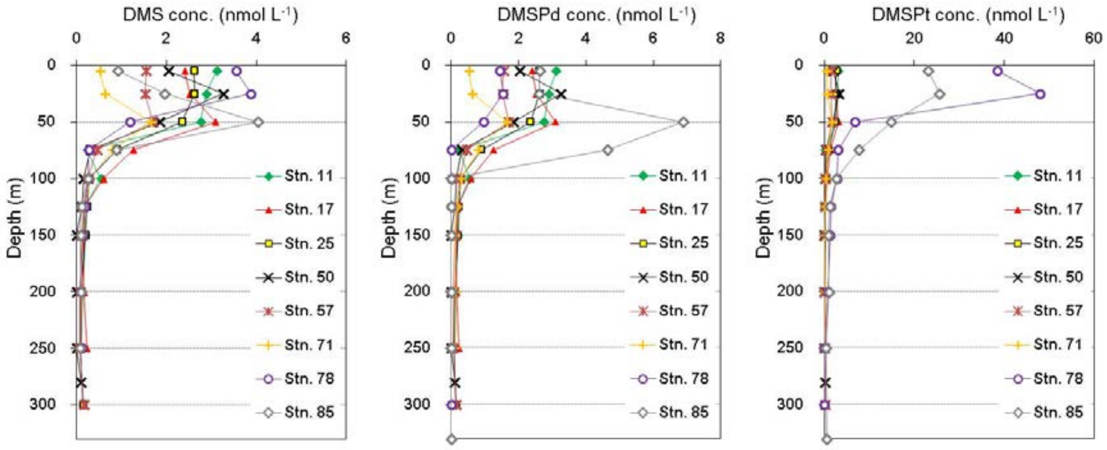

Figure 3-8-1. Vertical profiles of concentration of DMS, DMSPd and DMSPt during leg. 2 cruise.

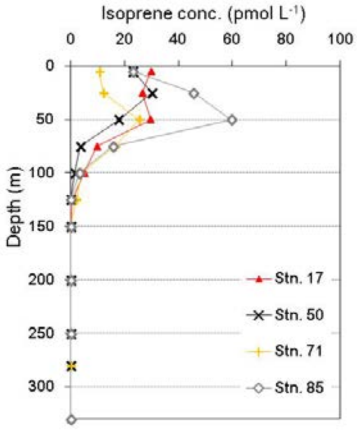

Figure 3-8-2. Vertical profiles of concentration of isoprene during leg. 2 cruise.

(6) Data archives

Remaining DMSP samples will be analyzed in the laboratory in Hokkaido University. All data will be opened within a year.

(7) References

Andreae, M. O. and H. Raemdonck (1983), Dimethyl sulfide in the surface ocean and the marine atmosphere: a global view, *Science*, *221*, 744–747.

.

Grenfell, J. L. (1999), An analysis of rapid increases in condensation nuclei concentrations at a remote coastal site in Western Ireland, *J. Geophys. Res.*, *104*, 13771–13780.

Kiene, R. P., and D. Slezak (2006), Low dissolved DMSP concentrations in seawater revealed by small-volume gravity filtration and dialysis sampling, *Limnol. Oceanogr. Methods*, *4*, 80–95.

.

3.9 Chlorophyll *a*

(1) Personnel

Hiroshi Uchida (JAMSTEC)
Osamu Yoshida (Rakuno Gakuen University) (Leg 3)
Haruka Tamada (Rakuno Gakuen University) (Leg 3)
Yuko Kanayama (Rakuno Gakuen University) (Leg 3)
Okura Shinozaki (Rakuno Gakuen University) (Leg 3)
Kanako Yoshida (MWJ) (Legs 1, 3)
Hideki Yamamoto (MWJ) (Leg 2)

(2) Objectives

Chlorophyll *a* is one of the most convenient indicators of phytoplankton stock, and has been used extensively for the estimation of phytoplankton abundance in various aquatic environments. In this study, we investigate horizontal and vertical distribution of phytoplankton. The chlorophyll *a* data is also used for calibration of fluorometers used in the surface water monitoring and the CTD profiler measurements.

(3) Instrument and Method

Seawater samples were collected in 500 or 250 ml brown Nalgene bottles without head-space. The whole sampled water were gently filtrated by low vacuum pressure (<0.02 MPa) through Whatman GF/F filter (diameter 25 mm) in the dark room. Whole volume of each sampling bottle was precisely measured in advance. Phytoplankton pigments were immediately extracted in 7 ml of N,N-dimethylformamide (DMF) after filtration and then, the samples were stored at –20°C under the dark condition to extract chlorophyll *a* for more than 24 hours. Fluorescence of the extracted samples was measured by the Turner fluorometer (10-AU-005, TURNER DESIGNS) which was previously calibrated against a pure chlorophyll *a* (Sigma-Aldrich Co., LLC). We applied the fluorometric “Non-acidification method” (Welschmeyer, 1994).

(4) Results

Chlorophyll *a* data obtained during the cruise are shown in Fig. 3.9.1. To estimate measurement precision, 20 pairs of replicate samples were obtained from hydrographic casts during leg 3. Ten pairs of the replicate samples were collected in 500 ml and 250 ml bottles. Difference between samples collected in 500 ml and 250 ml was small (≤ 0.02 μg/L). Standard deviation from 20 pairs of the replicate samples was 0.018 μg/L, although absolute difference was smaller than 0.01 μg/L for 16 pairs of the replicate samples.

Reference

Welschmeyer, N. A. (1994): Fluorometric analysis of chlorophyll a in the presence of chlorophyll b and pheopigments. Limnor. Oceanogr., 39, 1985-1992.

.

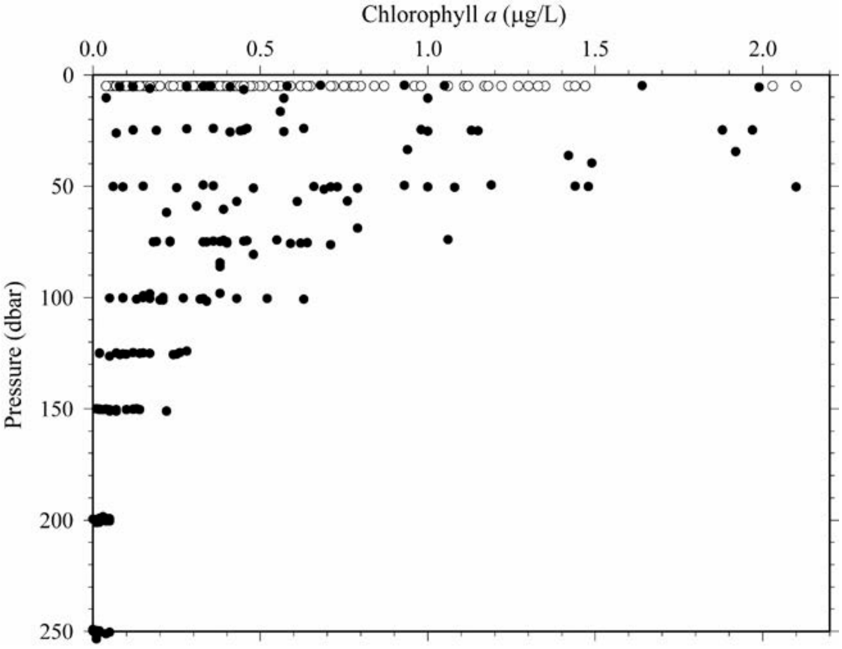

Figure 3.9.1. Vertical distribution of chlorophyll *a* obtained from hydrographic casts (closed circles) and surface water monitoring system (open circles).

.

3.10 pigment and bacterial abundance

(1) Personnel

Sohiko Kameyama (Hokkaido University/ Principal Investigator)

(2) Objective

It is broadly known that phytoplankton abundance and the community structure influences on biogenic gases in ocean surface (e.g., Bonsang et al., 1992; Kettle et al., 1999; Baker et al., 2000). Recently, analytical technique of remote sensing data is much improving to estimate phytoplankton community in ocean surface (Alvain et al., 2005). The Southern Ocean, however, is often covered thick cloud all year round, therefore, the estimation of the community structure still has large uncertainty. Therefore, the estimation still depends on the frequency of in-situ observation as for the Southern Ocean. In this study, we try to estimate the phytoplankton community structure over the broad area in the Southern Ocean by pigment analysis with high-performance liquid chromatography (HPLC). The distribution of the community structure will be compared with that of biogenic trace gas concentration. Moreover, the high-resolution pigment data may contribute to improve the estimation of the phytoplankton community with remote sensing technique in the Southern Ocean. Bacterial abundance also contributes to the trace gas production/consumption. We measure the bacterial abundance by flow cytometry (FCM).

(3) Parameters

Pigments contents

Bacterial abundance

(4) Instruments and Methods

Water samples for both pigment and bacterial analysis were collected from 5-m depth at the same stations of the sampling for trace gas measurements (see the chapter of " DMS and isoprene" in detail). Samples totaled 45 for HPLC analysis and 90 for FCM analysis, respectively. The samples will be analyzed on land by HPLC and FCM. For HPLC pigment analysis, the water samples were filtered onto Whatman GF/F filters. For FCM, 2-mL of duplicate seawater subsamples were taken into a cryotubes vial and 0.04-mL of paraformaldehyde (PFA) solution was added. After the treatments, samples were stored in deep freezer at −70°C.

(5) Data archives

All samples will be analyzed in the laboratory in Hokkaido University. All data will be opened within a year.

(6) References

Alvain, S., C. Moulin, Y. Dandonneau, and F. M. Breon (2005), Remote sensing of phytoplankton groups in case 1 waters from global SeaWiFS imagery, *Deep Sea Res. I*, *52*, 1989–2004.

Baker, A., S. Turner, W. Broadgate, A. Thompson, G. McFiggans, O. Vesperini, P. Nightingale, P. Liss, and T. Jickells (2000), Distribution and Sea-Air Fluxes of Biogenic Trace Gases in the Eastern Atlantic Ocean, *Global Biogeochem. Cycles*, *14*, 871–886.

.

Bonsang, B., C. Polle, and G. Lambert (1992), Evidence for marine production of isoprene, *Geophys. Res. Lett.*, *19*, 1129–1132.

Kettle, A. J., et al. (1999), A global database of sea surface dimethylsulfide (DMS) measurements and a procedure to predict sea surface DMS as a function of latitude, longitude, and month, *Global Biogeochem. Cycles*, *13*(2), 399–444

.

3.11 Chlorophyll isotope

April 19, 2013

(1) Personnel

Chisato Yoshikawa[1], Naohiro Yoshida[1], Osamu Yoshida[2,3], Haruka Tamada[3], Okura Shinozaki[3], and Yuko Kanayama[3]*

[1] *Interdisciplinary Graduate School of Science and Engineering, Tokyo Institute of Technology*

[2] *College of Agriculture, Food and Environment Sciences, Rakuno Gakuen University*

[3] *Faculty of Environment Systems, Rakuno Gakuen University*

* *Principal Investigator*

(2) Sampling elements

All sampling elements of Rakuno Gakuen University group at hydrographic stations are listed below.

Table 1. Parameters and hydrographic station numbers for samples collection.

1. Chl. *a* isotope	94,98,102,106,111,115,121,140,156,163

Water sample for isotope analysis of isotope analysis of Chlorophyll pigments were collected into six-ten 20L light-blocking polypropylene tanks. The samples were filtered under reduced pressure and collected on two-three Whatman GF/F filfers. The filters were wrapped in aluminum foil and stored at -20ºC until analysis. Chlorophyll pigments were extracted and split into each pigments by HPLS. Isotope ratios of Chlorophyll pigments were measured by using EA-IRMS (Ohkouchi et al., 2006).

(3) Expected results

Stable nitrogen isotopic composition provides significant information for nitrogen cycle in the surface ocean. Nitrogen isotopic ratios of nitrate are widely used as a tracer of nutrient utilization, atmospheric nitrogen input, nitrogen fixation and denitrification (Sigman et al., 2009; Elliott et al., 2009; Minagawa and Wada, 1986; De Pol-Holz, 2009). The levels of the nitrogen isotopic ratios of nitrate must transfer to the nitrogen isotopic ratios of phytoplankton, settling particles, and eventually benthic sediment. The nitrogen isotopic ratios of settling particles and sediments can therefore be used to trace the various time-scale of past nitrogenous nutrient environment. But in fact, various biogeochemical information (nutrient utilization, atmospheric nitrogen input, nitrogen fixation, denitrification, contamination and diagenesis) are recorded simultaneously in the nitrogen isotopic ratios of settling particles and sediments (Yoshikawa et al., submitted).

Recently Ohkouchi et al. (2006) developed an isotope analysis of Chlorophyll pigments. They applied this technique to the sediments and reconstructed the past nitrogen fixation process (Ohkouchi et al., 2006; Kasiyama et al., 2008). In this study nitrogen isotope ratios of Chlorophyll together with those ratios of substrate (NO_3^-) will reveal the surface nitrogen cycle in the Southern Ocean and will confirm the transfer of the levels of the nitrogen isotopic ratio from

.

nitrate to phytoplankton.

(4) References

De Pol-Holz, R., R. S. Robinson, D. Hebbeln, D. M. Sigman, and O. Ulloa: Controls on sedimentary nitrogen isotopes along the Chile margin, Deep-Sea Research II 56, 1042–1054, 2009.

Elliott, E. M., C. Kendall, E. W. Boyer, D. A. Burns, G. G. Lear, H. E. Golden, K. Harlin, A. Bytnerowicz, T. J. Butler, and R. Glatz: Dual nitrate isotopes in dry deposition: Utility for partitioning NOx source contributions to landscape nitrogen deposition, J. Geophys. Res., 114, G04020, doi:10.1029/2008 JG000889, 2009.

Kashiyama, Y., N. O. Ogawa, M. Shiro, R. Tada, H. Kitazato, and N. Ohkouchi: Reconstruction of the biogeochemistry and ecology of photoautotrophs based on the nitrogen and carbon isotopic compositions of vanadyl porphyrins from Miocene siliceous sediments, Biogeosciences, 5, 797–816, doi:10.5194/bg-5-797-2008, 2008.

Minagawa, M., and E. Wada: Nitrogen isotope ratio of red tide organisms in the East China Sea: A characterization of biological nitrogen fixation, Marine Chem., 19, 245–259, 1986.

Ohkouchi, N., Kashiyama, Y., Kuroda, J., Ogawa, N. O., and Kitazato, H.: The importance of diazotrophic cyanobacteria as primary producers during Cretaceous Oceanic Anoxic Event 2, Biogeosciences 3, 467-478, 2006.

Sigman, D. M., P. J. DiFiore, M. P. Hain, C. Deutsch, Y. Wang, D. M. Karl, A. N. Knapp, M. F. Lehmann, and S. Pantoja: The dual isotopes of deep nitrate as a constraint on the cycle and budget of oceanic fixed nitrogen, Deep-Sea Research I, doi:10.1016/j.dsr.2009.04.007, 2009.

Yoshikawa, C., A. Makabe, S. Toyoda, O. Yoshida and N. Yoshida, Nitrogenous nutrient inputs and losses in the subtropical South Pacific traced by nitrogen isotopes of nitrate, Submitted to Geophysical Research Letter.

.

3.12 Carbon isotopes

April 19, 2013
Yuichiro Kumamoto
Japan Agency for Marine-Earth Science and Technology (JAMSTEC)

(1) Personnel

Yuichiro Kumamoto (Japan Agency for Marine-Earth Science and Technology, JAMSTEC)

(2) Objective

In order to investigate the water circulation and carbon cycle in the Southern Ocean, seawaters for measurements of carbon-14 (radiocarbon) and carbon-13 (stable carbon) of total dissolved inorganic carbon (TDIC) were collected by the hydrocasts from surface to near bottom during MR12-05 cruise.

(3) Sample collection

The sampling stations and number of samples are summarized in Table 3.12.1. All samples for carbon isotope ratios (total 888 samples) were collected at 28 stations using 12-liter Niskin-X bottles. The seawater sample was siphoned into a 250 cm^3 glass bottle with enough seawater to fill the glass bottle 2 times. Immediately after sampling, 10 cm^3 of seawater was removed from the bottle and poisoned by 0.1 cm^3 μl of saturated $HgCl_2$ solution. Then the bottle was sealed by a glass stopper with Apiezon grease M and stored in a cool and dark space on board.

(4) Sample preparation and measurements

In our laboratory, dissolved inorganic carbon in the seawater samples will be stripped cryogenically and split into three aliquots: radiocarbon measurement (about 200 μmol), carbon-13 measurement (about 100 μmol), and archive (about 200 μmol). The extracted CO_2 gas for radiocarbon will be then converted to graphite catalytically on iron powder with pure hydrogen gas. The carbon-13 of the extracted CO_2 gas will be measured using Finnigan MAT252 mass spectrometer. The carbon-14 in the graphite sample will be measured by Accelerator Mass Spectrometry (AMS).

Table 3.12.1 The sampling stations and number of samples for carbon isotope ratios.

Station	Lat. (N)	Long. (E)	Sampling Date (UTC)	Number of samples	Number of replicate samples	Max. Pressure (dbar)

011	-56-59.67	173-59.15	2012/12/05	35	2	5551
015	-58-59.23	174-00.23	2012/12/07	35	2	5224
020	-61-30.39	174-00.92	2012/12/08	34	2	5134
025	-63-30.33	170-58.98	2012/12/09	23	1	2362
404	-63-59.70	167-27.69	2012/12/10	26	1	3222
050	-63-33.93	159-43.73	2012/12/12	24	1	2662
053	-63-26.07	156-39.16	2012/12/13	27	2	3223
057	-63-26.03	150-39.76	2012/12/15	28	2	3775
061	-62-36.05	145-02.59	2012/12/16	29	2	4061
064	-62-28.03	141-02.03	2012/12/16	30	2	4221
067	-62-00.15	137-00.81	2012/12/17	29	2	3997
071	-62-00.39	131-19.49	2012/12/20	32	2	4589
075	-62-00.17	125-39.34	2012/12/22	32	2	4378
078	-61-59.98	121-31.53	2012/12/22	30	2	4173
083	-61-56.29	115-04.34	2012/12/24	31	2	4329
087	-61-31.55	108-57.72	2012/12/25	30	2	4259
090	-62.08.62	105-16.46	2013/01/13	31	2	4317
094	-62-19.74	101-05.36	2013/01/14	31	2	4501
098	-62-15.13	94-45.57	2013/01/15	29	2	3860
104	-63-06.55	87-07.94	2013/01/17	29	2	3842
113	-61-24.93	80-29.39	2013/01/19	24	1	2463
116	-61-48.54	76-40.87	2013/01/19	30	2	4006
119	-62.00.57	71-38.06	2013/01/20	30	2	4151
123	-62-18.81	65-47.43	2013/01/21	31	2	4443
128	-63-30.37	59-26.84	2013/01/23	31	2	4365
133	-63-30.09	53-40.61	2013/01/27	32	2	4842
146	-63-44.22	46-24.17	2013/01/28	30	2	4283
153	-65-18.03	36-07.25	2013/01/30	33	2	4734
			Total	836	52	

.

3.13 Radioactive Cesium

April 19, 2013
Yuichiro Kumamoto
Japan Agency for Marine-Earth Science and Technology (JAMSTEC)

(1) Personnel

Yuichiro Kumamoto (Japan Agency for Marine-Earth Science and Technology)

(2) Objective

In order to investigate the water circulation and ventilation process in the western Pacific and Southern Oceans, during the leg-1 and -2 of MR12-05 cruise seawater samples were collected for measurements of radioactive cesium (Cs-134 and -137), which were released from the global fallout in the 1950s and 1960s and the Fukushima Daiichi nuclear power plant after its serious accident on the March 11 of 2011.

(3) Sample collection

The sampling stations and number of samples are summarized in Table 3.13.1. The total 180 of seawater samples for radioactive cesium were collected at 31 stations. At stations 051, 062, 070, and 084 during the leg-2 the seawaters were sampled vertically using 12-liter Niskin-X bottles. Surface seawater were collected from continuously-pumped-up water from about 4-m depth. The deep seawaters from stations C01 and C02 during the leg-1 were for evaluation of background contamination. The seawater sample for radioactive cesium was collected into a 20-L plastic container and after two time washing. Immediately after sampling, the seawater collected in layers shallower than 1000-m depth was filtrated using menbrane filter (Millipore HAWP14250, 142mm, 0.45μm). All the seawater samples were acidified by 40-cm^3 of concentrated nitric acid (RCI Labscan Ltd., Nitric Acid 70% , AR) on board.

(4) Sample preparation and measurements

In our laboratory on shore, radioactive cesium in the seawater samples will be concentrated using ammonium phosphomolybdate (AMP) that forms insoluble compound with cesium. The radioactive cesium in AMP will be measured using Ge γ-ray spectrometer. For the seawater samples collected in deeper than 1000-m depth, the radioactive cesium on AMP will be dissolved again then concentrated using insoluble platinate salt in which radioactive cesium will be analyzed using low-background Ge γ-ray detector.

Table 3.13.1 The sampling stations and number of samples for radioactive cesium.

Station	Lat. (N)	Long. (E)	Sampling Date (UTC)	Number of samples	Max. Pressure (dbar)
Surface-1,2	40-28.38	141-49.61	2012/11/6	2	4

Surface-3,4	39-58.18	142-09.11	2012/11/6	2	4
Surface-5,6	39-39.45	142-20.49	2012/11/6	2	4
Surface-7,8	39-00.47	142-26.32	2012/11/6	2	4
Surface-9,10	38-27.70	142-32.78	2012/11/6	2	4
Surface-11,12	38-02.14	142-37.30	2012/11/6	2	4
Surface-13,14	37-29.35	142-43.76	2012/11/7	2	4
Surface-15,16	37-01.59	142-49.45	2012/11/7	2	4
Surface-17,18	36-30.81	142-55.39	2012/11/7	2	4
Surface-19,20	36-02.46	143-01.34	2012/11/7	2	4
Surface-21,22	35-30.90	143-09.09	2012/11/7	2	4
Surface-23,24	35-02.89	143-15.30	2012/11/7	2	4
Surface-25,26	33-59.86	143-30.23	2012/11/8	2	4
Surface-27,28	33-00.80	143-43.91	2012/11/8	2	4
Surface-29,30	32-01.32	143-57.24	2012/11/8	2	4
Surface-31,32	31-04.57	144-10.38	2012/11/8	2	4
Surface-33,34	29-00.91	144-37.99	2012/11/9	2	4
Surface-35,36	27-03.13	145-03.34	2012/11/9	2	4
Surface-37,38	25-01.69	145-29.63	2012/11/9	2	4
Surface-39,40	14-04.45	149-14.15	2012/11/12	2	4
C01	14-00.13	149-15.84	2012/11/12	9	2000
C02	12-00.01	149-50.86	2012/11/12	9	2000
Surface-41,42	3-00.95	149-44.88	2012/11/15	2	4
Surface-43,44	-26-18.25	165-35.91	2012/11/22	2	4
Surface-45,46	-55-59.95	173-00.01	2012/12/5	2	4
Surface-47,48	-59-57.82	173-57.99	2012/12/7	2	4
Surface-49,50	-63-00.11	171-45.49	2012/12/9	2	4
051	-63-02.52	159-26.38	2012/12/13	24	800
062	-62-45.88	143-35.84	2012/12/16	24	770
070	-61-59.75	132-36.66	2012/12/20	41	4529
084	-62-03.04	113-49.74	2012/12/24	23	800
			Total	180	

.

3.14. Delta O18

(1) Personnel

Shigeru Aoki (Hokkaido University)

(2) Objectives

Salinity/freshwater budget in the high-latitude oceans is an essential factor in determining the stratification and hence global meridional overturning. Near-surface freshening is observed in the high-latitude Southern Ocean (eg. Boyer et al., 2005) and understanding the balance of freshwater input and its origins are of critical importance in climate change study related to global hydrological cycle.

In the freshwater input near surface, excess precipitation (over evaporation) is a dominant factor in relatively fresh nature of the Antarctic Surface Water. Near the Antarctic continent, net sea ice melt and iceberg melt can contribute to the freshwater input as well. However, relative contribution from each component is not sufficiently understood. Oxygen isotope is a good tracer in detecting the origin of freshwater since its value is significantly among the different freshwater sources such as local precipitation, ice shelf/iceberg melt water, and sea ice (Heywood et al., 1998). However, there is few observation of oxygen isotope in the Australian-Antarctic Basin until recently.

To obtain the oxygen isotope data for WHP S4 line for the first time, we collected water samples for the oxygen isotope analysis. This will hence lead to set the baseline for the future climate change study.

(3) Apparatus

The relative proportion of principal stable isotopes of oxygen in seawater is usually quoted as δ^{18}O, defined as the ratio of ^{18}O to ^{16}O relative to Vienna Standard Mean Ocean Water.

$$\delta^{18}O = \frac{(^{18}O/^{16}O)_{sample} - (^{18}O/^{16}O)_{VSMOW}}{(^{18}O/^{16}O)_{VSMOW}} \times 1000$$

We collected water samples for the δ^{18}O analysis from all Niskin bottles with 30ml glass vials at all stations. Total number of samples is 4,560 from 145 stations. The vials are stored in the refrigerator. The vials were sealed with Parafilms.

The samples are to be shipped to ILTS, Sapporo, and the analysis will be conducted with an IRMS mass spectrometer and CRDS isotope analyzer. The samples that well represent the watermass core property will be analyzed first and by Finnigan Delta Plus spectrometer. Water samples will be set in equilibrium with CO2 gas within the 18 degree Celcius water bath. The rest of the samples will be analyzed with a CRDS spectrum analyzer.

.

References

Boyer, T.P., S.Levitus, J.I.Antonov, R.A.Locarnini, and H.E.Garcia (2005) Linear trends in salinity for the World Ocean, 1955-1998, Geophys. Res. Lett., 32, L01604, doi:10.1029/2004GL021791.

Heywood, K., R.A. Locarnini, R.D. Frew, P.F. Dennis and B.A. King (1998), Ocean, Ice and Atmosphere: Interactions at Antarctic continental margin, Antarc. Res. Ser., Vol.75, 203-213.

3.15 Ocean origin gases

Methane (CH_4), Nitrous oxide (N_2O) and related substances

April 19, 2013

(1) Personnel

Osamu Yoshida[1,2], Haruka Tamada[2], Okura Shinozaki[2], Yuko Kanayama[2], Chisato Yoshikawa[3,4],*
and Naohiro Yoshida[3]

[1] *College of Agriculture, Food and Environment Sciences, Rakuno Gakuen University*
[2] *Faculty of Environment Systems, Rakuno Gakuen University*
[3] *Interdisciplinary Graduate School of Science and Engineering, Tokyo Institute of Technology*
[4] ***Japan Society for the Promotion of Science***
* *Principal Investigator*

(2) Sampling elements

Sampling elements of Rakuno Gakuen University group at hydrographic stations are listed below.

Table 3-15-1. Parameters and hydrographic station numbers for samples collection.

Parameters	Hydrographic Station Numbers (S04I)
1. Dissolved CH_4 (concentration)	90,94,98,102,106,111,115,121,125,131,135,140,146,150, 156,162
2. Dissolved CH_4 (carbon isotope ratio)	102,115,135,156
3. Dissolved N_2O (concentration)	90,94,98,102,106,111,115,121,125,131,135,140,146,150, 156,162
4. Dissolved N_2O (nitrogen and oxygen isotopomers)	102,115,135,156
5. CH_4 isotopomer (hydrogen isotope ratio)	102,115,135,156
6. NO_3^- (nitrogen isotope ratios)	102,115,135,156

.

(3) Methane

Methane concentration and stable isotopic distribution as indicators of biogenic methane dynamics in the Southern Ocean

i. Dissolved CH_4

i-a Introduction

Atmospheric methane (CH_4) is a trace gas playing an important role in the global carbon cycle as a greenhouse gas. Its concentration has increased by about 1050 ppbv from 700 ppbv since the pre-industrial era (IPCC, 2007). In order to understand the current global methane cycle, it is necessary to quantify its sources and sinks. At present, there remain large uncertainties in the estimated methane fluxes from sources to sinks. The ocean's source strength for atmospheric methane should be examined in more detail, even though it might be a relatively minor source, previously reported to be 0.005 to 3% of the total input to the atmosphere (Cicerone and Oremland, 1988; Bange et al., 1994; Lelieveld et al., 1998).

To estimate an accurate amount of the methane exchange from the ocean to the atmosphere, it is necessary to explore widely and vertically. Distribution of dissolved methane in surface waters from diverse locations in the world ocean is often reported as a characteristic subsurface maximum representing a supersaturation of several folds (Yoshida et al., 2004; 2011). Although the origin of the subsurface methane maximum is not clear, some suggestions include advection and/or diffusion from local anoxic environment nearby sources in shelf sediments, and *in situ* production by methanogenic bacteria, presumably in association with suspended particulate materials (Karl and Tilbrook, 1994; Katz et al., 1999). These bacteria are thought to probable live in the anaerobic microenvironments supplied by organic particles or guts of zooplankton (Alldredge and Cohen, 1987).

So, this study investigates in detail profile of methane concentration and stable isotopic distribution in the water column in the Southern Ocean to clarify methane dynamics and estimate the flux of methane to the atmosphere.

i-b Materials and methods

Seawater samples are taken by CTD-CAROUSEL system attached Niskin samplers of 12 L at 28 layers and surface layer taken by plastic bucket at 16 hydrographic stations as shown in Table 1. Each sample was carefully subsampled into 30, 125, 220 mL glass vials and 600 mL plastic bottles to avoid air contamination for analysis of methane concentration, carbon isotope ratio, and hydrogen isotope ratio respectively. The seawater samples were poisoned by 20 μL (30 ,125 and 220 mL vials) or 100 μL (600 mL vial) of mercuric chloride solution (Tilbrook and Karl, 1995; Watanabe et al., 1995), and were closed with rubber-aluminum and plastic caps. These were stored in a dark and cool place until we got to land, where we conducted gas chromatographic analysis of methane concentration and mass spectrometric analysis of carbon and hydrogen isotopic composition at the laboratory.

The analytical method briefly described here: The system consists of a purge and trap unit, a desiccant unit, rotary valves, a gas chromatograph equipped with a flame ionization detector for concentration of methane, GC/C/IRMS for carbon isotope ratio of methane, GC/TC/IRMS for hydrogen isotope ratio of methane, and data acquisition units. The entire volume of seawater in each glass vial was processed all at once to avoid contamination and loss of methane. Precision obtained from replicate determinations of methane concentration was estimated to be better than 5% for the

.

usual concentration of methane in seawater.

i-c Expected results

Subsurface maximum concentrations of methane (>3 nmol kg^{-1}) were expected to be observed in the Southern Ocean. A commonly-encountered distribution in the upper ocean with a methane peak within the pycnocline (e.g., Ward et al., 1987; Owens et al., 1991; Watanabe et al., 1995; Yoshida et al., 2011). Karl and Tilbrook (1994) suggested the suboxic conditions would further aid the development of microenvironments within particles in which methane could be produced. The organic particles are accumulated in the pycnocline, and methane is produced in the micro reducing environment by methanogenic bacteria. Moreover, *in situ* microbial methane production in the guts of zooplankton can be expected (e.g., Owens et al., 1991; de Angelis and Lee, 1994; Oudot et al., 2002; Sasakawa et al., 2008). Watanabe et al. (1995) pointed out that the diffusive flux of methane from subsurface maxima to air-sea interface is sufficient to account for its emission flux to the atmosphere. In the mixed layer above its boundary, the methane is formed and discharged to the atmosphere in part, in the below its boundary, methane diffused to the bottom vertically. By using concentration and isotopic composition of methane and hydrographic parameters for vertical water samples, it is possible to clarify its dynamics such as production and/or consumption in the water column.

ii. References

Alldredge, A. A., Y. Cohen: Can microscale chemical patches persist in the sea? Microelectrode study of marine snow, fecal pellets, Science, 235, 689-691, 1987.

Bange, H. W., U. H. Bartell, S. Rapsomanikis, and M. O. Andreae: Methane in the Baltic and the North seas and a reassessment of the marine emissions of methane, Global Biogeochem. Cycles, 8, 465–480, 1994.

Cicerone, R. J., and R. S. Oremland: Biogeochemical aspects of atmospheric methane, Global Biogeochem. Cycles, 2, 299–327, 1988.

de Angelis, M. A., and C. Lee: Methane production during zooplankton grazing on marine phytoplankton, Limnol. Oceanogr., 39, 1298-1308, 1994.

Intergovermental Panel on Climate Change: Couplings Between Change in the Climate System and Biogeochemistry, in Climate Change 2007: The Physical Science Basis: Contribution of Working Group I to the Fourth Assessment Report of the Intergovernment Panel on Climate Change, edited by S. Solomon, et al., pp. 501-568, Cambridge University Press, Cambridge, United Kingdom and New York, NY, USA, 2007.

Karl, D. M., and B. D. Tilbrook: Production and transport of methane in oceanic particulate organic matter, Nature, 368, 732–734, 1994.

Katz, M. E., D. K. Pak, G. R. Dickkens, and K. G. Miller: The source and fate of massive carbon input during the latest Paleocene thermal maximum, Scince, 286, 1531–1533, 1999.

Lelieveld, J., P. J. Crutzen, and F. J. Dentener: Changing concentration, lifetime and climate forcing of atmospheric methane, Tellus Ser. B, 50, 128–150, 1998.

Oudot, C., P. Jean-Baptiste, E. Fourre, C. Mormiche, M. Guevel, J-F. Ternon, and P. L. Corre: Transatlantic equatorial distribution of nitrous oxide and methane, Deep-Sea Res., Part I, 49, 1175–1193, 2002.

Owens, N. J. P., C. S. Law, R. F. C. Mantoura, P. H. Burkill, and C. A. Llewellyn: Methane flux to the atmosphere from

.

the Arabian Sea, Nature, 354, 293–296, 1991.

Sasakawa, M., U. Tsunogai, S. Kameyama, F. Nakagawa, Y. Nojiri, and A. Tsuda: Carbon isotopic characterization for the origin of excess methane in subsurface seawater, J. Geophys. Res., 113, C03012, doi: 10.1029/2007JC004217, 2008.

Tilbrook, B. D., and D. M. Karl: Methane sources, distributions and sinks from California coastal waters to the oligotrophic North Pacific gyre, Mar. Chem., 49, 51–64, 1995.

Ward, B. B., K. A. Kilpatrick, P. C. Novelli, and M. I. Scranton: Methane oxidation and methane fluxes in the ocean surface layer and deep anoxic waters, Nature, 327, 226–229, 1987.

Watanabe, S., N. Higashitani, N. Tsurushima, and S. Tsunogai: Methane in the western North Pacific, J. Oceanogr., 51, 39–60, 1995.

Yoshida, O., H. Y. Inoue , S. Watanabe, S. Noriki, M. Wakatsuchi: Methane in the western part of the Sea of Okhotsk in 1998-2000, J. Geophys. Res., 109, C09S12, doi:10.1029/2003JC001910, 2004.

Yoshida, O., H. Y. Inoue, S. Watanabe, K. Suzuki, and S. Noriki: Dissolved methane distribution in the South Pacific and the Southern Ocean in austral summer, J. Geophys. Res., 116, C07008, doi:10.1029/2009JC006089, 2011.

.

(4) Nitrous oxide and related substances

Nitrous oxide Production, consumptions and air-sea flux in the Southern Ocean

i. Introduction

Recently considerable attention has been focused on emission of biogenic trace gases from ecosystems, since the gases contain a significant amount of greenhouse gases. Isotopic signatures of these gases are well recognized to provide constraints for relative source strength and information on reaction dynamics concerning their formation and biological pathways. Nitrous oxide (N_2O) is a very effective heat-trapping gas in the atmosphere because it absorbs outgoing radiant heat in infrared wavelengths that are not captured by the other major greenhouse gases, such as water vapor and CO_2. The annual input of N_2O into the atmosphere is estimated to be about 16 Tg N_2O-N yr^{-1}, and the oceans are believed to contribute more than 20% of the total annual input (IPCC, 2007).

N_2O is produced by the biological processes of nitrification and denitrification (Dore et al., 1998; Knowles et al., 1981; Rysgaard et al., 1993; Svensson, 1998; Ueda et al., 1993). Depending on the redox conditions, N_2O is produced from inorganic nitrogenous compounds (NH_4 or NO_3^-), with subsequently different isotopic fractionation factors. The isotopic signatures of N_2O confer constraints on the relative source strength, and the reaction dynamics of N_2O biological production pathways are currently under investigation. Furthermore, isotopomers of N_2O contain more easily interpretable biogeochemical information as to their sources than obtained from conventional bulk ^{15}N and ^{18}O measurements (Yoshida and Toyoda, 2000).

The Southern Ocean is expected to be important for the biogeochemical and biological cycles. Thus, the study of N_2O production and nutrients dynamics are very important to examine the origins of N_2O in seawater and to estimate the inventory of N_2O from this region with respect to the troposphere.

ii. Materials and methods

The purpose of the expedition was to study on the heat and material transports and their variability of the general ocean circulation and a study on chemical environment and its changes in the ocean. In order to investigate the production and consumption of dissolved N_2O in the Southern Ocean, seawater samples for dissolved N_2O concentration/isotopomer ratio analysis and those for nitrate isotope ratio analysis were collected at total 12 and 4 stations, respectively (Table 1).

ii-a N_2O concentration and isotope analyses

Seawater samples collected by CTD-CAROUSEL system was subsampled into three glass vials: one 30 mL vial for concentration analysis and two or four 120 mL glass vials for isotopomer ratio analysis. The subsamples were then sterilized with saturated $HgCl_2$ solution (about 20 μL per 100 mL seawater). The vials were sealed with butyl-rubber septa and aluminum caps, taking care to avoid bubble formation, and then brought back to the laboratory and stored at 4°C until analysis. Dissolved N_2O concentrations and its isotopic compositions will be measured by GC/ECD and/or GC/IRMS.

.

ii-b Isotope ratios of NO_3^-

Water sample was collected into a 50 mL syringe equipped with a DISMIC® filter (pore size: 0.45 m). The sample was then filtrated and divided into five polypropylene tubes.The tubes was stored at -40ºC until analysis. Isotope ratios of NO_3^- will be measured by denitrifer method (Sigman et al., 2001) in which N_2O converted from nitrate is measured by using GC/IRMS.

iii. Expected results

In the surface layer, N_2O concentration of water affects the sea-air flux directly (Dore et al., 1998). However the pathway of N_2O production in surface layer is still unresolved. In the surface layer, N_2O is predominantly produced by nitrification, but also by denitrification if oxygen concentration is low (Maribeb and Laura, 2004). Moreover, it was reported that N_2O production by nitrification is photo-inhibited (Olson, 1981). Therefore, concentration and isotopomer ratios of N_2O/nitrate together with N_2O production rate from ammonium/nitrate obtained by this study will reveal the pathway of N_2O production and N_2O production rate in the surface layer (especially euphotic zone).

In deeper layer, N_2O could be produced through *in situ* biological processes of settling particles or fecal pellets derived from phytoplankton or zooplankton, and N_2O maximum was indeed observed at 600-800 m depth (Popp et al., 2002; Toyoda et al., 2002). However, following problems have not been resolved: (i) what the major pathway for the N_2O maximum is and (ii) whether the N_2O is produced *in situ* or transported from other area.

iv. References

Dore, J.E., Popp, B.N., Karl, D.M. and Sansone, F.J.: A large source of atmospheric nitrous oxide from subtropical North Pacific surface water, Nature, 396, 63-66, 1998.

IPCC, Climate Change 2007: The Physical Science Basis. Contribution of Working Group I to the Fourth Assessment Report of the Intergovernmental Panel on Climate Change, edited by S. Solomon et al., pp. 996, Cambridge University Press, Cambridge, United Kingdom and New York, NY, USA, 2007.

Knowles, R., Lean, D.R.S. and Chan, Y.K.: Nitrous oxide concentrations in lakes: variations with depth and time, Limnology and Oceanography, 26, 855-866, 1981.

Maribeb, C.-G. and Laura, F.: N_2O cycling at the core of the oxygen minimum zone off northern Chile, Marine Ecology Progress Series, 280, 1-11, 2004.

Olson, R.J.: Differential photoinhibition of marine nitrifying bacteria: a possible mechanism for the formation of the primary nitrite maximum, Journal of Marine Research, 39, 227-238, 1981.

Popp, B. N., et al.: Nitrogen and oxygen isotopomeric constraints on the origins and sea-to-air flux of N_2O in the oligotrophic subtropical North Pacific gyre, Global Biogeochem. Cycles, 16(4), 1064, 2002. doi: 10.1029/2001GB001806.

Rysgaard, S., Risgaard-Petersen, N., Nielsen, L.P. and Revsbech, N.P.: Nitrification and denitrification in lake and estuarine sediments measured by the ^{15}N dilution technique and isotope pairing, Applied and Environmental Microbiology, 59, 2093-2098, 1993.

Sigman, D. M., K. L. Casciotti, M. Andreani, C. Barford, M. Galanter, and J. K. Boehlke: A bacterial method for the nitrogen isotopic analysis of nitrate in seawater and freshwater, Anal. Chem., 73, 4145-4153, 2001.

.

Svensson, J.M.: Emission of N_2O, nitrification and denitrification in a eutrophic lake sediment bioturbated by Chironomus plumosus, Aquatic Microbial Ecology, 14, 289-299, 1998.

Toyoda, S., N. Yoshida, T. Miwa, Y. Matsui, H. Yamagishi, U. Tsunogai, Y. Nojiri, and N. Tsurushima: Production mechanism and global budget of N_2O inferred from its isotopomers in the western North Pacific, Geophys. Res. Lett., 29 (3), 7-1-7-4, 2002.

Ueda, S., Ogura, N. and Yoshinari, T.: Accumulation of nitrous oxide in aerobic ground water, Water Research, 27, 1787-1792, 1993

www.cia.gov/cia/publications/factbook/geos/zn.html

Yoshida, N. and Toyoda, S.: Constraining the atmospheric N_2O budget from intramolecular site preference in N_2O isotopomers, Nature, 405, 330-334, 2000.

.

3.16 PFASs (perfluoro alkyl substances)

(1) Personnel

Nobuyoshi Yamashita (National Institute of Advanced Industrial Science and Technology, AIST)

(2) Objectives

Environmentally persistent perfluoroalkyl substances (PFASs, shown in figure 3-16-1) have appeared as a new class of global pollutants for the last thirteen years. These compounds have recently emerged as a priority environmental pollutant due to its widespread finding in biota including both Arctic and Antarctic species and its persistent and bioaccumulative nature. The physicochemical properties of PFASs, especially of PFSAs (perfluoro sulfonic acids) and PFCAs (perfluoro carboxylic acids) are unique in that they have high water solubility despite the low reactivity of carbon-fluorine bond, which also imparts high stability in the environment. However, little is known on the distribution of PFASs in the oceans around the world, so far. We have conducted several international joint cruises, including South China Sea and Sulu Seas (KH-02-4), the central to Eastern Pacific Ocean (KH03-1 and MR11-08), North and middle Atlantic Ocean, Southern Pacific and Antarctic Ocean (KH04-5), Labrador Sea and coastal seawater from Asian countries (Japan, China, Hong Kong, Korea) (1, 2, 3). Vertical profiles of PFASs in the marine water column were associated with the global ocean circulation theory. We found that vertical profiles of PFASs in water columns from the Labrador Sea reflected the influx of the North Atlantic Current in surface waters, the Labrador Current in subsurface waters, and the Denmark Strait Overflow Water in deep layers below 2000 m. Striking differences in the vertical and spatial distribution of PFASs, depending on the oceans, suggest that these persistent organic acids can serve as useful chemical tracers to allow us to study oceanic transportation by major water currents. The results provide evidence that PFAS concentrations and profiles in the oceans adhere to a pattern consistent with the global ‘‘Broecker’s Conveyor Belt’’ theory of open ocean water circulation.

In MR12-05, we tried to confirm the vertical profiles of PFASs found in water columns from above cruises and the Pacific Ocean (KH03-1 and MR11-08) and obtained open ocean samples for further analysis..

(3) *Samples:*

Seawater samples were taken by Conductivity temperature depth profiler-Carousel multiple sampling system (CTD-CMS) attached X-Niskin samplers of 12 L, together with surface seawater samples taken by bucket at all the water sampling stations. At two sampling site, atmospheric materials taken with a comprehensive cryogenic moisture sampler (CMS; prototype, AIST/SIBATA Co.). The air sampler was operated with a flow rate of 3– 10 L/min. Samples were collected during underway to avoid contamination from exhaust gas from ship. Water, air samples were stored at below -20°C until chemical analysis in AIST laboratory.

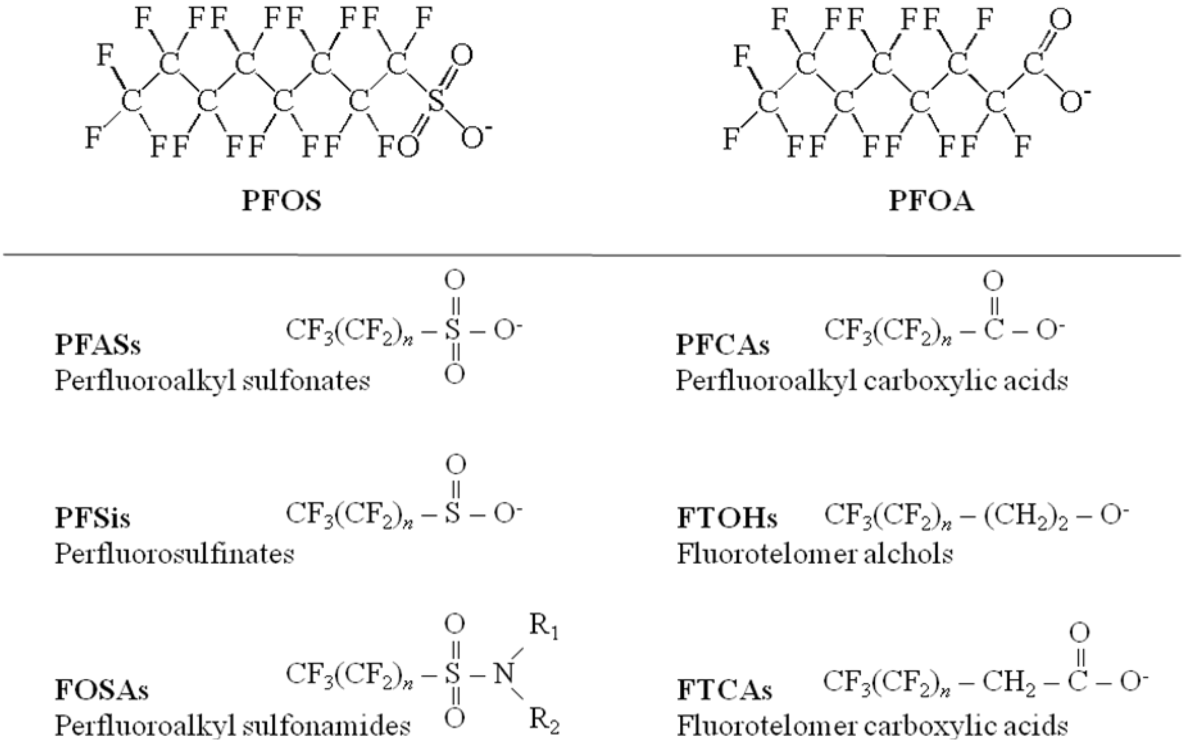

Figure 3-16-1. Perfluoroalkyl substances (PFASs)

(4) ***Chemical analysis**:*

Water samples were stored in clean 1 L polypropylene bottles and were kept frozen until analysis. Samples were thawed at room temperature, and a solid phase extraction method using WAX® cartridge (Waters Co.) was used for the determination of PFASs by HPLC tandem mass spectrometry (HPLC-MS/MS) as described elsewhere (4,5). Briefly, after preconditioning with 4 mL ammonium hydroxide in methanol, 4 mL methanol, and then 4 mL Millipore water, the cartridges were loaded with 900-1000 mL samples at approximately 1 drop sec-1. The cartridges were then washed with 4mL of 25 mM ammonium acetate buffer (pH 4) in Millipore water and dried by centrifugation at 3000rpmfor 2 min. The elution was then divided into two fractions. The first fraction was carried out with 4 mL methanol and the second with 4 mL 0.1%ammoniumhydroxide in methanol. Both fractions were reduced to 0.5 mL under a nitrogen stream and analyzed separately. HPLC-MS/MS, composed of a HP1100 liquid chromatograph (Agilent Technologies, Palo Alto, CA) interfaced with a Micromass® (Beverly, MA) Quattro Ultima Pt mass spectrometer was operated in the electrospray negative ionization mode.A 5 or 10-µL aliquot of the sample extract was injected into a Betasil C18 column (2.1 mm i.d.×50 mm length, 5µm; Termo Hypersil-Keystone, Bellefonte, PA). The capillary is held at 1.2 kV. Cone-gas and desolvation-gas flows are kept at 60 and 650 L/h, respectively. Source and desolvation temperatures were kept at 120 and 420°C respectively. MS/MS parameters are optimized so as to transmit the [M-K]- or [M-H]- ions.

MR12-05 is the fifth international research cruise that conducted measurement of POPs in Open ocean waters

.

using ISO method (ISO25101). Because of recent scene of analytical chemistry, uncertainty and reliability of measurement supported by suitable quality assurance and quality control (QAQC) becoming to the essential issue. Our experimental result with ISO25101 supported by the international QAQC (ISO17025 with Guide45) and Japanese Industrial Standard (JIS) will provide the most reliable information of environmental chemistry in Open ocean research for now.

(5) Results

List of water samples (surface, subsurface and deep water) collected during Leg 2 and Leg3 were presented in table 3-16-1, 3-16-2, 3-16-3 as follows Subsurface waters were collected from the out let tube of surface water analysis facility in MIRAI during Leg2. In Leg 3, same sample collection were kindly carried out by Dr. Uchida (the chief researcher of Leg 3).

Table 3-16-1. Summary of surface seawater sampling for PFASs analysis

Leg 2											
Sample ID	**Collected Date**			**Time**	**Longitude**			**Latitude**			**Depth**
	YYYY	**MM**	**DD**	**(UT)**	**Deg.**	**Min.**	**N/S**	**Deg.**	**Min.**	**E/W**	**(dbar)**
MR1205B01	2012	12	7	17:40	60	30.34	S	173	57.77	E	0
MR1205B03	2012	12	14	7:00	63	26.19	S	153	41.41	E	0
MR1205B04	2012	12	18	2:30	61	52.324	S	135	54.44930	E	0
MR1205B05	2012	12	20	00:40	62	01.29320	S	134	11.32230	E	0
MR1205B06	2012	12	23	9:10	61	59.12550	S	119	02.38350	E	0
MR1205B07	2012	12	23	14:45	62	00.30	S	118	01.60	E	0

Leg 3											
Sample ID	**Collected Date**			**Time**	**Longitude**			**Latitude**			**Depth**
	YYYY	**MM**	**DD**	**(UT)**	**Deg.**	**Min.**	**N/S**	**Deg.**	**Min.**	**E/W**	**(dbar)**
MR1205B08	2013	1	26	16:51	63	29.93	S	54	49.32	E	0
MR1205B09	2013	1	31	9:11	66	00.01	S	35	59.97	E	0

Atmospheric sampling those carried out using a comprehensive cryogenic moisture sampler (CMS) and list of samples were presented in table 3-16-4. Operation of CMS were carried out by AIST (Leg2) and GODI (Leg3). Because of unexpected malfunction of vacuum pump, limited air sample was collected in Leg 3.

Table 3-16-2. Summary of subsurface seawater sampling for PFASs analysis

Leg 1

Sample ID	Collected Date			Time	Longitude			Latitude			Depth
	YYYY	MM	DD	(UT)	Deg.	Min.	N/S	Deg.	Min.	E/W	(dbar)
MR1205S1	2012	11	6	8:03	40	36.277	N	141	38.048	E	4
MR1205S2	2012	11	6	12:33	40	00.333	N	142	08.333	E	4
MR1205S3	2012	11	8	22:14	29	24.892	N	144	32.481	E	4
MR1205S4	2012	11	10	22:12	19	47.317	N	147	19.044	E	4
MR1205S5	2012	11	13	7:38	10	18.130	N	150	21.617	E	4
MR1205S6	2012	11	15	21:34	0	04.212	N	151	29.936	E	4
MR1205S7	2012	11	18	4:38	9	52.082	S	156	34.687	E	4
MR1205S8	2012	11	20	8:39	19	08.960	S	161	29.646	E	4
MR1205S9	2012	11	23	19:42	30	24.035	S	169	44.369	E	4
MR1205S10	2012	11	25	3:55	34	31.624	S	174	20.836	E	4
MR1205S11	2012	11	25	6:57	34	50.818	S	174	43.275	E	4

Leg 2

Sample ID	Collected Date			Time	Longitude			Latitude			Depth
	YYYY	MM	DD	(UT)	Deg.	Min.	N/S	Deg.	Min.	E/W	(dbar)
MR1205S12	2012	12	1	2:02	45	59.565	S	171	55.884	E	4
MR1205S14	2012	12	7	17:40	60	30.34	S	173	57.77	E	4
MR1205S15	2012	12	14	7:14	63	26.19	S	153	41.41	E	4
MR1205S16	2012	12	18	2:30	61	52.324	S	135	54.44930	E	4
MR1205S17	2012	12	13	7:00	62	47.61540	S	158	09.38760	E	4
MR1205S18	2012	12	20	00:40	62	01.29320	S	134	11.32230	E	4
MR1205S19	2012	12	23	9:23	61	59.12550	S	119	02.38350	E	4
MR1205S20	2012	12	23	15:01	61	50.0720	S	118	01.44750	E	4
MR1205S21	2012	12	30	15:51	52	20.0148	S	136	50.099	E	4
MR1205S22	2013	1	1	4:19	47	10.207	S	143	09.365	E	4

Leg 3

Sample ID	Collected Date			Time	Longitude			Latitude			Depth
	YYYY	MM	DD	(UT)	Deg.	Min.	N/S	Deg.	Min.	E/W	(dbar)
MR1205S23	2013	1	15	0:32	62	06.62	S	98	01.39	E	4
MR1205S24	2013	1	16	17:13	63	21.43	S	90	10.59	E	4
MR1205S25	2013	1	17	13:22	63	06.21	S	85	58.61	E	4
MR1205S26	2013	1	17	23:32	63	00.67	S	84	01.22	E	4

Leg 3

MR1205S27	2013	1	19	4:08	61	24.93	S	80	29.38	E	4
MR1205S28	2013	1	20	19:13	62	00.62	S	71	38.04	E	4
MR1205S29	2013	1	21	22:14	62	18.88	S	65	47.61	E	4
MR1205S30	2013	1	25	3:12	65	22.31	S	53	14.76	E	4
MR1205S31	2013	1	25	19:55	64	26.05	S	53	04.29	E	4
MR1205S32	2013	1	26	11:18	63	30.00	S	55	59.50	E	4
MR1205S33	2013	02	12	6:57	66	29.96	S	36	00.00	E	4

Table 3-16-3. Summary of deep seawater sampling for PFASs analysis

Leg 2

Sample ID	Station	Collected Date			Time	Longitude			Latitude			Depth
	No.	YYYY	MM	DD	(UT)	Deg.	Min.	N/S	Deg.	Min.	E/W	(dbar)
MR1205DW10	17	2012	12	7	17:40	60	30.34	S	173	57.77	E	B-10
MR1205DW11	17	2012	12	7	17:40	60	30.34	S	173	57.77	E	4080
MR1205DW12	17	2012	12	7	17:40	60	30.34	S	173	57.77	E	3080
MR1205DW13	17	2012	12	7	17:40	60	30.34	S	173	57.77	E	2080
MR1205DW14	17	2012	12	7	17:40	60	30.34	S	173	57.77	E	1080
MR1205DW15	17	2012	12	7	17:40	60	30.34	S	173	57.77	E	830
MR1205DW16	17	2012	12	7	17:40	60	30.34	S	173	57.77	E	530
MR1205DW17	17	2012	12	7	17:40	60	30.34	S	173	57.77	E	330
MR1205DW18	17	2012	12	7	17:40	60	30.34	S	173	57.77	E	200
MR1205DW19	17	2012	12	7	17:40	60	30.34	S	173	57.77	E	100
MR1205DW20	17	2012	12	7	17:40	60	30.34	S	173	57.77	E	50
MR1205DW21	17	2012	12	7	17:40	60	30.34	S	173	57.77	E	5
MR1205DW22	55	2012	12	14	9:20	63	26.19	S	153	41.41	E	B-10
MR1205DW23	55	2012	12	14	9:20	63	26.19	S	153	41.41	E	3080
MR1205DW24	55	2012	12	14	9:20	63	26.19	S	153	41.41	E	2080
MR1205DW25	55	2012	12	14	9:20	63	26.19	S	153	41.41	E	1080
MR1205DW26	55	2012	12	14	9:20	63	26.19	S	153	41.41	E	830
MR1205DW27	55	2012	12	14	9:20	63	26.19	S	153	41.41	E	530
MR1205DW28	55	2012	12	14	9:20	63	26.19	S	153	41.41	E	330
MR1205DW29	55	2012	12	14	9:20	63	26.19	S	153	41.41	E	200
MR1205DW30	55	2012	12	14	9:20	63	26.19	S	153	41.41	E	100
MR1205DW31	55	2012	12	14	9:20	63	26.19	S	153	41.41	E	50
MR1205DW32	55	2012	12	14	9:20	63	26.19	S	153	41.41	E	5

Leg 2

MR1205DW33	4	2012	12	18	5:40	61	51.8703	S	135	55.39660	E	B-10
MR1205DW34	4	2012	12	18	5:40	61	51.8703	S	135	55.39660	E	4000
MR1205DW35	4	2012	12	18	5:40	61	51.8703	S	135	55.39660	E	3000
MR1205DW36	4	2012	12	18	5:40	61	51.8703	S	135	55.39660	E	2000
MR1205DW37	4	2012	12	18	5:40	61	51.8703	S	135	55.39660	E	1000
MR1205DW38	4	2012	12	18	5:40	61	51.8703	S	135	55.39660	E	800
MR1205DW39	4	2012	12	18	5:40	61	51.8703	S	135	55.39660	E	500
MR1205DW40	4	2012	12	18	5:40	61	51.8703	S	135	55.39660	E	300
MR1205DW41	4	2012	12	18	5:40	61	51.8703	S	135	55.39660	E	200
MR1205DW42	4	2012	12	18	5:40	61	51.8703	S	135	55.39660	E	100
MR1205DW43	4	2012	12	18	5:40	61	51.8703	S	135	55.39660	E	50
MR1205DW44	4	2012	12	18	5:40	61	51.8703	S	135	55.39660	E	5
MR1205DW45	69	2012	12	20	3:40	62	01.29320	S	134	11.32230	E	B-10
MR1205DW46	69	2012	12	20	3:40	62	01.29320	S	134	11.32230	E	4000
MR1205DW47	69	2012	12	20	3:40	62	01.29320	S	134	11.32230	E	3000
MR1205DW48	69	2012	12	20	3:40	62	01.29320	S	134	11.32230	E	2000
MR1205DW49	69	2012	12	20	3:40	62	01.29320	S	134	11.32230	E	1000
MR1205DW50	69	2012	12	20	3:40	62	01.29320	S	134	11.32230	E	800
MR1205DW51	69	2012	12	20	3:40	62	01.29320	S	134	11.32230	E	500
MR1205DW52	69	2012	12	20	3:40	62	01.29320	S	134	11.32230	E	300
MR1205DW53	69	2012	12	20	3:40	62	01.29320	S	134	11.32230	E	200
MR1205DW54	69	2012	12	20	3:40	62	01.29320	S	134	11.32230	E	100
MR1205DW55	69	2012	12	20	3:40	62	01.29320	S	134	11.32230	E	50
MR1205DW56	69	2012	12	20	3:40	62	01.29320	S	134	11.32230	E	5
MR1205DW57	81	2012	12	23	17:50	62	00.30	S	118	01.60	E	B-10
MR1205DW58	81	2012	12	23	17:50	62	00.30	S	118	01.60	E	4000
MR1205DW59	81	2012	12	23	17:50	62	00.30	S	118	01.60	E	3000
MR1205DW60	81	2012	12	23	17:50	62	00.30	S	118	01.60	E	2000
MR1205DW61	81	2012	12	23	17:50	62	00.30	S	118	01.60	E	1000
MR1205DW62	81	2012	12	23	17:50	62	00.30	S	118	01.60	E	800
MR1205DW63	81	2012	12	23	17:50	62	00.30	S	118	01.60	E	500
MR1205DW64	81	2012	12	23	17:50	62	00.30	S	118	01.60	E	300
MR1205DW65	81	2012	12	23	17:50	62	00.30	S	118	01.60	E	200
MR1205DW66	81	2012	12	23	17:50	62	00.30	S	118	01.60	E	100
MR1205DW67	81	2012	12	23	17:50	62	00.30	S	118	01.60	E	50
MR1205DW68	81	2012	12	23	17:50	62	00.30	S	118	01.60	E	5

Leg 3

.

Sample ID	Station	Collected Date			Time	Longitude			Latitude			Depth
	No.	YYYY	MM	DD	(UT)	Deg.	Min.	N/S	Deg.	Min.	E/W	(dbar)
MR1205DW69	132	2013	1	26	17:54	63	29.92	S	54	49.37	E	B-10
MR1205DW70	132	2013	1	26	17:54	63	29.92	S	54	49.37	E	4000
MR1205DW71	132	2013	1	26	17:54	63	29.92	S	54	49.37	E	3000
MR1205DW72	132	2013	1	26	17:54	63	29.92	S	54	49.37	E	2000
MR1205DW73	132	2013	1	26	17:54	63	29.92	S	54	49.37	E	1000
MR1205DW74	132	2013	1	26	17:54	63	29.92	S	54	49.37	E	800
MR1205DW75	132	2013	1	26	17:54	63	29.92	S	54	49.37	E	400
MR1205DW76	132	2013	1	26	17:54	63	29.92	S	54	49.37	E	300
MR1205DW77	132	2013	1	26	17:54	63	29.92	S	54	49.37	E	200
MR1205DW78	132	2013	1	26	17:54	63	29.92	S	54	49.37	E	100
MR1205DW79	132	2013	1	26	17:54	63	29.92	S	54	49.37	E	50
MR1205DW80	132	2013	1	26	17:54	63	29.92	S	54	49.37	E	5
MR1205DW81	157	2013	1	31	10:11	66	00.02	S	36	00.14	E	B-10
MR1205DW82	157	2013	1	31	10:11	66	00.02	S	36	00.14	E	4000
MR1205DW83	157	2013	1	31	10:11	66	00.02	S	36	00.14	E	3000
MR1205DW84	157	2013	1	31	10:11	66	00.02	S	36	00.14	E	2000
MR1205DW85	157	2013	1	31	10:11	66	00.02	S	36	00.14	E	1000
MR1205DW86	157	2013	1	31	10:11	66	00.02	S	36	00.14	E	800
MR1205DW87	157	2013	1	31	10:11	66	00.02	S	36	00.14	E	500
MR1205DW88	157	2013	1	31	10:11	66	00.02	S	36	00.14	E	300
MR1205DW89	157	2013	1	31	10:11	66	00.02	S	36	00.14	E	200
MR1205DW90	157	2013	1	31	10:11	66	00.02	S	36	00.14	E	100
MR1205DW91	157	2013	1	31	10:11	66	00.02	S	36	00.14	E	50
MR1205DW92	157	2013	1	31	10:11	66	00.02	S	36	00.14	E	5

Table 3-16-4. Summary of air sampling for PFASs analysis

Leg 2										
Sample ID	Collected Period			Time	Collected Location					
					Longitude			Latitude		
				(UT)	Deg.	Min.	N/S	Deg.	Min.	E/W
MR1205AR01	2012/11/30 9:29	-	2012/12/2 16:40	16:40	49	19.59600	S	169	59.82220	E
MR1205AR03	2012/12/6 2:40	-	2012/12/8 1:30	1:30	60	33.7983	S	173	58.48550	E
MR1205AR04	2012/12/8 2:16	-	2012/12/12 1:30	1:30	63	36.00490	S	160	27.34000	E
Leg 2										
MR1205AR05	2012/12/12 2:20	-	2012/12/17 23:10	23:10	62	23.32730	S	140	13.03840	E
MR1205AR06	2012/12/18 0:20	-	2012/12/19 23:08	23:08	60	02.35540	S	139	56.44820	E

MR1205AR07	2012/12/20 1:40	-	2012/12/24 1:22	1:22	61	57.55760	S	116	24.25310	E
MR1205AR08	2012/12/27 19:24	-	2012/12/30 4:05	4:02	54	42.53910	S	133	15.39590	E
MR1205AR09	2012/12/30 4:42	-	2012/1/1 3:55	3:55	47	46.68490	S	142	29.21110	E

Leg 3										
Sample ID	Collected Period			Time	Collected Location					
					Longitude			Latitude		
				(UT)	Deg.	Min.	N/S	Deg.	Min.	E/W
MR1205AR10	2013/1/7 2:01	-	2013/1/12 10:15	10:15	60	54.62	S	110	37.43	E
MR1205AR11	2013/2/3 9:48	-	2013/2/7 5:52	5:52	58	21.72	S	80	20.09	E
MR1205AR12	2013/2/7 7:46	-	2013/2/12 6:57	6:57	41	29.37	S	107	10.94	E

(6) Discussion

All samples are under chemical analysis in AIST. The final result will be published as out come of research project "Chemical Oceanography to Elucidate Global Kinetics of Persistent Perfluorinated Chemicals (project number B1106, funded by the Ministry of Environment, Japan)" in 2014.

As a possible discussion using above analysis of samples collected in MR12-05, we describe brief discussion of oceanographic research using PFASs analysis bellow.

The international joint research between AIST, Ocean Research Institute of Tokyo University and Leibniz Institute of Marine Science from 2002 conducted a joint study by collecting water samples from oceans worldwide for the analysis of PFASs and the results were reported in 2005. Earlier results of the monitoring survey revealed that there were remarkably higher concentrations of PFOS and PFOA in surface water from the northern and middle Atlantic Ocean compared to those from the southern Pacific Ocean. No reasonable hypothesis, including the traditional long range atmospheric transportation, could be possible to explain such global distribution of these compounds in the open ocean. It is known that the oceans are a three-dimensional compartments and the results of surface water analysis show only limited information of hydrodynamics of PFASs. In this study, ultra-trace level analysis of PFOA and PFOA was performed in five water columns up to a depth of 5500 m (3500 – 5500 m) collected from the middle Atlantic Ocean and the South Pacific Ocean.

Open ocean and offshore surface and subsurface water samples were collected between 2002 and 2006 from 62 locations around the world. The vertical profile of PFOS and PFOA in the Mid-Atlantic Ocean (AO3, AO4, AO5) seems to be typical of the profiles found for coastal and off-shore regions of the industrialized countries (Figure 3-16-2). PFOS and PFOA discharged into the surface waters in the Mid-Atlantic Ocean seemed to have long residence times due to the isolation of the surface waters from the deep waters, and due also to the circulation of the water mass by the Gulf Stream and the North Atlantic Drift. These factors provide an explanation for the highest concentrations found in the Mid-Atlantic Ocean.

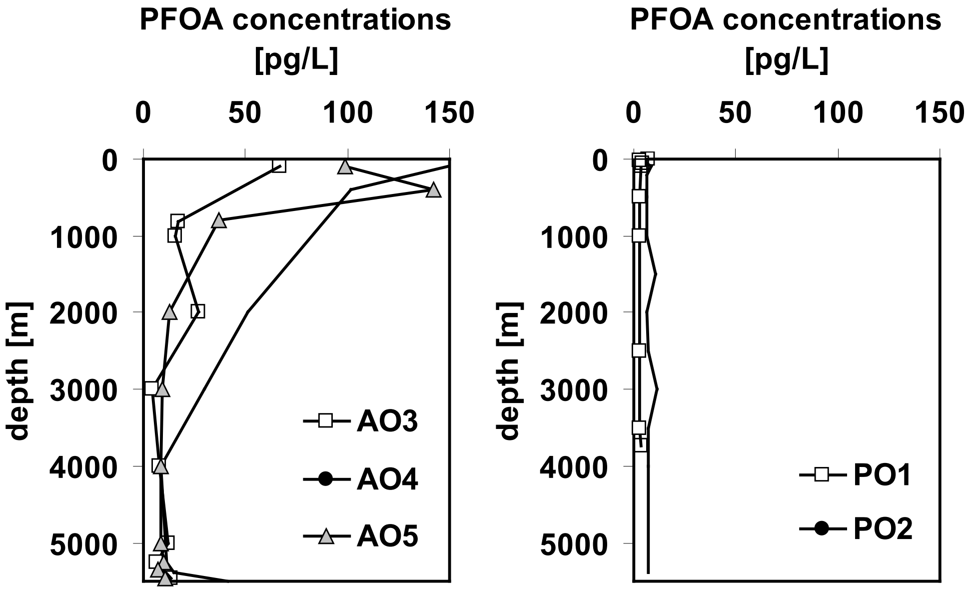

Figure 3-16-2. Vertical profiles of PFOA in water column in the Middle Atlantic Ocean (AO3, AO4, AO5) and the South Pacific Ocean (PO1, PO2).

The vertical profiles of PFOS and PFOA in two water columns, PO1 and PO2 from the South Pacific Ocean were completely different from the middle Atlantic Ocean. Concentrations of PFAs were consistently low (<10 pg/L) or below the limit of detection, from surface to bottom. These water columns are samplings of ocean currents that are more than 1000 years old, in terms of global circulation, as well as surface coastal streams derived from Antarctic circumpolar waters. Despite the fact that PO1 and PO2 are different masses of water, concentration profiles were constant throughout both columns. Negligible level of PFOS and PFOA in the water columns of the South Pacific Ocean showed that there is no direct input to this remote region. Thus, the open ocean water in the South Pacific is less contaminated by PFOS and PFOA than the water masses in the middle Atlantic Ocean.

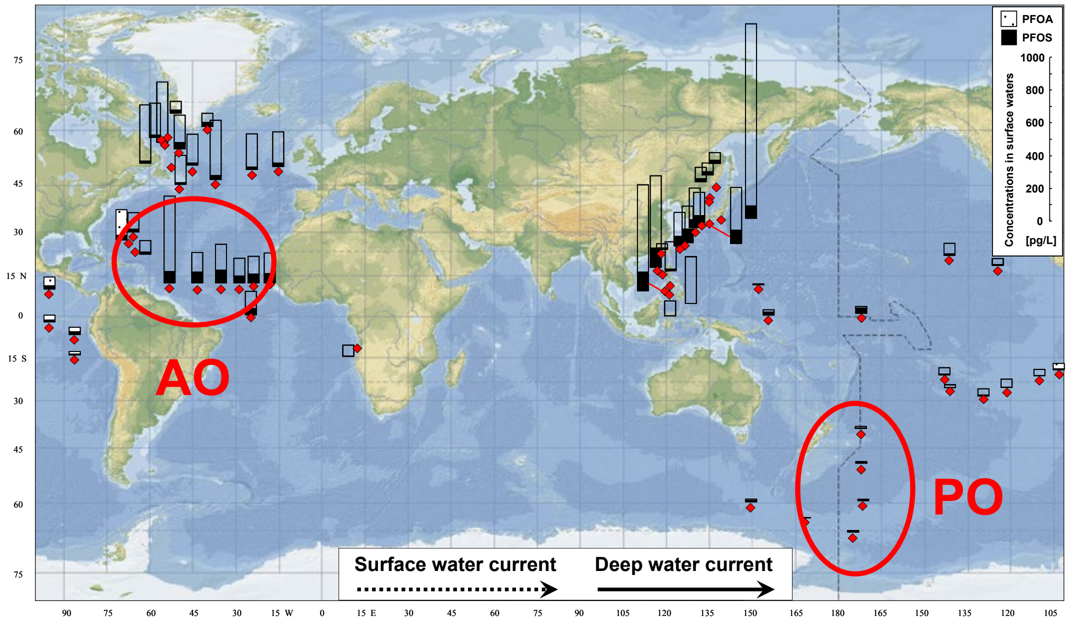

Figure 3-16-3. Global monitoring survey of PFOS and PFOA in surface water - possible long range transportation by global scale water current (modified from Broecker's conveyor belt).

The results presented above provide evidence that PFOS and PFOA concentrations and profiles in the oceans adhere to a pattern consistent with the global "Broecker's Conveyor Belt" theory of open ocean water circulation , as described in Figure 3-16-3. Striking differences in the vertical and spatial distribution of PFAs, depending on the oceans, suggest that these persistent acids can serve as useful chemical tracers to allow us to study oceanic transportation by major water currents.

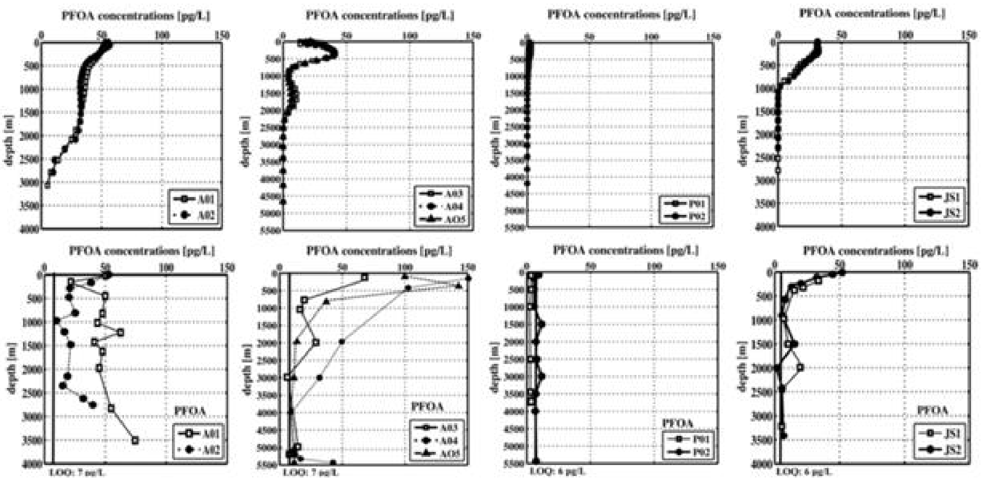

Figure 3-16-4. Comparison between real vertical profile of PFASs (lower) in oceans (from left, the Labrador Sea, the North Atlantic Ocean, the southern Pacific Ocean and the Japan Sea) and simulation model (upper). (modified from original figure by I. Stemmler and G. Lammel, Atmos. Chem. Phys., 10, 9965–9980, 2010, Pathways of PFOA to the Arctic: variabilities and contributions of oceanic currents and atmospheric transport and chemistry sources).

Above field survey result were utilized as important data set of PFASs monitoring in global scale and applied to several simulation using computer model (figure 3-16-4). Stemmler tried to develop simulation model to understand global distribution of PFAS in ocean and applied our data set published in 2008. The vertical profiles of PFOA in the southern Pacific Ocean and Japan Sea might similar between real concentration and simulation. However, significant differences between both were found in the Labrador Sea and the North Atlantic Ocean.

It suggest that unknown oceanographic phenomenon and/or kinetics of anthropogenic chemicals were expected in these oceans.

The global circulation of ocean water and deep seawater might play a major role in scavenging of several POPs and therefore their role in the global fate of PFASs must be examined to estimate the environmental destiny of persistent hazardous chemicals on our planet.

.

References

(1) Yamashita N, Kannan K, Taniyasu S, Horii Y, Petrick G, Gamo T, A global survey of perfluorinated acids in oceans, Marine Pollution Bulletin 51 (2005) 658–668

(2) Wei S, Chen LQ, Taniyasu S, So MK, Murphy MB, Yamashita N, Yeung LWY, Lam PKS, Distribution of perfluorinated compounds in surface seawaters between Asia and Antarctica, Marine Pollution Bulletin 54 (2007) 1813–1838

(3) Yamashita N, Taniyasu S, Petrick G, Wei S, Gamo T, Lam PKL, Kannan K, Perfluorinated acids as novel chemical tracers of global circulation of ocean waters, *Chemosphere* 70 (2008) 1247–1255

(4) Yamashita N, Kannan K, Taniyasu S, Horii Y, Okazawa T, Petrick G, Gamo T, Analysis of Perfluorinated Acids at Parts-Per-Quadrillion Levels in Seawater Using Liquid Chromatography-Tandem Mass Spectrometry, Environ. Sci. Technol. (2004) 38, 5522-5528

(5) Taniyasu S, Kannan K, So MK, Gulkowskad A, Sinclair E, Okazawa T, Yamashita N, Analysis of fluorotelomer alcohols, fluorotelomer acids, and short- and long-chain perfluorinated acids in water and biota, *Journal of Chromatography A*, 1093 (2005) 89–97

(6) ISO 25101 (2009 March 1st) Water quality — Determination of perfluorooctanesulfonate (PFOS) and perfluorooctanoate (PFOA) — Method for unfiltered samples using solid phase extraction and liquid chromatography/mass spectrometry

.

3.17 Distribution and ecology of oceanic *Halobates* inhabiting tropical area of Pacific Ocean and their responding system to several environmental factors

(1) Personnel

Tetsuo Harada (Kochi University)
Kentaro Emi (Kochi University)
Ryuta Ide (Kochi University)
Takero Sekimoto (Kochi University)

(2) Introduction

Many great voyages were launched to explore the oceans and what lies beyond, because they have always held a great fascination to us. A great variety of marine organisms were collected and describe during these voyages, but insects appear to have received little attention (Andersen and Chen, 2004). Although they are the most abundant animals on land, insects are relatively rare in marine environments (Cheng, 1985). However, a few thousand insect species belonging to more than 20 orders are considered to be marine (Cheng and Frank, 1993; Cheng, 2003). The majority of marine insects belong to the Coleoptera, Hemiptera, and Diptera, and they can be found in various marine habitats. However, the only insects to live in the open ocean are members of the genus *Halobates*, commonly known as sea-skaters. They belong to the family Gerridae (Heteroptera), which comprises the common pond-skaters or water-striders. Unlike most of its freshwater relatives, the genus *Halobates* is almost exclusively marine. Adults are small, measuring only about 0.5 cm in body length, but they have rather long legs and may have a leg span of 1.5 cm or more except for a new species, *Halobates megamoomario*. This new species which has very long boy length of 0.9 cm and large mid-leg span of 3.2 cm has been newly and recently collected in the tropical Pacific Ocean during the cruise, MR-06-05-Leg 3, and described (Harada et al., submitted). They are totally wingless at all stages of their life cycle and are confined to the air-sea interface, being an integral member of the pleuston community (Cheng, 1985). One may wonder how much tiny insects have managed to live in the open sea, battling waves and storms. In life, sea-skaters appear silvery. On calm days ocean-going scientists have probably seen them as shiny spiders skating over the sea surface. It is not known whether ancient mariners ever saw them, and no mention of their presence has been found in the logs of Christopher Columbus'S (1451-1506) ships or other ships that sailed to and from the New World (Andersen and Cheng, 2004).

Forty-seven species of *Halobates* are now known (Andersen and Cheng, 2004; Harada *et al.*, submitted). Six are oceanic and are widely distributed in the Pacific, Atlantic and the Indian Oceans. The remaining species occur in near-shore areas of the tropical seas associated with mangrove or other marine plants. Many are endemic to islands or island groups (Cheng, 1989).

The only insects that inhabit the open sea area are seven species of sea skaters: *Halobates micans, H. sericeus, H. germanus, H. splendens, H. sobrinus* (Cheng, 1985) and new two species of *H. megamoomario* and *H. moomario* under description (Harada *et al.*, submitted). Three species, *Halobates sericeus*, *H. micans* and *H. germanus* inhabit tropical and temperate areas of the Pacific Ocean in the northern hemisphere, including The Kuroshio Current and the East China Sea (Andersen and Polhemus, 1976, Cheng, 1985). *Halobates sericeus, H. micans and H germanus* are reported from latitudes of 13ºN-40ºN, 0ºN-35ºNand 0ºN-37ºN, respectively, in the Pacific Ocean (Miyamoto and Senta, 1960; Andersen and Polhemus, 1976; Ikawa et al., 2002). However, this information was collected on different cruises and in different times of the years. There have been several ecological studies based on samples collected in a specific area in a particular season during the six cruises of R/V HAKUHO-MARU: KH-02-01, KH-06-02, TANSEI-MARU: KT-07-19, KT-08-23 and R/V MIRAI: MR-06-05-Leg 3, MR-08-02.

During one cruise, KH-02-01, one sea skater species, *Halobates sericeus,* was collected at 18 locations in the East China Sea area (27°10' N- 33°24' N, 124º57' E - 129º30' E) (Harada, 2005), and *H. micans* and/or *H. germanus* at only 8 locations in the area south of 29° 47'N, where water temperatures were more than 25℃. At three locations, where the water temperature was less than 23℃, neither *H. micans* nor *H. germanus* were caught.

During another cruise, KH-06-02, in the latitude area of 12˚N to 14˚30’N, *Halobates micans* were caught at 6 of 7 locations, while *H.germanus* and *H. sericeus* were caught at only 3 and 1 location(s), respectively (Harada et al*,* 2006). However, at 15˚00’ N or northern area, *H. germanus* were caught at 14 of 19 locations, whereas *H. micans* and *H. cericeus* were caught at only 8 and 6 locations, respectively (Harada et al, 2006).

In the cruise, MR-06-05-Leg 3, larvae of both *H. micans* and *H. germanus* were very abundant at 6º N, whereas adults of *H. germanus* alone were completely dominant at 2º N on the longitudinal line of 130ºE. On the longitudinal line of 138ºE, larvae and adults of *H. micans* alone were dominant at points of 5 º and 8ºN, while adults of *H. germanus* were abundant between 0º and 2ºN. At the two stations of St. 37 (6º N, 130º E) and St. 52 (5º N, 138º E), relatively great number of larvae of *H. sericeus* were collected. This species has been known to be distributed in the northern area of the Pacific Ocean. At St. 52 (6º N, 138º E), it was heavily raining around the ship while trailed.

In the cruise, KT-07-19 on the northern edge of Kuroshio Current, *H. sericeus* was mainly collected in the northern-eastern area of 135º-140ºE, 34º-35ºN whereas *H. germanus and H. micans* were mainly collected in the relatively southern-western area of 131º-133ºE., 31º-33ºN. Only *H. sericeus* can be transferred by the Kuroshio Current onto the relatively northern-eastern area and to do reproduce at least in the summer season. In the cruise of KT-08-23, Most of “domestic” specimen collected in the area northern to Kuroshio current and near to Kyushu and Shikoku islands in September were *H. germanus* (Harada *et al.*, submitted).

All samplings of *Halobates* have been performed at different geographical positions in any cruise in the Pacific Ocean so far. However, there has been no information on the dynamics in species and individual compositions in relatively eastern area of 145-160ºE, 0-10ºN of tropical Pacific Ocean. This study aims, first, to perform samplings in this area of the Western Pacific Ocean and examine dynamics of the species composition and reproductive and growth activity and compare these data to the data in the past which were got in more western area of 130-137ºE, 0-10ºN in the cruise, MR-06-05- Leg 3 (Harada et al*.,* 2007; Harada et al., 2011a).

During the cruise, MR-08-02, on the longitudinal line of 130ºE, larvae of both *H. micans* and *H. germanus* were very abundant at 5-12º N, whereas adults of *H. sericeus* alone were dominant at 17º N. In the lower latitude area of 5-8 º N, all the three described species, *H. micans, H. germanus* and *H. sericeus* and un-described species, *Halobates moomario* (Harada *et al.,* unbublished) were collected. At a fixed point located at 12ºN, 135ºE, *H. micans* was dominant through the sampling period of 20 days, whereas *H. sericeus* was collected mainly in the

.

latter half of the period. Higher number of *Halobates* (593) was collected in the first half of the sampling period (8th – 17th June, 2008) when the weather was very fine than that (427) in the second half (18th – 27th June, 2008) when the typhoon No 6 was born and developed near the fixed sampling point.

In this cruise of MR-09-04, on the longitudinal line of 155-156ºE *H. germanus* was very dominant, whereas three adults of *H. micans*, *H. germanus* and *H. sericeus* were dominant at 5º N on the longitudinal line of 147 ºE during this cruise held in Nov 4-Dec 12, 2009 (Harada et al., 2009; Harada et al*.,* 2010a). Among several latitudes of 0-10 º N, peak of number of individuals collected was located at 8 º N, 5 º N and 0-2 º N for *H.m., H.g.* and *H.s.,* respectively, on the longitudinal line of 155-156 º E. From latitudinal point of view, *H. micans* and *H.germanus*. were abundant in 5-8 º N, whereas *H. sericeus* and *H. moomario* were in 0-5 º N. Except for St. 6 at 3 º N, 147 º E, more than half of specimen collected were larvae at the remaining St. 1-5 and St.7,8.. Un-described new species, *Halobates moomario* was mostly on the longitudinal line of 147ºE. On the longitudinal line of 147 º E, more newly hatched larvae were collected than those on the line of 155-156E. *Halobates micans* was dominantly inhabiting at a fixed point of 3N, 139E in the tropical Pacific Ocean during a science cruise of MR-10-03 administered in May and June of 2010.

In the cruise, KH-10-04-Leg. 1 (Harada et al., 2010b), the samplings of *Halobates* inhabiting temperate and subtropical Pacific Ocean along the cruise track from Tokyo to Honolulu for the 2 weeks showed that four species of *Halobates micans, H.germanus, H. sericeus, H. moomario* inhabited in the relatively northern and western area of 30ºN-34ºN and 140ºE-144ºE, although *H. sericeus* was dominant species. In the relatively southern and eastern area of 19 ºN-29ºN and 147ºE-163ºW, only *H. sericeus* was exclusively inhabiting. Many larvae of this species were collected through all the stations and the reproductive activity of *H. sericeus* seems to be active in this area. Significantly more female-adults were collected rather than male-adults in total (χ^2-test, P<0.01). The extent of positive phototaxis by females may be higher than that of males, or avoiding behavior from the opening of the Neuston Net might be more active by males than females.

In the cruise, KH-10-04-Leg 2(Harada *et al.*, 2010c), the samplings of *Halobates* in Central or Eastern Tropical Pacific Ocean showed that *Halobates sericeus* was dominant at 13º59'N, 162º06'W, while *Halobates megamoomario* and *Halobates moomario* were dominant in the areas of 2º35'N-2º45'N, 164ºW-166ºW and 14ºN-17ºN, 172ºW-176ºW, respectively. In the sampling area of the Central or Eastern Tropical Pacific ocean, the population density of *Halobates* is relatively low of 3626.4/km^2.

In the cruise, KH-10-05-Leg 1 (Harada et al., 2010d), the samplings of *Halobates* in Tropical Indian Ocean showed that *Halobates micans* was dominant with estimated population density of about 58000 individuals/km^2 along the cruise track from 04'09S, 094'26E to 08˚40'S, 084˚04'E, while *H. micans* was also dominant but estimated population density was relatively low of 0 -21523 /km^2 on the line of cruise track from 10˚12'S, 080˚24'E to 15˚23'S, 067˚48'E. Positive and negative correlations were shown between chlorophyll conc. and the number of *Halobates* (mostly *H. micans*) individuals collected and between oxygen and the number of sea skaters inhabiting in Tropical Indian Ocean, respectively.

In the cruise, MR-11-07-Leg 1, the samplings of *Halobates* inhabiting two locations at 01º55'S, 083º24'E (Station 1 and 08º00'S, 080º30'E (Stations 2-17) in subtropical Indian Ocean showed that two species of *Halobates micans* and *H.germanus* inhabited in the tropical Indian Ocean, although most of individuals collected

.

are *H. micans* and it was completely dominant species. This result coincides with results of the past study (Andersen and Cheng, 2004; Harada et al., 2010a; Harada et al., 2011b). At the fixed location of 08º00’S, 080º30’E, one third of the density of *H. micans* can be estimated, compared with the density in relatively wide area of 8ºN-6ºS, 76ºE-86ºE (KH-10-05) in the Indian Ocean. Probably the low activity of photosynthesis and relatively high oxygen consumption which can be suggested by low amount of chlorophyll in surface sea water in this fixed location may be related to relatively low density of *Halobates*, because low photosynthesis activity and high dissolved oxygen show extremely low amount of animals like as zooplankton and nekton which mean low amount of foods for sea skaters. Samplings at the fixed location at 08º00’S, 080º30’E showed that higher population density (20491.4 individuals/km^2) of *Halobates micans* was estimated at the stations where air temperature was 27.5ºC than that (12070.9 individuals/km^2) in the stations at which air temp. was less than 27.5 ºC (Mann-Whitney U-test: z=-2.614, p=0.009)(Fig. 2). Similar result in the population density of larvae (481 larvae of *H. micans* and 70 ones of *H. germanus* were collected in total at Stations 1-17) implies higher reproductive activity when the air temperature become higher than 27.5 ºC (z=-2.935, p=0.003).

In the cruise, KH-12-01-Leg 2, the samplings of *Halobates* inhabiting temperate and subtropical Pacific Ocean along the cruise track from Honolulu to Tokyo for the 2 weeks showed that 68-198 individuals of only one species of *H. sericeus,* were exclusively collected at the three stations around the cruise track from 24˚30’N, 177˚32’W to 26˚27’N, 174˚15’ E. At another station of 27˚42’N 169˚24’ E, the number of individuals of *H. sericeus* were small of 42. At the two stations located in northern area (30˚15’N, 159˚04’ E; 31˚27’N, 154˚07’ E), no individuals were collected any more in this season. Northern limit of the distribution of *H. sericeus* would be located between 27˚42’N and 30˚15’N in the season of late Feb and the beginning of Mar in the central Pacific Ocean. Andersen and Cheng (2004) mentioned about the lower limit for surface water temperature which can be located around 25℃. This study shows that *Halobates sericeus* which distributed also to the northern area of 40 degree north can be survived even in the sea surface temperature of 22℃.

This study aims, first, to examine the relationship between the individual number and species components of the oceanic sea skaters of *Halobates* and oceanic dynamism on several factors like as precipitation, waves, air temperature, chlorophyll conc. and dissolved oxygen conc. in surface water during samplings in the area of 14ºN-10ºN, 148ºE-150ºE of the tropical Pacific Ocean.

Fresh water species in Gerridae seem to have temperature tolerance from -3℃ to 42℃ (Harada, 2003), because water temperature in fresh water in ponds and river highly changes daily and seasonally. However, water temperatures in the ocean are relatively stable and only range from 24℃ to 30 ℃ in the center of Kuroshio current in southern front of western Japan (Harada, 2005). Adults of *Halobates germanus* showed semi-heat-paralysis (SHP: static posture with no or low frequency to skate on water surface), when they were exposed to temp. higher than 32℃ (Harada unpublished, data in the TANSEIMARU cruise: KT-05-27).

In contrast to the temperate ocean, water temperature in the tropical ocean area, is more stable around 30℃. Therefore, the tropical species of *H. micans* is hypothesized to have lower tolerances to temperature changes than the tropical-temperate species, *H. cericeus*. This hypothesis was true in the laboratory experiment during the cruise of KH-06-02-Leg 5 (Harada *et al.*, submitted). When the water temperature increased stepwise 1℃ every 1 hour, heat-paralysis (ventral surface of thorax attaché to water surface and unable to skate) occurred at 29℃ to >35 ℃ (increase by 1 to >7 ℃). Three of four specimens in *Halobates sericeus* were not paralyzed even at 35 ℃ and

.

highly resistant to temperature change, while only one of nine in *H. micans.* and only four of twelve in *H. germanus* were not paralyzed at 35 ℃. On average, *H. sericeus, H germanus and H. micans* were paralyzed at >35.6 ℃ (SD: 0.89), >32.9 ℃(SD: 2.17) and >31.6 ℃ (SD: 2.60) on average, respectively (Harada *et al.*, submitted).

As an index of cold hardiness, super cooling points (SCPs) have been used in many insects (Bale, 1987, 1993; Worland, 2005). The absence of ice-nucleating agents and/or the lack of an accumulation of cryo-protective elements can often promote higher super cooling points (Milonas and Savopoulou-Soultani, 1999). SCPs, however, might be estimated as only the lower limits of supercooling capacity and only a theoretical lower threshold for the survival of insects as freeze-non-tolerant organisms. Many insects show considerable non-freezing mortality at temperatures well above the SCPs, a "chill-injury" species (Carrillo et al., 2005; Liu et al., 2007). Liu et al. (2009) recently showed that SCPs change in accordance with the process of winter diapauses, decreasing in Dec-Feb and increasing rapidly in Feb-Apr (diapauses completing season) due to making glycogen from trehalose as a "blood suger" leading to lower osmotic pressure in haemolymph due to low "trehalose" level. This relation supports the possibility of SCPs available as an indirect indicator of cold hardiness of insects.

The 0-10ºN latitude-area in the Pacific Ocean has very complicated dynamic systems of ocean and atmosphere. Because of such complicated system, water/air temperatures and water conductivity (salinity) can be in dynamic change temporally and spatially. Sea skaters inhabiting this area of the Pacific Ocean show relatively high tolerance to temperature changes (heat tolerance) (Harada et al*.,* 2011a), and *H. sericeus* which is inhabiting wide latitude area of 40ºN-40ºS in the Pacific Ocean is more hardy to temperature increase than other two oceanic sea skaters, *H. germanus* and *H. micans* inhabiting narrower latitude range of 25ºS-25ºN and 20ºS-20ºN in the Indian and Pacific Ocean (Harada et al., 2011a). Adult specimens of *Halobates micans* living at 6ºS, 89ºE where currents from south and north directions hit and get together than those living at other places of 8ºN, 89ºE in the tropical Indian Ocean (Harada et al., 2011c). Due to 3 or 4ºC of temperature decrease when rain falls, tolerance to high temperature by *H. micans* becomes weaker in the tropical Pacific Ocean (Harada et al., 2011c). Recently, a cross-tolerance to high and low severe temperature has been reported by fresh water species of semi-aquatic bug, *Aquarius paludum* (Harada et al., 2010e). Also oceanic sea skaters (all four species of *H. micans, H. germanus, H. sericeus* and *H.sp.*) inhabiting tropical ocean showed a negative correlation between heat coma temperature and SCP (Harada et al., 2009: the cruise report of MR-09-04). Similar correlation was also observed only for males of *H. sericeus* collected on the cruise track between Tokyo and Honolulu, Hawaii (Harada et al., 2010b: the cruise report of KH-10-04-Leg 1).

This study aims, second, to examine whether sea skaters, living in the area of 14ºN-10ºN, 148ºE-150ºE of the tropical Pacific Ocean show a high cross tolerance of higher heat tolerance and lower super cooling points (SCP) and also to examine some relationship between the heat hardiness plus SCP as a index of cold hardiness of sea skaters and oceanic dynamism on several factors like as precipitation, waves, air temperature, chlorophyll conc. and dissolved oxygen conc. in surface water.

Insects which have chance to be exposed to sea water or brackish water are known to adopt one of two strategies to survive an stress as higher osmotic pressure, "osmoregulating" and "osmoconforming" (Bradley, 1987). In the former strategy, insect maintains the osmotic pressure in haemolymph relatively lower level against high salinity environment. For example, dipteran larvae including saline-water mosquitoss of the genus *Aedes* and chironomids (Neumann, 1976; Kokkin, 1986) constantly lose water in saline water. To prevent water loss, larvae drink the

.

external medium and at the same time excrete a concentrated “urine” to keep lower osmotic pressure in the haemolymph. In the latter strategy, osmoconforming, insects of other genera of mosquitoes (Bradley, 1987, 1994) and euryhaline species of other order genera (for example a dragon fly nymph, *Enallagma clausam*: Stobbart & Shaw, 1974) equilibrate the osmotic pressure of the haemolymph with that of the saline environment.

A semi-aquatic bug, *Aquarius paludum,* a fresh water and semi-cosmopolitan species in Palearctic area response to the exposure to the brackish water: the limit for nymph growth was 0.9% of NaCl, and even in 0.45% of salinity can depress the reproductive activity (down up to 2/3 of fecundity) in the population inhabiting fresh water habitat (Kishi et al., 2006, 2007, 2009). How do oceanic sea skaters adapt to the brackish and fresh water environment? In the open ocean, some heavy rain can make the sea water file leading to rapid decreasing of osmotic pressure.

In the cruise of KH-09-05-Leg.7 (Harada and Sekimoto, 2010: the cruise report), salinity experiment was performed at the first time on sea skaters of *Halobates* sp (under the description as *Halobates moomario*) inhabiting Tomini Bay in Indonesia. The movements of mid- and/or hind legs of all the specimen on the fresh water were paralyzed with unusual back position and quick fluctuating and all ones were dead within 2 hours after the occurrence of such so called “paralysis due to fresh-water shock” The paralysis and death after that occurred only on the fresh water 19-31hrs and 21-33 hrs, respectively. In total data from Experiments 1-3, females showed significantly longer hours of 27 hrs in survival on average than males only on the fresh. Individuals on 2/3 sea water tended to be in survival longer than those on 100% sea water in Experiments 1-3 (Wilcoxon test on average value: z= -1.604, p=0.109).

In the cruise of KH-10-04-Leg 2 (Harada et al., 2010c: the cruise report), on the fresh water, the movements of mid- and/or hind legs of all the specimen on the fresh water were paralyzed with unusual back position and quick fluctuating just after transferring to the fresh water and all ones were dead within 2-3 hours after the transferring to the fresh water in all three species of *Halobates sericeus*, *H. moomario* and *H. megamoomario* inhabiting open Pacific Ocean. In the case of *H. moomario* inhabiting in Tomini bay, such fresh water paralysis occurred 15-20hours after the transferring to the fresh water. Sea skaters inhabiting the open Ocean may be less resistant to fresh water than those living on Tomini Bay, because there are no effects of fresh water flowing from the rivers of lands. Even on the salinity of 11‰, all the three species of sea skaters survived for similar hours to those on the higher salinity of 22-36‰. They can survive when they are exposed to the heavy rain and following very low salinity level of the surface layer of the sea.

In the cruise of KH-10-05 (Harada et al., 2010d: the cruise report), the fresh water shock occurred very quickly within 2-9hrs for in all adult specimens of *H. micans* from the Oceans and dead within 2hrs thereafter. Significantly longer hours in survival were shown by the both species on 1/3 or 2/3 sea water than those on sea water. The longer hours in survival by oceanic sea skaters to “brackish waters” could be speculated to be adaptation to the occasional rain fall on the sea water film.

As a third aim of this study, another experiment is performed on oceanic sea skaters, *Halobates* inhabiting the area of 14ºN-10ºN, 148ºE-150ºE of the tropical Pacific Ocean to know an exact threshold of higher limit to trig the “fresh water shock” in relation to a salinity concentration (osmotic pressure) of haemolymph which should be sampled during this cruise. This experiment tries to clarify whether some relationship is among oceanic dynamics (for example, weather, precipitation, waves, salinity, air temperatures) in the day before the collection, survival days under several salinity levels and also the threshold to trig the “fresh water shock” and the haemolymph osmotic pressure.

(3) Materials and Methods

i. Samplings

Samplings were performed on 12th November, 15th November and 22nd November, 2012 with a Neuston NET (6 m long and with diameter of 1.3 m.) (Photos 1, 2). The Neuston NET was trailed for 15 mm x 6 times on the sea surface at 3 stations located at 14º00’N 149º00’E, 2º00’N 150º30’E and 26º18’S 165º35’E of the tropical Pacific Ocean on the starboard side of R/V MIRAI (8687t) which is owned by JAMSTEC (Japan Agency for Marine-earth Science and TECHnology). The trailing was performed for 15min exclusively at night with the ship speed of 2.0 knot to the sea water (Photo 1). It was repeated 5 or 8 times in each station. Surface area which was swept by Neuston NET was evaluated as an expression of [flow-meter value x 1.3m of width of the Neuston NET (Photo 1). Samples were transferred from the sample bottle at the end of the Neuston net to transparent aquarium (Photo 3). All the sea skaters were picked up with tweezers for planktons from the transparent aquarium on the white paper in a tray (Photo 4). The samples as sea skaters were examined very carefully and the species and stage of all the specimens were identified (after Andersen and Cheng, 2004) and the number of them was counted and recorded (Tables 3-17-1, 3-17-2, 3-17-3).

ii. Laboratory experiments

Sea skaters trapped in the pants (grey plastic bottle) (Photo 2) located and fixed at the end of Neuston NET (Photo 2) were paralyzed with the physical shock due to the trailing of the NET. Such paralyzed sea skaters were transferred on the surface of paper towel to respire. Then, the paralysis of some ones was discontinued within 20min. When sea skaters were trapped in the jelly of jelly fishes, the jelly was removed from the body of sea skaters very carefully and quickly by hand for the recovering out of the paralysis.

Adults and 5th instars which recovered out of the paralysis were moved on the sea water in the aquaria set in the laboratory for the Heat Coma Experiments (Photo 5) and measuring Super Cooling Points (Photo 6). Many white cube aquaria (30cm × 30cm × 40cm) were used in the laboratory of the ship for rearing of the adults and larvae which were recovered out of the paralysis due to the trailing. Each aquarium contained ten to twenty adults and/or larvae of *Halobates*. Both the room temperature and sea water temperature in the aquaria were kept at 29±2℃. For about 9 hours after the collection, sea skaters were kept in the aquaria before the Heat Coma Experiment. All the individuals of *Halobates* kept in the aquaria were fed on adult flies, *Lucillia illustris.* However, no foods were given at least 12 hours before measuring SCP, because the contents of alimentary canal would be possible to become ice-nuclei substances. The transparent round-shaped aquarium as the experimental arena has sea water with the same temperature (mostly 28 or 30℃) as that of the aquarium to keep sea skaters. 4 to 11 individuals at adult or larval stage were moved to the transparent aquarium. Temperature was stepwise increased by 1℃ every 1 hour till the high temperature coma occurring in all the experimental specimens. Four or five layers of cardboard were rapped around the round-shaped experimental aquarium and functioned as an insulator.

Temperature was very precisely controlled by handy on-off-switching to keep in ±0.3℃ of the current water temperature. Handy-stirring with 10cm air tube with 5mm diameter and ball stone with 3cm diameter was effective to keep the precise controlling of the current temperature. Sea skaters on the water surface of the aquarium were recorded with Digital Handy Video Camera (GZ-MG840-S: VICTOR) from above position for the last 15 min of each 1hour under the current temperature. Temperature at which Semi Heat Coma (Semi Heat Coma Temperature [HSCT]: little or no movement on the water surface more than 3 seconds) occurs and Temperature at which Heat Coma (HTP: ventral surface of the body was caught by sea water film and no ability to skate any more) occurs were recorded (Table 3-17-4).

iii. Determination of super cooling point (SCP)

Measurements of super cooling points and increasing temperature value at the moment of an exothermic event occurred in the body of the specimen (ITSCP: increased temperature at SCP) were performed for the specimen (mainly adults) paralyzed by high temperature of the two species of oceanic *Halobates* (*H. micans, H. germanus*) just after the heat paralysis experiment during this cruise (Table 3-17-4)

Surface of each adult was dried with filter paper, and thermocouples which consist of nickel and bronze were attached to the abdominal surface of the thorax and connected to automatic temperature digital recorders (Digital Thermometer, Yokogawa Co, LTD, Model 10, Made in Japan). The thermocouple was completely fixed to be attached to the ventral surface of abdomen by a kind of Scotch tape. The specimen attached to thermocouples was placed into a compressed-Styrofoam box (5×5×3 cm^3) which was again set inside another insulating larger compressed Styrofoam to ensure that the cooling rate was about 1ºC/min for recording the SCP in the freezer in which temperature was -35ºC. The lowest temperature which reached before an exothermic event occurred due to release of latent heat was regarded as the SCP (Zhao and Kang, 2000). All tested specimen were killed by the body-freezing when SCP was determined.

iv. Salinity experiment and collection of haemolymph

Adults of *H. germanus* collected during this cruise, MR-12-05-Leg 1 were used for the salinity experiment. All specimen (all female adults) for Experiment 1 were moved on the sea water in the aquaria set in the wet laboratory in R/V Mirai (temperature was kept within 30.0±2C). White cube aquaria with 30cm X 30cm X 40cm) (Photo 2) were used for the experiments. Experimental specimens were moved to one of the 2 salinity conditions, sea water or fresh waters with two salinity concentrations (A: sea water=36‰, B: distilled water: 0‰).

All specimens were female adults of *Halobates germanus* . Experimental specimens were kept more than 24 hours within 1 week after the collection and fed on the flies, *Lucilia illustris* (rate of one fly per 5-10 sea skaters per one day). After the transfer to the fresh water condition, the behavior of specimen was checked every 10 min. and the haemolymph was collected using a small handy-pump inside the small capillary (inside volume: 0.5 micro litter) when the specimen began to show leg-neurological-paralysis (3 or 4 hours after the transfer) due to zero salinity. The technical limitation cannot permit us to collect haemolymph from the bodies of males of *H.*

.

germanus, because the body volume is too small to collect haemolymph. For more than 12 hours before the transfer to one of two conditions and also during experiment, specimens were kept without foods to delete the effects of digested liquids inside the alimentary canal on the salinity concentration.

(4) Results and Discussion

i. Population density and other Meteorological factors

The samplings at 13°59'N, 149°16'E (Station 1), 02°00'S, 150°31'E (Stations 2) and 26°19'S, 165°34'E (Station 3) in subtropical Indian Ocean showed that two species of *Halobates micans* and *H.sericeus* inhabited and the latter was dominant at Station 1, two species of *H. germanus* and *H. micans* inhabited and the former was dominant, and one species of *H. sericeus* inhabited at Station 3 in the tropical Indian Ocean. These results coincides with results of the past study (Andersen, 1982; Andersen and Cheng, 2004; Harada et al., 2009; Harada et al., 2010a). Table 3-17-2 shows a comparison of population density of *Halobates* species among four tropical sampling ranges in Indian and Pacific Oceans. High density near to 100,000 individuals per 1 km^2 of *H. germanus* could be estimated at the Station 2 in this study could be related to high concentration of chlorophyll1 (solid square mark in Fig. 1).

ii. Laboratory experiments

Semi-Heat-coma temperature (SHCT), heat coma temperature (HCT), gap temperature for heat coma (GTHC) super cooling point (SCP) and Increased temperature at super cooling point (ITSCP) were ranged 31 ºC to 41 ºC, 31 ºC to 41ºC, 1.0ºC to 11.5ºC, -20.9ºC to -6.5ºC and 0.2ºC to 11.4Cº, respectively (Table 3-17-4).

Significant negative correlation between HCT (or GTHC) and SCP was shown only in female *H. germanus* (Figs. 2, 3). In *H. micans* collected at 5ºN, 140ºE, only females showed such negative correlation during the cruise of MR-10-03 (Harada et al., 2010f). Harada et al. (2010b) showed that clear negative correlation was shown not by female-adults but by male-adults of *H. sericeus* in the area of 34˚43'N, 140˚14'E to 19˚33'N, 164˚44'W in the temperate and subtropical Pacific Ocean. On the other hand, in the area of 00˚04'N-09˚59'N, 146˚59'E-156˚20'E of the central tropical Pacific Ocean, adults of *H. sericeus* showed very clear and significant negative correlation (Pearson's correlation test: r=-0.463, p=0.011, n=26) (Harada et al., 2009).

What is the physiological mechanism of the correlation between SCP and HCT? Heat shock protein (HSP) was well known to be in transcript and translated several times higher in response to the exposure to heat in insects, especially in *Drosophila* (Velazquez et al., 1983; Goto et al., 1998). Heat shock protein protect from the damage of functional or constructive protein due to heat, for example (Neven, 2000): the *HSP*70 protein may 'chaperone' the protein against the lysosome for degradation (Chiang et al.,1994) or help the protein re-fold after return to favorable temperatures (Parsell and Lindquist, 1994). The over expression of HSP might be speculated to promote the expression of other substances to increase the osmotic pressures in the case of oceanic sea skaters, because heat shock proteins accelerate the synthesis of sorbitol in white flies, polyol in whiteflies and aphids and also promote the trehalose synthesis in yeast Salvucci, 2000; Salvucci et al., 2000).

Opposite tendency as "positive" correlation between HCT and SCP was shown by female *H. sericeus* from the Station 1 and male *H. sericeus* from the Station 3 (Female *H. sericeus* at Station 1: r=0.415, p=0.025, n=31; No analysis on male *H. sericeus* at Station 1 because of few number of specimen collected; Female *H. sericeus* at Station 3: r=0.185, p=0.463, n=18; Male *H. sericeus* at Station 3: r=0.432, p=0.073). However, the exposure to high

.

temperature during the heat coma experiment increased by 2.5 the value of super cooling point in an experiment (Harada et al., 2011b). Therefore, longer exposure to high temperature during experiment might induce higher SCP as the side and artificial effects. As the result, positive correlation between SCP and "exposure time" to high temperature can occur.

(5) Additional Analyses

It will be analyzed how the data on field samplings in this study are related to environmental data as the oceanography data at the three sampling stations: 14º00'N 149º00'E, 2º00'N 150º30'E and 26º18'S 166º35'E in the Pacific Ocean at the cruise, KH-12-05-Leg 1. This relationship can be compared to other similar analyses on the data collected in the area of 4ºS to 13ºS and 8ºN to 6ºS in the Indian Ocean at two cruises, KH-10-05-Leg 1 (Harada et al., 2010d) and KH-07-04-Leg1 (Harada et al., 2008), respectively and also in the area of 30º-35ºN along the Kuroshio Current at the cruises, KT-07-19, KT-08-23, KT-09-20 and the other R/V TANSEIMARU cruises held in the past.

Cross tolerance between heat and cold hardiness was shown by female adults of *Halobates germanus* inhabiting the station at 2º00'N 150º30'E in the western tropical Pacific Ocean during the MR-12-05-04. SCP measurement and heat coma experiments were done during the other cruises in the past. The comparative studies will be done on the relationship between heat tolerance and SCP data as an index of cold hardiness, and other oceanographic data. Dissection data (for example reproductive maturation), chemical contents data (example lipids) and gene data of MtDNA from *Halobates* samples should be analyzed in the future.

Salinity concentration in the haemolymph of female adults of *Halobates germanus* and *Halobates sericeus* collected during this study will be measured by the special measurement machine as soon as possible.

ACKNOWLEDGEMENT

We would like to thank Dr. Katsuro KATSUMATA (Head Scientist of the cruise: MR-12-05-Leg 1) for the permission to do this study during the R/V MIRAI cruise, for his warm suggestion on ocean and atmosphere dynamics, and encouragement and help throughout this cruise. The samplings and the experimental study were also possible due to supports from all of the crew (Captain: Mr. Yoshiharu TSUTSUMI) and all the scientists and the engineers from GODI and MWJ in this cruise. We would like to give special thanks to them.

References

Andersen NM, Chen L 2004: The marine insect Halobates (Heteroptera: Gerridae): Biology, adaptations distribution, and phylogeny. *Oceanography and Marine Biology: An Annual Review* 42, 119-180.

Andersen NM, Polhemus JT 1976: Water-striders (Hemiptera: Gerridae, Vellidae, etc). In L. Cheng L. (ed): *Marine Insects.* North-Holland Publishing Company, Amsterdam, pp 187-224.

Bale JS 1987: Insect cold hardiness: freezing and supercooling- an ecophysiological perspective. *J. Insect Physiol.*, 33: 899-908.

Bale JS 1993: Classes of Insect Cold Hardiness. *Functional Ecol.* 7: 751–753.

Bradley TJ 1987: Physiology of osmoregulation in mosquitoes. *Annual Review of Entomology* 32:

.

439-462.

Bradley TJ 1994: The role of physiological capacity, morphology and phylogeny in determining habitat use in mosquitoes. *Ecological Morphology: Integrative Organisms Biology,* pp. 303-318, University of Chicago Press, Chicago.

Carrillo MA, Heimpel GE, Moon RD, Cannon CA, Hutchison WD 2005: Cold hardiness of *Habrobracon hebetor* (Say) (Hymnoptera: Braconidae), a parasitoid of pyralid moths. *J. Insect Physiol.* 51: 759-768.

Cheng L 1985: Biology of Halobates (Heteroptera: Gerridae) *Ann. Rev. Entomol.* 30, 111-135.

Cheng L 1989: Factors limiting the distribution of Halobates species. In Reproduction, Genetics and Distribution of Marine Orgaminisms, J.S. Ryland & P.A. Tyler (eds), Fredensbor, Denmark: Olsen & Olsen, 23rd European Marine Biology Symposium, pp. 357-362.

Cheng L 2003: Marine insects. In Resh VH & Carde RT (eds), *Encyclopedia of Insects*, pp. 679-682, Academic Press, San Diego.

Cheng L, Frank JH 1993: Marine insects and their reproduction. *Oceanography and Marine Biology: An Annual Review* 31, 479-506.

Chiang H, Terlecky SR, Plant CP, Dice JF 1994: A role for a 70-kilodaton heat shock protein in lysosomal degradation of intracellular proteins. *Science* 246, 382–385.

Goto SG, Yoshida KM, Kimura MT, 1998: Accumulation of Hsp70 mRNA under environmental stresses in diapausing and nondiapausing adults of *Drosophila triauraria. J. Insect Physiol.* 44, 1009-1015.

Harada T 2003: Hardiness to low temperature and drought in a water strider, *Aquarius paludum* in comparison with other insect groups *Trends in Entomology(Research Trends, Trivandrum, India)*, 3, 29-41.

Harada T 2005: Geographical distribution of three oceanic Halobates spp. and an account of the behaviour of *H. sericeus* (Heteroptera: Gerridae). *Eur. J. Entomol.* 102, 299-302.

Harada T, Sekimoto T 2010: Distribution and tolerance to brackish and fresh water bodies as habitat in oceanic sea skater of Halobates (Heteroptera: Gerridae). *The Cruise Report of KH-09-05-Leg 7.*

Harada T, Ishibashi T, Inoue T 2006: Geographical distribution and heat-tolerance in three oceanic *Halobates* species (Heteroptera: Gerridae). *The Cruise Report of KH-06-02-Leg 5.*

Harada T, Sekimoto T, Osumi Y, Ishigaki H 2008: Geographical distribution in the Indian Ocean and heat-tolerance in the oceanic sea skaters of Halobates. (Heteroptera: Gerridae) and oceanic dynamics.. *The Cruise Report of KH-07-04-Leg 1.*

Harada T, Nakajyo M, Inoue T 2007: Geographical distribution in the western tropical Pacific Ocean and heat-tolerance in the oceanic sea skaters of *Halobates*. (Heteroptera: Gerridae) and oceanic dynamics. *The Cruise Report of MR-06-05-Leg3.*

Harada T, Iyota K, Shiraki T, Katagiri C 2009: Distribution, heat-tolerance and super cooling point of the oceanic sea skaters of *Halobates*. (Heteroptera: Gerridae) inhabiting tropical area of western Pacific Ocean and oceanic dynamics. *The Cruise Report of MR-09-04*

Harada T, Sekimoto T, Iyota K, Shiraki T, Takenaka S, Nakajyo M, Osumi O and Katagiri C 2010a: Comparison of the population density of oceanic sea skater of *Halobates* (Heteroptera: Gerridae) among several areas in the tropical pacific ocean and the tropical Indian Ocean. *Formosan Entomol*, 30, 307-316.

.

Harada T, Iyota K, Osumi Y, Shiraki T, Sekimloto T, Yokogawa S, Oguma K 2010b: Distribution, heat-tolerance and supercooling point of the oceanic sea skaters of *Halobates* (Heteroptera: Gerridae) inhabiting temperate and

Subtropical Pacific Oceean along the cruise track from Tokyo to Honolulu. *The Cruise Report of KH-10-04-Leg 1.*

Harada T, Iyota K, Osumi Y, Shiraki T, Sekimoto T 2010c: Distribution and tolerance to brackish and fresh water bodies as a habitat in oceanic sea skater of Halobates (Heteroptera: Gerridae) inhabiting Eastern & Central Tropical Pacific Ocean. *The Cruise Report of KH-10-04-Leg 2.*

Harada T, Iyota K, Sekimoto T 2010d: Distribution and tolerance to brackish water bodies as habitat in oceanic sea Skater of Halobates (Heteroptera: Gerridae) inhabiting Tropical Indian Ocean. *The Cruise Report of KH-10-05-Leg 1.*

Harada T, Ikeda S, Ishibashi T 2010e: Cross tolerance between heat and cold stress by warm temperate *Aquarius paludum paludum* and subtropical *Aquarius paludum amamiensis*, semi-aguatic bugs (Gerridae, Heteroptera). *Formosan Entomol.*, 30:87-101.

Harada T, Iyota K, Osumi Y, Sekimoto T 2010f: Heat-tolerance and super cooling point of the oceanic sea skaters of *Halobates* (Heteroptera: Gerridae) inhabiting a fixed station (3ºN, 139ºE) of western tropical Pacific Ocean *The Cruise Report of MR-10-03* (3rd May, 2010 ~ 28th June, 2010)

Harada T, Takenaka S, Sekimoto T, Nakajyo M, Inoue T, Ishibashi T, Katagiri C 2011a: Heat coma as an indicator of resistance to environmental stress and its relationship to ocean dynamics in the sea skaters, *Halobates* (Heteroptera: Gerridae). *Insect Sci.*, 18, 73-711.

Harada T, Sekimoto T, Osumi Y, Kobayashi A, Shiraki T 2011b: Distribution and ecology of oceanic *Halobates* inhabiting tropical area of Indian Ocean and their responding system to several environmental factors. The Cruise Report of MR-11-07 (23rd September, 2011 ~ 2nd December, 2011)

Harada T, Takenaka S, Sekimoto T, Ohsumi Y, Nakajyo M, Katagiri C 2011c: Heat coma and its relationship to ocean dynamics in the oceanic sea skaters of *Halobates* (Heteroptera: Gerridae) inhabiting Indian and Pacific Oceans. *J. Thermal Biol.*, 36: 299–305.

Ikawa T, Okabe H, Hoshizaki S, Suzuki Y, Fuchi T, Cheng L 2002: Species composition and distribution of ocean skaters Halobates (Hemiptera: Gerridae) in the western pacific ocean. *Entomol. Sci.* 5, 1-6.

Kishi M, Fujisaki K, Harada T 2006: How do water striders, *Aquarius paludum*, react to brackish-water simulated by NaCl solutions? *Naturwissenschaften* 93: 33-37.

Kishi M, Harada T, Fujisaki K 2007: Dispersal and reproductive responses of the water strider, *Aquarius paludum* (Hemiptera: Gerridae), to changing NaCl concentrations. *Eur. J. Entomol.* 104: 377-383.

Kishi M, Harada T, Fujisaki K 2009: Responses of life-history traits of brackish- and freshwater populations of the water strider to NaCl *Aquarius paludum* (Hemiptera: Gerridae). *Eur. J. Entomol.* 106: 43-48.

Kokkinn MJ 1986: Osmoregulation, salinity tolerance and the site of ion excretion in the halobiont chironomid, *Tanytarsus baritarsis* Freeman. *Austarian Journal of Marine and Freshwater*

Researches 37: 243 -250.

Liu ZD, Gong PY, Wu KJ, Wei W, Sun JH, Li DM 2007: Effects of larval host plants on over-wintering preparedness and survival of the cotton ballwarm, *Helicoverpa armigera* (Hübner) (Lepidoptera: Noctuidae). *J. Insect Physiol.* 53: 1016-1026.

Liu ZD, Gong PY, Heckel DG, Wei W, Sun JH, Li DM 2009: Effects of larval host plants on over-wintering physiological dynamics and survival of the cotton bollwarm, *Helicoverpa armigera* (Hübner)(Lepidoptera: Noctuidae). *J. Insect Physiol.* 55: 1-9.

Milonas P, Savopoulou-Soultani M 1999: Cold hardiness in diapause and non-diapause larvae of the summer fruit tortorix, *Adoxophes orana* (Lepidoptera: Tortricidae). *Eur. J. Entomol.* 96: 183-187.

Miyamoto S, Senta T 1960: Distribution, marine condition and other biological notes of marine water-striders, *Halobates* spp., in the south-western sea area of Kyushu and western area of Japan Sea. *Sieboldia* (In Japanese with English summary). 2, 171-186.

Neumann D 1976: Adaptations of chironomids to intertidal environments. *Annual Review of Entomology,* 21: 387-414.

Neven LG 2000: Physiological responses of insects to heat. *Postharvest Biology and Technology* 21, 103–111.

Parsell DA, Lindquist S 1994: In: Morimoto, R.I., Tissieres, A., Georgopoulos, C., (Eds.), *The Biology of Heat Shock Proteins and Molecular Chaperones*, Cold Spring Harbor Laboratory Press, New York, 457–494.

Salvucci ME 2000: Sorbitol accumulation in whiteflies: evidence for a role in protecting proteins during heat stress. *J. Therm. Biol.* 25, 353-361.

Salvucci ME, Stecher DS, Henneberry TJ 2000: Heat shock proteins in whiteflies, an insect that accumulates sorbitol in response to heat stress. *J. Therm. Biol.* 25, 363-371.

Stobbart RH, Shaw J 1974: Salt and water balance: excretion. *The Physiology of Insecta,*. pp. 362-446, Academic Press, New York.

Worland M. R. 2005: Factors that influence freezing in the sub-antarctic springtail *Tullbergia antarctica*. *J. Insect Physiol.* 51: 881-894.

Velazquez JM, Sonoda S, Bugaisky G, Lindquist S 1983: Is the major *Drosophila* heat shock protein present in cells that have not been heat shocked? J. Cell Biol. 96, 286-290.

Zhao YX, Kang L. 2000: Cold tolerance of the leafminer *Liriomyza sativae* (Dipt., Agromyzidae). *J. Appl. Entomol.* 124: 185-189.

Table 3-17-1-A. Number of *Halobates* collected at locations in the tropical Pacific Ocean in Nov. 12th, 15th and 22nd 2012 (N: Total number of individuals collected; *H.m.: Halobates micans; H.g.: Halobates germanus; H.s.: Halobates sericeus*; Stat: Station number; WT: Water temperature (℃); AT: Air temp.; L: N of larvae; A: N of adults, E: N of exuviae; Date: sampling date; Sampling was performed for 45min. EG: eggs on some substrates like as polystyrene form thousands of eggs laid on the substrate. S: Surface area which was swept by Neuston NET was expressed as value of flow-meter x 1.3m of width of Neuston NET; WS: wind speed (m/s); W: weather; TD: Time of day; WS: Wind speed, CS: Current speed(m/s)CD: Current direction; F: female; M: male; DO: dissolved oxygen (μmol/kg); Chl: Chlorophyll-A conc.(relative fluorescent value); SL: salinity(‰)

Latitude	Longitude	N	L	A		*H.m.*	*H.g.*	*H.s.*	EG	E	Stat	WT	AT	WS	W	CS	CD	TD	Date	S(x1.3 m^2)	DO	Chl	SL
				F	M																		
13º59'N	149º16'E	14	4	7	3	0	0	14	0	1	St.1-1	29.4	30.5	10.0	F/R	0.4	254º	17:57~18:12	Nov 12	844.0	204.60	0.285	32
13º59'N	149º16'E	32	12	15	5	12	0	20	0	1	St.1-2	29.4	30.5	9.3	F/R	0.5	256º	18:18-33	Nov 12	958.0	204.60	0.285	32
13º59'N	149º17'E	25	14	9	2	15	0	10	0	0	St.1-3	29.4	30.5	9.9	F/R	0.5	298º	18:38-53	Nov 12	813.0	204.60	0.285	32
13º58'N	149º17'E	15	6	5	4	9	0	6	0	1	St.1-4	29.4	30.5	8.9	F/R	0.3	235º	18:53~19:08	Nov 12	638.0	204.60	0.285	32
13º58'N	149º17'E	14	3	10	1	4	0	10	0	0	St.1-5	29.4	30.5	8.3	F/R	0.4	256º	19:18~33	Nov 12	838.0	204.60	0.285	32
13º57'N	149º18'E	17	5	11	1	3	0	14	0	0	St.1-6	29.4	30.5	9.6	F/R	0.3	241º	19:38~ 53	Nov 12	652.0	204.60	0.285	32
01º55'N	150º31'E	53	6	24	23	2	51	0	0	1	St.2-1	29.6	27.1	4.3	Cloudy	0.5	319º	18:43~58	Nov 15	-	206.6 3	0.915	32
01º56'N	150º31'E	67	9	28	30	1	66	0	0	0	St.2-2	29.6	27.1	5.1	Cloudy	0.6	309º	19:06~21	Nov 15	-	206.63	0.915	32
01º57'N	150º31'E	75	13	25	37	2	73	0	0	0	St.2-3	29.6	27.1	5.6	Cloudy	0.4	321º	19:28~43	Nov 15	-	206.63	0.915	32
01º58'N	150º31'E	83	19	31	33	1	82	0	0	0	St.2-4	29.6	27.1	6.4	Cloudy	0.5	305º	19:49~20:04	Nov 15	-	206.63	0.915	32
01º59'N	150º31'E	85	5	34	46	1	84	0	0	0	St.2-5	29.6	27.1	4.6	Cloudy	0.5	313º	20:10~25	Nov 15	-	206.63	0.915	32
01º59'N	150º31'E	82	14	37	31	1	81	0	0	0	St.2-6	29.6	27.1	6.1	Cloudy	0.5	321º	20:31~46	Nov 15	563.0	206.63	0.915	32
26º18'S	165º36'E	9	3	2	4	0	0	9	0	0	St.-3-1	23.2	22.0	9.6	F/C	0.5	021º	19:32-48	Nov 22	719.0	224.53	0.375	34
26º19'S	165º35'E	42	9	20	13	0	0	42	0	3	St.3-2	23.2	22.0	8.5	F/C	0.4	014º	19:54~20:11	Nov 22	895.0	224.53	0.375	34
26º19'S	165º34'E	17	5	8	4	0	0	17	0	0	St.3-3	23.2	22.0	10.6	F/C	0.4	339º	20:13~28	Nov 22	874.0	224.53	0.375	34
26°19'S	165°34' E	46	11	18	17	0	0	46	0	0	St.3-4	23.2	22.0	10.4	F/C	0.3	356 º	20:33-48	Nov 22	868.0	224.53	0.375	34
26°19'S	165°33' E	73	22	29	22	0	0	73	0	0	St.3-5	23.2	22.0	10.1	F/C	0.3	338º	20:54-21:09	Nov 22	896.0	224.53	0.375	34
26°19'S	165°32' E	67	21	28	18	0	0	67	0	0	St.3-6	23.2	22.0	9.3	F/C	0.3	347	21:15-30	Nov 22	882.0	224..53	0.375	34

Table 3-17-2: A comparison of population density of oceanic sea skaters, *Halobates* among four areas of open Indian and Pacific Oceans. Samplings were performed during the four cruises including this cruise. *H.m: Halobates micans: H.g.: H. germanus; H.s.: H. sericeus; H.p.: H. princeps;* sp.: *H.* sp.: Density: individual number/km^2

1. MR-10-03: Western Tropical Pacific Ocean, 5ºN, 139º30'E (Harada et al., 2010f)

	Total		*H.m*	*H.g*	*H. s .*	*H. p or* sp	AS#
	Nymphs	Adults					
Number	3772	383	4059	66	1	28	0.105310
Density	35834.0	3638.5	38560.5	627.0	9.5	266.0	-

2.KH-07-04-Leg 1: Eastern Tropical Indian Ocean, 8ºN-6º35'S, 86ºE- 76º36'E) (Harada et al., 2008)

	Total		*H.m*	*H.g*	*H. s .*	*H. p or* sp	AS#
	Nymphs	Adults					
Number	1291	706	1886	111	0	0	0.044292
Density	29147.5	15939.7	42581.1	2506.1	0	0	-

3. MR-11-07-Leg 1 (this cruise, Stations 1-17): Eastern Tropical Indian Ocean, 01º55'S, 083º24E; 8ºS, 80º30'E) (Harada et al., 2011b)

	Total		*H.m*	*H.g*	*H. s .*	*H. p or* sp	AS#
	Nymphs	Adults					
Number	551	255	697	109	0	0	0.0438607
Density	12562.5	5813.9	15891.2	2485.1	0	0	-

4. MR-12-05-Leg 1 (this cruise, Stations 1-3): Western Subtropical and Tropical Pacific Ocean, at 13º59'N 149º16'E, 01º55'N 150º31'E and 27ºS 168ºE

	Total		*H.m*	*H.g*	*H. s .*	*H. p or* sp	AS#
	Nymphs	Adults					
A. 13º59'N 149º16'E							
Number	44	73	43	0	74	0	0.0061659
Density	7136.0	11839.3	6973.8	0	12001.5	0	-

	Total		*H.m*	*H.g*	*H. s .*	*H. p or* sp	AS#
	Nymphs	Adults					
B. 01º55'N 150º31'E							

Number	66	379	8	437	0	0	0.0043914
Density	15029.4	86305.1	1821.7	99512.7	0	0	-
C. 26º55'S 165º34'E							
Number	71	183	0	0	254	0	0.0066742
Density	10638.0	27419.0	0	0	38057.0	0	-

AS$^{\#}$: Area of surface where the Neuston net has swept (km^2)

.

Table 3-17-3-A. Components of instars of larvae and adults of oceanic sea skaters, *Halobates micans*, *H. germanus* and *H. sericeus* sampled mostly sampled at 8000N, 8030E in the tropical Indian Ocean.

	Halobates micans							*H. germanus*							*H. sericeus*						
						Adults							Adults							Adults	
	1st	2nd	3rd	4th	5th	F	M	1st	2nd	3rd	4th	5th	F	M	1st	2nd	3rd	4th	5th	F	M
St1-1	**0**	**0**	**0**	**0**	**0**	**0**	**0**	**0**	**0**	**0**	**0**	**0**	**0**	**0**	**0**	**0**	**0**	**1**	**3**	**7**	**3**
St1-2	**0**	**3**	**2**	**5**	**1**	**1**	**0**	**0**	**0**	**0**	**0**	**0**	**0**	**0**	**0**	**0**	**0**	**0**	**1**	**14**	**5**
St1-3	**0**	**1**	**5**	**5**	**2**	**0**	**2**	**0**	**0**	**0**	**0**	**0**	**0**	**0**	**0**	**1**	**0**	**0**	**0**	**9**	**0**
St1-4	**0**	**0**	**2**	**1**	**3**	**0**	**3**	**0**	**0**	**0**	**0**	**0**	**0**	**0**	**0**	**0**	**0**	**0**	**0**	**5**	**1**
St1-5	**0**	**0**	**0**	**3**	**0**	**1**	**0**	**0**	**0**	**0**	**0**	**0**	**0**	**0**	**0**	**0**	**0**	**0**	**0**	**10**	**0**
St1-6	**0**	**0**	**1**	**0**	**2**	**0**	**0**	**0**	**0**	**0**	**0**	**0**	**0**	**0**	**0**	**0**	**0**	**0**	**2**	**11**	**1**
St2-1	**0**	**0**	**0**	**0**	**0**	**4**	**0**	**0**	**0**	**0**	**0**	**6**	**20**	**23**	**0**	**0**	**0**	**0**	**0**	**0**	**0**
St2-2	**0**	**0**	**0**	**0**	**0**	**0**	**1**	**0**	**0**	**0**	**2**	**7**	**28**	**29**	**0**	**0**	**0**	**0**	**0**	**0**	**0**
St2-3	**0**	**0**	**0**	**0**	**0**	**2**	**0**	**0**	**0**	**0**	**2**	**11**	**23**	**37**	**0**	**0**	**0**	**0**	**0**	**0**	**0**
St2-4	**0**	**0**	**0**	**0**	**0**	**1**	**0**	**0**	**0**	**1**	**4**	**14**	**30**	**33**	**0**	**0**	**0**	**0**	**0**	**0**	**0**
St2-5	**0**	**0**	**0**	**0**	**0**	**1**	**0**	**0**	**1**	**0**	**1**	**3**	**33**	**46**	**0**	**0**	**0**	**0**	**0**	**0**	**0**
St2-6	**0**	**0**	**0**	**0**	**0**	**0**	**1**	**0**	**1**	**3**	**5**	**5**	**37**	**30**	**0**	**0**	**0**	**0**	**0**	**0**	**0**
St3-1	**0**	**0**	**0**	**0**	**0**	**0**	**0**	**0**	**0**	**0**	**0**	**0**	**0**	**0**	**0**	**0**	**1**	**0**	**2**	**2**	**4**
St3-2	**0**	**0**	**0**	**0**	**0**	**0**	**0**	**0**	**0**	**0**	**0**	**0**	**0**	**0**	**0**	**0**	**0**	**2**	**7**	**20**	**13**
St3-3	**0**	**0**	**0**	**0**	**0**	**0**	**0**	**0**	**0**	**0**	**0**	**0**	**0**	**0**	**0**	**1**	**0**	**0**	**4**	**8**	**4**
St3-4	**0**	**0**	**0**	**0**	**0**	**0**	**0**	**0**	**0**	**0**	**0**	**0**	**0**	**0**	**0**	**0**	**0**	**1**	**10**	**18**	**17**
St3-5	**0**	**0**	**0**	**0**	**0**	**0**	**0**	**0**	**0**	**0**	**0**	**0**	**0**	**0**	**0**	**2**	**2**	**8**	**10**	**29**	**22**
St3-6	**0**	**0**	**0**	**0**	**0**	**0**	**0**	**0**	**0**	**0**	**0**	**0**	**0**	**0**	**0**	**1**	**1**	**8**	**11**	**28**	**18**

Table 3-17-4-Sheet 1. Results of "heat-coma" experiments and SCP (Super Cooling Point) measurement performed on adults of *Halobates germanus* (H.g.) and *H. sericeus* (H.s.); TA: temp. at which specimen adapted, SHCT: temp. at which semi-heat coma occurred; HCT: temp. at which heat coma occurred ; GTHC: gap temp. for heat coma (from base temp.); "Date and Time of Day" when experiments were performed. (MR-12-05-Leg 1: Nov. 5-Nov. 26, 2012), ITSCP: Increased temperature at SCP was detected; TD: Time of day when heat-paralysis experiment was performed

St.No.	Latitude	Longitude	Exp.No.	TA	SHCT	HCT	GTHC	SCP	ITSCP	Species	Stage (sex)	Date	TD
St. 1	13°59'N	149°16'E	1	30	32	32	2	-20.2	4.6	H.s.	Adult (female)	Nov 13	06:50~
St. 1	13°59'N	149°16'E	1	30	32	36	6	-20.9	6.4	H.s.	Adult(female)	Nov 13	06:50~
St. 1	13°59'N	149°16'E	1	30	32	36	6	-15.6	2.7	H.s.	Adult(female)	Nov 13	06:50~
St. 1	13°59'N	149°16'E	1	30	32	37	7	-16.9	4.1	H.s.	Adult (female)	Nov 13	06:50~
St. 1	13°59'N	149°16'E	1	30	33	37	7	-17.6	3.9	H.s.	Adult (female)	Nov 13	06:50~
St. 1	13°59'N	149°16'E	1	30	36	38	8	-15.1	3.7	H.s.	Adult (female)	Nov 13	06:50~
St. 1	13°59'N	149°16'E	1	30	36	38	8	-11.7	4.0	H.s.	Adult(female)	Nov 13	06:50~
St. 1	13°59'N	149°16'E	1	30	37	38	8	-16.7	5.7	H.s.	Adult (female)	Nov 13	06:50~
St. 1	13°59'N	149°16'E	1	30	37	38	8	-13.7	6.7	H.s.	Adult (female)	Nov 13	06:50~
St. 1	13°59'N	149°16'E	1	30	37	38	8	-16.6	5.7	H.s.	Adult (male)	Nov 13	06:50~
St. 1	13°59'N	149°16'E	1	30	37	38	8	-12.2	8.5	H.s.	Adult(female)	Nov 13	06:50~
St. 1	13°59'N	149°16'E	2	29	30	37	8	-16.5	2.4	H.s.	Adult(female)	Nov 14	06:55~
St. 1	13°59'N	149°16'E	2	29	30	38	9	-18.4	3.9	H.s.	Adult(female)	Nov 14	06:55~
St. 1	13°59'N	149°16'E	2	29	32	38	9	-19.6	4.1	H.s.	Adult(female)	Nov 14	06:55~
St. 1	13°59'N	149°16'E	2	29	33	38	9	-	-	H.s.	Adult(female)	Nov 14	06:55~
St. 1	13°59'N	149°16'E	2	29	36	38	9	-13.5	2.8	H.s.	Adult (female)	Nov 14	06:55~
St. 1	13°59'N	149°16'E	2	29	37	39	10	-15.8	4.1	H.s.	Adult (female)	Nov 14	06:55~
St. 1	13°59'N	149°16'E	2	29	37	39	10	-15.8	1.2	H.s.	Adult (female)	Nov 14	06:55~
St. 1	13°59'N	149°16'E	2	29	37	39	10	-16.0	5.6	H.s.	Adult (female)	Nov 14	06:55~
St. 1	13°59'N	149°16'E	2	29	38	39	10	-	-	H.s.	Adult (female)	Nov 14	06:55~
St. 1	13°59'N	149°16'E	2	29	38	39	10	-15.8	3.8	H.s.	Adult(female)	Nov 14	06:55~
St. 1	13°59'N	149°16'E	2	29	38	39	10	-19.5	4.0	H.s.	Adult(female)	Nov 14	06:55~
St. 1	13°59'N	149°16'E	3	29.5	31	31	1.5	-17.4	4.6	H.s.	Adult(female)	Nov 15	06:40~
St. 1	13°59'N	149°16'E	3	29.5	32	32	2.5	-18.7	2.0	H.s.	Adult(male)	Nov 15	06:40~
St. 1	13°59'N	149°16'E	3	29.5	32	34	4.5	-18.7	8.7	H.s.	Adult(female)	Nov 15	06:40~
St. 1	13°59'N	149°16'E	3	29.5	33	36	6.5	-13.5	4.5	H.s.	Adult(female)	Nov 15	06:40~
St. 1	13°59'N	149°16'E	3	29.5	33	37	7.5	-11.8	1.5	H.s.	Adult(female)	Nov 15	06:40~
St. 1	13°59'N	149°16'E	3	29.5	34	38	8.5	-12.8	4.1	H.s.	Adult(female)	Nov 15	06:40~
St. 1	13°59'N	149°16'E	3	29.5	37	38	8.5	-12.2	7.6	H.s.	Adult(male)	Nov 15	06:40~
St. 1	13°59'N	149°16'E	3	29.5	37	38	8.5	-13.1	0.4	H.s.	Adult(female)	Nov 15	06:40~

Table 3-17-4-Sheet 2. Results of “heat-coma” experiments and SCP (Super Cooling Point) measurement performed on adults of *Halobates germanus* (H.g.) and *H. sericeus* (H.s.); TA: temp. at which specimen adapted, SHCT: temp. at which semi-heat coma occurred; HCT: temp. at which heat coma occurred ; GTHC: gap temp. for heat coma (from base temp.); “Date and Time of Day” when experiments were performed. (MR-12-05-Leg 1: Nov. 5-Nov. 26, 2012), ITSCP: Increased temperature at SCP was detected; TD: Time of day when heat-paralysis experiment was performed

St.No.	Latitude	Longitude	Exp.No.	TA	SHCT	HCT	GTHC	SCP	ITSCP	Species	Stage (sex)	Date	TD
St. 1	13°59’N	149°16’E	3	29.5	37	38	8.5	-12.2	2.5	H.s.	Adult (female)	Nov 15	06:40~
St. 1	13°59’N	149°16’E	3	29.5	37	38	8.5	-10.2	3.4	H.s.	Adult(female)	Nov 15	06:40~
St. 1	13°59’N	149°16’E	3	29.5	38	38	8.5	-11.8	6.1	H.s.	Adult(female)	Nov 15	06:40~
St. 2	01°55’N	150°31’E	4	29.5	31	34	4.5	-18.7	4.4	H.g.	Adult (male)	Nov 16	06:35~
St. 2	01°55’N	150°31’E	4	29.5	31	36	6.5	-14.4	5.8	H.g.	Adult (male)	Nov 16	06:35~
St. 2	01°55’N	150°31’E	4	29.5	36	37	7.5	-14.8	7.0	H.g.	Adult(male)	Nov 16	06:35~
St. 2	01°55’N	150°31’E	4	29.5	32	38	8.5	-18.5	2.7	H.g.	Adult (female)	Nov 16	06:35~
St. 2	01°55’N	150°31’E	4	29.5	37	38	8.5	-11.4	3.3	H.g.	Adult (female)	Nov 16	06:35~
St. 2	01°55’N	150°31’E	4	29.5	38	38	8.5	-17.0	1.5	H.g.	Adult(female)	Nov 16	06:35~
St. 2	01°55’N	150°31’E	4	29.5	37	40	10.5	-17.7	2.7	H.g.	Adult (male)	Nov 16	06:35~
St. 2	01°55’N	150°31’E	4	29.5	39	40	10.5	-12.8	7.3	H.g.	Adult (female)	Nov 16	06:35~
St. 2	01°55’N	150°31’E	4	29.5	39	40	10.5	-11.9	7.1	H.g.	Adult (female)	Nov 16	06:35~
St. 2	01°55’N	150°31’E	4	29.5	38	40	10.5	- 13.0	2.8	H.g.	Adult(male)	Nov 16	06:35~
St. 2	01°55’N	150°31’E	4	29.5	41	41	11.5	-17.9	5.9	H.g.	Adult (male)	Nov 16	06:35~
St. 2	01°55’N	150°31’E	4	29.5	40	41	11.5	-15.2	0.5	H.g.	Adult (female)	Nov 16	06:35~
St. 2	01°55’N	150°31’E	5	29.5	31	31	1.5	-9.1	3.2	H.g.	Adult(female)	Nov 17	06:40~
St. 2	01°55’N	150°31’E	5	29.5	32	32	2.5	-16.5	6.2	H.g.	Adult (male)	Nov 17	06:40~
St. 2	01°55’N	150°31’E	5	29.5	33	33	3.5	-16.7	5.8	H.g.	Adult (male)	Nov 17	06:40~
St. 2	01°55’N	150°31’E	5	29.5	33	35	5.5	-11.7	5.6	H.g.	Adult (female)	Nov 17	06:40~
St. 2	01°55’N	150°31’E	5	29.5	35	37	7.5	-15.7	3.9	H.g.	Adult(female)	Nov 17	06:40~
St. 2	01°55’N	150°31’E	5	29.5	33	37	7.5	-10.9	4.7	H.g.	Adult (male)	Nov 17	06:40~
St. 2	01°55’N	150°31’E	5	29.5	37	37	7.5	-16.7	3.8	H.g.	Adult (male)	Nov 17	06:40~
St. 2	01°55’N	150°31’E	5	29.5	38	38	8.5	-13.0	6.4	H.g.	Adult (male)	Nov 17	06:40~
St. 2	01°55’N	150°31’E	5	29.5	37	39	9.5	-17.4	9.9	H.g.	Adult (female)	Nov 17	06:40~
St. 2	01°55’N	150°31’E	5	29.5	37	39	9.5	-	-	H.g.	Adult (female)	Nov 17	06:40~
St. 2	01°55’N	150°31’E	5	29.5	37	40	10.5	- 16.4	10.4	H.g.	Adult(female)	Nov 17	06:40~
St. 2	01°55’N	150°31’E	5	29.5	39	40	10.5	-16.8	2.6	H.g.	Adult (female)	Nov 17	06:40~
St. 2	01°55’N	150°31’E	6	30	31	31	1.0	-19.8	6.0	H.g.	Adult (male)	Nov 18	06:40~
St. 2	01°55’N	150°31’E	6	30	31	31	1.0	-11.6	3.5	H.g.	Adult (female)	Nov 18	06:40~
St. 2	01°55’N	150°31’E	6	30	31	31	1.0	-12.0	5.5	H.g.	Adult (male)	Nov 18	06:40~

Table 3-17-4-Sheet 3. Results of “heat-coma” experiments and SCP (Super Cooling Point) measurement performed on adults of *Halobates germanus* (H.g.) and *H. sericeus* (H.s.); TA: temp. at which specimen adapted, SHCT: temp. at which semi-heat coma occurred; HCT: temp. at which heat coma occurred ; GTHC: gap temp. for heat coma (from base temp.); “Date and Time of Day” when experiments were performed. (MR-12-05-Leg 1: Nov. 5-Nov. 26, 2012), ITSCP: Increased temperature at SCP was detected; TD: Time of day when heat-paralysis experiment was performed

St.No.	Latitude	Longitude	Exp.No.	TA	SHCT	HCT	GTHC	SCP	ITSCP	Species	Stage (sex)	Date	TD
St. 2	01°55’N	150°31’E	6	30	31	32	2.0	-11.7	3.9	H.g.	Adult (male)	Nov 18	06:40~
St. 2	01°55’N	150°31’E	6	30	32	32	2.0	-10.5	4.0	H.g.	Adult (female)	Nov 18	06:40~
St. 2	01°55’N	150°31’E	6	30	33	33	3.0	-06.5	3.7	H.g.	Adult (female)	Nov 18	06:40~
St. 2	01°55’N	150°31’E	6	30	32	33	3.0	-10.1	4.3	H.g.	Adult (male)	Nov 18	06:40~
St. 2	01°55’N	150°31’E	6	30	33	37	7.0	-20.9	9.4	H.g.	Adult (male)	Nov 18	06:40~
St. 2	01°55’N	150°31’E	6	30	33	37	7.0	-08.7	2.6	H.g.	Adult (female)	Nov 18	06:40~
St. 2	01°55’N	150°31’E	6	30	37	37	7.0	-10.7	0.9	H.g.	Adult (male)	Nov 18	06:40~
St. 2	01°55’N	150°31’E	6	30	37	37	7.0	-13.1	5.6	H.g.	Adult (female)	Nov 18	06:40~
St. 2	01°55’N	150°31’E	6	30	37	38	8.0	-15.4	6.8	H.g.	Adult (female)	Nov 18	06:40~
St. 2	01°55’N	150°31’E	7	29.5	31	37	7.5	-11.0	3.9	H.g.	Adult (male)	Nov 19	06:35~
St. 2	01°55’N	150°31’E	7	29.5	37	37	7.5	-10.8	2.0	H.g.	Adult (male)	Nov 19	06:35~
St. 2	01°55’N	150°31’E	7	29.5	32	38	8.5	-16.8	2.1	H.g.	Adult (female)	Nov 19	06:35~
St. 2	01°55’N	150°31’E	7	29.5	35	38	8.5	-13.2	0.2	H.g.	Adult (female)	Nov 19	06:35~
St. 2	01°55’N	150°31’E	7	29.5	38	38	8.5	-11.1	1.9	H.g.	Adult (female)	Nov 19	06:35~
St. 2	01°55’N	150°31’E	7	29.5	38	38	8.5	-12.3	8.9	H.g.	Adult (female)	Nov 19	06:35~
St. 2	01°55’N	150°31’E	7	29.5	38	38	8.5	-10.4	6.9	H.g.	Adult (male)	Nov 19	06:35~
St. 2	01°55’N	150°31’E	7	29.5	38	38	8.5	-11.6	3.9	H.g.	Adult(female)	Nov 19	06:35~
St. 2	01°55’N	150°31’E	7	29.5	38	38	8.5	-10.6	7.0	H.g.	Adult (male)	Nov 19	06:35~
St. 2	01°55’N	150°31’E	7	29.5	38	38	8.5	-12.6	1.6	H.g.	Adult (male)	Nov 19	06:35~
St. 2	01°55’N	150°31’E	7	29.5	38	38	8.5	-13.1	6.5	H.g.	Adult (male)	Nov 19	06:35~
St. 2	01°55’N	150°31’E	7	29.5	38	39	9.5	-13.3	4.0	H.g.	Adult (female)	Nov 19	06:35~
St. 2	01°55’N	150°31’E	8	29.5	33	34	4.5	-16.8	7.6	H.g.	Adult (female)	Nov 20	06:40~
St. 2	01°55’N	150°31’E	8	29.5	34	35	5.5	-17.5	9.1	H.g.	Adult (female)	Nov 20	06:40~
St. 2	01°55’N	150°31’E	8	29.5	35	37	7.5	-15.4	7.6	H.g.	Adult (female)	Nov 20	06:40~
St. 2	01°55’N	150°31’E	8	29.5	34	37	7.5	-15.2	5.0	H.g.	Adult(male)	Nov 20	06:40~
St. 2	01°55’N	150°31’E	8	29.5	37	37	7.5	-13.9	8.6	H.g.	Adult(male)	Nov 20	06:40~
St. 2	01°55’N	150°31’E	8	29.5	36	37	7.5	-09.4	4.4	H.g.	Adult (female)	Nov 20	06:40~
St. 2	01°55’N	150°31’E	8	29.5	37	37	7.5	-19.8	4.6	H.g.	Adult (male)	Nov 20	06:40~
St. 2	01°55’N	150°31’E	8	29.5	37	38	8.5	-09.9	6.6	H.g.	Adult (female)	Nov 20	06:40~
St. 2	01°55’N	150°31’E	8	29.5	37	38	8.5	-09.7	7.3	H.g.	Adult (male)	Nov 20	06:40~

Table 3-17-4-Sheet 4. Results of “heat-coma” experiments and SCP (Super Cooling Point) measurement performed on adults of *Halobates germanus* (H.g.) and *H. sericeus* (H.s.); TA: temp. at which specimen adapted, SHCT: temp. at which semi-heat coma occurred; HCT: temp. at which heat coma occurred ; GTHC: gap temp. for heat coma (from base temp.); “Date and Time of Day” when experiments were performed. (MR-12-05-Leg 1: Nov. 5-Nov. 26, 2012), ITSCP: Increased temperature at SCP was detected; TD: Time of day when heat-paralysis experiment was performed

St.No.	Latitude	Longitude	Exp.No.	TA	SHCT	HCT	GTHC	SCP	ITSCP	Species	Stage (sex)	Date	TD
St. 2	01°55’N	150°31’E	8	29.5	38	38	8.5	-10.7	7.4	H.g.	Adult (male)	Nov 20	06:40~
St. 2	01°55’N	150°31’E	8	29.5	39	39	9.5	-09.5	5.5	H.g.	Adult (male)	Nov 20	06:40~
St. 2	01°55’N	150°31’E	8	29.5	38	39	9.5	-11.2	6.7	H.g.	Adult (female)	Nov 20	06:40~
St. 2	01°55’N	150°31’E	9	29.5	32	32	2.5	-18.3	11.4	H.g.	Adult (female)*	Nov 21	06:40~
St. 2	01°55’N	150°31’E	9	29.5	32	33	3.5	-18.2	10.2	H.g.	Adult(male)	Nov 21	06:40~
St. 2	01°55’N	150°31’E	9	29.5	32	36	6.5	-09.0	0.7	H.g.	Adult(male)	Nov 21	06:40~
St. 2	01°55’N	150°31’E	9	29.5	36	36	6.5	-10.0	0.2	H.g.	Adult (male)	Nov 21	06:40~
St. 2	01°55’N	150°31’E	9	29.5	36	37	7.5	-16.4	3.0	H.g.	Adult (male)	Nov 21	06:40~
St. 3	26°18’S	165°36’E	10	30	31	31	1	-19.2	2.2	H.s.	Adult (male)	Nov 23	06:40~
St. 3	26°18’S	165°36’E	10	30	31	32	2	-14.6	5.1	H.s.	Adult (female)	Nov 23	06:40~
St. 3	26°18’S	165°36’E	10	30	32	32	2	-15.7	7.5	H.s.	Adult (female)	Nov 23	06:40~
St. 3	26°18’S	165°36’E	10	30	32	32	2	-12.1	6.2	H.s.	Adult (female)	Nov 23	06:40~
St. 3	26°18’S	165°36’E	10	30	32	32	2	-11.2	5.3	H.s.	Adult (male)	Nov 23	06:40~
St. 3	26°18’S	165°36’E	10	30	32	32	2	-11.8	6.4	H.s.	Adult (male)	Nov 23	06:40~
St. 3	26°18’S	165°36’E	10	30	32	33	3	-12.0	5.9	H.s.	Adult(male)	Nov 23	06:40~
St. 3	26°18’S	165°36’E	10	30	33	34	4	-17.5	0.3	H.s.	Adult (male)	Nov 23	06:40~
St. 3	26°18’S	165°36’E	10	30	34	35	5	-17.0	1.3	H.s.	Adult (female)	Nov 23	06:40~
St. 3	26°18’S	165°36’E	10	30	35	36	6	-15.6	7.2	H.s.	Adult (male)	Nov 23	06:40~
St. 3	26°18’S	165°36’E	10	30	36	36	6	-17.9	0.4	H.s.	Adult (female)	Nov 23	06:40~
St. 3	26°18’S	165°36’E	10	30	36	36	6	-12.3	0.3	H.s.	Adult (female)	Nov 23	06:40~
St. 3	26°18’S	165°36’E	11	29.5	31	31	1.5	-16.6	8.0	H.s.	Adult (female)	Nov 24	06:40~
St. 3	26°18’S	165°36’E	11	29.5	31	31	1.5	-17.7	11.5	H.s.	Adult (male)	Nov 24	06:40~
St. 3	26°18’S	165°36’E	11	29.5	32	32	2.5	-17.5	5.3	H.s.	Adult (female)	Nov 24	06:40~
St. 3	26°18’S	165°36’E	11	29.5	31	32	2.5	-15.7	8.8	H.s.	Adult (male)	Nov 24	06:40~
St. 3	26°18’S	165°36’E	11	29.5	32	32	2.5	-14.9	5.6	H.s.	Adult (female)	Nov 24	06:40~
St. 3	26°18’S	165°36’E	11	29.5	32	32	2.5	-14.3	9.2	H.s.	Adult (male)	Nov 24	06:40~
St. 3	26°18’S	165°36’E	11	29.5	32	32	2.5	-16.0	9.0	H.s.	Adult (male)	Nov 24	06:40~
St. 3	26°18’S	165°36’E	11	29.5	32	32	2.5	-16.6	9.9	H.s.	Adult (female)	Nov 24	06:40~

*Lack of femur and tarsus of left middle leg

Table 3-17-4-Sheet 5. Results of “heat-coma” experiments and SCP (Super Cooling Point) measurement performed on adults of *Halobates germanus* (H.g.) and *H. sericeus* (H.s.); TA: temp. at which specimen adapted, SHCT: temp. at which semi-heat coma occurred; HCT: temp. at which heat coma occurred ; GTHC: gap temp. for heat coma (from base temp.); “Date and Time of Day” when experiments were performed. (MR-12-05-Leg 1: Nov. 5-Nov. 26, 2012), ITSCP: Increased temperature at SCP was detected; TD: Time of day when heat-paralysis experiment was performed

St.No.	Latitude	Longitude	Exp.No.	TA	SHCT	HCT	GTHC	SCP	ITSCP	Species	Stage (sex)	Date	TD
St. 3	26°18’S	165°36’E	11	29.5	32	32	2.5	-15.8	7.1	H.s.	Adult (male)	Nov 24	06:40~
St. 3	26°18’S	165°36’E	11	29.5	32	33	3.5	-12.1	6.9	H.s.	Adult (female)	Nov 24	06:40~
St. 3	26°18’S	165°36’E	11	29.5	32	33	3.5	-11.2	4.3	H.s.	Adult (female)	Nov 24	06:40~
St. 3	26°18’S	165°36’E	11	29.5	32	33	3.5	-10.5	5.8	H.s.	Adult (male)	Nov 24	06:40~
St. 3	26°18’S	165°36’E	12	29.5	31	31	1.5	-17.7	6.1	H.s.	Adult (female)	Nov 25	06:40~
St. 3	26°18’S	165°36’E	12	29.5	32	32	2.5	-16.1	6.8	H.s.	Adult (female)	Nov 25	06:40~
St. 3	26°18’S	165°36’E	12	29.5	32	32	2.5	-15.0	7.9	H.s.	Adult (female)	Nov 25	06:40~
St. 3	26°18’S	165°36’E	12	29.5	33	33	3.5	-15.2	4.9	H.s.	Adult (female)	Nov 25	06:40~
St. 3	26°18’S	165°36’E	12	29.5	33	33	3.5	-19.4	8.4	H.s.	Adult (female)	Nov 25	06:40~
St. 3	26°18’S	165°36’E	12	29.5	32	34	4.5	-18.2	8.1	H.s.	Adult (male)	Nov 25	06:40~
St. 3	26°18’S	165°36’E	12	29.5	34	34	4.5	-14.3	8.7	H.s.	Adult (male)	Nov 25	06:40~
St. 3	26°18’S	165°36’E	12	29.5	35	35	5.5	-12.1	3.6	H.s.	Adult (female)	Nov 25	06:40~
St. 3	26°18’S	165°36’E	12	29.5	34	35	5.5	-19.7	6.2	H.s.	Adult (male)	Nov 25	06:40~
St. 3	26°18’S	165°36’E	12	29.5	34	35	5.5	-10.0	7.2	H.s.	Adult (male)	Nov 25	06:40~
St. 3	26°18’S	165°36’E	12	29.5	35	35	5.5	-10.4	6.8	H.s.	Adult (male)	Nov 25	06:40~
St. 3	26°18’S	165°36’E	12	29.5	35	35	5.5	-10.4	6.5	H.s.	Adult (male)	Nov 25	06:40~

.

Table 3-17-5-A. Comparison of Semi-Heat-Coma Temperature (SHCT), Heat Coma Temperature (HCT), Gap Temperature for Heat Coma (GTHC), Super-Cooling Temperature (SCP) and Increased Temperature at Super Coolig Point (ITSCP) between *Halobates germanus* and *H. sericeus.* Experiments were performed in the period of 13th Nov to 25th Nov, 2012 in the wet-lab. 2 of R/V Mirai during the cruise of MR-12-05-Leg1 [Mean±SD(n)]

1. Combined data of specimens collected in the Tropical Pacific Region at 14º00'N and 2º00'N (Station 1 & 2)

	SHCT	**HCT**	**GTHC**	**SCP**	**ITSCP**
H .germanus	35.5±2.8(63)	36.8±2.6(63)	7.2±2.7(63)	-13.6±3.3(62)	5.0±2.5(62)
H. sericeus	34.7±2.7(34)	37.1±2.0(34)	7.6±2.2(34)	-15.3±3.1(32)	4.2±2.1(32)
Total	35.2.±2.8(97)	36.9±2.4(97)	7.3±2.6(97)	-14.2±3.3(94)	4.7±2.4(94)
Mann-Whitney U-test between H. germanus and H. sericeus					
Z	*-1.488*	*-0.753*	*-0.758*	*-2.362*	*-1.505*
P	*0.137*	*0.452*	*0.448*	*0.018*	*0.132*

2. Data of specimens collected in the Temperate Pacific Region at 26º18'S (Station 3)

	SHCT	**HCT**	**GTHC**	**SCP**	**ITSCP**
H. sericeus	32.7±1.5(36)	33.1±1.5(36)	3.4±1.5(36)	-14.6±2.9(36)	6.1±2.7(36)
Mann-Whitney U-test between population at Station 1(2º00'N) and Station 3(26º18'S) in H. sericeus					
Z	*-3.356*	*-6.094*	*-6.056*	*-1.063*	*-3.447*
P	*0.001*	*<0.001*	*<0.001*	*0.288*	*0.001*

Table 3-17-5-B. Comparison of Semi-Heat-Coma Temperature (HSCT), Heat Coma Temperature (HCT), Gap Temperature for Heat Coma (GTHC), Super-Cooling Temperature (SCP) and Increased Temperature at Super Cooling Point (ITSCP) between females and males of the two species, *Halobates germanus* and *H.sericeus.* Experiments were performed in the period of 13th Nov to 25th Nov 2012 in the wet-lab. 2 of R/V Mirai during the cruise of MR-12-05-Leg 1 [Mean±SD(n)]

1. Combined data of specimens collected in the Tropical Pacific Region at 14º00'N and 2º00'N (Station 1 & 2)

Adult stage	**SHCT**	**HCT**	**GTHC**	**SCP**	**ITSCP**
Females	35.2±2.7(62)	37.2±2.4(62)	7.6±2.5(62)	-14.4±3.2(59)	4.5±2.4(59)
Males	35.3±3.0(35)	36.5±2.5(35)	6.9±2.6(35)	-13.9±3.5(35)	5.1±2.4(35)
Total	35.2±2.8(97)	36.9±2.4(97)	7.3±2.6(97)	-14.2±3.3(94)	4.7±2.4(94)
Mann-Whitney U-test between females and males					
Z	*-0.004*	*-1.989*	*-1.904*	*-1.005*	*-1.467*
P	*0.997*	*0.047*	*0.057*	*0.315*	*0.142*

2. Data of specimens collected in the Temperate Pacific Region at 26º18'S (Station 3)

Adult stage	**SHCT**	**HCT**	**GTHC**	**SCP**	**ITSCP**
Females	32.7±1.6(18)	32.9±1.6(18)	3.2±1.5(18)	-15.2±2.4(18)	5.5±2.7(18)
Males	32.7±1.4(18)	33.2±1.6(18)	3.6±1.6(18)	-13.9±3.2(18)	6.8±2.5(18)
Total	32.7±1.5(36)	33.1±1.5(36)	3.4±1.5(36)	-14.6±2.9(36)	6.1±2.7(36)
Mann-Whitney U-test between females and males					
Z	*-0.185*	*-0.623*	*-0.609*	*-1.488*	*-1.646*
P	*0.853*	*0.533*	*0.543*	*0.137*	*0.100*

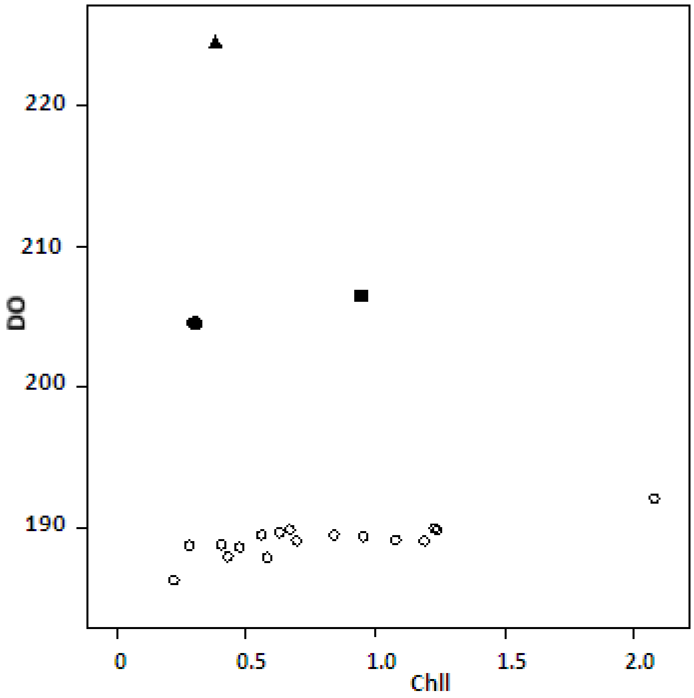

Fig.3-17-1 : Relationship between dissolved oxygen (µmol/kg) and chlorophyll (relative fluorescent value) contents in surface sea water. Open circles: at the fixed station, 8°00'S, 80°30'E in the Indian Ocean during the cruise, MR-11-07; solid circle: 13°59'N, 149°16'E, solid square: 01°55'N, 150°31'E and solid triangle: 26°19'S, 165°34'E in the Pacific Ocean during the cruise, MR-12-05-Leg 1. An extremely high density of about 100,000 individuals per 1km^2 of oceanic sea skaters mainly *Halobates germanus* can be related to the relatively high scores of chlorophyll (solid square).

.

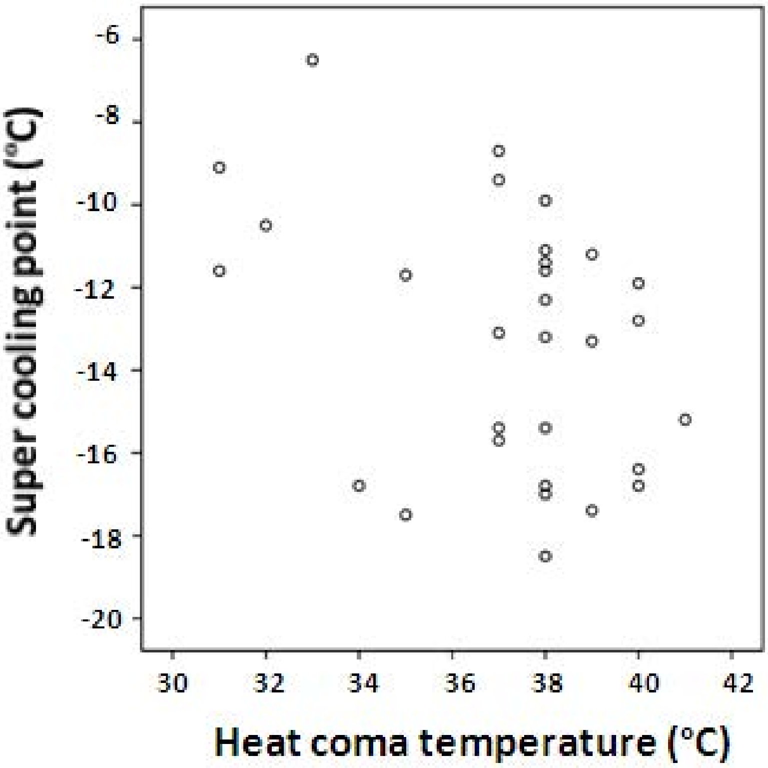

Fig. 3-17-2: Correlative analysis of super-cooling point (SCP) and heat coma temperature. Data on the female specimens of *Halobates germanus* collected at Station 2 (2º00'N, 150º30'E) . A significant negative correlation was shown (Pearson's correlation test: r=-0.378, p=0.039, n=30).

.

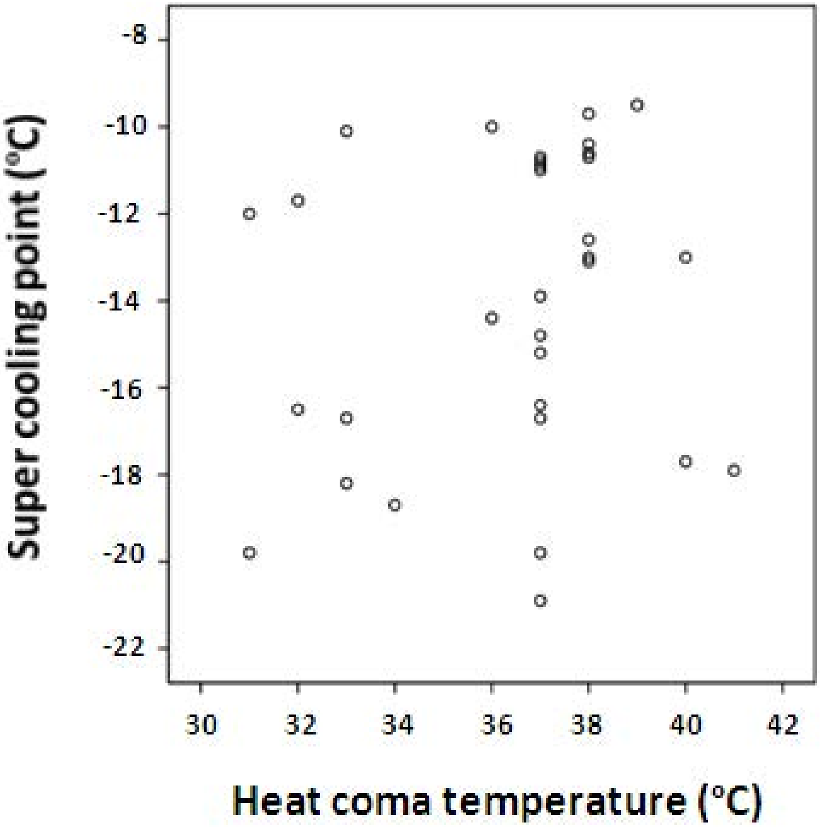

Fig. 3-17-3: Correlative analysis of super-cooling point (SCP) and heat coma temperature. Data on the male specimens of *Halobates germanus* collected at Station 2 (2º00'N, 150º30'E) . A significant negative correlation was shown (Pearson's correlation test: r=-0.177, p=0.332, n=32).

.

Photo 1: A trailing scene of Neuston-NET

Photo 2: Washing the sample bottle so called the “pants” of the Neuston net just after the trailing to collect all the *Halobates* individuals into the round-shaped transparent aquarium.

.

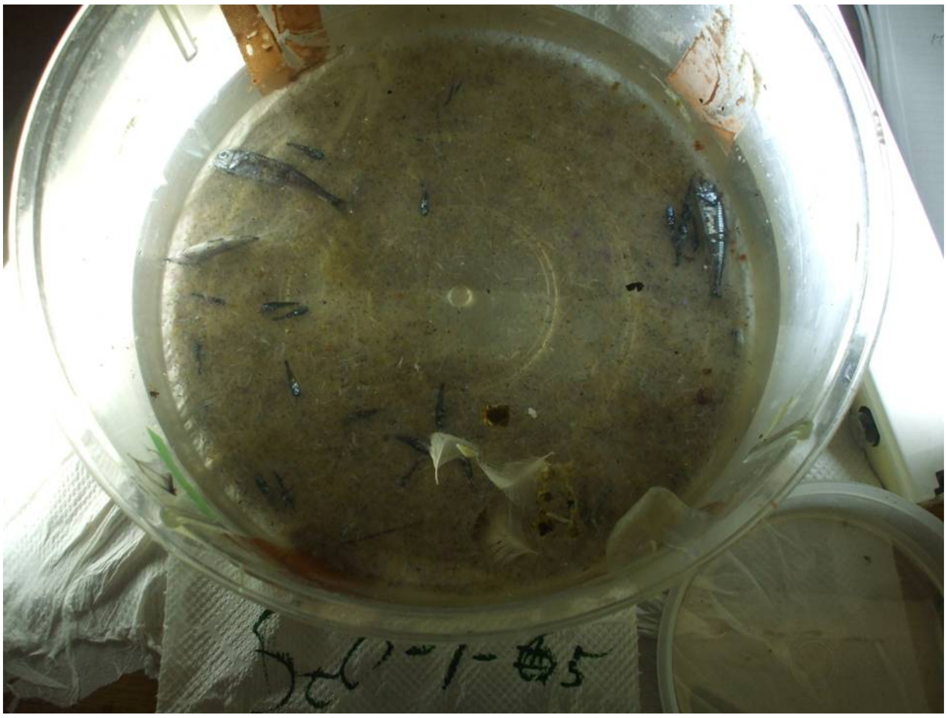

Photo 3: An example of the sample of Neuston-NET trailing

3.18 LADCP

(1) Personnel

Shinya Kouketsu (JAMSTEC)
Hiroshi Uchida (JAMSTEC)
Katsurou Katsumata (JAMSTEC)
Toshimasa Doi (JAMSTEC)

(2) Overview of the equipment

An acoustic Doppler current profiler (ADCP) was integrated with the CTD/RMS package. The lowered ADCP (LADCP), Workhorse Monitor WHM300 (Teledyne RD Instruments, San Diego, California, USA), which has 4 downward facing transducers with 20-degree beam angles, rated to 6000 m. The LADCP makes direct current measurements at the depth of the CTD, thus providing a full profile of velocity. The LADCP was powered during the CTD casts by a 50.4 volts expendable Alkali battery pack. The LADCP unit was set for recording internally prior to each cast. After each cast the internally stored observed data was uploaded to the computer on-board. By combining the measured velocity of the sea water and bottom with respect to the instrument, and shipboard navigation data during the CTD cast, the absolute velocity profile can be obtained (e.g., Visbeck, 2002).

The instrument used in this cruise were Teledyne RD Instruments, WHM300(S/N 183240).

(3) Data collection

In this cruise, data were collected with the following configuration.

Bin size: 4 m
Number of bins: 25
Pings per ensemble: 1
Ping interval: 1 sec

(4) Data collection problems

Echo intensities are sufficiently high along the section (Fig. 3-18-1), except at the stations of 9. Since the weak echo were observed for all the beams, the weakness was not due to the instrument problem.

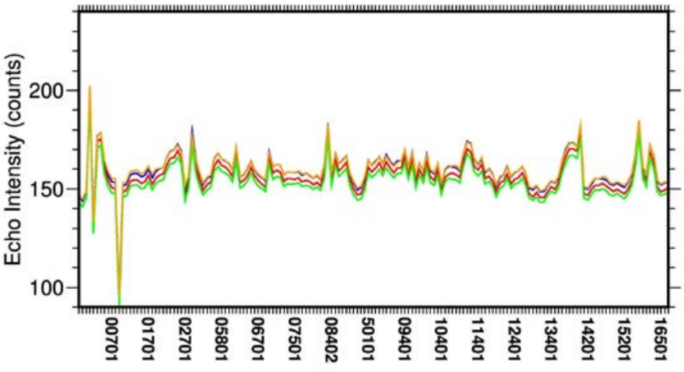

Fig. 3-18-1. Cast-averaged echo intensities at the first bin. Red, blue, green and orange denote beam 1, 2, 3, and 4 respectively.

(4) Data process

Vertical profiles of velocity are obtained by the inversion method (Visbeck, 2002). Since the first bin from LADCP is influenced by the turbulence generated by CTD frame, the weight for the inversion is set to 0.1. GPS navigation data and the bottom-track data are used in the calculation of the reference velocities. Shipboard ADCP data averaged for 1 minute are also included in the calculation. The CTD data are used for the sound speed and depth calculation. The directions of velocity are corrected using the magnetic deviation estimated with International Geomagnetic reference field data.

However, the inversion method doesn’t work well due to no-good velocity data due to the instrument problems as well as weak echo intensity at deep layers. We again plan to process carefully after the cruise.

Reference

Visbeck, M. (2002): Deep velocity profiling using Lowered Acoustic Doppler Current Profilers: Bottom track and inverse solutions. *J. Atmos. Oceanic Technol.*, 19, 794-807.

.

3.19 XCTD

(1) Personnel

H*iroshi Uchida (JAMSTEC)*
Soichiro Sueyoshi (GODI) (Legs 1 and 3)
Koichi Inagaki (GODI) (Legs 1 and 3)
Kazuho Yoshida (GODI) (Leg 2)
Shinya Okumura (GODI) (Leg 2)
Masanori Murakami (GODI) (Leg 2)
Katsuhisa Maeno (GODI) (Leg 3)

(2) Objectives

In this cruise, XCTD (eXpendable Conductivity, Temperature and Depth profiler) measurements were carried out to evaluate the fall rate equation and temperature by comparing with CTD (Conductivity, Temperature and Depth profiler) measurements, and to substitute for CTD measurements.

(3) Instrument and Method

The XCTDs used were XCTD-1, XCTD-2 and XCTD-4 (Tsurumi-Seiki Co., Ltd., Yokohama, Kanagawa, Japan) with an MK-150N deck unit (Tsurumi-Seiki Co., Ltd.). The manufacturer's specifications are listed in Table 3.19.1. In this cruise, the XCTD probes were deployed by using 8-loading automatic launcher or hand launcher (Tsurumi-Seiki Co., Ltd.). For comparison with CTD, XCTD was deployed at about 10 minutes after the beginning of the down cast of the CTD (999_C02, 999_C03, P14S_25, S04_402, S04I_166, and S04I_167).

The fall-rate equation provided by the manufacturer was used to infer depth Z (m), $Z = at - bt^2$, where t is the elapsed time in seconds from probe entry into the water, and a (terminal velocity) and b (acceleration) are the empirical coefficients (Table 3.19.2).

(4) Data Processing and Quality Control

The XCTD data were processed and quality controlled based on a method by Uchida et al. (2011). Differences between XCTD and CTD depths were shown in Fig. 3.19.1. The terminal velocity error was estimated for the XCTD-2 and for the XCTD-4 (Table 3.19.2). Difference of temperature on pressure surfaces were examined by using side-by-side XCTD and CTD data (Fig. 3.19.2). The XCTD data were corrected for the depth error by using the estimated terminal velocities. Average thermal bias below 400 dbar was 0.009 °C. Mean of the thermal biases of XCTD data estimated from four cruises was 0.015 ± 0.004 °C (Table 3.19.3). The mean thermal bias (0.015 °C) was corrected for the XCTD data obtained in this cruise. Difference of salinity on reference temperature surfaces were examined by using neighboring CTD data (Table 3.19.4). The estimated salinity biases were corrected for the XCTD data (Fig. 3.19.3) except for the XCTD data obtained at 999_326 and 999_329, because neighboring CTD data was not available in this cruise.

.

Reference

Kizu, S., H. Onishi, T. Suga, K. Hanawa, T. Watanabe, and H. Iwamiya (2008): Evaluation of the fall rates of the present and developmental XCTDs. *Deep-Sea Res I*, **55**, 571–586.

Uchida, H., K. Shimada, and T. Kawano (2011): A method for data processing to obtain high-quality XCTD data. *J. Atmos. Oceanic Technol.*, **28**, 816–826.

Uchida, H., A. Murata, and T. Doi (2013): WHP P10 Revisit in 2011 Data Book (in prep.).

Table 3.19.1. Manufacturer's specifications of XCTD-1, XCTD-2 and XCTD-4.

Parameter	Range	Accuracy
Conductivity	0 ~ 60 mS cm^{-1}	±0.03 mS cm^{-1}
Temperature	–2 ~ 35 °C	±0.02 °C
Depth	0 ~ 1000 m (for XCTD-1) 0 ~ 1850 m (for XCTD-2 and XCTD-4)	5 m or 2%, whichever is greater *

* Depth error is shown in Kizu et al (2008).

Table 3.19.2. Manufacturer's coefficients for the fall-rate equation.

Model	*a* (terminal velocity, m/s)	*b* (acceleration, m/s^2)	*e* (terminal velocity error, m/s)
XCTD-1	3.42543	0.00047	not estimated
XCTD-2	3.43898	0.00031	–0.0239
XCTD-4	3.68081	0.00047	–0.0075

Table 3.19.3. Thermal biases of the XCTD temperature data.

Cruise	Average thermal bias (°C)	Depth range	Source
MR09-01	0.016	>= 1100 dbar	Uchida et al. (2011)
KH-02-3	0.019	>= 1100 dbar	Uchida et al. (2011)
MR11-08	0.014	>= 1100 dbar	Uchida et al. (2013)
MR12-05	0.009	>= 400 dbar	This report

Mean 0.015 ± 0.004

Table 3.19.4. Salinity biases of the XCTD data.

XCTD station	Salinity bias	Reference temperature (°C)	Reference salinity	Reference CTD stations
999_C02	0.007	2.3	34.6251	999_C02
999_C03	0.018	2.3	34.6293	999_C03
P14S_25	0.001	0.9	34.7122	*1
S04_401	0.001	0.9	34.7122	*1
S04_402	0.001	0.9	34.7122	*1
S04_403	–0.006	0.9	34.7122	*1
S04_405	–0.009	0.9	34.7122	*1
S04_407	–0.009	0.9	34.7122	*1
S04_409	0.004	0.9	34.7122	*1
S04_411	–0.003	0.9	34.7122	*1
999_C04	0.017	1.2	34.7279	999_C04
S04I_166	–0.015	0.9	34.7065	S04I_166, S04I_167
S04I_167	–0.021	0.9	34.7065	S04I_166, S04I_167

*1: P14S_25, P14S_27, S04_50, S04_402, S04_404, S04_406, S04_408, S04_410

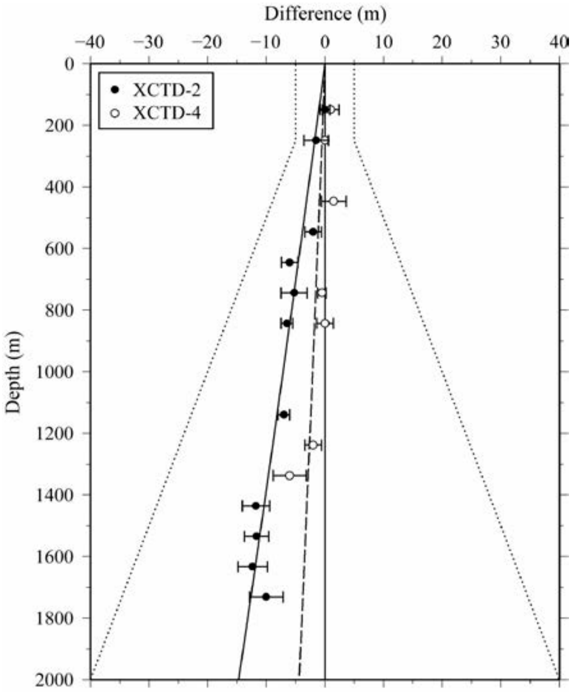

Figure 3.19.1. Differences between XCTD and CTD depths for XTD-2 and XCTD-4. Differences were estimated with the same method as Uchida et al. (2011). Standard deviation of the estimates (horizontal bars) and the manufacturer's specification for XCTD depth error (dotted lines) are shown. The regressions for the XCTD-2 data (solid line) and for the XCTD-4 data (broken line) are also shown.

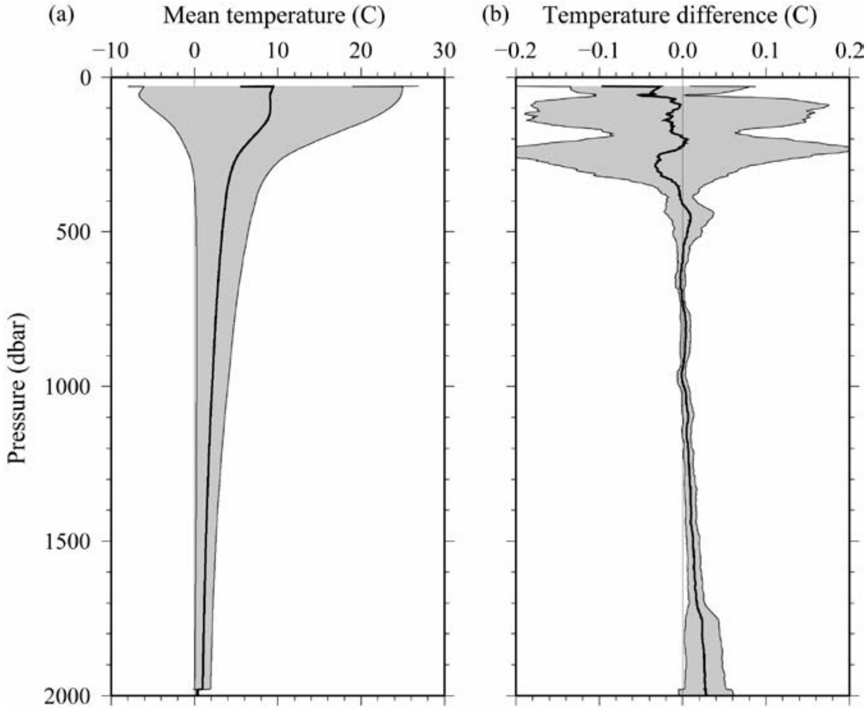

Figure 3.19.2. Comparison between XCTD and CTD temperature profiles. (a) Mean temperature files of CTD profiles with standard deviation (shade) and (b) mean temperature difference with standard deviation (shade) between the XCTD and CTD. Mean profiles were low-pass filtered by a running mean with a window of 51 dbar.

.

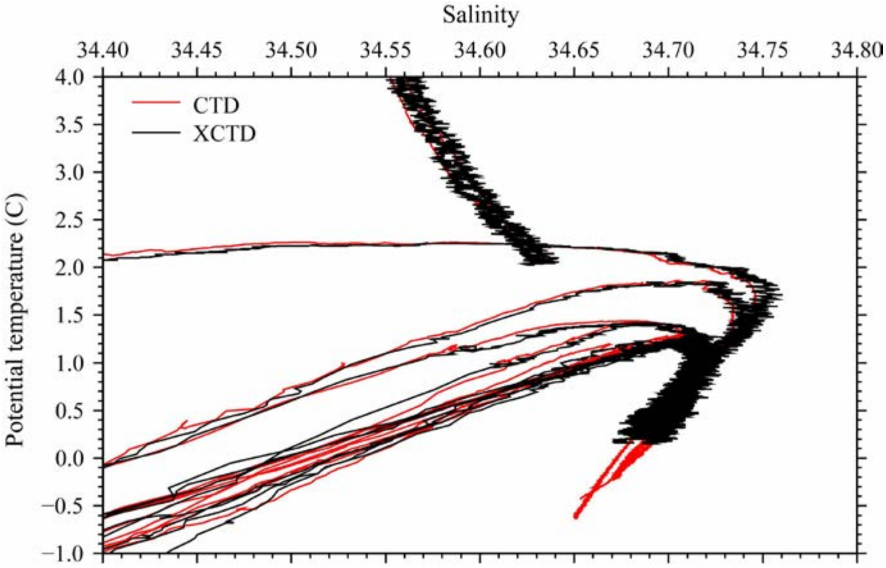

Figure 3.19.3. Comparison of temperature-salinity profiles of CTD (red lines) data used for the XCTD salinity bias estimation and salinity bias-corrected XCTD (black lines) data.

.

3.20. Expendable Microstructure Profiler

(1) Personnel

K. Katsumata (JAMSTEC)

(2) Objectives

Turbulence mixing in the ocean has been a difficult quantity to measure directly despite its important role in the ocean energy budget and general circulation dynamics. Recent improvements on materials such as optic fibre and on sensors such as high precision shear sensors now enable the measurement using expendable microstructure profilers (XMP).

(3) Apparatus

XMP probe and its tow frame were manufactured by Rockland Scientific International, Canada. The expendable sensor has a cylindrical shape with the length of about 152 cm and a diameter of 18 cm. Two shear sensors, one temperature sensor, a pressure sensor, and an accelerometer are mounted on the deeper tip of the cylinder. The tail is fringed with plastic drag brushes to stabilise its drop rate.

The shear sensors measure the shear at a 2.5×10^{-3} s^{-1} rms resolution. Least squares fit of the shear spectrum to the Nasmyth theoretical curve yields an estimate of the turbulent kinetic energy dissipation rate. The instrument oscillation is measured by the accelerometer and corrected during the spectrum estimation

Mirai's A-frame was used to deploy the prove attached to the tow frame. The prove was released underwater. The measured data were transmitted to the deck PC through an optic fibre. Twlelve kilometre of the fibre on a spool was used and the fibre freely came off the spool as the prove descended underwater. The fall rate was about 0.8 m/s initially but slowed down to less than 0.5 m/s at 2000 dbar as more fibre was dragged in the water. The fibre spool was mounted underwater (about 10 m depth) in a tow frame which was towed from the stern of the vessel. The vessel travelled no faster than 2 knots *relative to water.*

The turbulent kinetic energy dissipation rate ϵ was estimated by

$$\varepsilon=\frac{15}{2}\nu\overline{u_z^2}\ ,$$

where ν is the kinematic molecular viscosity of water and u_z is the vertical derivative of the horizontal velocity and the overbar denotes a spatial or ensemble averaging. Detailed description of the principle and sensors can lsbe found in Lueck *et al.*, (2002).

(4) Deployments

Six probes were deployed at six different CTD stations right after the CTD cast. Two were deployed within an area where, at the time of writing, a problem was detected in foreign clearance request documents, hence the data are not disclosed.

.

The detail of other deployments are shown below. The year is 2012.

S/N	Latitude	Longitude	Depth	Start (UT)	End (UT)
30	58-01.52°S	173-59.97°E	5201 m	6 Dec 13:06	6 Dec 14:47
31	58-30.33°S	173-58.98°E	5005 m	6 Dec 20:42	7 Dec 00:11
28	62-45.99°S	172-12.97°E	4264 m	9 Dec 05:34	9 Dec 05:37
26	63-59.72°S	171-07.46°E	2557 m	9 Dec 20:55	9 Dec 22:23

(5) Results

The realtime pressure reading indicated that Serial Number (SN) 31 and 26 survived to the sea bottom. SN 30 and 28 lost connection at about 2500 dbar and 30 dbar, respectively. Figs 3.20.1 shows the vertical distribution of the eddy kinetic energy dissipation rate, tentatively estimated by quick_look_XMP.m in the ODAS library. The method for estimating the dissipation rate follows that of Lueck *et al.* (2002).

References

Lueck, R.G., F. Wolk, and H. Yamazaki (2002) Oceanic Velocity Microstructure Measurements in the 20th Century. Journal of Oceanography 58, 153-174.

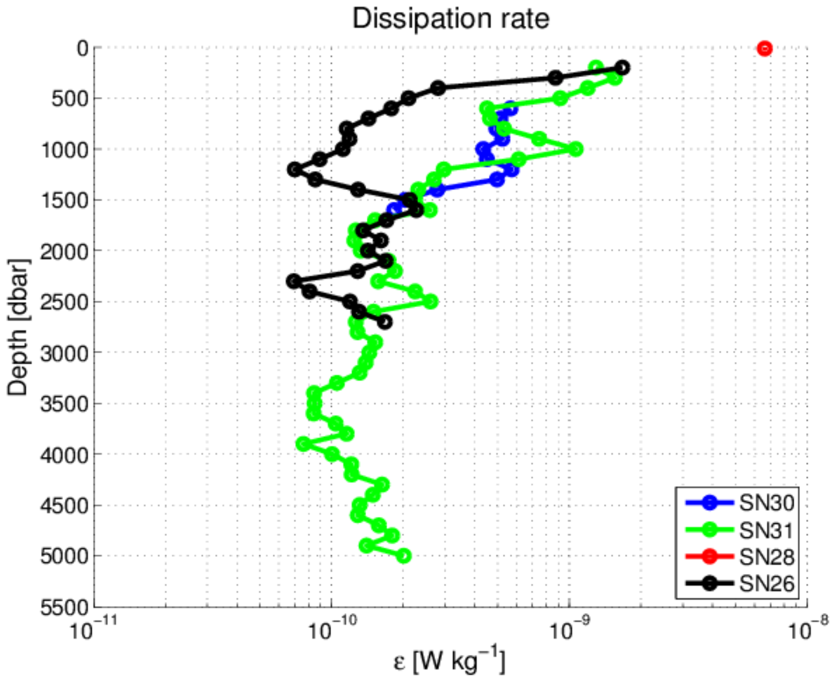

Fig. 3.20.1 Kinetic energy dissipation rate estimated at intervals of 100-300 dbar, 200-400 dbar and so forth using quick_look_XMP.m in the ODAS library. Out of two sensors, the one which produced smaller dissipation estimate was plotted.

4. Floats, Drifters, and Moorings

4.1 Argo floats

(1) Personnel

Toshio Suga	***(JAMSTEC/RIGC): Principal Investigator (not on board)***
Shigeki Hosoda	***(JAMSTEC/RIGC): not on board***
Taiyo Kobayashi	***(JAMSTEC/RIGC): not on board***
Mizue Hirano	***(JAMSTEC/RIGC): not on board***
Tatsuya Tanaka	***(MWJ): Chief Technical Staff (Operation Leader Leg.1)***
Tomonori Watai	***(MWJ): Technical Staff (Leg.1)***
Tomoyuki Takamori	***(MWJ): Chief Technical Staff (Operation Leader Leg.2)***
Naoko Takahashi	***(MWJ): Technical Staff (Leg.2)***

(2) Objectives

North Pacific

The objective of deployment is to clarify the structure and temporal/spatial variability of water masses in the North Pacific such as North Pacific Tropical Water in the subtropical North Pacific.

The profiling floats launched in this cruise measure vertical profiles of temperature and salinity automatically every ten days. As the vertical resolution of the profiles is very fine, the structure and variability of the water mass can be displayed well. Therefore, the profile data from the floats will enable us to understand the variability and the formation mechanism of the water mass.

Southern Ocean

The objective of deployment is to observe (seasonal) variation of Antarctic Bottom Water (AABW) formed off the coast of Adelie Coast, Antarctica and to detect its signal transferred into the Pacific Basins with deep floats newly developed.

The profiling floats launched in this cruise measure vertical profiles of temperature and salinity automatically every ten days. As the vertical resolution of the profiles is very fine, the structure and variability of the water mass can be displayed well. Therefore, the profile data from the floats will enable us to understand the variability and the formation mechanism of the water mass.

(3) Parameters

- water temperature, salinity, and pressure

(4) Methods

i. Profiling float deployment

North Pacific

We launched Arvor floats manufactured by nke. These floats equip a SBE41cp CTD sensor manufactured by Sea-Bird Electronics Inc.

The floats usually drift at a depth of 1000 dbar (called the parking depth), diving to a depth of 2000 dbar and rising up to the sea surface by decreasing and increasing their volume and thus changing the buoyancy in ten-day cycles. During the ascent, they measure temperature, salinity, and pressure. They stay at the sea surface for approximately nine hours, transmitting the CTD data to the land via the ARGOS system, and then return to the parking depth by decreasing volume. The status of floats and their launches are shown in Table 4.1.1.

Southern Ocean

We launched Deep NINJA floats newly developed by Tsurumi Seiki Co. Ltd. and JAMSTEC. These floats equip a SBE41cp CTD sensor manufactured by Sea-Bird Electronics Inc.

The floats usually drift at a depth of 1000 dbar (called the parking depth), diving to a depth of 4000 dbar or 2000 dbar and rising up to the sea surface by decreasing and increasing their volume and thus changing the buoyancy in ten-day cycles. During the ascent, they measure temperature, salinity, and pressure. They stay at the sea surface for approximately one hour, transmitting the CTD data to the land via the Iridium Short Burst Data survice, and then return to the parking depth by decreasing volume. The status of floats and their launches are shown in Table 4.1.2.

Table 4.1.1 Status of floats deployed in the North Pacific and their launches

Float (2000dbar)

Float Type	Arvor float manufactured by nke.
CTD sensor	SBE41cp manufactured by Sea-Bird Electronics Inc.
Cycle	10 days (approximately 9 hours at the sea surface)
ARGOS transmit interval	30 sec
Target Parking Pressure	1000 dbar
Sampling layers	115 (2000,1950,1900,1850,1800,1750,1700,1650,1600,1550,1500, 1450, 1400, 1350, 1300, 1250, 1200, 1150, 1100, 1050, 1000, 980, 960, 940, 920, 900, 880, 860, 840, 820, 800, 780, 760, 740, 720, 700, 680, 660, 640, 620, 600, 580, 560, 540, 520, 500, 490, 480, 470, 460, 450, 440, 430, 420, 410, 400, 390, 380, 370, 360, 350, 340, 330, 320, 310, 300, 290, 280, 270, 260, 250, 240, 230, 220,210, 200, 195, 190, 185, 180, 175, 170, 165, 160, 155, 150, 145, 140, 135, 130, 125, 120, 115, 110, 105, 100, 95, 90, 85, 80, 75, 70, 65, 60, 55, 50, 45, 40, 35, 30, 25, 20, 15, 10, 4 or surface dbar)

Launches

Float S/N	ARGOS ID	Date and Time of Reset (UTC)	Date and Time of Launch(UTC)	Location of Launch	WMO ID	CTD St. No.
11029	**112258**	**2012/11/12 06:43**	**2012/11/12 07:44**	**14-00.21[N] 149-15.77[E]**	5904211	C01
11026	**112255**	**2012/11/12 22:52**	**2012/11/12 23:38**	**12-00.13[N] 149-50.82[E]**	5904212	C02
11027	**112256**	**2012/11/13 10:02**	**2012/11/13 10:57**	**10-00.31[N] 150-26.62[E]**	5904213	C03

.

Table 4.1.2 Status of floats deployed in the Southern Ocean and their launches

Float (4000dbar)

Float Type	Deep NINJA manufactured by Tsurumi Seiki Co. Ltd.
CTD sensor	SBE41cp manufactured by Sea-Bird Electronics Inc.
Cycle	10 days (approximately one hour at the sea surface)
Method of data transmit	Iridium Short Burst Data survice
Target Parking Pressure	1000 dbar
Sampling layers	400 (Deepest, 20 dbar interval between 4000 dbar and 2000 dbar, 10 dbar interval between 2000 dbar and 1000 dbar, 5 dbar interval between 1000 dbar and 4 or surface dbar)

Launches

Float S/N	IMEI ID	Date and Time of Reset (UTC)	Date and Time of Launch (UTC)	Location of Launch	WMO ID	CTD St. No.
0004	**300234011980570**	**2012/12/5 21:54**	**2012/12/5 23:29**	**56-59.87 [S]** **173-59.31 [E]**	TBD	11
0006	**300234011988560**	**2012/12/16 09:20**	**2012/12/16 10:20**	**62-45.73 [S]** **143-36.05 [E]**	TBD	62
0005	**300234011981560**	**2012/12/17 15:34**	**2012/12/17 16:33**	**62-00.38 [S]** **137-00.42 [E]**	TBD	67
0003	**300234010565570**	**2012/12/19 04:12**	**2012/12/19 05:42**	**60-00.62 [S]** **139-56.12 [E]**	TBD	C04

(5) Data archive

The real-time data are provided to meteorological organizations, research institutes, and universities via Global Data Assembly Center (GDAC: http://www.usgodae.org/argo/argo.html, http://www.coriolis.eu.org/) and Global Telecommunication System (GTS), and utilized for analysis and forecasts of sea conditions.

The data observed by the Deep NINJA floats will be provided as soon as its technical issues on the data decoding are resolved.

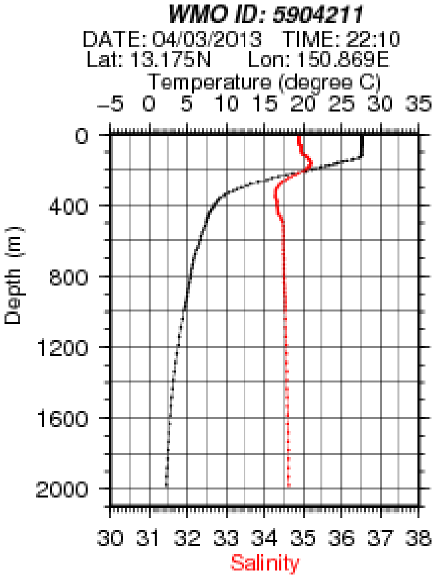
WMO ID: 5904211
DATE: 04/03/2013 TIME: 22:10
Lat: 13.175N Lon: 150.869E

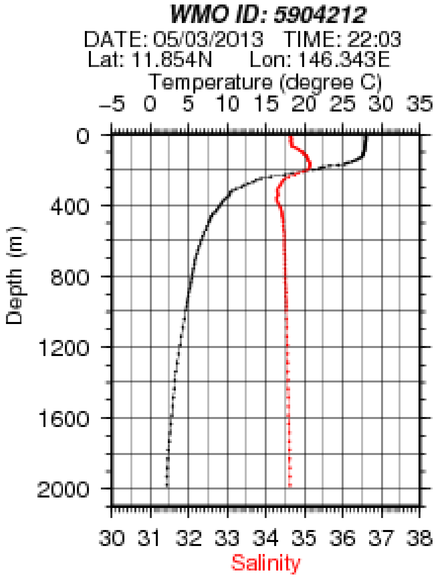
WMO ID: 5904212
DATE: 05/03/2013 TIME: 22:03
Lat: 11.854N Lon: 146.343E

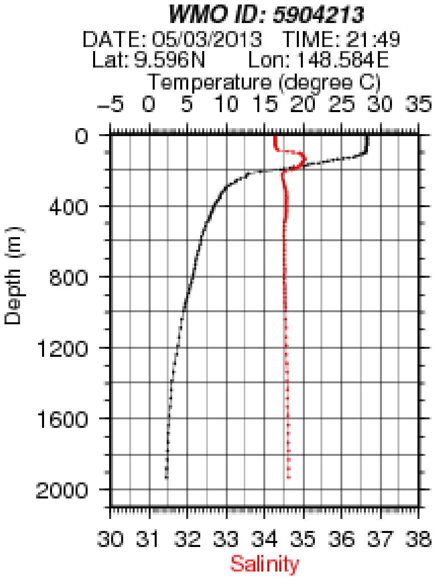
WMO ID: 5904213
DATE: 05/03/2013 TIME: 21:49
Lat: 9.596N Lon: 148.584E

.

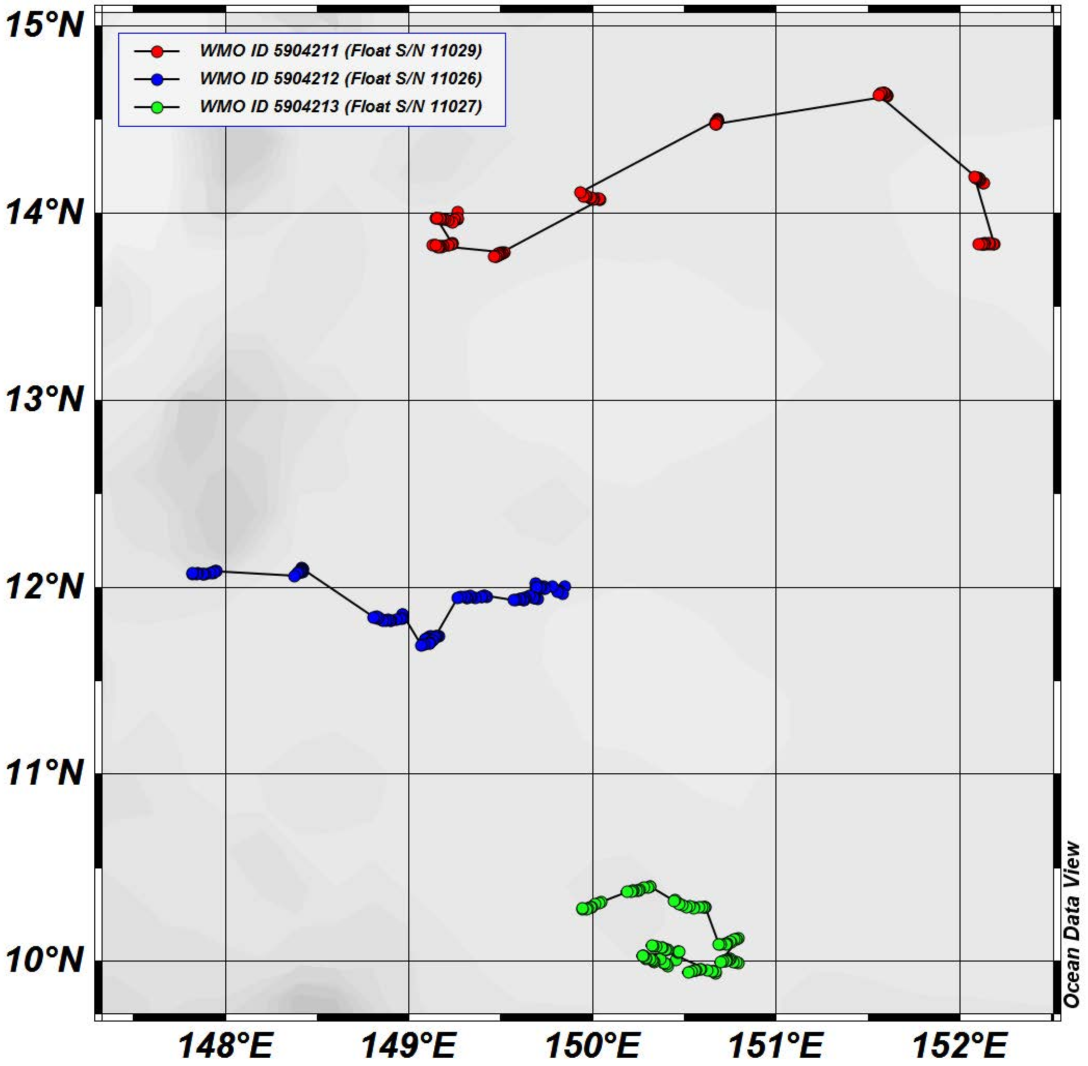

Fig. 4.1.1. The profile and trajectory of the float launched during MR12-05 (North Pacific).

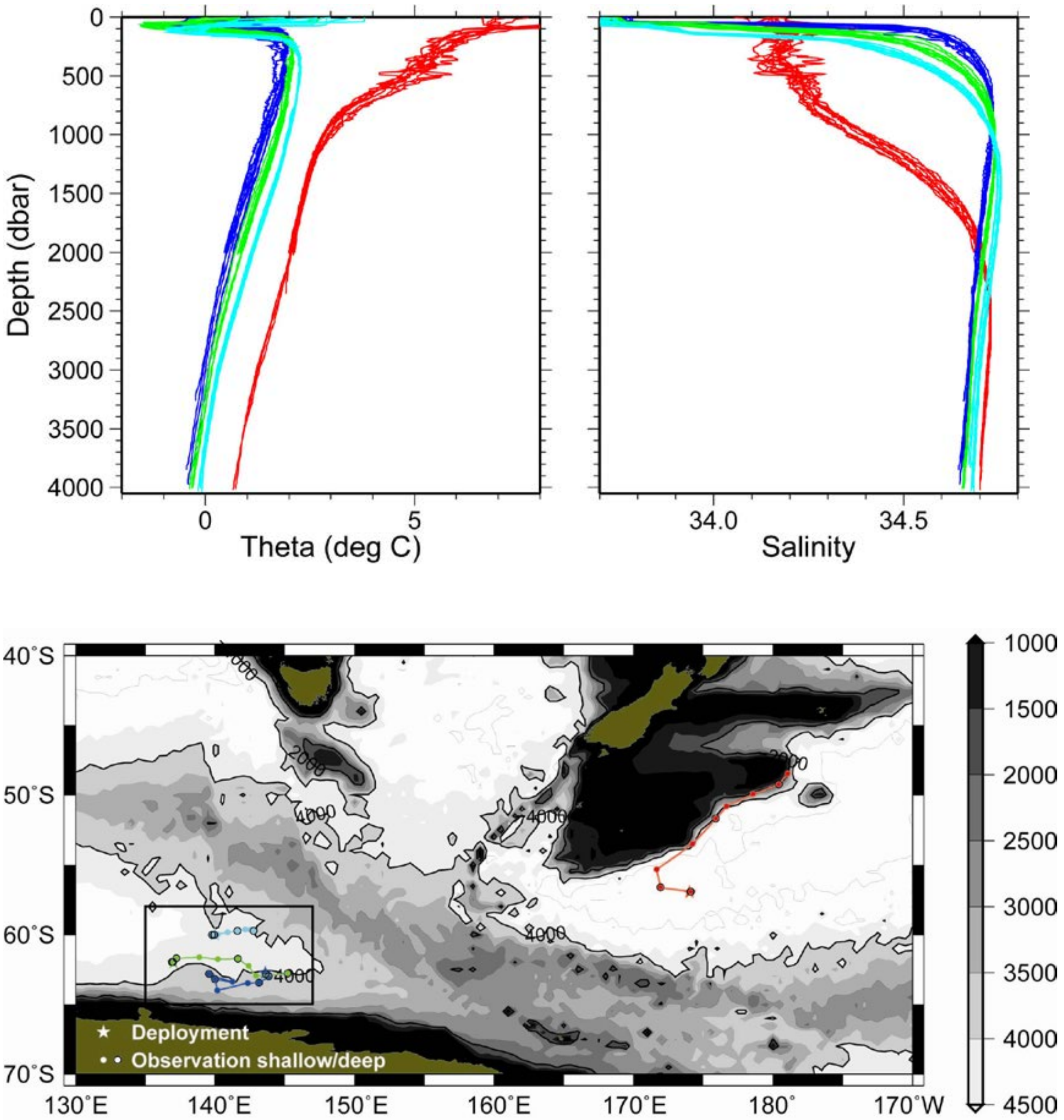

Fig. 4.1.2. The profile and trajectory of the float launched during MR12-05 (Southern Ocean).

(6) Preliminary results

Deep NINJA, which was developed by JAMSTEC and Tsurumi Seiki Co. Ltd. recently, is the first practical float for deeper ocean than 2000m depth. The small fleet of three floats deployed off the Adelie Coast has directly observed the Antarctic Bottom Water located in the deeper layers than 3000 m depth. The float observations, the salinity biases by up to 0.01 of which were corrected, are almost consistent with the CTD observations conducted by R/V Mirai.

Compared with the historical observations carried out near the deployed region including the high quality data obtained under WOCE and Repeat Hydrography Program, warmer and fresher AABW was observed by the floats. The warming and freshening trends seem to be continued since the 1970s, at least, and their rates could be accelerated recently.

.

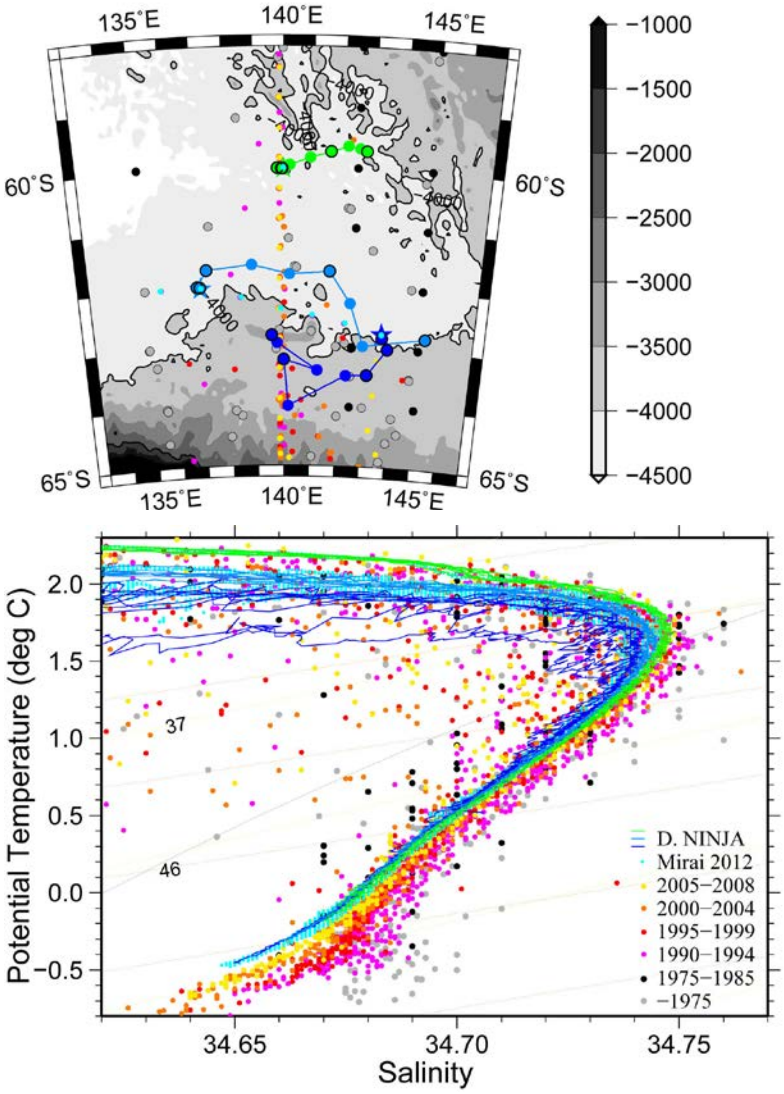

Fig. 4.1.3. Float measurements compared with the historical observations conducted near the deployed region. The salinity of float measurements was corrected with that of R/V Mirai's CTD profiles in the potential temperature around 0.5-1.2 degree C.

.

4.2 Southern Ocean flux mooring (Recovery of the Southern Ocean buoy)

(1) Personnel

Shoichiro Baba (JAMSTEC)
Tomohide Noguchi (MWJ)
Tomoyuki Takamori (MWJ)
Shinsuke Toyoda (MWJ)
Tatsuya Tanaka (MWJ)
Rei Ito (MWJ)
Shungo Oshitani (MWJ)
Eitaro Matsumoto (MWJ)

(2) Objectives

The ocean off the Antarctic Continent coast is a region of cold, heavy Antarctic bottom water formation. It supplies bottom and deep water to oceans around the world, and it is an atmosphere-heating region as it releases large volumes of heat to the atmosphere in the course of deep-water formation. Changes in the deep-water configuration are closely related to the phenomena of global warming and other climate changes. Deployment off the Adelie Coast of moored surface buoys capable of measuring air-sea flux in these waters would be ideal for verification of events and hypotheses that have been derived from ship-borne observations in the Antarctica coastal regions and related data analysis. Establishment of a continuous meteorological observation network is also regarded as highly desirable by the Southern Ocean Observation System (SOOS) and other international scientific organizations, particularly in regions of “data blanks” in which little or no meteorological observations. Because of the harsh environment with rough seas and low temperatures, however, surface buoy deployment south of 60°S latitude has not yet been practicable. If the problems posed by this environment can be resolved through technological development to enable surface-buoy mooring and acquisition of time-course data on air-sea interaction changes, it may contribute to break through in research relating to global environment observation, assessment, and prediction.

As a result, JAMSTEC has begun developing buoys that have countermeasures to account for rough seas and low temperatures based on the m-TRITON buoys which have been operating in equatorial seas. A developing prototype buoy was succeeded in deploying at about 60° south, 140° east off the Adelie Coast on 16/01/2012. And it had been able to be moored for 11 months in the Southern Ocean.

In this cruise, we tried to recover the southern ocean buoy under rough sea conditions where we had never recovered them.

(3) Measured parameters

1) Meteorological parameters: Wind speed/direction, Atmospheric pressure, Air temperature, Relative humidity, Short wave radiation, Precipitation

2) Oceanic parameters: Water temperature and conductivity at 1.5 m, 10 m, 30 m, 50 m, 75 m, 100 m, 125 m, 150 m, 200 m, 400 m, 800 m, 1300 m, 4100 m(bottom – 400 m), 4300 m(bottom – 200 m), 4400 m(bottom – 100 m), 4450 m(bottom

.

– 50 m), Depth at 10 m, 50 m, 100 m, 150 m, 200 m, 400 m, 800 m, 1300 m, 4100 m(bottom – 400 m), 4300 m(bottom – 200 m), 4450 m(bottom – 50 m), Current profilers(ADCP) below 2.5 m and 4400 m(bottom – 100 m)

3) Engineering parameters: Monitoring cameras for the wind direction velocimetry with heater and the deck of the buoy, Water-gauge at 1.5 m, Tension meter at the end of the center pole, Attitude meter in the electric equipment, GPS compass on the deck, Magnetic compasses in the electric equipment and at 4400 m beside the ADCP

(4) Instruments

1) Meteorological sensors

Wind speed/direction, air temperature, relative humidity, atmospheric pressure, precipitation 2sets One is equipped with the heater.

Vaisala Weather Transmitter WXT520
Sampling interval: 1200 sec
Atmospheric pressure
JAMMET BAR & model DP4000
Sampling interval: 1200 sec
Air temperature, relative humidity
JAMMET HRH & model MP103A
Sampling interval: 1200 sec
Short Wave Radiation
JAMMET SWR & model EPSP
Sampling interval: 1200 sec
Precipitation
JAMMET RAN & model Y50202
Sampling interval: 1200 sec

2) Underwater sensors

Water temperature, conductivity and depth 16sets
11 sets of those are equipped with depth sensor.
Sea-Bird Electronics, Inc. SBE37 (except 1.5 m, 200 m)
Sampling interval: 1200 sec
JFE Advantech INFINITY-CTW (at 1.5 m)
Sampling interval: 1200 sec
JAMSTEC JES10 (prototype) (at 200 m)
Sampling interval: 600 sec
Current profilers 2 sets
Teledyne RD Instruments Workhorse sentinel ADCP 300 kHz
Sampling interval: 1200 sec, sampling time: 3 min / 50 times
Layer: 8 m, maximum measuring range: 154 m

3) Engineering sensors

Monitoring cameras 2 sets
  TAMAYA TECHNICS INC. KADEC21-EYE II
  Shooting interval: 1 hour
Water-gauge
  RIGO CO., LTD. RMD N5225
    Sampling interval: 600 sec
    Measurement range: 0-5m
Tension meter
  Unipulse Corporation LT-50KNG79
    Sampling interval: 3 hours, sampling time: 4 min / 10 Hz
    Measurement range: 0-50kN
Attitude meter
  Silicon Sensing Systems Japan, Ltd. AMU-1802-BR
    Sampling interval: 3 hours, sampling time: 4 min / 10 Hz
    Measurement range roll: ± 180 deg
    Measurement range pitch: ± 85 deg
    Measurement range angle velocity: ± 180 deg/s
    Measurement range accelerated velocity: ± 2 G
GPS compass
  Hemisphere GPS V102GPS
    Sampling interval: 1 hour, sampling time: 10 sec / 12 times
    Horizontal accuracy: < 1.0 m 95 % confidence
    Heading accuracy: 0.75 deg RMS
Magnetic compass in the electric equipment
  Honeywell HMR3400
    Sampling interval: 3 hours, sampling time: 4 min / 10 Hz
    Heading accuracy (Level): 1.0 deg RMS
    Heading resolution: 1.0 deg
    Magnetic field range: ± 2 gauss
    Magnetic field resolution: 0.1 milli-gauss
Magnetic compass at 4400 m (bottom – 100 m (beside ADCP))
  Honeywell HMR3400
    Sampling interval: 1200 sec, sampling time: 3 min / 50 times
    Heading accuracy (Level): 1.0 deg RMS
    Heading resolution: 1.0 deg
    Magnetic field range: ± 2 gauss

.

Magnetic field resolution: 0.1 milli-gauss

(5) Location of recovery

Nominal location	59°59’S, 140°00’E
ID number at JAMSTEC	Nantaiyo
ARGOS PTT number	29040 (Emergency ARGOS PPT number 13066)
Deployed date	16th Jan. 2012
Recovered date	18th Dec. 2012
Exact location	59°59.9550’S, 139°59.9330’E
Depth	4497m

(6) Results

Both acoustic releasers in underwater around 0 °C were started up by a first enabling command from the transducer equipped with Mirai. And we succeeded in recovering the all gear of the deployed buoy under rough sea conditions where wind speed is 9.2 m/s, current speed 0.5 knot, sea surface temperature is 1.3 °C, wave height is 1.5 m. On the mechanical point of view, all gear were not damaged except 2 signal cable attached the right below of the top buoy float. One of which is a signal cable for the tension meter was cut off right close to the sensor. The other modem cable for the underwater sensors also was cut off at the top of the wire cable. Therefore tension data had not only been able to be measured until the cable was cut off. On the other hand, cutting the modem cable caused underwater date transmission to stop. Each underwater sensors, however, can sample the date due to fit a storage medium in itself. Fig.4.1 shows the time series data of underwater temperature at 4,400m depth taken from the fitted storage medium. The underwater sensor was functioning correctly all over 11 months in the southern ocean at 4,400 depth to be plotted appropriate values. Other data we have gathered, for instance meteorological and engineering data, are still be taking form the each devices or analyzing.

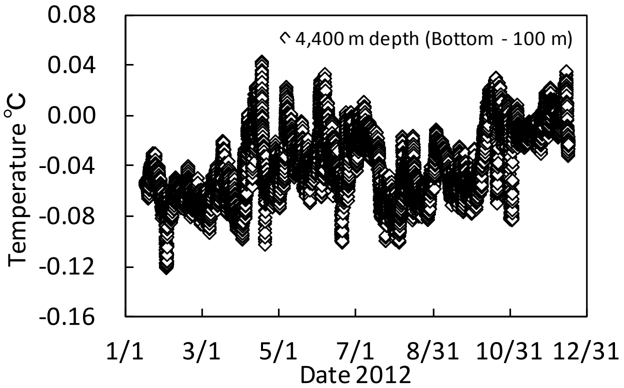

Fig. 4.1. 11 months time series variability of under water temperature at 4,400 m depth

III. Notice on Using

This cruise report is a preliminary documentation as of the end of the cruise.

This report may not be corrected even if changes on contents (i.e. taxonomic classifications) may be found after its publication. This report may also be changed without notice. Data on the cruise report may be raw or unprocessed. If you are going to use or refer to the data written on this report, please ask the Chief Scientist for latest information.

Users of data or results on this cruise report are requested to submit their results to the Data Management Group of JAMSTEC.